UNIVERSITAT DE BARCELONA

Genetics of natural variation and environmental modulation of immune-related hybrid incompatibilities in *Arabidopsis*

Kostadin Evgeniev Atanasov

UNIVERSITAT DE BARCELONA

FACULTAT DE FARMÀCIA I CIÈNCIES DE L'ALIMENTACIÓ

Genetics of natural variation and environmental modulation of immune-related hybrid incompatibilities in *Arabidopsis*

Kostadin Evgeniev Atanasov

2019

UNIVERSITAT DE BARCELONA

FACULTAT DE FARMÀCIA I CIÈNCIES DE L'ALIMENTACIÓ

DOCTORAT EN BIOTECNOLOGIA

Genetics of natural variation and environmental modulation of immune-related hybrid incompatibilities in *Arabidopsis*

Memòria presentada per Kostadin Evgeniev Atanasov per optar al títol de doctor per la Universitat de Barcelona

Rubén Alcázar Hernández
Director/Tutor

Antonio Fernández Tiburcio
Director/Tutor

Kostadin Evgeniev Atanasov
Doctorand

A mis abuelos, Kostadin y Magdalena.

A mi pareja, Jennifer.

AGRADECIMIENTOS

A mis directores de tesis, Dr. Antonio Fernández Tiburcio y Rubén Alcázar Hernández.

Al Ministerio de Economía y Competitividad, por el proyecto BFU2013-44337-P en el marco del cual he podido realizar mis estudios de doctorado con la beca para la Formación de Personal Investigador BES-2014-068041.

A todos los compañeros de la Sección de Fisiología Vegetal de la Facultad de Farmacia y Ciencias de la Alimentación. A Raúl Sánchez, por ser un gran amigo durante todos estos años.

A los profesores con los que he compartido espacio, por ser unas personas envidiables. A Laura, Eli, Jaume, Francesc, Rosa Maria, Mercè, Javier, Marius Mumbrú y Teresa. ¡Por ser tan cercanos y profesionales!

A los compañeros del grupo de investigación en Genética Molecular de la Tolerancia al Estrés, Changxin Liu y Nazanin Arafaty.

Antonio, gracias por haberme acogido inicialmente en tú grupo, por ser una persona maravillosa, por tu amistad y por todos los buenos momentos que hemos vivido.

A Xavier Zarza por los años que hemos trabajado juntos, por estar siempre tan cercano a pesar de las distancias, por su amistad y consejos, por disfrutar de la ciencia y motivar a los demás. ¡Gracias!

A Rubén, por la oportunidad que me brindaste, haber sido mi director y tutor durante estos años. Por haberme enseñado y ayudado tanto. Por orientar mi formación. Por todos esos momentos en que adaptar los recursos para investigar, se convertía en juego de niños. Por tu rigor científico. ¡Gracias!

A mi esposa, amiga y compañera, Jennifer. ¡Gracias por haber estado conmigo estos años tan difíciles!

A mi suegra, Maria Carmen Jiménez. ¡Gracias por quererme cómo un hijo!

Layout of the thesis

The main topic of this thesis is the investigation of genetic and molecular mechanisms underlying the temperature-dependent immune incompatibility between natural accessions of *Arabidopsis thaliana* from North Europe (L*er*) and Central Asia (Kas-2). Environmental modulation by mineral nutrient variation was investigated on immune-related hybrid incompatibility. Last, I've used genetics of natural variation and GWAS mapping to identify genes associated with natural variation to guazatine tolerance.

In the **Introduction** I summarize some aspects of *A. thaliana* that are useful to introduce the reader to the genetics of the natural variation, gene mapping and evolutionary analyses described in chapters 1, 2 and 3. Afterwards, I summarize the current models for pathogen recognition and defense mechanisms, which are related with post-zygotic hybrid incompatibilities described in the Bateson-Dobzhansky-Muller model

In **Chapter 1,** I describe the contribution of *RPP1-like* L*e*r genes to the immune-related hybrid incompatibility (HI) between L*e*r and Kas-2. I perform a suppressor screen of L*er*/Kas-2 HI by EMS mutagenesis that is complemented with the generation of directed mutations by CRISPR/Cas9. I map a number of intragenic mutations leading to suppression of incompatibility and analyze the effects of such mutations on primary metabolism, global gene expression and disease resistance to bacteria and a local *Hpa* isolate.

In **Chapter 2**, I study abiotic factors that modulate the plant immune response, taking as model the L*er*/Kas-2 HI. I test light intensity, humidity, CO_2 and nutrient composition. I find that HI is conditioned by ammonium or nitrate concentrations in soil or media. I then analyze the potential contribution of NPR1 to such responses.

Chapter 3 aims to study the natural variation against the PAOs inhibitor, guazatine, on a set of *A. thaliana* natural accessions. I establish the minimal dose suitable to detect quantitative differences and I perform a GWAS mapping. The study provided an association between the measured phenotype with a gene encoding for the

enzyme *CHLOROPHYLLASE 1* (*CLH1*). The association was confirmed by studying loss-of-function mutants for this gene and its paralog. A model that explains the association between guazatine tolerance and chlorophyll degradation is suggested.

In the **Discussion** I summarize key findings from the three chapters and discuss about the outcomes of my research to end with main conclusions and future perspectives.

List of abbreviations

AAT: aspartate aminotransferase

AMM: accelerated mixed model

AS: asparagine synthase

BDM: Bateson-Dobzhansky-Muller

BTH: 2,1,3-benzothiadiazole

Cad: Cadaverine

CAPS: cleaved amplified polymorphic sequences

CC: coiled-coil domain

Clh: chlorophyll

CLH: chlorophyllase

CN: CC-NB-LRR receptor

cPTIO: 2-(4-carboxyphenyl)-4,4,5,5-tetramethylimidazoline-1-oxyl-3-oxide

CRISPR: clustered regularly interspaced short palindromic repeats

CuAO: copper amino oxidases

DAMP: damage-associated molecular pattern

DM: dangerous mix

DMTU: 1,3-dimethyl-2-thiourea

EDS1: enhanced disease susceptibility 1

EMS: ethyl methanesulfonate

ETI: effector-triggered immunity

ETS: effector-triggered susceptibility

Flg22: flagellin 22

GS/GOGAT: glutamine synthetase / glutamate synthase

GC-MS/MS: gas chromatography tandem-mass spectrometry

GSNO: S-nitrosoglutathione

GST1: Glutathione S-transferase 1

Guaza: Guazatine

Gw: Gorzów

GWAS: genome-wide association study

HCA: hierarchical cluster analysis

HI: hybrid incompatibility

Hpa: *Hyaloperonospora arabidopsidis*

HPLC: high performance liquid chromatography

HR: hypersensitive response

HRP: horseradish peroxidase

HS: Hoagland and Arnon solution

HTD: 1.7-diaminoheptane

IPA: isopropanol

LD: linkage disequilibrium

LRR: leucine-rich repeat domain

MAMP: microbe-associated molecular pattern

MAPK: mitogen-activated protein kinase

MES: 2-(N-morpholino) ethanesulfonic acid

MS: Murashige & Skoog media

NB: nucleotide binding domain

NIL: near isogenic line

NiR: nitrite reductase

NJ: neighbor-joining

NO: nitric oxide

NPR1: non expressor of pathogenesis-related 1

NR: nitrate reductase

PAMP: pathogen-associated molecular pattern

PAO: polyamine oxidase

PCA: principal component analysis

PCD: programmed cell death

PMSF: phenylmethyl sulfonyl fluoride

PPH: pheophytinase

PR1: pathogenesis-related 1

PRR: Pattern Recognition Receptors

Pst: *Pseudomonas syringae*

PTI: PAMP-triggered immunity

Put: putrescine

PVP: polyvinylpyrrolidone

QTL: quantitative trait locus

RH: relative humidity

RIL: recombinant inbred line

rMS: reconstituted MS

RNS: reactive nitrogen species

ROS: reactive oxygen species

RPP1: recognition of *Peronospora parasitica* 1

SA: salicylic acid

SAR: systemic acquired resistance

SNK: Student-Newman-Keuls

SNP: single nucleotide polymorphism

Spd: spermidine

Spm: spermine

SRF3: strubbelig receptor family 3

T3SS: type three secretion system

TCA: trichloroacetic acid

TIR: toll/interleukin-1 receptor domain

TNL: TIR-NB-LRR receptor

t-Spm: thermosperimine

Table of contents

General introduction

Highlights into the *Brassicaceae* family

During the Ordovician period, about 485,4 – 443,8 million years ago (Mya), the first terrestrial plants emerged that initiated hostile-habitat colonization of the primitive Earth and created the current levels of oxygen (Lenton *et al*., 2016). Part of their success was due to high adaptation capacity through genomic and phenotypic plasticity. Genomic plasticity is based on the capacity to generate large genomic rearrangements, change the ploidy and accumulate mutations. The combination of new genes, either by genome duplication, hybridization or polyploidism, enabled the generation of new enzymatic activities, metabolic pathways and structural modifications essential for plant adaptation and evolution (Alonso-Blanco *et al*., 2009).

The Brassicales order was originated during the Cretaceous (70 million years ago) and was split at the end of this period originating three different family groups: Capparaceae, Cleomaceae, and Brassicaceae (Cruciferae). Within the group of Brassicaceae several tribes and more than 300 genera with 3.709 species appeared (Warwick and Al-Shehbaz, 2006). Within Brassicaceae, the Brassiceae tribe is a monophyletic group that contains about 66 genus and more than 200 plant species (Lysak *et al*., 2005). Among them, cultivated plants of *Brassica* such as the *B. napus*, *B. rapa*, *B. juncea*, *B. nigra*, *B. carinata* and *B. oleracea*, are used in agriculture. Brassicaceae crops represent one of the most economically important plants in the world. Brassica vegetables can be edible, used as a condiment, oilseed extraction, etc. (Warwick, 2010). They contain bioactive health-promoting secondary products (Raiola *et al*., 2018). Secondary metabolites, such as glucosinolates, are defense compounds synthesized by the Brassicaceae with direct antimicrobial and anti-inflammatory activities in humans (Bischoff, 2016). In addition, the Brassicaceae have traits of interest for plant research and plant breeding like the adaptation to abiotic and biotic stresses. Some of these traits are due to genomic rearrangements. The wild populations are thought to have adapted to different environments, at least for certain traits. This might involve the adaptation to different abiotic stresses such as salinity, drought, cold, heavy metals, xenobiotics among others (Sonah *et al*., 2017). The evolution from polyploidism to diploidism includes events of gene loss, chromosomic rearrangements and natural variation which are common in the Brassicaceae (Hohmann *et al*., 2015). Previous investigations on the evolution of the *Brassica* genus proposed an hexaploid

ancestry and explains the current diploidism by genetic reduction, dispersal and gene fragmentation (Town, 2006). In nature, diploid species of *B. oleracea*, *B. nigra* and *B. rapa* can be found (*see* **Annex I, Supplemental Table ST1**). These three species constitute the so-called "Triangle of U", from which allotetraploid hybrids are considered to be derived, such as *B. juncea*, *B. napus* and *B. curinata* (Østergaard and King, 2008). Hybridization between close-related *Brassica* species and varieties has produced genotypes with new biological features and hybrid vigor phenotypes (Chen, 2010).

An exciting event of plant diversification within the Brassicaceae family is the origin of the genus *Arabidopsis*. About 20 to 40 Mya, the tribes of Brassiceae and Camelinae diverged from Brassicaceae (Kagale *et al*., 2014) (*see* **Figure 1**). This tribe contains the genera of *Brassica*, *Capsella*, and *Arabidopsis* (Beilstein *et al*., 2010). The estimated number of *Arabidopsis* species is ten, with more than 20 subspecies (Johnston *et al*., 2005; Elven *et al*., 2007; Wolf *et al*., 2014; Briskine *et al*., 2017) (*see* **Annex I, Supplemental Table ST2**) . The *Arabidopsis* genus can be distinguished from others not only by genetic traits, but also morphological characters (Al-Shehbaz and O'Kane, 2002). Sequencing of several members of the *Arabidopsis* genus has highlighted a complex history of non-bifurcating speciation and trans-specific polymorphism (Novikova *et al*., 2016). In addition, a gene flow shared with ancestry and ploidies among species was reported within the genus members (Hohmann *et al*., 2014). Recent studies in *Capsella bursa-pastoris*, close related taxa to *A. thaliana*, have demonstrated that polyploidism originated during the last 100,000-300,000 years (Douglas *et al*., 2015). It is thought that polyploidization enhanced *C. bursa-pastoris* plasticity to deal with temperature and light changes enabling the spreading of this ruderal weed (Kasianov *et al*., 2017).

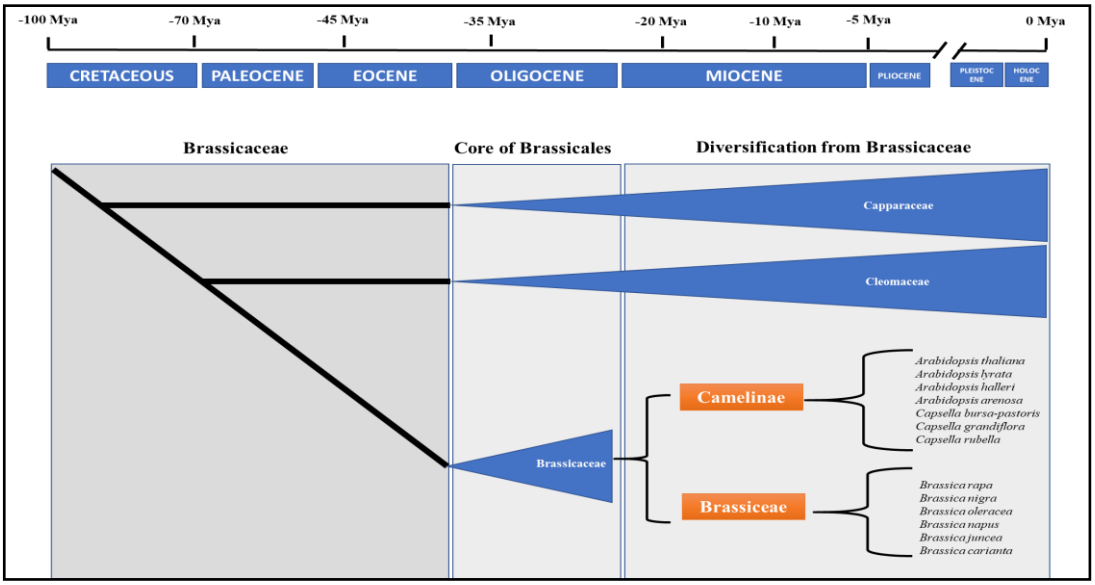

Figure 1: Time-scale of Brassicaceae diversification into the Capparaceae and Cleomaceae families during the Oligocene period. Camelinae and Brassiceae tribes diverged later from the Brassicaceae family (Core of Brassicales) during the Miocene, and these tribes originated actual species of *Arabidopsis* and *Capsella* and the *Brassica* genus, among others.

The model plant *Arabidopsis thaliana*

A. thaliana was discovered by Johannes Thal (1542-1583; Germany) in the sixteenth century at the Harz Mountains (Germany). Hence its species name "*thaliana*". However, the first one to summarize the potential of the species as a model for plant genetics was Prof. Friedrich Laibach (Laibach, 1943, 1951), with prominent contributions from other plant researchers afterwards. *A. thaliana* was the first plant with the whole genome sequenced and a T-DNA mutant collection developed (Kaul *et al.*, 2000).

Evolutionarily, *A. thaliana* was also the first one to diverge from its relatives (3,8-5 Mya), whereas the remaining species began to separate 2 Mya (Hunter and Bomblies, 2010). For example, when *A. thaliana* is compared with its closest relative, *A. lyrata*, 56 % of the genome cannot be aligned and their genome size varies by 40 %. This is because *A. thaliana* has less transposable mobile elements (TE) than *A. lyrata*. These TE are important for gene expression regulation of neighboring genes.

Morphologically, *A. thaliana* has a well-defined basal rosette, with small-ovate juvenile leaves of smooth margins, and bigger ovate adult leaves with partially serrated margins. Leaves have long and simple-forked trichomes. The central inflorescence has bifurcations emerging secondary inflorescences, carrying lanceolate caulinar leaves, and

white-color flowers with four sepals, four petals, six stamens and two carpels. Fruits in siliques contain about 20 seeds per fruit (Rodriguez *et al.*, 2014). *A. thaliana* has a short life-cycle and produces a large number of seeds. It has a small size but a large plasticity to adapt to different environments and growth conditions. *A. thaliana* is currently one of the best models to investigate basic biological processes: primary metabolism, defense, seed-dormancy, abiotic stress adaptation, and evolutionary biology (Bomblies and Weigel, 2007; Koornneef and Meinke, 2010; Corream *et al.*, 2012; Kerwin *et al.*, 2015; Blackman, 2017).

Moreover, one of the main characteristics that distinguishes *A. thaliana* from other *Arabidopsis* relative species is the capacity of self-fertilization, being *A. thaliana* an autogamous plant, not like other *Arabidopsis* genus species. The capacity of self-pollination provides some short-term advantages (Guo *et al*., 2009). Autogamous plants can produce more seeds than the outcrossing ones. This enables a proper seed dissemination and the capacity to colonize new unoccupied niches (Barrett, 2002). Acquired mutations or genomic variants are maintained in the progeny and will become fixed in the population, also depending on fitness effects of such mutations. However, self-pollination produces inbreeding negative effects such as the inbreeding depression (ID) associated with the increased homozygosity (Jarne and Charlesworth, 1993; Johnston, 1998).

The capacity for autogamous reproduction is determined by the *S* locus. This locus encodes two proteins: The *S-locus* Receptor Kinase (SRK), located at the epidermal surface of stigma, and the *S-locus* soluble ligand cysteine-rich protein (SCR) localized at the pollen wall. The recognition between SRK and SRC from the same haplotype initiates a downstream response that inhibits fertilization. In *Arabidopsis,* the *S-locus* is highly polymorphic and strongly inactivate to avoid the expression of SRK and SCR genes. Almost all *A. thaliana* natural accessions carry loss-of-function mutations at the self-incompatibility (*SI*) locus or other *SI-locus* modifiers, whereas a single point mutation in this locus has been described as causal for the restoration of self-incompatibility in the C24 accession (Iwano *et al*., 2014; Nasrallah *et al*., 2004). *A. thaliana* recently became a self-compatible plant through independent and gradual fixation of disabling mutations at the *S-locus* (Bechsgaard *et al*., 2006; Tang *et al*., 2007). The loss of outcrossing capacity can produce differences in traits, such as floral morphology and flowering time that, together with chromosomic rearrangements,

reduce gene flow between populations leading to genetic isolation and eventually, speciation (Charlesworth and Vekemans, 2005; Rieseberg and Willis, 2007) (*see* **Box 1**). An example for the importance of self-incompatibility breakdown for speciation are the diploid species *Capsella rubella* and *C. grandiflora* (2n = 2x = 16). Recent studies have suggested the occurrence of a self-incompatibility breakdown event in a local Greek population of *C. grandiflora*. This population was likely exposed to an extreme bottleneck and forced to self-reproduce from a single or few individuals, and to generate a fertile offspring with the consequent appearance of *C. rubella*. Finally, *C. rubella* has spread in the Mediterranean region together with agriculture practices (Guo *et al*., 2009).

BOX 1 Self-incompatibility

The self-compatibility produced by loss-of function mutations at the *SI-locus* can trigger negative effects. One of this negative effect is the decrease in genetic recombination between individuals that can produce lower diversity and plant adaptation capacity. On the other hand, self-compatibility provides in some cases a reproductive-improvement when the pollinator is absent or lacks the synchrony of flowering-time. Hence, self-compatibility and the acquisition of loss-of-function mutations at the *SI locus* can be considered important for speciation by reproductive isolation.

Natural genetic variation in *Arabidopsis thaliana*

Ecologic and geographic isolation drive genetic divergence and the accumulation of polymorphism. Natural variation refers to the differences in the genetic material between individuals and populations that may (or not) have adapted to deal with different local environmental conditions (Mitchell-Olds and Schmitt, 2006). Humans are the unique animal species on Earth able to see and exploit natural variation for its benefit. Crosses between species have resulted in plant domestication and the advance of agriculture (Henderson and Salt, 2017).

Arabidopsis thaliana has a worldwide geographical distribution with a strong anthropogenic influence of dispersal and colonization of new habitats (Picó *et al*., Alonso-Blanco, 2008). It is native from the Northern Hemisphere (Eurasia) but has spread by human activity and naturalized in other geographical regions such as North and South America, Africa, Oceania, and some islands (Horton *et al*., 2012). *Arabidopsis* is thought to have adapted to different habitats, accumulating and maintaining beneficial traits for its ecological niche conditions. Researchers and botanists have collected individuals from natural populations (accessions). For example, Prof. F. Laibach, one of the founders of the *Arabidopsis* research, collected in 1920 the Bla-5 and Sf-2 accessions in Blanes and San Feliu de Guixols, respectively.

During the last decades, several studies based on natural variation have been performed, resulting in a large number of genes identified that have essential biological activities (*see* **Annex I**, **Supplemental Table ST3)**. Importantly, many of these genes are not exclusive for *Arabidopsis*. As such, plant-breeders can extrapolate basic knowledge to cultivated plants, aiming at improving crop yields (Litrico and Violle, 2015). This is feasible because many pathways in development and defense have conserved mechanisms, signaling hubs or even similar genes. In conclusion, *A. thaliana* natural variation is considered a powerful tool to investigate the genetics and molecular changes involved in plant adaptation and genome evolution (Alonso-Blanco *et al*., 2009).

Today, a big effort is being performed to sequence a large number of accessions for evolutionary studies (https://1001genomes.org/). Next generation sequencing (NGS) techniques are providing thousands of genetic variations and markers across genomic regions, not only in *Arabidopsis* but also in maize, rice, soybean and wheat, among other cultivars. These data enable to apply quantitative genetics to determine casual regions underlying a measurable phenotypic trait (Trontin *et al*., Loudet, 2011).

One of the approaches to localize or map a locus associated with an observed phenotype is the Quantitative Trait Loci (QTL) mapping. The availability of genetic markers enables to apply QTL analysis using Recombinant Inbred Lines (RILs) or other genotyped populations suitable for such analyses. The power of QTL analysis and fine-scale mapping, relies not only on the low economical cost and quickness of genetic mapping, but also on the historical recombination event produced in nature that reduces

the degree of linkage disequilibrium (LD) and the tight physical distance between causal loci and the polymorphism (Slatkin, 2008). On the other hand, QTL analysis fails when there is allelic segregation between the parental lines or when a huge number of recombination occurs in the RIL population.

LD is a nonrandom association of alleles at two or more loci in the general population and its use is crucial for genetic association studies. The chromosomic extent of LD in haplotypes is crucial because it determines how dense can be the map of the associated genomic loci (Nordborg *et al*., 2002). LD is broken by recombination events and is shaped by local adaptation, genetic divergence, natural selection and population history. In autogamous plants with high homozygosity, such as *A. thaliana*, LD is strong because of the self-style of reproduction, whereas some events of recombination can also be found and interfere with the assumed association (Yang *et al*., 2012).

The strong LD in *Arabidopsis* produced through several self-pollination events, its genomic data availability, and the development of statistical methods, makes *Arabidopsis* a suitable plant for Genome-Wide Association Studies (GWAS). GWAS is a technique that uses global high-density SNP data in a large set of accessions, and it is an alternative, or probably better to say a complementary method, to QTL mapping (*see* **Box 2**).

GWAS requires major statistical improvements for an accurate polymorphism-loci association (Korte and Farlow, 2013). GWAS analysis has some limitations that can lead to misleading associations (Platt *et al.*, 2010). These involve the existence of strong and complex population structure due to isolation, accessions relatedness, genetic heterogeneity, trait heritability and population size. Narrow sense heritability is telling us how strong contributes the genetic variant to the phenotype variation or in other words, how much connected is the genotype to the phenotype. There are many ways to measure LD, all related to the difference between the frequency of co-occurrence for two alleles and the frequency expected when the two markers are independent. Furthermore, there are two commonly used LD measures: D' and r^2 (Belmont *et al*., 2005; Devlin and Risch, 1995). The statistical mixed-linear-model (MLM) method takes the population structure into account by using a genetic estimated marker data matrix and can overcome the population-structure limitation as well to predict the heritability (Yu *et al*., 2006; Zhang *et al*., 2010). Increasing the population size will

improve meaningful association but, can reduce variant recovery by weakening the polymorphism-loci correlation or decreasing allelic frequency (Korte and Farlow, 2013). Once the analysis is performed, it is time to analyze the significance of the outcome. Hence, more statistical analyzes are applied, for example, the 5 % Bonferroni threshold (Westfall *et al.*, 1993), Q-Q plots and Manhattan plot for *P* value inflation (Almli *et al.*, 2014), and false discovery ratio (FDR) (Benajmini *et al*., 1995).

BOX 2 Genome-wide association study

GWAS is a genetic study that attempts to identify commonly occurring genetic variants (SNP) that contribute to the observed phenotype. To apply the study, it is required numerical discrete or continue data because they improve the power of SNP detection. When data is a phenotypic trait with a non-numerical value, the observed trait must be categorized in numerical by categorizing it in binary (e.g. 0 = non-affected; 1 = affected) or in multiple-numerical categories. There are online-free applications that enable GWAS analyses, whereas the most powerful analyses are performed in Linux and R scripts. Nevertheless, findings obtained by GWAS must be validated by other complementary genetic approaches.

In *Arabidopsis*, Genome-Wide Association Studies were reported in 2010 (Atwell et al., 2010) identifying disease resistance genes against the plant pathogenic bacteria, *Pseudomonas syringae*. Recently, GWAS has demonstrated the capacity to identify the genetic bases for defense traits not only in *Arabidopsis*, but also in other species such as rice, tobacco, maize, soybean and wheat, among others, and it is widely used for the identification of genes that influence other complex traits (Chang *et al*., 2016; Gurung *et al*., 2014; Olukolu *et al*., 2014; Turuspekov *et al*., 2016; Wang *et al*., 2016) including tolerance to high magnesium supply (Niu *et al*., 2018), identification of genes shaping the leaf microbiota (Horton *et al*., 2014), identification of new components involved in hydrogen peroxide signaling an tolerance *(*Sadhukhan *et al*., 2017), abscisic acid accumulation during abiotic stress (Kalladan *et al*., 2017), herbicide resistance in wheat (Zandkamiri *et al*., 2017), salt tolerance, secondary metabolites variation, morphological

and yield-trait identification in rice (Begum *et al*., 2015; Matsuda *et al*., 2015; Meyer *et al*., 2016).

We carried out a GWAS analysis to study the genetics basis for the natural variation to guazatine (*see* **Chapter 3**). Guazatine is a mixture of long chain guanylate-polyamines derived from polyamines (PAs) that inhibits plant polyamine oxidases (PAOs). PAs are small polycationic compounds present in all living organisms. In *A. thaliana* the most abundant PAs are putrescine (Put), spermidine (Spd), spermine (Spm), and thermospermine (t-Spm). The role for PAs in plants is associated with protection against abiotic stress (Alcázar *et al*., 2006; Tiburcio *et al.,* 2014; Zarza *et al*., 2016), but also biotic stress (Lou *et al*., 2016; Sagor *et al*., 2015; Takahashi *et al*., 2003; Vilas *et al*., 2018). The mechanism underling biotic stress protection can be explained through PA oxidation by polyamine oxidases (PAO) or diamino oxidases such as the Copper amino oxidases (CuAOs) which produce reactive species of oxygen (ROS), a potent messenger that stimulates the plant immune system (Liu *et al*., 2015; Planas-Portell *et al*., 2013; Tavladoraki *et al.,* 2016).

The plant immune system

Biotic stress causes between 30 % to 40 % of crop losses with huge economical costs, while abiotic stress has an impact of 6 % to 20 % (Shamee *et al.,* 2018). In addition, biotic stress has a strong negative impact on crop yield, not only on the quality of the product but also decreasing the potential of plant growth due to the metabolic cost of maintaining an activated immune system (Huot *et al.,* 2014). Plants are sessile organisms with no cellular, humoral or adaptative immune system. Their capacity to resist to pathogen colonization is based on the innate immune response and the capacity to recognize pathogens through resistance (*R*) proteins encoded by *R* genes or other receptors at the plasma membrane (Dangl and Jones, 2001).

To deal with pathogen attack, the plant has different layers of defense according to the nature of the pathogen that is threating the plant. However, plant pathogens have different strategies to survive and adapt to their hosts. Pathogens can be herbivores insects, nematodes, fungi and viruses or microorganisms such as bacteria and oomycetes. Hence, fungi and bacteria have similar mechanisms to avoid plant recognition. The interference mechanism is based on the capacity to deliver into the host

cell proteins known as effectors (virulence factors) in such a way that pathogen fitness is enhanced (Jones and Dangl, 2006).

The plant immune system can be represented in a "zig-zag" model (*see* **Figure 2**). Molecules at the surface of bacteria, fungi or oomycetes, might represent molecular fingerprints called Pathogen Associated Molecular Patterns (PAMPs) and Microbial Associated Molecular Patterns (MAMPs) (Zipfel and Felix, 2005). Recognition PAMPs or MAMPs by Pattern Recognition Receptors (PRR) results in a PTI response that arrests pathogen invasion. At a second stage, pathogen successfully use effector or avirulence proteins (*Avr*) that contribute to pathogen virulence by interfering in a spatial and temporal manner with PTI signaling and delay plant immune responses (Toruño, Stergiopoulos, and Coaker, 2016) thus resulting in Effector Triggered Susceptibility (ETS). To counteract this, plants have developed a second line of defense comprising intracellular receptors or R proteins which mainly are Nucleotide-Binding site Leucine-Rich Repeat (NB-LRR) type. Their conformational activation leads to ETI (effector triggered immunity). ETI triggers global transcriptional reprogramming, generation of ROS and RNS, induction of Programmed Cell Death (PCD) and Hypersensitive Response (HR) at the infection sites (Dangl and McDowell, 2006; Jones and Dangl, 2006).

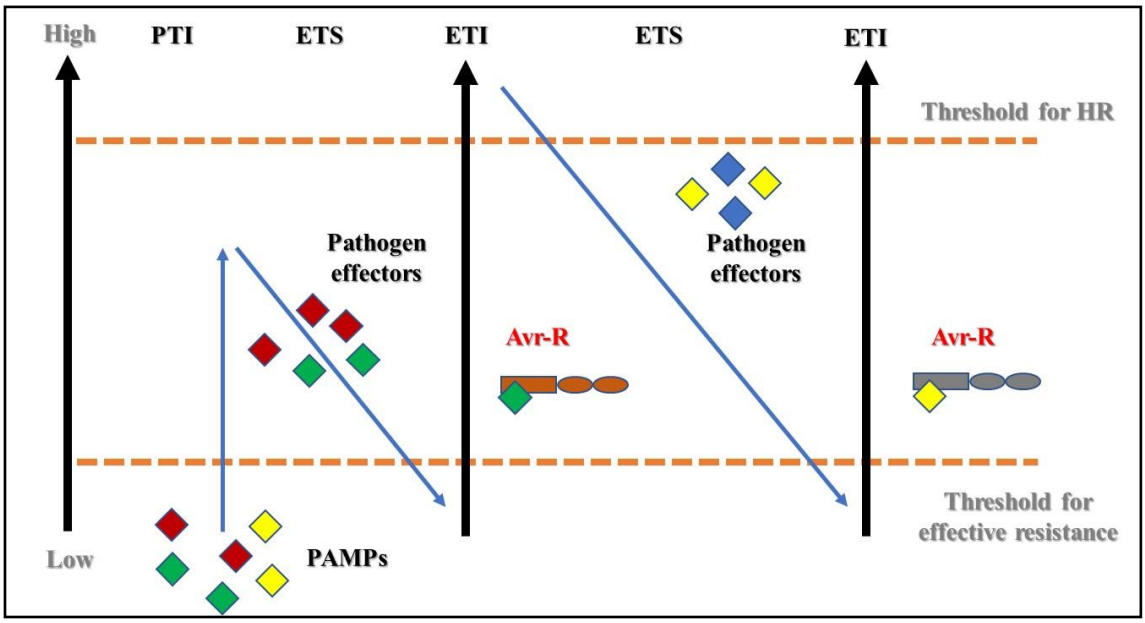

Figure 2: Zig-zag model for the illustration of the quantitative output of the plant immune-system interaction with pathogen effectors. Adapted from Jones and Dangl, 2006.

PAMP and DAMP triggered immunity

When PAMPs or MAMPs are recognized by PRRs, the PAMP-Triggered Immunity (PTI) initiates. PTI is an early and broad-range specific immune response against non-host specialized pathogens (An *et al.,* 2017). For example, bacterial PAMPs such as Flagellin 22 (flg22) or the Elongation Factor Tu 18 (elf18) are recognized by membrane-anchored PRR (FLS2 and EFR, respectively). Recognition stimulates the recruitment of the leucine-rich repeat receptor-like kinase BAK1 (*Brassinosteroid Insensitive Associated Receptor Kinase 1*) and the *receptor-like cytoplasmatic kinase* BIK1 that, upon trans-phosphorylation, activates a plasma membrane-anchored specific *NADPH oxidase* (RBOH) and *mitogen-activated protein kinases* (MAPK). RBOH are responsible for ROS production or oxidative burst, whereas MAPK cascades promote the expression of *Resistance* genes, biosynthesis of antimicrobial compounds and strengthening of cell wall structures (Qi *et al.,* 2017; Withers and Dong, 2017; Zipfel and Robatzek, 2010) (*see* **Box 3**).

BOX 3 *Arabidopsis* NADPH oxidases

In *A. thaliana*, there are 10 different isoforms for RBOH NADPH oxidases (RbohA-J). Only isoforms RbohD and RbohF have been reported to participate during PTI and are known to trigger the oxidative burst after PAMPs/MAMPs and DAMPs recognition.

RBOH activity is regulated at post-translational level by phosphatidic acid (PA), Ca^{2+}, FADH, NADPH and phosphorylation by BIK1 and CPKs (*Ca^{2+}-dependent protein kinases*).

Due to the pathogen invasive activity, cell structures are damaged. This process produces and delivers Damage-Associated Molecular Patterns (DAMPs) initiating the DAMP-Triggered Immunity (DTI) which enhances and maintains both PTI and ETI responses (Albert, 2013; Choi and Klessig, 2016; Huffaker and Ryan, 2007). Different defense triggering molecules, their origin, receptors and observed responses are summarized in **Annex I, Supplemental Table ST5**. Because of the continuous co-evolution with environmental pathogens, plants can recognize, in an innate way, pathogen-model molecules different from PAMPs or MAMPs and initiate immunity.

Thus, fingerprinting molecules have different nature and involve proteins, lipids, sugars, nucleotides, cell-wall degradation-derived products and maybe also polycationic molecules such as polyamines.

Effector triggered immunity

Host-specialized and non-specialized pathogens have different invasive mechanisms. The non-specialized ones can only be recognized by PRR receptors and trigger PTI whereas host-specialized pathogens deliver avirulence proteins (effectors) that are recognized by intracellular *Nucleotide Binding Leucine-Rich Repeats* (NLR) receptors that trigger ETI and hypersensitive response (HR). Very often, these intracellular receptors are not binding directly to the effectors, but they guard a host protein that is the target of such effectors. NLRs are present in plants, animals, and fungi, revealing their evolutive importance to recognize intracellular pathogens or their effectors. Plant NLR proteins can be found in angiosperms, gymnosperms, bryophytes, and liverworts (*Hepaticophyta*) but not in the unicellular alga *Chlamydomonas.* In animals, NLR receptors are found in mammals (also known as NOD-like receptors), chordates and sponges but not in nematodes or arthropods (Dyrka *et al*., 2014; Hamada *et al*., 2013; Huang *et al*., 2008; Rast *et al*., 2006).

In gram-negative bacteria, such as *Pseudomonas syringae*, effector delivery is mediated through the Type Three Secretion System (TTSS) (Toruño *et al*., 2016). An example of the guard-guardee model is RIN4, a plasma-membrane associated protein that is target of TTSS effectors AvrRpm1, AvrB and AvrRpt2. RIN4 is guarded by the NB-LRR proteins RPM1 and RPS2, which sense perturbations in RIN4 homeostasis. When AvrRpm1 or AvrB target RIN4, this protein becomes phosphorylated and activates RPM1. In contrast, AvrRpt2 cleaves RIN4 and this leads to RPS2 activation. Activation of ETI via NB-LRR receptors induces an HR response at the site of infection and promotes disease resistance (Grant *et al*., 1995; Hou *et al.,* 2011; Jones and Dangl, 2006b; Kim *et al.,* 2009). Filamentous pathogens can deliver effectors from the intercellular space by hyphae or haustoria (Torto *et al*., 2003). *Hyaloperonospora arabidopsidis (Hpa)* is an obligate biotrophic oomycete that grows under high humidity and can infect *A. thaliana* (Koch and Slusarenko, 1990; Slusarenko and Schlaich, 2003). *Arabidopsis* has NB-LRR receptors (Recognition of *Peronospora parasitica* 1, RPP1) that recognize allelic variants of the *Hpa* ATR1 effector. Some additional receptors

show sequence similarity to *RPP1* and are referred to as *RPP1-like* (Alcázar *et al.*, 2009; Botella *et al*., 1998), although their recognition specificities are still unknown (Rehmany, 2005).

It is widely accepted that NB-LRR mediated immune responses are only effective in obligate biotrophs (e.g. *Hpa*, *Ustilago spp.*, *Uromyces spp.*, *Phytophthora spp.*) that require living hosts to exploit their metabolites, but not effective against necroptrophic pathogens (e.g. *Botrytis spp.*, *Fusarium spp.*, *Sclerotinia spp.*, *Pythium spp*.). Necrotrophs kill and destroy the host by exhaustive use of the organic material and nutrients for its own growth (Glazebrook, 2005). Moreover, some hemibiotrophic pathogens establish a biotrophic interaction with the host at the beginning but switch to a necrotrophic lifestyle afterwards (Sukno *et al*., 2012).

NLR regulation and signaling

NLR receptors can be categorized according to their N-terminal domain. TIR-NB-LRR (TNL) receptors carry a *Toll-interleukin-1 domain* in their N-terminus. CC-NB-LRR (CNL) carry a *coiled-coil domain* in their N-terminus and RPW8-NB-LRR (RNL) have a *powdery mildew-8 domain* (Neupane *et al.*, 2018). TIR and CC domains of NLR receptors are required for downstream signaling and are able to trigger cell death (Casey *et al*., 2016; Wang *et al*., 2015). The NB domain contains STAND motifs with a regulatory activity via ATP hydrolysis that induces protein conformation changes (McHale, Tan, Koehl, and Michelmore, 2006). Between the NB domain and the LRR, an interspace separating sequence can be found (NL-LINKER). Structural variation of the NL-LINKER sometimes correlates with NLR activity, suggesting an intrinsic variation that modulates receptor activity (Zhu *et al*., 2018). The C-terminal sequence of NLR is composed of several *leucine-rich repeats* (LRR) domains. This region is highly variable and can bind effector proteins and interact with the NB domain thus inducing the conformation changes required for activation (Proell *et al*., 2008; Tran *et al*., 2017; Wang *et al*., 2015). Mutations in the different NLR domains can affect receptor activity and lead to self-activation, incapacity to bind molecules (e.g. effectors and nucleotides) or to oligomerize and trigger an autoimmune response (*see* **Chapter 1**).

TNL signaling requires the nucleocytoplasmatic lipase-like protein, *Enhanced Disease Susceptibility 1* gene (EDS1), its coreceptor *Phytoalexin Deficient 4* (PAD4) and *Senescence Associated Gene 101* (SAG101) that promotes SA biosynthesis by

stimulating *Salicylic acid Induction Deficient 2* (*SID2*) / *Isochorismate Synthase 1 (ICS1)* gene expression (Dempsey *et al.*, 2012; Gantner *et al*., 2019). SA and *EDS1*/*PAD4* have a positive feed-back relationship. CNL receptors are almost EDS1/PAD4 independent, but NDR1 dependent (Day *et al.*, 2006; Wiermer *et al.*, 2005; Wildermuth *et al.*, 2001). ETI activation induces a global immune response that can be transmitted throughout the plant to prevent disease (Fu and Dong, 2013). This broad-spectrum immune response is the Systemic Acquired Resistance (SAR) and requires SA gradient accumulation and conformational changes (S-nitrosylation) of the master SAR protein NPR1 (non-expressor of *PR-1*) that translocates into nuclei and promotes gene expression (via TGA transcription factors) of WRKY transcription factors, redox regulation, DNA repairment and membrane traffic readjustments (Fan and Dong, 2002; Gu *et al.*, 2017; Henry *et al.*, 2013; Kinkema *et al.*, 2000; Tada *et al*., 2008; Withers and Dong, 2017; Xu *et al*., 2017).

Autoimmunity in *A. thaliana* and the Bateson-Dobzhansky-Muller (BDM) model of reproductive isolation

Arabidopsis natural variation can be a useful tool to study underlying speciation processes derived from genetic divergence (Bomblies and Weigel, 2007). How natural populations with genomic variants evolve to new species without being incompatible in the ancestral population and without passing through any deep adaptive valley was an enigma for Darwin an others evolutionary biologists (Boero, 2015; Chen *et al.*, 2016). Studies have described ways of plant speciation through the occurrence of reproductive barriers at pre-zygotic or post-zygotic stages. Zygote formation can be affected during the step of pre pollination or postpollination. Handicaps of prepollination underlie ecological isolation (when fitness is reduced in heterospecific habitat), phenological isolation (e.g. differences in flowering time) and/or pollinator specialization. On the other hand, reproductive barriers after pollination are related to pollen-stigma interactions in which foreign pollen is recognized and ovule fertilization blocked (Baack *et al.*, 2015). Furthermore, postzygotic reproductive barriers occur when the zygote is formed but the hybrid exhibits sterility or is not viable. Hybrid seeds can also be defective, and germination or fitness strongly affected in F1 or F2 generations (Chen *et al*., 2016).

The BDM or Bateson-Dobzhansky-Muller (Bateson, 1909; Dobzhansky, 1951; Muller, 1942) model of genetic incompatibilities explains the process of speciation through postzygotic reproductive isolation (*see* **Figure 3**). The theory underlying this speciation model considers an ancestral population where two alleles (*AABB*) coexist with no impact on growth and fitness. When the ancestral population is split in two, alleles *A* and *B* mutate and generate new alleles (*a* and *b*) in the respective populations. Through transition states (*AaBB* or *AABb*) variants become fixed in the two populations (*aaBB* vs *AAbb*) with no costs on fitness. The problem emerges when individuals from these two diverged populations mate and evolved alleles are forced to co-exist in the same genome, leading to a lethal epistatic interaction between them that is the basis for hybrid incompatibility. Incompatible hybrids are sterile or lethal. Other symptoms such as hybrid weakness, might be related to intermediate stages towards the complete reproductive isolation.

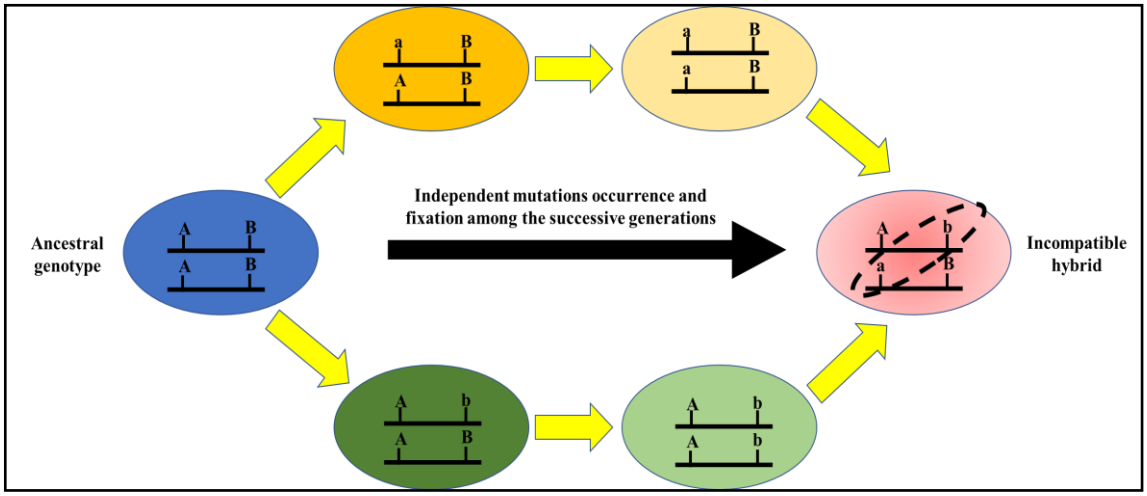

Figure 3: The Bateson-Dobzhansky-Muller (BDM) model for genetic incompatibilities. An ancestral population has two coexisting alleles (AABB). After a split, two new populations appear and exhibit independent allele divergence originating alternative alleles "a" or "b" which become fixed. When individuals from these two diverged populations are crossed, an epistasic deleterious interaction between the two new alleles occurs that leads to hybrid incompatibility.

There are many examples of HI in different plant species involving epistatic interactions with at least one immune *R* gene. These hybrids exhibit an autoimmune response which has a strong impact on plant growth and fitness. Dwarfism, cell death and sterility are hallmarks for immune-related HI. These hybrids are not only useful to study underlying mechanisms of reproductive isolation, but they also highlight molecular mechanisms that enable fine-tuning defense responses or guard-guardee relationships. Other mechanisms of hybrid incompatibility have been reported such as

cytonuclear incompatibilities and differences in ploidy (Fishman and Sweigart, 2018), but these are not the focus of this study. In the recent years, immune-related HI have been focused on the identification of causal genes. Here, we have studied what are the effects from the genetic suppression of immune-related hybrid incompatibilities on plant growth, overall fitness and resistance against pathogens (*see* **Chapters 1** and **2)**.

Most of the described HI in plants include incompatible interactions between *R* genes and other immune-signaling pathway related proteins (e.g. NLR receptors, RLK, receptors like proteins, and other types of immune-signaling proteins). Among the NLR-based HI, TIR-NB-LRR receptors are the most frequent, but involved although CC-NB-LRR incompatibilities have been described (van Wersch *et al.,* 2016) (*see* **Annex I, Supplemental Table ST4**). In rice, deleterious interactions leading to self-immune activation were described between NLR-RLK, two CNL receptors, and two RLK proteins (Césari *et al.,* 2014; Chen *et al.,* 2014; Yamamoto *et al.,* 2010). In other species such as, wheat, lettuce and *Capsella spp.*, incompatibilities involving CNL (Gong *et al*., 2013), RIN4 (Jeuken *et al*., 2009) and NPR1 were reported, too (Sicard *et al*., 2015). In *Arabidopsis* TNL-based incompatible interaction was first described by Bomblies *et al*., 2007. Alcázar *et al*., 2009, 2010, 2012, 2014, and Chae *et al*., 2014 identified additional genetic deleterious interactions often involving a common locus, *RPP1-like*.

Autoimmune phenotypes

Loss-of-function in RLK proteins such as BAK1, BAK1-like (BKK1), and BAK1-*interacting receptor-like kinase* (BIR1) produce strong autoimmunity (Gao *et al*., 2009; Kai He *et al*., 2007). In addition, gain-of-function mutations at RLK protein, *Suppressor of* NPR1-1 *constitutive 4* (SNC4), *Chitin Elicitor Receptor Kinase* (CERK) or the RLP (receptors like proteins), and the *Suppressor of NPR1-1 constitutive 2* (SNC2) also produce autoimmunity (Bi *et al.,* 2010; Petutschnig *et al*., 2014; Yang *et al*., 2010). Loss-of-function mutations in other type of genes such as *Constitutive expressor of PR genes* (e.g. *cpr1-1*), *Suppressors of RPS4-RLD1* (*srfr1*), *Accelerated Cell Death* (*ACD*), *MAP Kinase 4* (*mpk4*) or the *Non-expressor of PR* (*npr1*), among other genes also trigger autoimmunity with SA accumulation, programmed cell death (PCD), and dwarfism (Bowling *et al*., 1997; Bowling *et al*., 1994; Brodersen *et al*., 2002; Kuai *et al*., 2015; Li *et al*., 2010; Lu *et al*., 2009; Petersen *et al*., 2000; Yoshioka

et al., 2001; Zhang *et al*., 2006). Also, loss-of-function of *A. thaliana Nudix hydrolase 6* and *7* (AtNUDT6/7), described as a negative regulator of EDS1, exhibits an autoimmune phenotype but not so strong as e.g. *cpr1-1* or *mpk4* (Wang *et al*., 2013). A dominant mutation in *hopZ-ETI-deficient1 (*ZED1*)* produces high-temperature-dependent autoimmunity. ZED1 cooperates with some ZED1-*related kinases* and modulates SNC1, a TNL receptor involved in SAR (Wang *et al*., 2017). Loss-of-function mutations in calcium-dependent, *phospholipid binding proteins copines* (*cpn1-1*), generate plants with self-immune activation at low humidity (Jambunathan, Siani, and McNellis, 2001). During the last years, a large number of autoimmune temperature-dependent mutants have also been identified, including snc1, *bonzai1-1* (bon1-1), *npr1-5* (*ssi4*), the *chilling-sensitive 2* and *3* (*chs2* and *chs3*), *bir1* (bak1-*kinase phosphatase 1*), *bap1* (bon *associated protein 1*), *cpr1* and *mkp1* (*map kinase phosphatase 1*), among others (Buchala *et al*., 2009; Cheng *et al*., 2011; Wang *et al*., Yang, 2011; Yang, Li, and Hua, 2006; Yang and Hua, 2004). Remarkably, *BON1*, *BAP1*, *BIR1*, *SRFR1*, *MKP* and *CPR1* are known negative regulators of *SNC1* (Bartels *et al*., 2009;. Cheng *et al*., 2011; Gao *et al*., 2009; Gou and Hua, 2012; Kim *et al*., 2010; Li *et al*., 2010; Wang *et al*., 2011; Yang *et al*., 2006). Nevertheless, the link between temperature/humidity and defense remains unsolved (Wang *et al*., 2017).

The Ler/Kas-2 hybrid incompatibility

An immune-related hybrid incompatibility was reported by Alcázar et al., (Alcázar *et al*., 2009) between geographically isolated *A. thaliana* natural populations: L*e*r (Gorzów Wielkopolski, Poland) and Kas-2 (Kashmir mountains, Central Asia) or Kondara (Kond, Tajikistan, Central Asia). The nature of this interaction is similar to the BDM model but with incomplete reproductive isolation because the incompatible hybrid was still able to produce viable seeds at a permissive temperature.

The authors examined growth defects in two different RIL populations (L*e*r/Kas-2 and L*e*r/Kond) grown at 14 ºC - 16 ºC, and by QTL mapping three regions underlying the incompatibility were detected: L*e*r QTL3, Kas-2/Kond QTL4, and Kas-2/Kond QTL5, on the chromosomes 3, 4 and 5, respectively. QTL3 was mapped to the Col-0 genomic interval of *At3g44600-At3g44700* which contains 11 genes, two of them *RPP1-like* genes (*At3g44630* and *At3g44670*) and three transposable elements. Sequencing this locus from a L*e*r BAC library, identified a 65 Kb genomic insertion in

L*er* that increased the number of *RPP1-like* genes to eight (*R1-R8*). Because *A. lyrata* also contains two *RPP1*-like genes, it is assumed that the L*er* haplotype is a derived form.

Interestingly, Bomblies et al., (Bomblies *et al*., 2007b) found the same locus as involved in the temperature-dependent hybrid necrosis between Uk-1 and Uk-3 accessions. However, crosses between L*er* and Uk-1 or L*er* and Uk-3 resulted in a fully compatible offspring. The L*er*/Kas-2 or L*er*/Kond incompatibility was explained by the recessive interaction between QTL3 and QTL4, and an additional interaction with QTL5 that was dominant and behaves like a growth modifier.

The L*er*/Kas-2 incompatible hybrid exhibited enhanced resistance against Cala-2 *Hpa* infection and higher expression of SA oxidative stress (e.g. *GST1*) marker genes. The contribution of SA to the HI phenotype was corroborated by different approaches. L*er*/Kas-2 NIL plants were transformed with the *NahG* gene (bacterial *Salicylate Hydroxylase*), a gene that catabolizes SA to catechol, and the HI was suppressed. The same suppressive phenotype was reproduced when crossing Kas-2 with L*er* *eds1-2* or L*er*/Kas-2 hybrid with *sid2-1*, demonstrating that this type of HI requires SA and *EDS1*.

Alcázar *et al*., 2010 reported the fine mapping and sequence of a 30 KB region from Kas-2, on chromosome 4 (QTL4) that identified the causal gene interacting with the *RPP1-like* cluster. A receptor-like kinase *SRF3* was identified (*At4g03390*) and the epistatic interaction validated by complementation of the L*er*/Kas-2 NIL line with a Ler *SRF3* allele (cNIL). When *SRF3* allelic variation was analyzed in accessions from Northern Europe, Southern Europe and Central Asia, no incompatible alleles were found in Europe. Crosses between L*er* and North or South Europe accessions produced fully compatible plants, whereas crosses of L*er* with Central Asian accessions produced different degrees of HI suggesting high frequency of incompatible alleles in Central Asia.

On the other hand, when the authors analyzed by crossing the incompatibility of Kas-2 with accessions from all Europe, they reported no incompatibility and concluded that the L*er* *RPP1-like* haplotype is rare in Europe. Moreover, authors tested whether Kas-2 SRF3 was providing a positive contribution to pathogen resistance. To address this question, authors used cNIL, complemented Kas-2 (cKas-2) and complemented RIL (cRIL) plants for infection with *Hpa*, virulent *Pseudomonas syringae DC3000*

(*PstDC3000*), and the avirulent *Pseudomonas syringae DC3000 hrcC*$^{-}$. In addition, MPK3, MPK4 and MPK6 activities were determined after flg22 treatment in these genotypes. The results from these experiments provided strong evidence that SRF3 is involved in defense responses to pathogenic bacteria (Alcázar et al., 2010).

A deeper analysis about the genetics and occurrence of the *RPP1-like* locus in the nature was reported afterwards by Alcázar et al., (Alcázar *et al*., 2014). In this work, authors measured the contribution of the *RPP1-like* genes to incompatibility by transformation of the L*er*/Kas-2 incompatible NIL with artificial microRNAs (amiRNA) designed against the *RPP1-like* genes in Uk-1 accession (kindly provided by Dr. D. Weigel). Two amiRNA constructs (*KB209* and *KB212*) were identified that suppressed incompatibility. In these amiRNA lines, *RPP1-like* genes *R1*, *R3*, *R4*, *R5* and *R7* were silenced, whereas *R3* and *R8* were not. Additional amiRNA lines were analyzed, too. The constructs *KB228* did not suppress incompatibility and *R3* gene expression was increased more than two-fold. According to this, authors suggested that the incompatibility was determined by two or more *RPP1-like* genes, and it associated with higher *R3* expression. Researchers also measured the trade-off between growth and disease resistance by transforming Col-0 plants with single L*er* *RPP1-like* genes and infecting the transgenic plants with two isolates of *Hpa*, Cala-2 and Noco-2. No alteration on basal disease resistance was observed in the transgenic lines *R1*, *R2*, *R3*, *R4*, *R5*, *R7*, and *R8*. On the other hand, Col-0 *R3* over-expressor line (*R3ox*) was displaying HI-like phenotype and caused increased cell-death response against *Hpa* Noco-2, suggesting that *R3* overexpression affects the trade-off between growth and disease resistance. Moreover, the different *RPP1*-like transgenic lines crossed with Kas-2 produced compatible F2 populations, thus reinforcing that two or more *RPP1-like* genes were required for HI.

When the distribution of the *RPP1-like* L*er* haplotype was analyzed in a local population in Gorzów (Poland), from which L*er* was collected in 1939, authors still found individuals carrying a conserved *RPP1-like* haplotype (Gw^{+}) but also others not carrying it (Gw^{-}). Principal component analysis (PCA) based on 149 genome-wide SNPs, on Gw^{+}, Gw^{-}, and other geographical separated accessions revealed that Gw^{+}/Gw^{-} and L*er* are similar to other Central European accessions. The *RPP1-like* haplotype analysis on Gw local population revealed a L*er* haplotype frequency of about 30%. This high frequency was not due to a recent bottleneck (because of the large level

of polymorphism between individuals) but by introgression of the *RPP1-like* cluster into different Gw genetic backgrounds by outcrossing over 72 years, and maintenance of the haplotype due to low recombination. Nevertheless, the increase in frequency by genetic drift, selection or demography was not completely discarded (Alcázar *et al.,* 2014).

More recently, Stuttmann *et al*., 2016 obtained a transgenic line carrying a C-terminal YFP tag fused to EDS1 in which a nuclear localization sequence (NLS) was introduced (EDS1-YFP^{NLS}). In this publication, they reported that EDS1 residual-nuclear low-accumulation is enough to confer resistance against *Hpa* and *Pst DC3000*. Furthermore, EDS1-YFP^{NLS} nuclear-enrichment was enough to trigger autoimmunity and produce plants with stunted growth, SA accumulation and HR. By applying EMS mutagenesis (*see* **Box 4**), they performed a suppressor screen on an EDS1-YFP^{NLS} and isolated extragenic mutants, mapping at the *DM2h (R8)* a member of the L*er* *RPP1-like* gene cluster. Stuttmann et al., suggested that DM2h (R8) is upstream of EDS1/PAD4 and the autoimmunity becomes deleterious once EDS1 accumulates in nuclei.

BOX 4 Basic techniques on plant mutagenesis

Plant breeders have used different strategies in order to obtain new plant varieties with specific commercial or adventurous traits. Plant researchers use mutagenesis techniques as basic tool to study gene function and investigate main plant physiology. First mutagenesis techniques were based on the use of energetic radiations such as X-ray, γ-ray and fast neutron bombardment. X-ray produces high destructive changes and, in many cases, leads to a non-viable plant. γ-ray is less destructive and causes point mutations and small deletions, whereas fast neutron bombardment is used to induce large deletions and chromosomic translocations. UV-B and UV-C are non-atomic radiations that are also used for plant mutagenesis with different degrees of success.

Chemical mutagenesis is an alternative. The advantage of this technique relies on the easiness of application in a basic equipped laboratory and the known nature of induced mutations. For example, the Ethyl-methane sulfonate (EMS) alkylates guanine bases causing the shift GC to AT during DNA-polymerase replication. Sodium azide (Az) and methylnitrosourea (MNU) are chemicals also used in combination (Az-MNU). They induce a GC to AT or AT to GC shifts but are less stable, more toxic and tedious for work.

Finally, since the development of *CRISPR/Cas9* genome editing tools in plants, one can induce specific changes in a target gene with high precision. For instance, loss-of function mutants can be isolated when gene-mutant is not available or for non-model plants.

Objectives

Plant hybrid incompatibilities (HI) are one of the main problems that plant breeders face when they attempt to obtain a new variety with improved traits. The mechanism underlying such incompatibilities can be pre-zygotic or post-zygotic. However, post-zygotic incompatibilities are more frequent than pre-zygotic ones and involve complex genetic interactions that, in some cases, produce autoimmunity. Constitutive activation of defense has a direct negative impact on plant physiology in such a way that incompatible hybrids exhibit severe growth defects and reduced fitness. Hence, it is required to provide genetic strategies to overcome this barrier. However, any approach should consider maintaining an appropriate immune response against environmental pathogens, because they are the main factor for worldwide crop and economical losses.

HI between natural populations of *Arabidopsis thaliana* are a good model to investigate plant immunity and evolution of HI in the wild. Arabidopsis evolution is not forced by artificial selection towards certain traits. It is assumed that some of its variation is due to adaptation to local environmental conditions. Moreover, because one of the forces driving plant evolution are plant-pathogen interactions, investigations on the capacity of recognition of wild pathogens or isolates, can provide insights into plant-pathogen coevolution. In addition, HIs are suggested to act as an incipient process of speciation according to the Bateson-Dobzhansky-Muller genetic model of reproductive isolation. Therefore, understanding how local adaptation and the environment shapes genetic evolution and the occurrence of gene flow barriers is fundamental from a basic perspective but also from an applied view.

In this Thesis I have investigated the effects from suppression of HI on disease resistance and fitness traits. In addition, I have studied natural variation for the tolerance against guazatine, a fungicide which we have found it is also herbicide. Overall, my work provides insights into the genetics of reproductive isolation and local adaptation to pathogens and herbicides.

The specific objectives followed for each chapter are described bellow:

1- Chapter 1

a. Identification of L*er* *RPP1-like* genes and polymorphisms underlying the immune-based hybrid incompatibility interaction with the receptor-like kinase *SRF3*, from Kas-2 and Kond. Analysis of *RPP1-like* L*er* individual gene contribution to incompatibility and defense.

b. Determination of the metabolic costs and gene expression reprogramming during the immune activation and suppression of L*er*/Kas-2 HI.

c. Functional analysis of the L*er* *RPP1-like* gene cluster in the recognition of a natural *Hyaloperonospora arabidopsidis* isolate from Gorzów, Poland, were the L*er* accession is originated.

2- Chapter 2

a. Determination of the environmental factors modulating plant hybrid incompatibilities (L*er*/Kas-2 and Uk-1/Uk-3) with a focus on plant nutrition.

b. Involvement of ROS and RNS on ammonium-based modulation of HI.

c. Biochemical and genetic analysis of NO-dependency of HI. Identification of HI suppressors by *NPR1* mutation.

3- Chapter 3

a. Identification of genes providing tolerance to the herbicide guazatine in Arabidopsis, using natural variation and GWAS mapping.

b. Validation of associations found by GWAS using loss-of-function mutants.

c. Study of potential geographical or population structure signatures and allelic variation of validated genes.

d. Potential mode of action of guazatine as herbicide.

Supervisor's report

Dr. Rubén Alcázar Hernández (Professor Agregat) and Dr. Antonio Fernández Tiburcio (Catedràtic d'Universitat), at the Department of Biologia, Sanitat i Medi Ambient of the Facultat de Farmàcia i Ciències de l'Alimentació (Universitat de Barcelona), Directors of the PhD Thesis entitled **"Genetics of natural variation and environmental modulation of immune-related hybrid incompatibilities in *Arabidopsis*"** declare that:

The Thesis hereby presented is the result of the work performed by **Kostadin Evgeniev Atanasov** under our supervision and guidance.

The contribution of the PhD candidate to different articles and chapters included in this Thesis is detailed below.

Chapter 1: NLR mutations suppressing immune hybrid incompatibility and their effects on disease resistance

Kostadin E. Atanasov*, Changxin Liu, Alexander Erban, Joachim Kopka, Jane E. Parker, and Rubén Alcázar

Plant Physiology (2018) 177:1152-1169
Impact Factor (2018): 5.949
Position: Plant Scis 11 out of 212
Quartile: 1

Contribution of listed authors (as stated in the published article): **K.E.A.,*** J.K., J.E.P., and R.A. designed the research; **K.E.A.** and R.A. performed research with contributions from C.L. and A.E.; **K.E.A.**, A.E., J.K., J.E.P., and R.A. analyzed data; R.A. conceived the project and wrote the article with contributions from all authors.

*This article is part of **Kostadin E. Atanasov** PhD Thesis

Chapter 2: High ammonium suppresses NLR-mediated hybrid incompatibilities in *Arabidopsis thaliana* by *NPR1* modulation

Kostadin E. Atanasov* and Rubén Alcázar

Publication status: Submission in preparation. This work is published as an attached chapter in this Thesis.

Contribution of listed authors: **K.E.A** and RA designed the experiments. **K.E.A** performed all experiments and analyzed the data with contribution of R.A. **K.E.A** wrote the chapter under the guidance and contribution of R.A.

Chapter 3: Genome Wide Association Mapping for the Tolerance to the Polyamine Oxidase Inhibitor Guazatine in *Arabidopsis thaliana*

Kostadin E. Atanasov*, Luis Barboza-Baquero, Antonio F. Tiburcio and Rubén Alcázar

Frontiers in Plant Sci (2016) 7:401
Impact Factor (2016): 4.291
Position: Plant Scis, 20 out of 212
Quartile: 1

Contribution of listed authors (as stated in the published article): **K.E.A** performed all the experimental research. L.B performed the GWAS analyses. **K.E.A**, A.T and R.A planned the experiments. R.A analyzed the data and wrote the paper with contributions from all authors.

*This article is part of **Kostadin E. Atanasov** PhD Thesis

Barcelona, 8 d'abril de 2019.

Rubén Alcázar Hernández (Director i Tutor)

Antonio Fernández Tiburcio (Director)

CHAPTER 1

NLR Mutations Suppressing Immune Hybrid Incompatibility and Their Effects on Disease Resistance

NLR Mutations Suppressing Immune Hybrid Incompatibility and Their Effects on Disease Resistance

Kostadin E. Atanasov[1], Changxin[1], Alexander Erban[2], Joachim Kopka[2], Jane E. Parker[3], and Rubén Alcázar[1]

[1]Department of Biology, Healthcare and Environment, Section of Plant Physiology, Faculty of Pharmacy and Food Sciences
Sciences, University of Barcelona, 08028 Barcelona, Spain.
[2]Max Planck Institute for Mol Plant Physiology, 14476 Potsdam, Germany.
[3]Department of Plant-Microbe Interactions, Max Planck Institute for Plant Breeding Research, 50829 Cologne,
Germany.

Published as: Research publication in Plant Physiology. July 2018.

DOI: 10.1104/pp.18.00462

*Supplemental data is included in Annex II (page 157).

SPANISH SUMMARY

La divergencia genética entre poblaciones puede llevar a un aislamiento reproductivo. Las incompatibilidades híbridas (IH) son un ejemplo de eventos puntuales que se dan durante el incipiente proceso de especiación. En organismos, tales como las plantas, las variaciones genéticas en genes de resistencia a patógenos (*R*) son la base genética y molecular de buena parte de las IH descritas. Los descendientes del cruce entre los "*accessions*" de *Arabidopsis thaliana*, Landsberg erecta (L*e*r, Polonia) y Kashmir-2 (Kas-2, Asia Central), muestran un IH con base inmunológica. Concretamente, este caso de incompatibilidad es fruto de la interacción entre el clúster génico en L*e*r, formado por ocho genes *TNL* (*TOLL/INTERLEUKIN1 RECEPTOR-NUCLEOTIDE BINDING-LEU RICH REPEAT*) *RPP1-like* (*RECOGNITION OF PERONOSPORA PARASITICA1-like*; *R1–R8*) y alelos del receptor quinasa *Strubbelig-receptor family* (*SRF3*), presente en "*accessions*" de Asia Central, como Kas-2 o Kondara (Kond). En el presente trabajo, hemos caracterizado múltiples mutaciones en el clúster *RPP1-like* que alteran la incompatibilidad entre L*e*r y Kas-2. Un análisis más detallado de los mutantes supresores, *suppressors of the* L*e*r/Kas-2 *incompatibility* (*sulki*), ha revelado una interacción epistásica dentro del mismo clúster que altera la actividad de los genes que lo conforman. Se han medido los efectos de estas mutaciones en procesos fisiológicos cómo el metabolismo, transcriptoma global, inmunidad basal y resistencia al oomiceto *Hyaloperonospora arabidopsidis* aislado a partir de una población local de *Arabidopsis* de la región polaca de Gorzów Wielkopolski (*Hpa Gw*) de donde L*e*r es originaria. El perfil de expresión génica y rasgos metabólicos identificados para esta IH son dependientes de algunos miembros *RPP1-like*. A la vez, hemos establecido que los mutantes supresores de la IH, *sulki*, no tienen alteración alguna en su resistencia frente a *Hpa Gw*. Mediante el mapeo QTL (*Quantitative Trait of Loci*), tras la inoculación de *Hpa Gw*, se ha puesto el foco sobre un nuevo locus génico, *RPP7*, que estaría relacionado con la resistencia a la infección. En este trabajo proporcionamos más conocimiento sobre la compleja arquitectura intrínseca del clúster *RPP1-like*, las incompatibilidades híbridas con base inmunitaria y la contribución de los genes *R1-R8* a la IH y defensa.

NLR Mutations Suppressing Immune Hybrid Incompatibility and Their Effects on Disease Resistance[1][OPEN]

Kostadin E. Atanasov,[a] Changxin Liu,[a] Alexander Erban,[b] Joachim Kopka,[b] Jane E. Parker,[c] and Rubén Alcázar[a,2]

[a]Department of Biology, Healthcare and Environment, Section of Plant Physiology, Faculty of Pharmacy and Food Sciences, University of Barcelona, 08028 Barcelona, Spain
[b]Max Planck Institute for Molecular Plant Physiology, 14476 Potsdam, Germany
[c]Department of Plant-Microbe Interactions, Max Planck Institute for Plant Breeding Research, 50829 Cologne, Germany

ORCID IDs: 0000-0002-5538-895X (K.E.A.) (K.E.A.); 0000-0003-0723-7812 (C.L.); 0000-0003-1794-588X (A.E.) (A.E.); 0000-0001-9675-4883 (J.K.); 0000-0002-4700-6480 (J.E.P.); 0000-0002-3567-7586 (R.A.)

Genetic divergence between populations can lead to reproductive isolation. Hybrid incompatibilities (HI) represent intermediate points along a continuum toward speciation. In plants, genetic variation in disease resistance (*R*) genes underlies several cases of HI. The progeny of a cross between Arabidopsis (*Arabidopsis thaliana*) accessions Landsberg *erecta* (L*er*, Poland) and Kashmir2 (Kas2, central Asia) exhibits immune-related HI. This incompatibility is due to a genetic interaction between a cluster of eight *TNL (TOLL/INTERLEUKIN1 RECEPTOR-NUCLEOTIDE BINDING-LEU RICH REPEAT) RPP1 (RECOGNITION OF PERONOSPORA PARASITICA1)-like* genes (*R1–R8*) from L*er* and central Asian alleles of a *Strubbelig*-family receptor-like kinase (*SRF3*) from Kas2. In characterizing mutants altered in L*er*/Kas2 HI, we mapped multiple mutations to the *RPP1*-like L*er* locus. Analysis of these *suppressor of Ler/Kas2 incompatibility* (*sulki*) mutants reveals complex, additive and epistatic interactions underlying *RPP1-like* L*er* locus activity. The effects of these mutations were measured on basal defense, global gene expression, primary metabolism, and disease resistance to a local *Hyaloperonospora arabidopsidis* isolate (*Hpa* Gw) collected from Gorzów (Gw), where the Landsberg accession originated. Gene expression sectors and metabolic hallmarks identified for HI are both dependent and independent of *RPP1-like* L*er* members. We establish that mutations suppressing immune-related L*er*/Kas2 HI do not compromise resistance to *Hpa* Gw. QTL mapping analysis of *Hpa* Gw resistance point to *RPP7* as the causal locus. This work provides insight into the complex genetic architecture of the *RPP1-like* L*er* locus and immune-related HI in Arabidopsis and into the contributions of *RPP1-like* genes to HI and defense.

Hybrid vigor is a common phenomenon in plants. Genetic differentiation between individuals of the same species at specific loci can also lead to a dramatic reduction of hybrid fitness in the F1 or later generations, due to negative epistasis. Certain interacting alleles are not deleterious in their respective backgrounds, but they can become lethal when combined in the same hybrid genome. Such negative genetic interactions might constitute an early stage of species isolation (Coyne, 1992; Coyne and Orr, 2004). Plant hybrid necrosis or hybrid weakness has been documented in crops and model species (Bomblies and Weigel, 2007). In the last decade, identification of genetic determinants of some hybrid incompatibilities (HIs) revealed that immune gene variability could underlie this phenomenon. Immune-related incompatible hybrids are temperature dependent and exhibit reduced growth, deregulated cell death, and sterility (Bomblies et al., 2007; Alcázar et al., 2009; Jeuken et al., 2009; Yamamoto et al., 2010; Chen et al., 2014). The metabolic costs of maintaining a constitutively active immune system might contribute to reduced fitness. In many cases, mapping of causal genes identified at least one polymorphic *Nucleotide-binding/Leu-rich-repeat* (*NLR*) locus encoding intracellular pathogen recognition (NLR) receptors (Alcázar et al., 2012; Chae et al., 2014). *NLR*-interacting loci include other disease *Resistance* (*R*) genes or genes with diverse functions (Bomblies and Weigel, 2007; Alcázar et al., 2009; Yamamoto et al., 2010; Chae et al., 2014). In Arabidopsis (*Arabidopsis thaliana*), the *DANGEROUS MIX2* (*DM2*) locus mapping to a

[1]This work was supported by the Ramón y Cajal Program (RYC-2011-07847) of the Ministerio de Ciencia e Innovación (Spain), by grants from the Programa Estatal de Fomento de la Investigación Científica y Técnica de Excelencia (Ministerio de Economía y Competitividad, Spain; BFU2013-41337-P and BFU2017-87742-R) cofinanced with FEDER (Fondo Europeo de Desarrollo Regional), and by a Marie Curie Career Integration grant (DISEASENVIRON, PCIG10-GA-2011-303568) of the European Union. K.E.A., C.L., and R.A. are members of the Grup de Recerca Consolidat 2017 SGR-604 of the Generalitat de Catalunya. K.E.A. acknowledges support from the Subprograma Estatal de Formación del Ministerio de Economía y Competitividad (BES-2014-068041). R.A. and J.E.P. acknowledge support of Deutsche Forschungsgemeinschaft (CRC 680) for part of this work.

[2]Address correspondence to ralcazar@ub.edu.

The author responsible for distribution of materials integral to the findings presented in this article in accordance with the policy described in the Instructions for Authors (www.plantphysiol.org) is: Rubén Alcázar (ralcazar@ub.edu).

K.E.A., J.K., J.E.P., and R.A. designed the research; K.E.A. and R.A. performed research with contributions from C.L. and A.E.; K.E.A., A.E., J.K., J.E.P., and R.A. analyzed data; R.A. conceived the project and wrote the article with contributions from all authors.

[OPEN]Articles can be viewed without a subscription.
www.plantphysiol.org/cgi/doi/10.1104/pp.18.00462

polymorphic *RPP1* (*RECOGNITION OF PERONOSPORA PARASITICA1*)-*like* gene cluster underlies at least five documented cases of immune-related HIs between accessions Uk-1 (*DM2*, *RPP1-like*)/Uk-3 (*DANGEROUS MIX1*, *SUPPRESSOR OF SALICYLIC ACID INSENSITIVE4*; Bomblies et al., 2007), Landsberg *erecta* (L*er*) (DM2, *RPP1-like*)/Kas2 (*STRUBBELIG RECEPTOR FAMILY3*; Alcázar et al., 2009), Bla-1 (*DM2*, *RPP1-like*)/Hh-0 (*DANGEROUS MIX3*, prolyl aminopeptidase *At3g61540*), Dog-4 (*DM2*, *RPP1-like*)/ICE163 (*DANGEROUS MIX5*), and TueWa1-2 (*RPP1-like*)/ICE163 (*DANGEROUS MIX4*, overlapping with *RPP8*; Chae et al., 2014). Therefore, the *RPP1-like* locus is a hotspot for temperature-dependent immune-related HI in Arabidopsis (Alcázar et al., 2009; Chae et al., 2014; Stuttmann et al., 2016).

Immune-related HIs have also been reported in rice (*Oryza sativa*), lettuce (*Lactuca sativa*), tomato (*Solanum lycopersicum*), the genus *Capsella*, and other species. An interspecific hybrid weakness in rice involves two dominant loci and three genes (Chen et al., 2014). One locus (*HYBRID WEAKNESS I1*) contains two *LRR RECEPTOR-LIKE KINASE* genes, both required for incompatibility with the *HYBRID WEAKNESS I2* locus, which maps to a *SUBTILISIN-LIKE PROTEASE* gene (Chen et al., 2014). Also in rice, a two-way recessive interaction causing hybrid breakdown involves the *CASEIN KINASE I* gene and an *NLR* cluster (Yamamoto et al., 2010). In lettuce, temperature-dependent hybrid necrosis in an interspecific cross involves two loci, one of them mapping to *RPM1 INTERACTING PROTEIN4*, encoding an acylated plasma membrane-associated protein that is a negative regulator of basal antimicrobial defense targeted by different *Pseudomonas syringae* effectors (Jeuken et al., 2009; Khan et al., 2016). In tomato, HI was observed in an interspecific cross involving allelic variants at *Rcr3* and *Cf2* loci, the latter conferring resistance to the fungus *Cladosporium fulvum* (Krüger et al., 2002). In the genus *Capsella*, HI has been described between *Capsella grandiflora* and *Capsella rubella* involving a two-way epistatic interaction between *NPR1* and *RPP5* loci (Sicard et al., 2015). The Dobzhansky-Muller model on genetic incompatibilities is agnostic on whether causal genes diverge into incompatible alleles by drift or selection (Coyne and Orr, 2004). The frequency of immune receptor genes underlying HI is likely a consequence of their rapid evolution in response to pathogen infection pressure (Chae et al., 2014).

The majority of plant disease *R* genes encode NLR proteins. These are classified into two main groups: TNLs (TIR-NLRs) and CNLs (CC-NLRs), based on the presence of a Toll/IL-1 receptor (TIR) or a coiled-coil CC domain at their N terminus (Sukarta et al., 2016). *R* genes often reside in clusters and exhibit high polymorphism and copy number variation, through illegitimate recombination, duplication, and gene conversion events (Bakker et al., 2006; Hurwitz et al., 2010; McHale et al., 2012; Muñoz-Amatriaín et al., 2013). Indeed, together with *RECEPTOR-LIKE KINASE* genes, *NLRs* exhibit signatures of rapid expansion and diversification (Cao et al., 2011; Xu et al., 2011). The *RPP1-like* locus contains a variable number of *TNL* genes in different Arabidopsis accessions, from two in Col-0 to four in Ws2 (Botella et al., 1998), five to six in Zdr1 and Est1 (Goritschnig et al., 2016) and eight in L*er*, Uk-1, and Bla-1 (Alcázar et al., 2009; Chae et al., 2014). *RPP* genes recognize the obligate biotrophic oomycete pathogen, *Hyaloperonospora arabidopsidis* (*Hpa*, formerly *Peronospora parasitica*), which causes downy mildew disease (Botella et al., 1998; Coates and Beynon, 2010). As a naturally coevolving host-pathogen system, different *Hpa* isolates have been identified that elicit accession-specific resistance responses due to the recognition of different avirulence gene products/effectors (*Arabidopsis thaliana* Recognized [ATR]) or effector variants. The *RPP1* resistance locus in Ws2 and Nd1 contains *RPP1* genes that exhibit partially overlapping recognition of *Hpa* isolates (Botella et al., 1998; Rehmany et al., 2005). Using an F2 mapping population derived from a cross between *Hpa* isolates Emoy2 (avirulent) and Maks9 (virulent), $ATR1^{NdWsB}$ was found to be recognized by RPP1-NdA (Rehmany et al., 2005). Genetic variation at *ATR1* conditions *Hpa* recognition by different *RPP1* genes, e.g. *RPP1*-WsB, *RPP1*-NdA, *RPP1*-EstA, and *RPP1*-ZdrA (Rehmany et al., 2005; Sohn et al., 2007; Goritschnig et al., 2016). RPP1 receptors likely also perceive other *ATR* gene products (Botella et al., 1998; Rehmany et al., 2005). An intriguing question is whether *RPP1* genes involved in immune-related HIs provide disease resistance to locally adapted *Hpa* isolates or their activities in pathogen resistance and incompatibility can be separated.

Here, we determine the contribution of different *RPP1-like* genes to L*er*/Kas2 HI and resistance to a local *Hpa* isolate collected in Gorzów Wielkopolski (Poland), where Landsberg was collected in 1939. In this population, 30% of genetically differentiated Gorzów (Gw) individuals contain a conserved *RPP1-like* L*er* haplotype. This derived haplotype increased in frequency and has been maintained locally for many generations (Alcázar et al., 2014). Through ethyl methanesulfonate (EMS) mutagenesis, we identify multiple *suppressors of Ler/Kas2 incompatibility* (*sulki*) mutants, which map to *RPP1-like* L*er R3* and *R8* genes. Generation of CRISPR/Cas9 *RPP1-like* L*er R2*, *R3*, *R4*, and *R8* loss-of-function mutants in a L*er*/Kas2 near-isogenic line (NIL) background reveals that additive and epistatic interactions between *RPP1-like* gene members contribute to immune-related HI. Global gene expression and metabolite profiling of L*er*/Kas2 incompatible hybrids and *sulki* suppressors identify metabolic and expression hallmarks for immune-related HIs, which are *RPP1-like R8* dependent or independent. Through QTL mapping, we find that resistance to the local *Hpa* isolate from Gorzów (denoted here *Hpa* Gw) in L*er* is not mediated by genes at the *RPP1-like* locus but maps to a region containing the previously defined *RPP7* CNL *Resistance* gene (McDowell et al., 2000). Resistance conferred by *RPP7* to *Hpa* Gw is genetically independent of

salicylic acid (SA) and *EDS1*. Because certain *RPP1-like* proteins recognize allelic variants of the *Hpa* ATR1 effector, we tested whether RPP1-like L*er* proteins could induce host cell death, reflecting a hypersensitive response (HR) when transiently expressed with *Hpa* Gw ATR1 in tobacco (*Nicotiana tabacum*). Coexpression of *RPP1-like* L*er* R2, R3, R4, or R8 protein with *Hpa* Gw ATR1δ51 does not trigger cell death in tobacco. Our results show that the *RPP1-like*-incompatible haplotype does not provide disease resistance to a local *Hpa* Gw isolate. We provide evidence for complex genetic interactions underlying the *RPP1-like* L*er* locus HI with Kas2. Our results also help differentiate *RPP1-like* gene actions in incompatibility and defense.

RESULTS

Identification of *RPP1-like* L*er* Suppressors of Ler/Kas2 Incompatibility

An incompatible L*er*/Kas2 NIL that contains a L*er* introgression spanning the *RPP1-like* locus in an otherwise Kas2 genetic background (Alcázar et al., 2009) was used for the isolation of *suppressor of Ler/Kas2 incompatibility* (*sulki*) mutants. Mutagenized L*er*/Kas2 NIL plants were generated by treating L*er*/Kas2 NIL seeds with EMS, and 25,000 M1 individuals were propagated in 200 pools. Approximately 1,000 M2 generation plants from each pool were grown to identify suppressors of HI at 14°C to 16°C. Twenty dominant *sulki* mutants were isolated, which suppressed dwarfism at 14°C to 16°C, indicative of a loss or amelioration of L*er*/Kas2 HI. The different *sulki* mutants were backcrossed at least five times with the parental L*er*/Kas2 NIL. The genomes of *sulki* BC_5F_1 and L*er*/Kas2 NIL were then sequenced by next-generation sequencing, and unique SNPs were identified for each mutant compared with the L*er*/Kas2 NIL.

DNA sequence analysis identified eleven *sulki* mutants carrying single mutations within the *RPP1-like* L*er* locus, which were further confirmed by SANGER sequencing (Fig. 1A). Ten intragenic mutations (*sulki1-1* to *sulki1-10*) were dominant, mapping to different domains of *RPP1-like* L*er R8*, and fully suppressed both dwarfism and cell death at low temperature (14°C–16°C; Figs. 1A and 2; Supplemental Fig. S1; Supplemental Table S1). *RPP1-like* L*er R8* is a homolog of *DANGEROUS MIX 2h* (*DM2h*) in Arabidopsis accessions Uk-1 and Bla-1 (Chae et al., 2014). In Col-0, it is homologous to *At3g44670* (Alcázar et al., 2014), although with a high level of polymorphism especially in the LRR domain (Chae et al., 2014). A recessive mutation (*sulki2-1*) mapped to the TIR domain of *RPP1-like* L*er R3* (T78I), which partially suppressed dwarfism and cell death (Fig. 2; Supplemental Fig. S1; Supplemental Table S1). In all cases, except for one 8-nucleotide deletion (*sulki1-7*), only G/C to A/T transition mutations were observed, as expected for mutations generated by EMS treatment (Fig. 1A).

Distribution of *sulki* Mutations within TIR, NB, and LRR Domains

In *RPP1-like* L*er R8*, five and three suppressor mutations were found in the NB and LRR domains, respectively (Fig. 1B), consistent with the importance of these domains in TNL function (Meyers et al., 2003). Amino acid changes were found within the conserved RNBS-C (P428S, *sulki1-2*) and GLPL (P466L, *sulki1-3*) motifs. Two additional amino acid substitutions (G500E in *sulki1-5* and G509A in *sulki1-6*) and one stop codon (W484*, *sulki1-4*) were in a stretch of 40 amino acids that connects GLPL and RNBS-D motifs. The presence of three close mutations leading to the same suppressive phenotype suggests that the GLPL-to-RNBS-D region is crucial for *RPP1-like* L*er* R8 function. Three additional amino acid changes were found in the LRR domain of *RPP1-like* L*er R8*, in the junction between LRR2 and LRR3 (S758F, *sulki1-8*), within LRR5 (R821H, *sulki1-9*) and LRR8 (G877E, *sulki1-10*) motifs. A small 8-nucleotide deletion was identified in the splice donor site of *sulki1-7*, preceding the LRR exon. In the TIR domain of *RPP1-like* L*er R8*, one G202E nonsynonymous substitution was detected between TIR3 and TIR4 in *sulki1-1* (Fig. 1B). Most suppressive nonsynonymous substitutions were found in invariant or highly conserved NLR residues, except for Gly-509, which appears to be specific to *RPP1-like* L*er* R8 homologs *At3g44670* $^{Col-0}$ and *DM2h* $^{Bla-1}$ (Supplemental Fig. S2).

All together, we identified multiple independent mutations within the NB or LRR domains of *RPP1-like* L*er R8* and single mutations in the TIR domains of *RPP1-like* L*er R8* and *R3* genes suppressing L*er*/Kas2 NIL immune-related HI. These data strongly reinforce previous studies identifying *RPP1-like* L*er R3* and *R8* as genes contributing to L*er*/Kas2 HI (Alcázar et al., 2014; Stuttmann et al., 2016). We concluded that single point mutations within the *RPP1-like* locus are sufficient for full (*sulki1*, *RPP1-like* L*er R8*) or partial (*sulki2*, *RPP1-like* L*er R3*) suppression of L*er*/Kas2 HIs.

Expression of SA-Responsive and Oxidative Stress Marker Genes in *sulki1* and *sulki2*

L*er*/Kas2 HI is associated with constitutive activation of TNL receptor-triggered defense programs, including high expression of *PR1*, *EDS1*, *GST1*, and *RPP1-like* L*er R3* at 14°C to 16°C (Alcázar et al., 2009, 2014). We analyzed transcripts of these and other *RPP1-like* L*er* genes (*R2*, *R4*, and *R8*) to determine the defense status of *sulki1* and *sulki2*. Expression of *PR1*, *EDS1*, and *GST1* was much lower in *sulki1* and *sulki2-1* mutants compared to the L*er*/Kas2 NIL but similar or slightly lower than L*er* or Kas2 (Fig. 3). These results suggest that constitutive activation of defenses in the L*er*/Kas2 NIL at 14°C to 16°C is suppressed in *sulki1* and *sulki2*. The expression of *RPP1-like* L*er R3* and *R8* was also significantly lower in *sulki1* and *sulki2* than in L*er*/Kas2 NIL (Fig. 3). We hypothesized that SA, which accumulates in L*er*/Kas2 NIL (Alcázar et al.,

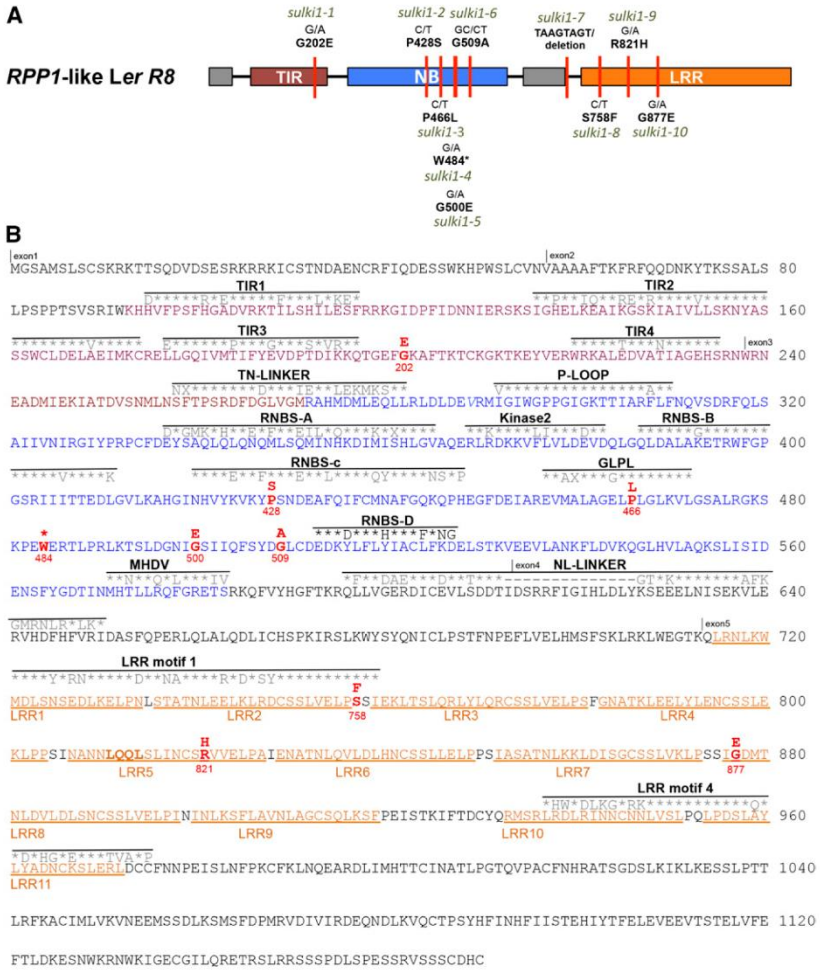

Figure 1. *sulki1* mutations mapping to *RPP1-like R8* L*er*. A, Schematic representation of nonsynonymous substitutions identified in *sulki1* mutants. Exon/intron organization and Toll-IL receptor (TIR), nucleotide binding (NB), and Leu-rich repeat (LRR) domains are shown. B, Detailed representation of *RPP1-like R8* L*er* amino acid sequence, conserved motifs (Meyers et al., 2003), and position of *sulki1* mutations.

2009), causes up-regulation of some *RPP1-like* genes. Indeed, we found that *RPP1-like* L*er R3* and *R8*, but not *R2* or *R4*, expression was induced in L*er* by SA or benzo (1,2,3) thiadiazole-7-carbothioic acid *S*-methyl ester application at 8 to 24 h (Supplemental Fig. S3). Therefore, we concluded that there is SA-positive feedback regulation of *RPP1-like* L*er* genes *R3* and *R8* involved in immune-related HI.

Allelism and Complementation Tests of *sulki1 and sulki2* Mutants

To confirm that the causal mutations in *sulki1* map to *RPP1-like* L*er R8*, we performed allelism tests with *RPP1-like* L*er R8* loss-of-function mutants generated by CRISPR/Cas9 in the L*er*/Kas2 NIL background (referred to as Cas9-*r8*; Supplemental Fig. S4). Cas9-*r8* mutants that contained early stop codons in the TIR domain of *RPP1-like* L*er R8* suppressed dwarfism and cell death at 14°C to 16°C in a dominant manner, consistent with the involvement of *RPP1-like* L*er R8* in the incompatibility with Kas2 (Fig. 4A; Supplemental Fig. S5; Supplemental Table S1). To confirm that *sulki1* mutations were allelic to Cas9-*r8*, homozygous *sulki1* and Cas9-*r8-1* (after removal of the *Cas9* transgene) were crossed, and F2 populations were obtained by selfing. The F2 populations were screened for the occurrence of incompatible phenotypes at 14°C to 16°C (Supplemental Table S1). The absence of segregation for

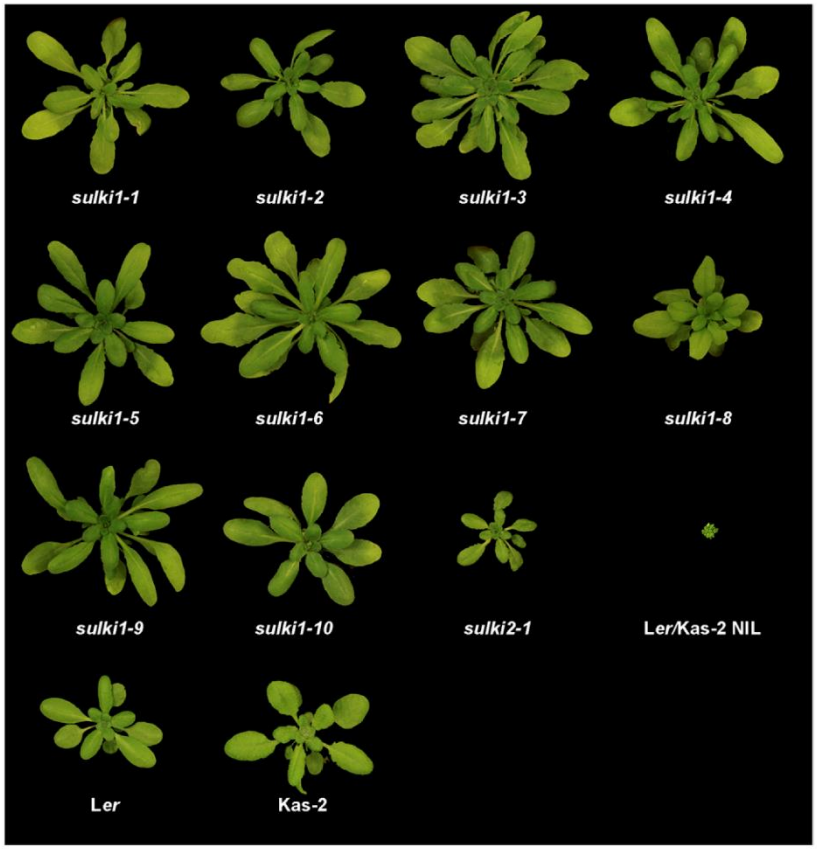

Figure 2. Composite image of *sulki* phenotypes. Five-week-old *sulki1*, *sulki2*, and Ler/Kas2 NIL grown at 14°C to 16°C under 12-h-light/12-h-dark cycles and light intensity of 120 µmol m^{-2} s^{-1}.

incompatibility confirmed that *sulki1* mutants are allelic to Cas9-*r8*.

To confirm the causality of the *sulki2-1* mutation mapping to *RPP1-like* L*er R3*, we transformed *sulki2-1* plants with a genomic construct of *RPP1-like* L*er R3* (Alcázar et al., 2014). Complemented lines, which also were nonoverexpressors of the *RPP1-like R3* L*er* transgene, reconstituted the incompatible phenotype at 14°C to 16°C (Supplemental Fig. S6). These results are in agreement with a gene dosage effect underlying the recessive nature of the *RPP1-like* L*er* locus. In summary, we confirmed that mutations underlying *sulki1* and *sulki2*-1 suppressive phenotypes map to *RPP1-like* L*er R8* and *R3* genes, respectively.

Generation of *RPP1-Like* L*er* Loss-of-Function Mutants in L*er*/Kas2 NIL by CRISPR/Cas9

We next analyzed the contribution of other *RPP1-like* L*er* genes to L*er*/Kas2 immune-related HI by isolating CRISPR/Cas9-induced mutations in the L*er*/Kas2 NIL. Based on mRNA-seq data (see below), *RPP1-like* L*er R2*, *R3*, *R4*, and *R8* genes within the *RPP1-like* L*er* locus are predicted to encode full-length TNL proteins. *RPP1-like* L*er R1*, *R5*, *R6*, or *R7* genes contain stop codons in their TIR or NB domains. Therefore, we focused on *RPP1-like* L*er R2*, *R3*, *R4*, and *R8* to introduce frameshift mutations by CRISPR/Cas9 in TIR or NB domains. For each TNL-encoding gene, we designed protospacers next to unique NGG motifs (protospacer adjacent motif [PAM]; Fauser et al., 2014; Supplemental Fig. S4). Indel mutations resulting in early stop codons were identified in transgenic lines expressing specific *RPP1-like* L*er R2*, *R3*, *R4*, and *R8* RNA-guided endonucleases (Supplemental Fig. S4). The different mutants were then crossed with L*er*/Kas2 NIL and Cas9-free homozygous mutants isolated from the F2 progeny. To confirm the absence of mutations in other genes within the *RPP1-like* cluster, the eight *RPP1-like* L*er* genes were sequenced in the different CRISPR/Cas9 mutants (Alcázar et al., 2014).

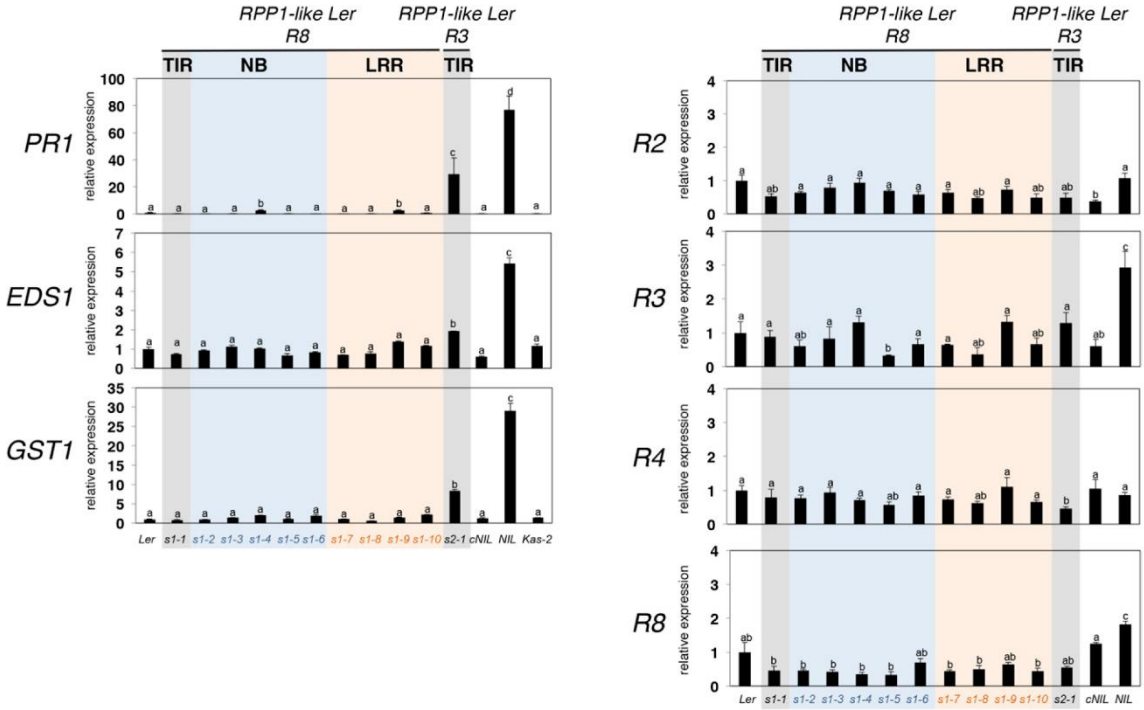

Figure 3. Expression of SA and oxidative stress marker genes. Quantitative reverse transcription PCR (RT-qPCR) analyses of *PR1*, *EDS1*, *GST1*, *RPP1-like* L*er* *R2*, *R3*, *R4*, and *R8* genes in *sulki1-1* (*s1-1*) to *sulki 1-10* (*s1-10*), *sulki2-1* (*s2-1*), Ler, Kas2, Ler/Kas2 NIL, and NIL complemented with *SRF3* Ler (cNIL; Alcázar et al., 2010). Values are relative to L*er* and are the mean of three biological replicates, each with three technical replicates. Letters indicate values that are significantly different according to Student-Newman-Keuls test at $P < 0.05$. Error bars indicate SD.

Loss-of-function mutations at *RPP1-like* L*er* *R2* (Cas9-*r2-1* and *r2-2*), *R3* (Cas9-*r3-1* and *r3-2*), and *R4* (Cas9-*r4-1* and *r4-2*) in the L*er*/Kas2 NIL were recessive and resulted in partial suppression of dwarfism and cell death (Fig. 4A; Supplemental Fig. S5; Supplemental Table S1). Lower expression of *PR1*, *EDS1*, *GST1*, and *RPP1-like* L*er* *R3* in 5-week-old Cas9 lines grown at 14°C to 16°C was consistent with suppression of the autoimmune response (Fig. 4B). Notably, cell death (Supplemental Fig. S5C) and *PR1*, *EDS1*, *GST1*, and *RPP1-like* L*er* *R3* expression (Supplemental Fig. S7) increased over time in Cas9-*r2*, *-r3* and *-r4* lines, although to a lower extent than in the L*er*/Kas2 NIL. Mutations in *RPP1-like* L*er* *R8* alone fully suppress incompatibility, regardless of other incompatible genes contributing to HI being present (*RPP1-like* L*er* *R2*, *R3*, and *R4*). Therefore, incompatibility is not simply an additive effect of various *RPP1-like* L*er* genes with *R8* having stronger effects than the others. These results indicate that *RPP1-like* L*er* *R2*, *R3*, and *R4* genes contribute additively to L*er*/Kas2 HI, whereas *RPP1-like* L*er* *R8* is epistatic to other *RPP1-like* L*er* members. Thus, additive and epistatic interactions underlie the complex nature of *RPP1-like* L*er* cluster incompatibility with Kas2. The data are consistent with the involvement of two or more *RPP1-like* L*er* genes in HI between L*er* and Kas2 (Alcázar et al., 2014; Stuttmann et al., 2016).

Bacterial Pathogen Resistance Phenotypes in *sulki1*, *sulki2*, and Cas9 *RPP1-like* L*er* Mutants

We determined the effect of *sulki1*, *sulki2*, Cas9-*r2*, Cas9-*r3*, Cas9-*r4*, and Cas9-*r8* mutations on basal disease resistance by measuring the growth of virulent *P. syringae* pv. *tomato* strain DC3000 (*Pst* DC3000) and the type III secretion-disabled *Pst hrcC* mutant, which fails to deliver virulence factors (effectors) and induces only PAMP-triggered immunity (Yuan and He, 1996). At 14°C to 16°C and 20°C to 22°C, the L*er*/Kas2 NIL exhibited higher basal resistance to *Pst* DC3000 than all other tested genotypes (Fig. 5). At both temperatures, *sulki1* and Cas9-*r8* mutations suppressed L*er*/Kas2 basal resistance to similar levels as the parents (L*er* or Kas2). By contrast, *sulki2-1*, Cas9-*r2*, Cas9-*r3*, and Cas9-*r4* mutations exhibited partial suppression of basal resistance at 14°C to 16°C but full suppression at 20°C to 22°C (similar to L*er* and Kas2). These results show that *RPP1-like* L*er* *R8* mutations in *sulki1*

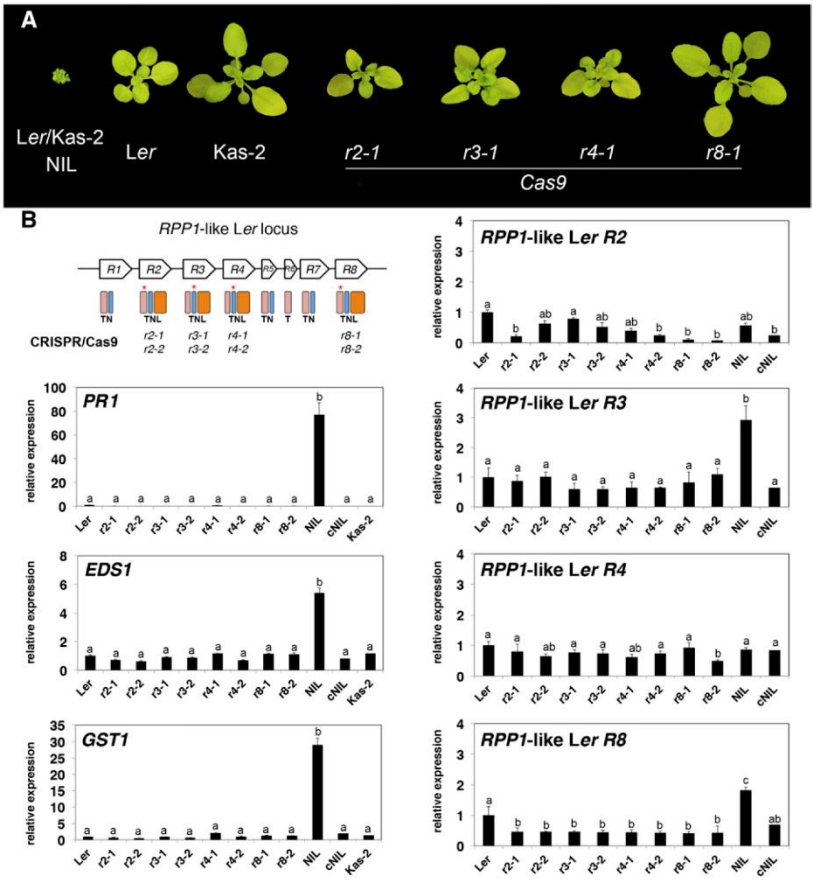

Figure 4. Growth phenotypes and expression analyses of Cas9 *RPP1*-like L*er* mutants. A, Composite image of 5-week-old Cas9-*r2-1*, Cas9-*r3-1*, Cas9-*r4-1*, Cas9-*r8-1* mutants in the L*er*/Kas2 NIL background, L*er*/Kas2 NIL, and parental lines (L*er* and Kas2) grown at 14°C to16°C. The position of stop codons in TIR (T) or NB (N) domains of *RPP1-like* genes is marked with an asterisk. B, Gene expression analyses of *PR1*, *EDS1*, *GST1*, *RPP1-like* L*er R2*, *R3*, *R4*, and *R8* in Cas9 *r2-1*, *r2-2*, *r3-1*, *r3-2*, *r4-1*, *r4-2*, *r8-1*, and *r8-2* mutant alleles L*er*, Kas2, L*er*/Kas2 NIL, and cNIL plants grown at 14°C to 16°C during 5 weeks. Analyses were performed as described in Figure 3.

and Cas9-*r8* suppress L*er*/Kas2 NIL defenses at both temperatures. A suppressive effect was observed in Cas9-*r2*, Cas9-*r3*, and Cas9-*r4* mutants only at 20°C to 22°C, consistent with their partial suppression of immune-related HI. No differences were detected between lines in response to *Pst hrcC* at either temperature (Fig. 5). Notably, mutation in *RPP1-like* L*er R8* did not lead to full susceptibility of the *eds1-2* mutant at both temperatures (Fig. 5). From these results, we concluded that suppression of *RPP1-like* L*er R8* function does not lead to a general dampening of basal defenses against *Pst* bacteria.

Gene Expression Analyses

To determine the effect of *sulki1* mutations suppressing immune-related HI on global expression profiles, we performed RNA-seq analyses in *sulki1-8*, the L*er*/Kas2 NIL, and Kas2 plants grown at 14°C to 16°C. A total of 9,564 genes exhibited significant expression differences (fold change ≥2; *P* value and false discovery rate ≤ 0.05) in the comparison between Kas2 and L*er*/Kas2 NIL (Fig. 6; Supplemental Tables 2-1 and 2-2). Of these, 5,882 genes (61.5%) were common between *sulki1-8* and L*er*/Kas2 NIL. Gene Ontology analysis of these common genes revealed an enrichment of stress-related terms (Supplemental Table S2-2). These genes represent transcriptional responses associated with incompatibility, which are suppressed in *sulki1-8*. However, 3,682 other genes were still differentially expressed in the comparison between Kas2 and L*er*/Kas2 NIL. These expression changes might be due to differences in the genetic background between Kas2 and the L*er*/Kas2 NIL not associated with incompatibility

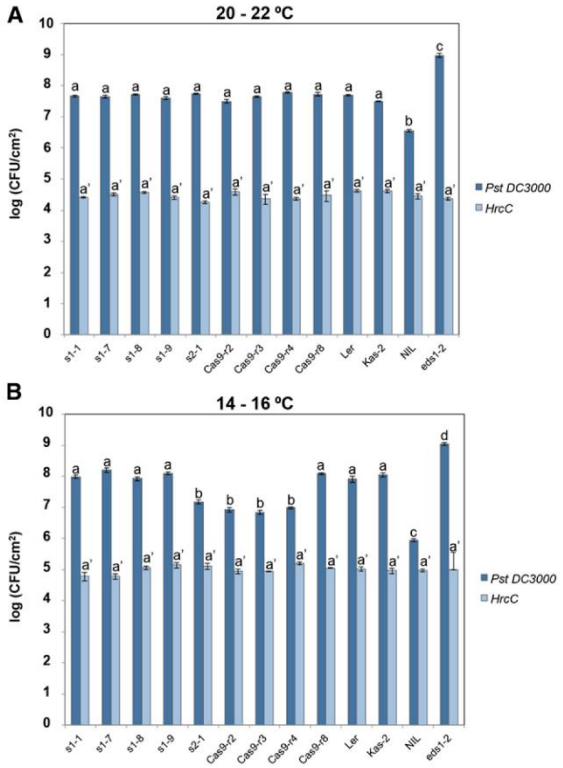

Figure 5. Growth of *Pst* DC3000 and *hrcC* mutant, 3 d after spray inoculation of *sulki1-1* (*s1-1*), *sulki1-7* (*s1-7*), *sulki1-8* (*s1-8*), *sulki1-9* (*s1-9*), *sulki2-1* (*s2-1*), Cas9- *r2-1*, *r3-1*, *r4-1*, and *r8-1* mutants in the L*er*/Kas2 NIL background, Ler, Kas2, L*er*/Kas2 NIL, and *eds1-2* L*er* plants grown at 20°C to 22°C (A) or 14°C to 16°C (B). Different letters indicate significant differences ($P < 0.01$) in a Student-Newman-Keuls test. Error bars indicate SD.

(Supplemental Table S2-1). Gene Ontology analysis in this subset of genes identified an enrichment of nitrogen metabolism-related terms (Supplemental Table S2-1). Finally, RNA-seq analysis identified 622 other genes differentially expressed in *sulki1-8* versus L*er*/Kas2 NIL that did not show significant expression differences in Kas2 versus L*er*/Kas2 NIL. These *sulki1-8*-specific genes were related to oxidation-reduction based on Gene Ontology (Supplemental Table S2-3).

Global Metabolite Profiling

We determined the effects of *sulki1* mutations on primary metabolism through global metabolite profiling by gas chromatography/mass spectrometry (GC/MS) in L*er*/Kas2 NIL, *sulki1* (*sulki1-1*, *sulki1-7*, *sulki1-8*, and *sulki1-9*) and the parents (L*er* and Kas2) at 14°C to 16°C. The metabolomics analysis identified 57 metabolites in the analyzed samples, 36 of which were consistently detected in all genotypes and used for principal component analysis (PCA; Fig. 7A). The nature of 23 of these 36 metabolites was known and annotated according to the MPIMP-Golm inventory list (Kopka et al., 2005). Among the identified metabolites, we detected amino acids, polyhydroxy acids, sugars, and TCA cycle intermediates (Supplemental Table S3). In the PCA analysis, PC1 explained 50.3% of the total variance and differentiated between the incompatible L*er*/Kas2 NIL and other genotypes. PC1 indicated that the *sulki1* mutations cause a reversal of a large part of the altered primary metabolome in L*er*/Kas2 NIL to L*er* or Kas2 parent levels. This metabolic reversal was consistent with suppression of the dwarf phenotype (Fig. 2), the absence of cell death at low temperature (Supplemental Fig. S1B), and deactivation of transcriptional defense responses (Fig. 3) in the *sulki* mutants. Conversely, PC2 (21.9% of the total variance) revealed that some metabolic differences remained between *sulki1* mutants or L*er*/Kas2 NIL and the parents (Fig. 7A; Supplemental Table S4).

Hierarchical cluster analysis (HCA) with Pearson's correlation and average linkage of metabolites and genotypes identified metabolic differences between the strongly deviating L*er*/Kas2 NIL, the parents, and the *sulki1* mutants (Fig. 7B). The heat map representation indicated a large cluster of metabolites that differentially accumulated in L*er*/Kas2 NIL (Fig. 7B). Compared with L*er* and Kas2, the incompatible L*er*/Kas2 NIL accumulated amino acids, such as Gln/pyro-Glu, Asp, Thr, or Ala, lipid-related phosphate, glycerol, ethanolamine, carbohydrate metabolism related glyceric acid, Glc-6P, and Suc (Fig. 7C). The levels of ascorbate, a substrate of the glutathione-ascorbate cycle for hydrogen peroxide detoxification, were much lower in L*er*/Kas2 NIL than in the isogenic Kas2, consistent with the occurrence of oxidative stress induced by HI. On the other hand, dehydroascorbate levels were similar in the two genotypes. These metabolic changes appear to be associated with HI, specifically with growth reduction in combination with metabolic recycling caused by the increased frequency of cell death in L*er*/Kas2 NIL leaf tissue.

As expected, most metabolic reprogramming associated with HI was reverted in *sulki1* mutants to Kas2 levels, e.g. ascorbate, Suc, phosphate, glycerol, Asp, Gln/pyro-Glu, and Thr (Fig. 7C). However, *sulki1* mutants exhibited metabolic changes that differed from L*er*/Kas2 NIL, L*er*, or Kas2 (Fig. 7C). These changes in the *sulki1* mutants might be linked to *RPP1-like* L*er R8*-independent transcriptional defense activation (Fig. 6). Levels of Glu, Asp, Thr, Ala, and dehydroascorbate were lower than in the parents. In parallel, Glc and Fru levels were consistently higher in *sulki1-1*, *sulki1-7*, *sulki1-8*, and *sulki1-9* compared to the parents L*er*, Kas2, and the incompatible L*er*/Kas2 NIL. However, such differences were not observed in the levels of Suc or Glc-6P (Fig. 7C). Quantification of starch at the end of the day (light) and before dawn (dark) in the above genotypes indicated the lower capacity of L*er*/Kas2 NIL to accumulate starch during the day, although its

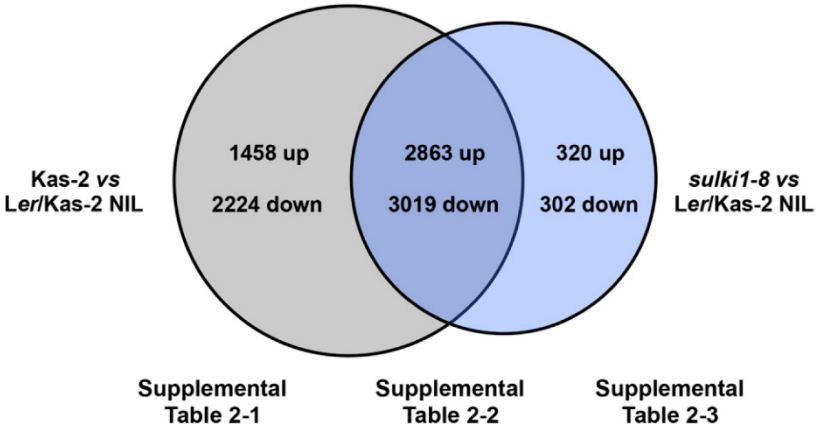

Figure 6. Venn diagram of genes differentially expressed in the comparisons between (Kas2 versus L*er*/Kas2 NIL) and (*sulki1-8* versus L*er*/Kas2 NIL). Lists of genes and Gene Ontology analyses are included in Supplemental Tables S2-1 to S2-3.

levels were not depleted at dawn (Supplemental Fig. S8). Interestingly, the L*er*/Kas2 NIL also exhibited higher apoplastic invertase activity than L*er*, Kas2, or *sulki1*, whereas vacuolar invertase was barely affected (Supplemental Fig. S9). These results can be explained by the suggested role of cell wall invertase in plant defense (Tauzin and Giardina, 2014). The absence of Glc or Fru accumulation in the L*er*/Kas2 NIL, despite the presence of high apoplastic invertase activity, suggests the use of carbohydrates in the biosynthesis of secondary metabolites involved in defense or cell wall strengthening. These demands might contribute to the metabolic costs of diverting resources away from growth in the L*er*/Kas2 NIL.

All together, global metabolite profiling confirmed a physiological reversal of the L*er*/Kas2 HI metabolic phenotype in *sulki1*. It also reinforced *RPP1-like* L*er R8*-independent responses at a metabolic level that were indicated by transcriptome profiling (Fig. 6). We concluded that the L*er*/Kas2-incompatible hybrids are growth inhibited, but that this inhibition is likely not due to limited C, N, or P resources.

Characterization of a Pathogenic *Hpa* Isolate in the Arabidopsis Gorzów Population

Previously, we collected a population of L*er* relatives (Gw) in Gorzów Wielkopolski (Poland), in which 30% of individuals carried a conserved *RPP1-like* L*er* haplotype (Alcázar et al., 2014). In 2014, we revisited the population site and isolated *Hpa* naturally infecting Gw plants, for which a basic population structure was already established (Alcázar et al., 2014). *Hpa* was found sporulating on cauline leaves of the susceptible genotype Gw-16. We refer to this local oomycete as *Hpa* Gw, which was propagated as a mass conidiospore culture from a single plant. The *Hpa ATR1* gene, encoding an effector recognized by certain *RPP1-like* TNL receptors, was used to establish a phylogenetic relationship between *Hpa* Gw and other known *Hpa* isolates. Sequencing of *ATR1* from *Hpa* Gw did not identify segregating polymorphisms within this population, which would be indicative of mixed *Hpa* populations. *Hpa* Gw was found to be more related to *Hpa* isolate Cala2 and Emwa1 than other *Hpa* isolates (Supplemental Fig. S10).

Examination of *Hpa* Gw disease resistance in 40 genetically different Arabidopsis Gw lines identified seven genotypes (17.5%) that were susceptible to *Hpa* Gw (e.g. Gw-16 in Supplemental Fig. S11; Supplemental Table S5). The remaining genotypes, as well as L*er*, Col-0, Kas2, L*er*/Kas2 NIL, and cNIL (Alcázar et al., 2010) exhibited a HR indicative of resistance to *Hpa* Gw infection and consistent with host *RPP*-mediated pathogen recognition (Supplemental Fig. S11). T-DNA insertion mutants of *RPP1* and *RPP1-like* genes in Col-0 *At3g44400* (N632237 and N518157), *At3g44480* (N599581 and N655327), *At3g44630* (N644159 and N658450), and *At3g44670* (N529707 and N477722) did not support the growth of *Hpa* Gw and exhibited HR (Supplemental Fig. S11). Susceptible and resistant Gw genotypes were not differentiated from each other in PCA analyses based on 134 genome-wide distributed SNPs (Alcázar et al., 2014; Supplemental Fig. S12). Notably, however, all genotypes carrying the conserved *RPP1-like* L*er* haplotype were resistant to *Hpa* Gw infection (Supplemental Fig. S12; Supplemental Table S5). Despite this, resistance is not strictly associated with the presence of an *RPP1-like* L*er* haplotype because it is expressed in accessions that do not carry the haplotype (e.g. Col-0).

Effect of Suppressive Mutations on *Hpa* Gw Disease Resistance in L*er*/Kas2 NIL

Next, we studied the effect of the L*er*/Kas2 HI suppressor (*sulki*) mutations on resistance to the local *Hpa* Gw isolate in the L*er*/Kas2 NIL. For this, we inoculated Cas9-*r2*, Cas9-*r3*, Cas9-*r4*, Cas9-*r8*, *sulki1* (*sulki1-3*, *sulki1-7*, *sulki1-8*, *and sulki1-9*), *sulki2-1*, and *near death experience1-3* (*nde1-3*), which carries a deletion between *RPP1-like R3-R8* L*er* genes (Stuttmann et al., 2016).

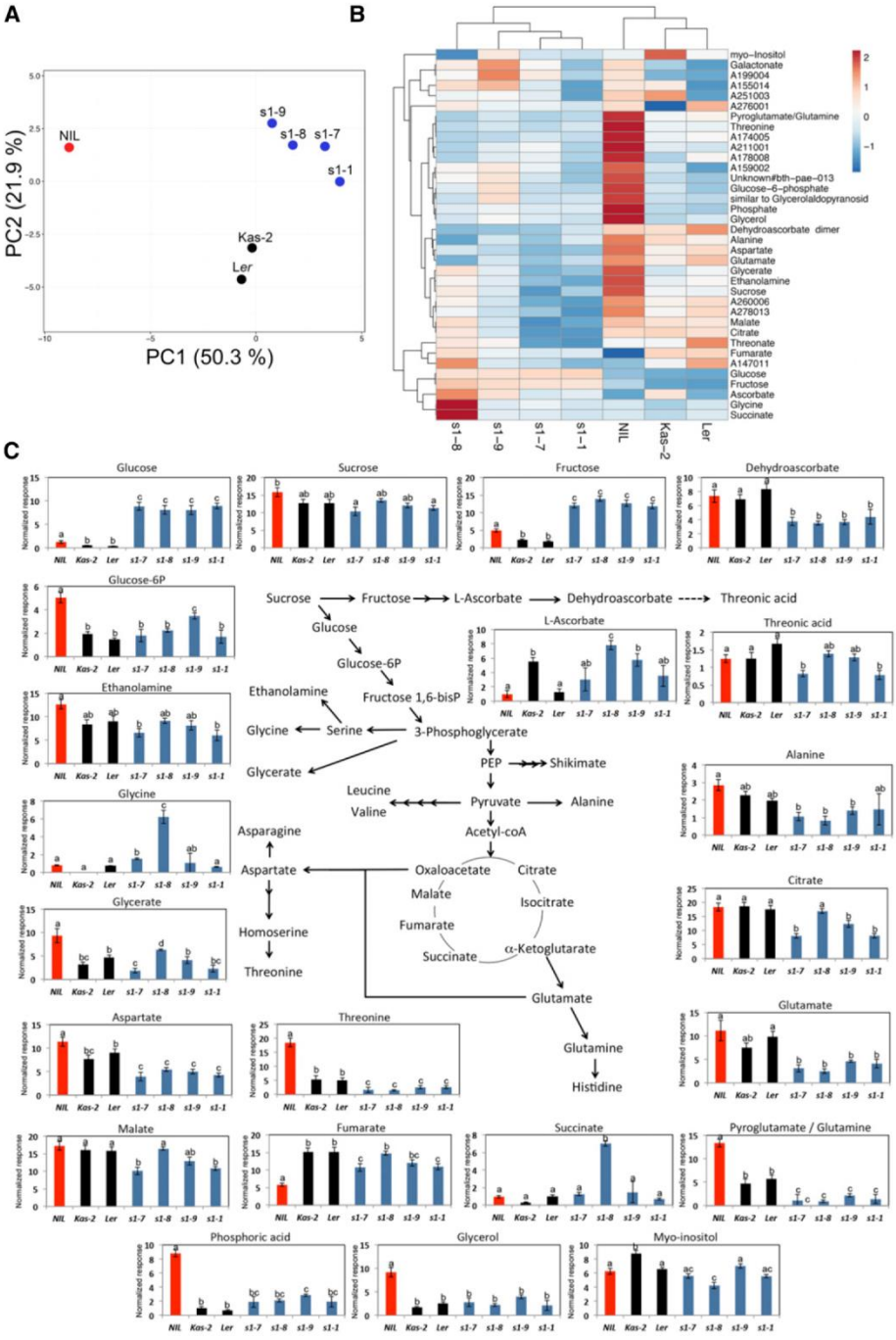

Figure 7. Principal component analysis (A) and HCA (B) with Pearson's correlation and average linkage of samples and metabolites from 5-week-old *sulki1-1* (*s1-1*), *sulki1-7* (*s1-7*), *sulki1-8* (*s1-8*), *sulki1-9* (*s1-9*), Ler, Kas2, and Ler/Kas2 NIL plants grown at 14°C to16°C. C, Log_2-normalized responses for some metabolites determined by GC/MS in the above genotypes, and schematic representation of their metabolic pathways. Different letters indicate significant differences ($P < 0.01$) in a Student-Newman-Keuls test. Error bars indicate SD. A complete list of analyzed metabolites is provided in Supplemental Table S3.

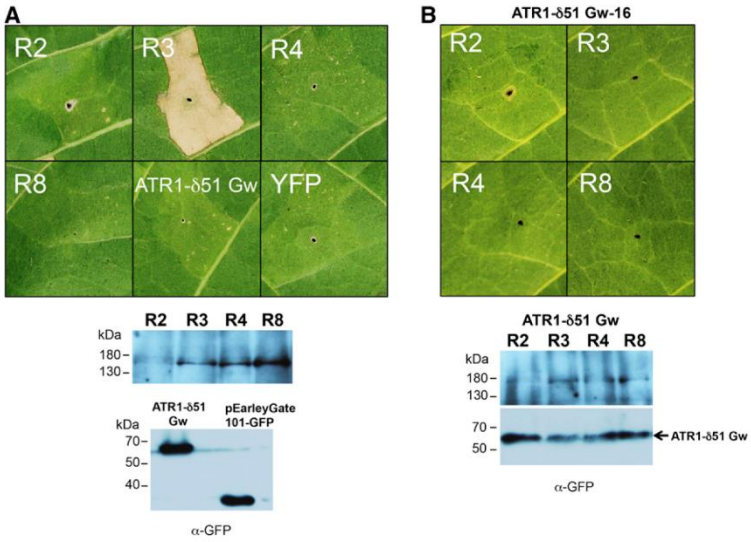

Figure 8. Transient expression assays in tobacco. A, Transient expression of genomic versions of 35s: *RPP1-like* L*er R2, R3, R4, R8,* and ATR1-δ51 Gw, tagged with C terminus YFP. B, Coinfiltration of *RPP1-like* L*er R2, R3, R4,* and *R8* with ATR1-δ51 Gw. Pictures in A and B were taken 48 h after infiltration. Samples for western-blot analyses in A and B were collected 24 h after infiltration. No symptoms of cell death were observed at later time points of coinfiltration in B.

Resistance to *Hpa* Gw was observed in all genotypes tested (Supplemental Fig. S11). We concluded that mutations suppressing L*er*/Kas2 incompatibility do not compromise disease resistance to a local *Hpa* isolate.

Analysis of ATR1 Gw Recognition by RPP1-Like L*er* Proteins in Tobacco

RPP1-like TNL receptors directly recognizing ATR1 effector variants from different *Hpa* isolates have been characterized (Rehmany et al., 2005; Sohn et al., 2007; Krasileva et al., 2010). We determined the capacity of TNL RPP1-like L*er* R2, R3, R4, and R8 proteins to recognize ATR1 cloned from Gw leading to cell death in tobacco transient expression assays. For this, C-terminal YFP fusions of *RPP1-like* L*er R2, R3, R4, R8* genomic constructs, and ATR1-δ51 *Hpa* Gw (lacking the ATR1 secretory signal peptide; Steinbrenner et al., 2015) were generated for *Agrobacterium tumefaciens* infiltration of tobacco leaves. Accumulation of *RPP1-like* L*er* R3 protein over a threshold triggered cell death in tobacco leaves (Fig. 8A), consistent with L*er*/Kas2 NIL phenotypes induced by *R3* overexpression in Arabidopsis (Alcázar et al., 2014) and its involvement in L*er*/Kas2 immune-related HI (Fig. 4). However, 1:1 coinfiltration of δ51-ATR1 *Hpa* Gw with *RPP1-like* L*er* R2, R3, R4, or R8, which resulted in lower but detectable RPP1 protein expression in tobacco leaves, did not induce cell death (Fig. 8B). These results suggest that ATR1 *Hpa* Gw is not recognized by any of the RPP1-like L*er* variants tested.

Hpa Gw Disease Resistance Is Independent of *EDS1*- and *ICS1*-Generated SA

We tested whether resistance to *Hpa* Gw was compromised in *eds1-2* (Col-0; Bartsch et al., 2006), *eds1-2*; L*er*; Feys et al., 2005), the SA-deficient *ISOCHORISMATE SYNTHASE1 sid2-1* mutant (Col-0; Wildermuth et al., 2001), or L*er-NahG* transgenic plants that metabolize SA into catechol (Bowling et al., 1994). Neither *eds1-2* nor SA depletion affected resistance to *Hpa* Gw (Supplemental Fig. S11). Because *TNL immunity* relies on *EDS1* (Aarts et al., 1998; Feys et al., 2001, 2005) and the *RPP1-like* L*er* locus only contains *TNL* genes (Alcázar et al., 2009), we reasoned that resistance to *Hpa* Gw is governed by other *RPP* loci in the genome.

Mapping of *Hpa* Gw Disease Resistance

Whereas L*er* is resistant to *Hpa* Gw, we found that the Shakdara (Sha) accession is susceptible, which enabled us to exploit a L*er*/Sha recombinant inbred line (RIL) population (Clerkx et al., 2004) in QTL mapping of *Hpa* Gw resistance loci (Supplemental Table S6). QTL analyses identified one major-effect QTL on chromosome 1 explaining 52% of the phenotypic variation, with L*er* alleles contributing most resistance to isolate *Hpa* Gw. L*er*/Sha RILs carrying Sha alleles at this QTL but L*er* alleles at the *RPP1-like* locus were susceptible to *Hpa* Gw infection (Supplemental Table S6). Therefore, the *RPP1-like* L*er* locus does not confer resistance to *Hpa* Gw. The QTL spanned 2.83 Mb between markers F6D8-94 and GENEA. This region contains at least nine *CNL*

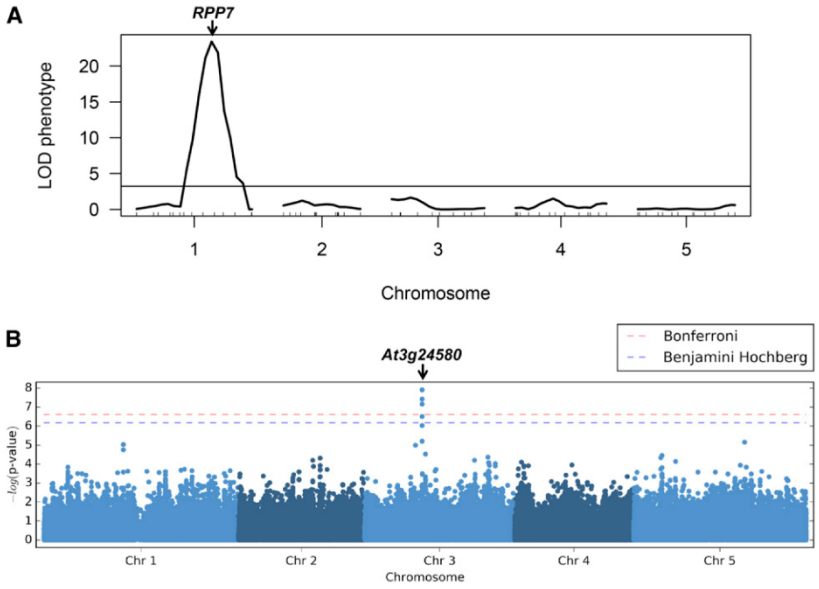

Figure 9. QTL and GWAS mapping. A, QTL mapping of disease resistance to *Hpa* isolate Gw in the L*er*/Sha RIL population (Clerkx et al., 2004; see Supplemental Table S6). The position of *RPP7* on chromosome 1 is indicated. B, Manhattan plot of GWAS mapping for disease resistance to *Hpa* Gw in 288 accessions (see Supplemental Table S8). The list of most significant gene associations is shown in Supplemental Table S9.

genes, among them *RPP7* (*At1g58602*; Supplemental Table S7), which was reported to confer resistance to *Hpa* isolate Hiks1 in an SA- and *EDS1*-independent manner (McDowell et al., 2000; Fig. 9A). Therefore, we consider *RPP7* as a strong candidate gene in L*er* resistance to *Hpa* Gw.

In addition to QTL analyses, we performed GWAS mapping using 288 Arabidopsis accessions distributed worldwide. Of the total phenotyped accessions, 78 (27%) were susceptible to *Hpa* Gw infection. Disease resistance phenotypes did not follow obvious geographical or population structure patterns and were segregated between and within populations (Supplemental Table S8). GWAS analysis for *Hpa* Gw disease resistance identified a significant association with multiple SNPs belonging to gene *At3g24580*, encoding an F-box protein of unknown function (Fig. 9B; Supplemental Table S9). However, no genetic variation at *At3g24580* was found between *Hpa* Gw-resistant (Gw-30, Gw-31, Gw-112, Gw-127, and Gw-144) and -susceptible (Gw-16, Gw-50, Gw-107, Gw-148, and Gw-167) genotypes, which all carried *At3g24580* Col-0 alleles (Supplemental Table S5). We concluded that *At3g24580* does not condition differences in disease resistance to *Hpa* Gw in the Gorzów population, although its epistatic interaction with other genes cannot be excluded in other genetic backgrounds. Together, the QTL and GWAS mapping identified candidate *RPP* genes outside the *RPP1-like* locus as conferring resistance to *Hpa* Gw.

DISCUSSION

Epistasis, defined as the nonadditive interaction between mutations, is the basis for many postzygotic immune-related HI in plants (Bomblies, 2010). The environment can affect the consequences of epistasis on fitness (Flynn et al., 2013). Indeed, growth defects in L*er*/Kas2 NIL at 14°C to 16°C are suppressed at 20°C to 22°C (Alcázar et al., 2009), a temperature at which basal disease resistance to *Pst* DC3000 is retained (Fig. 5). HI is not the result of direct action by natural selection but rather a byproduct of divergence through evolutionary processes acting on other traits (Coyne and Orr, 2004). Selective forces acting on *R* genes involve arms races between plants and pathogens, in addition to environmental factors (Dodds and Rathjen, 2010; Ariga et al., 2017). Such divergence might thus be shaped by adaptation to different environments (ecological speciation) or through different pathways within the same environment (Sherlock and Petrov, 2017). Adaptive mutations increasing fitness can be retrieved by experimental evolution, an approach facilitated by the study of microbial populations during multiple generations. In yeast, adaptation to divergent and identical environments has been shown to promote the emergence of reproductive isolation (Dettman et al., 2007; Ono et al., 2017). However, the intrinsic lethal nature of incompatible hybrids hinders the identification of potential mutations suppressing negative epistasis. Here, we circumvented this limitation by inducing random and

CRISPR/Cas9-guided mutagenesis in a large population of L*er*/Kas2 NIL plants. Through this approach, we identified *RPP1* intragenic mutations that suppress L*er*/Kas2 immune-related HI and observed different degrees of phenotypic adaptation.

The mutagenesis screen identified a large number of intragenic *suppressors of Ler/Kas2 incompatibility* (*sulki*) mapping to *RPP1-like* L*er R8* (*sulki1-1* to *sulki1-10*) and one mutation mapping to *RPP1-like* L*er R3 (sulki2-1)* that suppressed HI (Fig. 2). Due to the presence of moderate suppressor phenotypes in the EMS population, we reasoned that intragenic mutations leading to intermediate phenotypes might have been overlooked, including mutations in other potential *RPP1-like R3* alleles. Therefore, to provide a comprehensive analysis of the *RPP1-like* L*er* locus, we mutated each *RPP1-like* L*er* TNL encoding gene by CRISPR/Cas9 in the L*er*/Kas2 NIL background (Cas9-*r2*, Cas9-*r3*, Cas9-*r4*, and Cas9-*r8*) and studied the effects of the mutations on growth, cell death, gene expression, and disease resistance. EMS and CRISPR/Cas9 mutagenesis revealed epistatic interactions between *RPP1-like* L*er R8* and other *RPP1-like* L*er* members (*R2*, *R3*, and *R4*), with the latter contributing additively to immune-related HI (Fig. 4). These results are consistent with the involvement of two or more *RPP1-like* genes in L*er*/Kas2 incompatibility and suggest coaction between *RPP1-like* members for defense activation in Arabidopsis (Alcázar et al., 2014). The dominant nature of *RPP1-like* L*er R8* loss-of-function mutations suggests that a certain dosage of incompatible RPP1-like protein is required for the autoimmunity phenotype, and loss-of-function alleles in *RPP1-like* L*er R8* lower this dosage below a critical level when heterozygous. This might also explain the recessive nature of the *RPP1-like* haplotype in L*er*/Kas2 immune-related HI (Alcázar et al., 2009, 2014).

L*er*/Kas2 HI suppressor mutations mapped to different domains of *RPP1-like* L*er R8* (Fig. 1). The different mutations behaved like Cas9-*r8* loss-of-function alleles, indicating that *sulki1* mutations disrupt *RPP1-like* L*er R8* function in L*er*/Kas2 HI (Fig. 4). RNA-seq analyses in *sulki1-8* show that many transcriptional changes in incompatible L*er*/Kas2 hybrids are suppressed by *RPP1-like* L*er R8* mutation. However, the expression of other genes related with oxidation reduction was modified in *sulki1-8* mutants compared to its isogenic Kas2 genotype (Fig. 6; Supplemental Tables S2-1 to S2-3). The occurrence of these *RPP1-like* L*er R8*-independent expression sectors supports a multigenic basis for the *RPP1-like* L*er*-incompatible haplotype. Importantly, such expression sectors alone are not sufficient to trigger incompatibility, which requires a functional R8 protein.

Most *sulki1* suppressor mutations in *RPP1-like* L*er R8* were found in NB- or LRR-domain-conserved motifs and invariable residues. The NB-ARC domain is involved in nucleotide binding and hydrolysis and acts as a molecular switch for NLR activation (van Ooijen et al., 2008; Takken and Goverse, 2012). The NB-ARC is required for RPP1 self-association and cell death activation, probably assisted by TIR-TIR interactions (Schreiber et al., 2016). The LRR domain of TNL proteins is often involved in effector recognition, inducing a conformational change that switches the protein to an active state (van Ooijen et al., 2008; Takken and Goverse, 2012; Steinbrenner et al., 2015). Nonsynonymous substitutions in the LRR domain of *DM2h* Bla-1 are responsible for incompatibility with *DM1* Hh-0. Certain ATR1 alleles from *Hpa* isolates are recognized by the LRR domain of *RPP1* Ws-0 and Nd-1 (Krasileva et al., 2010; Steinbrenner et al., 2015). The identification of *DM2h* Bla-1 incompatible-trigger mutations in the *LQQL* motif of LRR4, next to a modeled ATR1 docking site, suggested that incompatible *RPP1* variants originate from an arms race between the immune receptor and pathogen ligands (Chae et al., 2014). Notably, the *sulki1-9* mutation (R821H) in LRR5 of *RPP1-like* R8 L*er* is adjacent to this *LQQL* motif (Fig. 1). A frameshift mutation in LRR2 of *RPP1-like* L*er R8* in the *nde1-1* mutant also suppresses incompatibility with Kas2. The *nde1-1* mutant was isolated from a suppressor screen for autoimmune phenotypes associated with EDS1 nuclear enrichment and suggested a role for *RPP1-like* L*er R8* in EDS1/PAD4 defense amplification (Stuttmann et al., 2016). Thus, polymorphism at the LRR domain of *RPP1-like* L*er R8* and its homolog in Bla-1 (*DM2h*) seems to be relevant for incompatibility (Chae et al., 2014; Stuttmann et al., 2016).

Here, we find that mutations in the TIR domains of RPP1-like L*er R3* and *R8* also suppress L*er*/Kas2 immune-related HI (Fig. 1). The TIR domain is necessary for receptor signaling, and in some TNLs, including RPP1, this domain self-associates and is sufficient for triggering cell death (Swiderski et al., 2009; Bernoux et al., 2011; Williams et al., 2014; Steinbrenner et al., 2015; Schreiber et al., 2016; Zhang et al., 2017). Whether *sulki1-1* and *sulki2-1* mutations disrupt potential self-association of *RPP1-like* L*er* R3 or R8 proteins needs to be determined.

We investigated whether the *RPP1* L*er* genes contributing to HI also participate in *Hpa* Gw recognition (Krasileva et al., 2010; Steinbrenner et al., 2015). Our analysis, using a local *Hpa* Gw isolate, indicated that the incompatible *RPP1* L*er* haplotype does not contribute to disease resistance to this local pathogen and that the resistance is SA and *EDS1* independent (Supplemental Fig. S11). Furthermore, we found that coexpression of *RPP1-like* L*er* R2, R3, R4, or R8 proteins with ATR1-*δ*51 *Hpa* Gw did not trigger HR in tobacco transient expression assays (Fig. 8B). Moreover, QTL mapping in the L*er*/Sha RIL population identified a major QTL on chromosome 1 that contained L*er* alleles contributing to resistance (Fig. 9A). The QTL interval spanned several *R* genes, including *RPP7*, a known *CNL* gene governing resistance to the *Hpa* Hiks1 isolate in an SA- and *EDS1*-independent manner (McDowell et al., 2000; Supplemental Table S7). From these data, we concluded that the incompatible *RPP1-like* L*er* haplotype does not contribute to disease resistance to a local *Hpa* isolate. Also, intragenic

mutations suppressing L*er*/Kas2 incompatibility do not incur on a fitness cost in terms of *Hpa* resistance (Supplemental Fig. S11). However, such mutations dampen disease resistance to *Pst* DC3000 of the L*er*/Kas2 NIL at 20°C to 22°C (Fig. 5), which might represent a trade-off between growth and basal defenses against virulent leaf-colonizing *P. syringae* bacteria.

Hpa populations might have diverged or even been extinguished since the birth of the *RPP1-like* L*er* haplotype, which was already present in the Gorzów population in 1939 (Alcázar et al., 2014). Thus, the contemporary *Hpa* Gw isolate might not represent a selective force for the *RPP1-like* L*er*-incompatible haplotype. However, fine-tuning *RPP1-like* L*er R3* expression may benefit disease resistance to other pathogenic strains (Alcázar et al., 2014), thereby favoring selection of the incompatible haplotype. Interestingly, *RPP1-like* L*er R3* and *R4* are homologs of *At3g44400* Col-0 (Alcázar et al., 2014) and whole-genome sequencing revealed the absence of *At3g44400* Col-0 gene in L*er* (Supplemental Fig. S13). This suggests that *RPP1-like R3* and *R4* in L*er* are derived from a gene transposition and duplication event from *At3g44400* during the formation of the incompatible *RPP1-like* haplotype.

Incompatible L*er*/Kas2 NIL plants exhibit metabolic hallmarks of HI, which can be explained by a combination of growth arrest and metabolic recycling of material from dead or dying leaf cells. Recycling likely also involves proteolysis and triglyceride degradation accompanied by oxidative stress (Fig. 7C). We further detected a promotion of Suc degradation through cell wall invertase, but not vacuolar invertase activities (Supplemental Fig. S9). Activation of cell wall invertase is triggered by defense responses to various pathogens, including oomycetes and bacteria (Tauzin and Giardina, 2014). Glc and Fru can be used as carbon sources for the biosynthesis of defense-related metabolites, potentially leading to a metabolic cost that reduces growth in the dwarf L*er*/Kas2 NIL (Bolton, 2009). Remarkably, these metabolic costs are fully suppressed in *sulki1* mutants, which also suppress oxidative stress symptoms. Nevertheless, *sulki1* mutants accumulate higher levels of Glc, Fru, and starch than the L*er*/Kas2 NIL (Fig. 7C), possibly due to *RPP1-like* L*er R8*-independent transcriptional activation of defense responses.

Our data shed light on the complex genetic nature of the *RPP1-like* L*er* locus triggering incompatibility with Kas2. Through random and guided mutagenesis, mutations can be generated that mitigate fitness costs of L*er*/Kas2 HI, while retaining resistance to a local *Hpa* Gw isolate. However, trade-offs are also inherent to such compensatory mutations.

MATERIALS AND METHODS

Plant Material and Growth Conditions

A complete list of Arabidopsis (*Arabidopsis thaliana*) accessions used in this study is provided in Supplemental Table S8. Seeds were obtained from the Nottingham Arabidopsis Stock Center or collected by authors (Alcázar et al., 2014). The incompatible L*er*/Kas2 NIL and cNIL used in this study were described previously (Alcázar et al., 2009, 2010). Plants were grown on soil at indicated temperatures under 12-h-dark/12-h-light cycles and 70% relative humidity and 120 µmol m^{-2} s^{-1} of light intensity.

EMS Mutagenesis

Seeds of L*er*/Kas2 NIL were soaked overnight in 1 mg/mL KCl at 4°C. After seed imbibition, the solution was discarded and replaced with 0.2% EMS (v/v) and incubated for 16 h. Seeds were then washed 10 times with 50 mL of water and suspended in 0.1% agarose for sowing on soil. Approximately 25,000 M1 plants were allowed to self at 20°C to 22°C. M2 seeds were collected in pools of 100 to 150 M1 plants. M2 plants were grown at 14°C to 16°C to identify suppressors of L*er*/Kas2 incompatibility (*sulki*).

Whole-Genome Sequencing

Genomic DNA from Arabidopsis plants was extracted from leaves of 5-week-old plants grown on soil using the CTAB method (Doyle, 1991). DNA quality was checked on 0.8% agarose gel electrophoresis stained with ethidium bromide. DNA concentration was determined by fluorometric quantitation using the dsDNA HS assay kit and the Qubit device (Thermo Fisher). Whole-genome sequencing was performed at the Centro Nacional de Análisis Genómico (CNAG, Spain). A standard Illumina protocol was followed to create paired-end libraries, which were run on Illumina sequencers HiSeq 3000/4000 2x150 according to standard procedures. Sample statistics are shown in Supplemental Table S10. Read mapping and variant detection were performed using the CLC Genomics Workbench 10 version 10.1.1 (Qiagen).

RT-qPCR Expression Analyses

Total RNA was extracted using Trizol reagent (Thermo Fisher). Reverse transcription and quantitative real-time PCR was performed as described (Alcázar et al., 2014). A complete list of primers used for expression analyses is reported in Alcázar et al. (2014).

RNA-Seq Expression Analyses

Total RNA was extracted from fully expanded leaves of 5-week-old *sulki1-8*, Kas2, and L*er*/Kas2 NIL plants grown at 14°C to 16°C. Three biological replicates, each from pooled leaves of at least three independent plants grown in individual pots were used for the analysis. Total RNA was extracted using Trizol (Thermo Fisher), quantified in a Nanodrop ND-1000 spectrophotometer, and checked for purity and integrity in a Bioanalyzer-2100 device (Agilent Technologies). RNA samples were further processed by the CNAG (Spain) for library preparation and RNA sequencing. Libraries were prepared using the Illumina TruSeq Sample Preparation Kit according to the manufacturer's instructions. Each library was paired-end sequenced (2 × 75 bp) on HiSeq 2000 Illumina sequencers. Sample statistics are shown in Supplemental Table S10. Read mapping and expression analyses were performed using the CLC Genomics Workbench 10 version 10.1.1 (Qiagen). Only significant expression differences (fold change ≥ 2; *P* value and false discovery rate ≤ 0.05) were considered.

CRISPR/Cas9 Mutagenesis

To identify specific PAM motifs in *RPP1-like* L*er* genes, their sequences were aligned using multiple sequence comparison by Log-Expectation (http://www.ebi.ac.uk/Tools/msa/muscle/) and unique NGG motifs identified in TIR or NB domains of *RPP1-like* L*er R2*, *R3*, *R4*, and *R8*. Generation of CRISPR/Cas9 lines was based on the system reported by Fauser et al. (2014). Spacers were designed next to unique PAM sites and annealed oligonucleotides containing *Bbs*I sites were used for the generation of customized RNA chimeras in the pEn-Chimera vector (Supplemental Table S11). The customized RNA chimeras were transferred into pDe-CAS9 by Gateway LR reaction (Thermo Fisher). The final clones were sequenced and transformed into *Agrobacterium tumefaciens* GV3101 pMP90. L*er*/Kas2 NIL plants were transformed by floral dipping and transgenic lines isolated by selection with 20 µg/mL

glufosinate-ammonium (Sigma-Aldrich). Individual lines were checked for the presence of indel mutations by SANGER sequencing of all *RPP1-like* L*er* genes (Alcázar et al., 2014), crossed to L*er*/Kas2 NIL, and Cas9-free homozygous mutants isolated in the F2 by gene sequencing and Cas9 genotyping (Supplemental Table S11).

Histochemical Analyses and Determination of Leaf Area

Plant cell death and *Hpa* structures were determined by staining leaves with lactophenol trypan blue (Alcázar et al., 2009). Samples were mounted on glycerol 70% and observed under light microscope (Axioplan; Carl Zeiss) coupled to a Leica DFC490 digital camera. Leaf area was quantified using Image Pro Analyzer (Media Cybernetics) as reported by Alcázar et al. (2009).

Isolation of *Hyaloperonospora arabidopsidis* Gw and Pathogen Inoculation Assays

Original spores from *H. arabidopsidis* Gw were collected from the Gw-16 accession naturally growing in the Gorzów population during spring of 2014. Spores were resuspended in 100 µL of water and inoculated on the susceptible Ws *eds1-1* genotype (Falk et al., 1999). Thereafter, the *Hpa* Gw isolate has been maintained by weekly propagation on the susceptible Gw-16 accession. *Hpa* inoculation assays were performed as described by Alcázar et al. (2009). *Pseudomonas syringae* spray inoculation and growth quantitation assays were performed as described by Alcázar et al. (2010).

Cloning of *ATR1*

The genomic DNA from *Hpa* Gw mass conidiospores was extracted using TriZol (Thermo Fisher) and used for PCR amplification of *ATR1* gene using primer combinations listed in Supplemental Table S11 (Rehmany et al., 2005). The PCR product was treated with ExoSap (Thermo Fisher) and sequenced by SANGER with primers described in Supplemental Table S11.

Global Metabolite Profiling

Metabolite profiling was performed from leaf samples (120 mg) using at least 10 biological replicates. Polar primary metabolite extraction and gas chromatography coupled to electron impact ionization-time of flight-mass spectrometry analysis was performed as described (Zarza et al., 2017). Only metabolites identified in all genotypes and at least 8 of 10 replicates were considered. Normalized values are referred to the internal standard. Principal component analysis was determined using *R* (www.r-project.org). HCA with Pearson correlation was obtained using the MultiExperiment Viewer software (http://mev.tm4.org/; version 27 4.8.1).

Starch Quantification

The entire shoot of 5-week-old plants was used for the analyses. Samples were harvested 1 h before the end of the light or dark periods. Starch levels were quantified according to Smith and Zeeman (2006) using at least five biological replicates per genotype.

Invertase Activities

Cell-wall-bound and soluble acid invertase activities were performed according to Appeldoorn et al. (1997) from leaves of 5-week-old Arabidopsis plants using at least five biological replicates per genotype.

Transient Expression Assays

Genomic versions of *RPP1-like* L*er* *R2*, *R3*, *R4*, and *R8* were obtained by PCR amplification from L*er* gDNA using the primers combinations listed in Supplemental Table S11. The PCR products were purified and cloned into the pSPARKII vector (Canvax). The resulting clones were sequenced using primers already described (Alcázar et al., 2014) and subcloned *Sal*I/*Not*I into a modified version of pENTR1A providing gentamycin resistance. The resulting construct was used for LR Gateway (Thermo Fisher) reaction with pEarley101 (Earley et al., 2006) to generate C terminus YFP-HA fusions of genomic clones under the control of the *Cauliflower mosaic virus* 35s promoter. The different constructs were sequenced, transformed into *A. tumefaciens* GV3101 pMP90, and used for infiltration of tobacco (*Nicotiana tabacum*; Samsun, SNN) leaves. Transformed agrobacteria were inoculated into 30 mL YEB media and incubated by shaking at 250 rpm and 28°C overnight. Cultures were centrifuged at 4,000*g* for 5 min and resuspended on 10 mM $MgCl_2$ and 10 mM MES, pH 5.6, to an OD_{600} of 0.45. For induction of agrobacteria virulence, 150 µM acetosyringone was added to the cells for 3 h. Discs from inoculated leaves were collected at indicated time points using a cork borer (1.2 cm diameter) and frozen immediately in liquid nitrogen. Pictures were taken at indicated time points with a Canon EOS 450D digital camera.

Western-Blot Analysis

Frozen samples were disrupted in 1.5-mL tubes along with 1-mm glass beads in a homogenizer device. Samples were suspended on 200 µL of protein extraction buffer (0.24 M Tris, pH 6.8, 6% SDS, 30% glycerol, 16% 2-mercaptoethanol, 0.01% bromophenol blue, and 10 M urea), boiled for 5 min, and centrifuged for 5 min at 12,000*g*. The supernatant was then transferred to a new tube. Fifteen microliters were used for 8% SDS-PAGE and transferred by blotting to a polyvinylidene difluoride membrane. Anti-GFP monoclonal antibody (clones 7.1 and 13.1; Roche) at 1:1,000 dilution and rabbit anti-mouse HRP (Sigma-Aldrich) secondary antibody at 1:10,000 were used for detection of YFP-tagged proteins with SuperSignal West Femto Maximum Sensitivity Chemiluminescent Substrate (Thermo Fisher).

QTL and GWAS Mapping

QTL mapping was performed using *R/qtl* with the genetic data of the L*er*/Sha RIL population from Clerkx et al. (2004) and phenotype evaluation of *Hpa* Gw disease resistance in Supplemental Table S6. For phenotypic evaluation, values from 0 to 2 were assigned to each genotype (0, no sporulation; 1, sporulation only observed on cotyledons; 2, sporulation observed in cotyledons and fully expanded leaves). LOD scores were calculated with a single-QTL model implemented in *R/qtl*. LOD score significance threshold was established using 1,000 permutations. GWAS mapping was performed using accessions and phenotypes listed in Supplemental Table S8. Manhattan plots were determined using 250 k SNP data and the accelerated mixed model (Kang et al., 2010; Zhang et al., 2010) implemented in GWAPP (Seren et al., 2012). To ensure adequate correction for population stratification, we constructed a *quantile-quantile* plot (Supplemental Fig. S14). A list of most significant associations is found in Supplemental Table S9.

Accession Numbers

RNA-seq data have been deposited to ArrayExpress (www.ebi.ac.uk/arrayexpress/) under accession number E-MTAB-6755.

Supplemental Data

The following supplemental materials are available.

Supplemental Figure S1. Leaf area and trypan blue staining in 5-week-old *sulki1*, *sulki2*, L*er*/Kas2 NIL, cNIL (Alcázar et al., 2010), and parental accessions grown at 14°C to 16°C.

Supplemental Figure S2. Alignment of amino acid sequences for *RPP1-like* genes in L*er*, Col-0, Uk-1, Bla-1, and Ws.

Supplemental Figure S3. RT-qPCR expression analyses of *PR1*, *RPP1-like* L*er* *R2*, *R3*, *R4*, and *R8* genes in L*er* plants treated with 100 µM benzo (1,2,3) thiadiazole-7-carbothioic acid *S*-methyl ester or 100 µM SA.

Supplemental Figure S4. CRISPR/Cas9-induced indel mutations in Cas9-*r2*, Cas9-*r3*, Cas9-*r4*, and Cas9-*r8* and their effects on protein translation.

Supplemental Figure S5. Leaf area and trypan blue staining of 5-week-old CRISPR/Cas9 *RPP1-like* L*er* mutants grown at 14°C to 16°C.

Supplemental Figure S6. Complementation of *sulki2-1* with *RPP1-like* L*er R3* gene reconstitutes L*er*/Kas2 NIL phenotype.

Supplemental Figure S7. *PR1*, *EDS1*, and *GST1* expression analyses in 5- and 7-week-old (w-o) Cas9 *r2-1*, *r2-2*, *r3-1*, *r3-2*, *r4-1*, *r4-2*, *r8-1*, and *r8-2*, L*er*, Kas2, L*er*/Kas2 NIL, and cNIL plants grown at 14°C to 16°C.

Supplemental Figure S8. Starch levels determined in leaves of 5-week-old incompatible L*er*/Kas2 NIL, Kas2, L*er*, *sulki1-1*, *sulki1-7*, *sulki1-8*, and *sulki1-9* grown at 14°C to 16°C.

Supplemental Figure S9. Apoplastic and vacuolar invertase activities of 5-week-old incompatible L*er*/Kas2 NIL, Kas2, L*er*, *sulki1-1*, *sulki1-7*, *sulki1-8*, and *sulki1-9* grown at 14°C to 16°C.

Supplemental Figure S10. Neighbor-joining phylogenetic analysis of ATR1 amino acid sequences from different *Hpa* isolates.

Supplemental Figure S11. Disease resistance phenotypes to *Hpa* Gw infection in different genotypes.

Supplemental Figure S12. Principal component analysis of the Gw population based on 134 genome-wide SNPs.

Supplemental Figure S13. Coverage of Illumina reads mapping to the *At3g44400-At3g44480* interval in L*er*.

Supplemental Figure S14. Quantile-quantile (Q-Q) plot for GWAS analysis of *Hpa* Gw disease resistance using the accelerated mixed model method.

Supplemental Table S1. Segregation analyses of *sulki* and CRISPR/Cas9 mutants.

Supplemental Table S2. List of differentially expressed genes in the comparisons between Kas2 versus L*er*/Kas2 NIL and *sulki1-8* versus L*er*/Kas2 NIL and their Gene Ontology analyses.

Supplemental Table S3. List of metabolites and raw data from GC/MS analyses in L*er*/Kas2 NIL, Kas2, L*er*, *sulki1-1*, *sulki1-7*, *sulki1-8*, and *sulki1-9*.

Supplemental Table S4. PC1 and PC2 loadings of L*er*/Kas2 NIL, L*er*, Kas2, and *sulki1* metabolite profiles.

Supplemental Table S5. Genotype data and disease resistance phenotypes to *Hpa* Gw infection in the Gorzów population.

Supplemental Table S6. Phenotype data for disease resistance to *Hpa* Gw in the L*er*/Sha RIL population.

Supplemental Table S7. List of *NLR* genes in the QTL interval of chromosome one for *Hpa* Gw disease resistance in the L*er*/Sha RIL population.

Supplemental Table S8. List of accessions used in GWAS mapping for disease resistance to *Hpa* Gw infection.

Supplemental Table S9. List of genes with highest associations in GWAS mapping for disease resistance to *Hpa* Gw.

Supplemental Table S10. Summary statistics of whole-genome sequencing and RNA-seq reads.

Supplemental Table S11. List of oligonucleotides used in this work.

ACKNOWLEDGMENTS

We thank Maarten Koornneef for biological materials and critical reading of the manuscript. We acknowledge support from the CNAG (Spain) in next-generation sequencing experiments.

Received April 18, 2018; accepted May 15, 2018; published May 23, 2018.

LITERATURE CITED

Aarts N, Metz M, Holub E, Staskawicz BJ, Daniels MJ, Parker JE (1998) Different requirements for EDS1 and NDR1 by disease resistance genes define at least two *R* gene-mediated signaling pathways in *Arabidopsis*. Proc Natl Acad Sci USA **95**: 10306–10311

Alcázar R, García AV, Parker JE, Reymond M (2009) Incremental steps toward incompatibility revealed by *Arabidopsis* epistatic interactions modulating salicylic acid pathway activation. Proc Natl Acad Sci USA **106**: 334–339

Alcázar R, García AV, Kronholm I, de Meaux J, Koornneef M, Parker JE, Reymond M (2010) Natural variation at *Strubbelig Receptor Kinase 3* drives immune-triggered incompatibilities between *Arabidopsis thaliana* accessions. Nat Genet **42**: 1135–1139

Alcázar R, Pecinka A, Aarts MGM, Fransz PF, Koornneef M (2012) Signals of speciation within *Arabidopsis thaliana* in comparison with its relatives. Curr Opin Plant Biol **15**: 205–211

Alcázar R, von Reth M, Bautor J, Chae E, Weigel D, Koornneef M, Parker JE (2014) Analysis of a plant complex *resistance* gene locus underlying immune-related hybrid incompatibility and its occurrence in nature. PLoS Genet **10**: e1004848

Appeldoorn NJG, de Bruijn SM, Koot-Gronsveld EAM, Visser RGF, Vreugdenhil D, van der Plas LHW (1997) Developmental changes of enzymes involved in conversion of sucrose to hexose-phosphate during early tuberisation of potato. Planta **202**: 220–226

Ariga H, Katori T, Tsuchimatsu T, Hirase T, Tajima Y, Parker JE, Alcázar R, Koornneef M, Hoekenga O, Lipka AE, (2017) NLR locus-mediated trade-off between abiotic and biotic stress adaptation in *Arabidopsis*. Nat Plants **3**: 17072

Bakker EG, Toomajian C, Kreitman M, Bergelson J (2006) A genome-wide survey of *R* gene polymorphisms in *Arabidopsis*. Plant Cell **18**: 1803–1818

Bartsch M, Gobbato E, Bednarek P, Debey S, Schultze JL, Bautor J, Parker JE (2006) Salicylic acid-independent ENHANCED DISEASE SUSCEPTIBILITY1 signaling in *Arabidopsis* immunity and cell death is regulated by the monooxygenase FMO1 and the Nudix hydrolase NUDT7. Plant Cell **18**: 1038–1051

Bernoux M, Ve T, Williams S, Warren C, Hatters D, Valkov E, Zhang X, Ellis JG, Kobe B, Dodds PN (2011) Structural and functional analysis of a plant resistance protein TIR domain reveals interfaces for self-association, signaling, and autoregulation. Cell Host Microbe **9**: 200–211

Bolton MD (2009) Primary metabolism and plant defense--fuel for the fire. Mol Plant Microbe Interact **22**: 487–497

Bomblies K (2010) Doomed lovers: mechanisms of isolation and incompatibility in plants. Annu Rev Plant Biol **61**: 109–124

Bomblies K, Weigel D (2007) Hybrid necrosis: autoimmunity as a potential gene-flow barrier in plant species. Nat Rev Genet **8**: 382–393

Bomblies K, Lempe J, Epple P, Warthmann N, Lanz C, Dangl JL, Weigel D (2007) Autoimmune response as a mechanism for a Dobzhansky-Muller-type incompatibility syndrome in plants. PLoS Biol **5**: e236

Botella MA, Parker JE, Frost LN, Bittner-Eddy PD, Beynon JL, Daniels MJ, Holub EB, Jones JD (1998) Three genes of the *Arabidopsis RPP1* complex resistance locus recognize distinct *Peronospora parasitica* avirulence determinants. Plant Cell **10**: 1847–1860

Bowling SA, Guo A, Cao H, Gordon AS, Klessig DF, Dong X (1994) A mutation in *Arabidopsis* that leads to constitutive expression of systemic acquired resistance. Plant Cell **6**: 1845–1857

Cao J, Schneeberger K, Ossowski S, Günther T, Bender S, Fitz J, Koenig D, Lanz C, Stegle O, Lippert C, (2011) Whole-genome sequencing of multiple *Arabidopsis thaliana* populations. Nat Genet **43**: 956–963

Chae E, Bomblies K, Kim S-TT, Karelina D, Zaidem M, Ossowski S, Martín-Pizarro C, Laitinen RAE AE, Rowan BAA, Tenenboim H, (2014) Species-wide

genetic incompatibility analysis identifies immune genes as hot spots of deleterious epistasis. Cell **159**: 1341–1351

Chen C, Chen H, Lin Y-S, Shen J-B, Shan J-X, Qi P, Shi M, Zhu M-Z, Huang X-H, Feng Q, (2014) A two-locus interaction causes interspecific hybrid weakness in rice. Nat Commun **5**: 3357

Clerkx EJM, El-Lithy ME, Vierling E, Ruys GJ, Blankestijn-De Vries H, Groot SPC, Vreugdenhil D, Koornneef M (2004) Analysis of natural allelic variation of Arabidopsis seed germination and seed longevity traits between the accessions Landsberg *erecta* and Shakdara, using a new recombinant inbred line population. Plant Physiol **135**: 432–443

Coates ME, Beynon JL (2010) *Hyaloperonospora Arabidopsidis* as a pathogen model. Annu Rev Phytopathol **48**: 329–345

Coyne JA (1992) Genetics and speciation. Nature **355**: 511–515

Coyne JA, Orr HA (2004) Speciation. Sinauer Associates, Sunderland, MA

Dettman JR, Sirjusingh C, Kohn LM, Anderson JB (2007) Incipient speciation by divergent adaptation and antagonistic epistasis in yeast. Nature **447**: 585–588

Dodds PN, Rathjen JP (2010) Plant immunity: towards an integrated view of plant-pathogen interactions. Nat Rev Genet **11**: 539–548

Doyle J (1991) DNA protocols for plants. *In* **GM Hewitt, AWB Johnston, JPW Young**, eds, Molecular Techniques in Taxonomy, Springer, Berlin, pp 283–293

Earley KW, Haag JR, Pontes O, Opper K, Juehne T, Song K, Pikaard CS (2006) Gateway-compatible vectors for plant functional genomics and proteomics. Plant J **45**: 616–629

Falk A, Feys BJ, Frost LN, Jones JD, Daniels MJ, Parker JE (1999) EDS1, an essential component of R gene-mediated disease resistance in *Arabidopsis* has homology to eukaryotic lipases. Proc Natl Acad Sci USA **96**: 3292–3297

Fauser F, Schiml S, Puchta H (2014) Both CRISPR/Cas-based nucleases and nickases can be used efficiently for genome engineering in *Arabidopsis thaliana*. Plant J **79**: 348–359

Feys BJ, Moisan LJ, Newman MA, Parker JE (2001) Direct interaction between the *Arabidopsis* disease resistance signaling proteins, EDS1 and PAD4. EMBO J **20**: 5400–5411

Feys BJ, Wiermer M, Bhat RA, Moisan LJ, Medina-Escobar N, Neu C, Cabral A, Parker JE (2005) Arabidopsis SENESCENCE-ASSOCIATED GENE101 stabilizes and signals within an ENHANCED DISEASE SUSCEPTIBILITY1 complex in plant innate immunity. Plant Cell **17**: 2601–2613

Flynn KM, Cooper TF, Moore FB-G, Cooper VS (2013) The environment affects epistatic interactions to alter the topology of an empirical fitness landscape. PLoS Genet **9**: e1003426

Goritschnig S, Steinbrenner AD, Grunwald DJ, Staskawicz BJ (2016) Structurally distinct *Arabidopsis thaliana* NLR immune receptors recognize tandem WY domains of an oomycete effector. New Phytol **210**: 984–996

Hurwitz BL, Kudrna D, Yu Y, Sebastian A, Zuccolo A, Jackson SA, Ware D, Wing RA, Stein L (2010) Rice structural variation: a comparative analysis of structural variation between rice and three of its closest relatives in the genus Oryza. Plant J **63**: 990–1003

Jeuken MJW, Zhang NW, McHale LK, Pelgrom K, den Boer E, Lindhout P, Michelmore RW, Visser RGF, Niks RE (2009) Rin4 causes hybrid necrosis and race-specific resistance in an interspecific lettuce hybrid. Plant Cell **21**: 3368–3378

Kang HM, Sul JH, Service SK, Zaitlen NA, Kong SY, Freimer NB, Sabatti C, Eskin E (2010) Variance component model to account for sample structure in genome-wide association studies. Nat Genet **42**: 348–354

Khan M, Subramaniam R, Desveaux D (2016) Of guards, decoys, baits and traps: pathogen perception in plants by type III effector sensors. Curr Opin Microbiol **29**: 49–55

Kopka J, Schauer N, Krueger S, Birkemeyer C, Usadel B, Bergmüller E, Dörmann P, Weckwerth W, Gibon Y, Stitt M, (2005) GMD@CSB.DB: the Golm Metabolome Database. Bioinformatics **21**: 1635–1638

Krasileva KV, Dahlbeck D, Staskawicz BJ (2010) Activation of an *Arabidopsis* resistance protein is specified by the in planta association of its leucine-rich repeat domain with the cognate oomycete effector. Plant Cell **22**: 2444–2458

Krüger J, Thomas CM, Golstein C, Dixon MS, Smoker M, Tang S, Mulder L, Jones JDG (2002) A tomato cysteine protease required for Cf-2-dependent disease resistance and suppression of autonecrosis. Science **296**: 744–747

McDowell JM, Cuzick A, Can C, Beynon J, Dangl JL, Holub EB (2000) Downy mildew (*Peronospora parasitica*) resistance genes in *Arabidopsis* vary in functional requirements for NDR1, EDS1, NPR1 and salicylic acid accumulation. Plant J **22**: 523–529

McHale LK, Haun WJ, Xu WW, Bhaskar PB, Anderson JE, Hyten DL, Gerhardt DJ, Jeddeloh JA, Stupar RM (2012) Structural variants in the soybean genome localize to clusters of biotic stress-response genes. Plant Physiol **159**: 1295–1308

Meyers BC, Kozik A, Griego A, Kuang H, Michelmore RW (2003) Genome-wide analysis of NBS-LRR-encoding genes in *Arabidopsis*. Plant Cell **15**: 809–834

Muñoz-Amatriaín M, Eichten SR, Wicker T, Richmond TA, Mascher M, Steuernagel B, Scholz U, Ariyadasa R, Spannagl M, Nussbaumer T, (2013) Distribution, functional impact, and origin mechanisms of copy number variation in the barley genome. Genome Biol **14**: R58

Ono J, Gerstein AC, Otto SP (2017) Widespread genetic incompatibilities between first-step mutations during parallel adaptation of *Saccharomyces cerevisiae* to a common environment. PLoS Biol **15**: e1002591

Rehmany AP, Gordon A, Rose LE, Allen RL, Armstrong MR, Whisson SC, Kamoun S, Tyler BM, Birch PRJ, Beynon JL (2005) Differential recognition of highly divergent downy mildew avirulence gene alleles by *RPP1* resistance genes from two *Arabidopsis* lines. Plant Cell **17**: 1839–1850

Schreiber KJ, Bentham A, Williams SJ, Kobe B, Staskawicz BJ (2016) Multiple domain associations within the *Arabidopsis* immune receptor RPP1 regulate the activation of programmed cell death. PLoS Pathog **12**: e1005769

Seren Ü, Vilhjálmsson BJ, Horton MW, Meng D, Forai P, Huang YS, Long Q, Segura V, Nordborg M (2012) GWAPP: a web application for genome-wide association mapping in *Arabidopsis*. Plant Cell **24**: 4793–4805

Sherlock G, Petrov DA (2017) Seeking goldilocks during evolution of drug resistance. PLoS Biol **15**: e2001872

Sicard A, Kappel C, Josephs EB, Lee YW, Marona C, Stinchcombe JR, Wright SI, Lenhard M (2015) Divergent sorting of a balanced ancestral polymorphism underlies the establishment of gene-flow barriers in Capsella. Nat Commun **6**: 7960

Smith AM, Zeeman SC (2006) Quantification of starch in plant tissues. Nat Protoc **1**: 1342–1345

Sohn KH, Lei R, Nemri A, Jones JDG (2007) The downy mildew effector proteins ATR1 and ATR13 promote disease susceptibility in *Arabidopsis thaliana*. Plant Cell **19**: 4077–4090

Steinbrenner AD, Goritschnig S, Staskawicz BJ (2015) Recognition and activation domains contribute to allele-specific responses of an Arabidopsis NLR receptor to an oomycete effector protein. PLoS Pathog **11**: e1004665

Stuttmann J, Peine N, Garcia AV, Wagner C, Choudhury SR, Wang Y, James GV, Griebel T, Alcázar R, Tsuda K, (2016) *Arabidopsis thaliana* DM2h (R8) within the Landsberg *RPP1-like* resistance locus underlies three different cases of EDS1-conditioned autoimmunity. PLoS Genet **12**: e1005990

Sukarta OCA, Slootweg EJ, Goverse A (2016) Structure-informed insights for NLR functioning in plant immunity. Semin Cell Dev Biol **56**: 134–149

Swiderski MR, Birker D, Jones JDG (2009) The TIR domain of TIR-NB-LRR resistance proteins is a signaling domain involved in cell death induction. Mol Plant Microbe Interact **22**: 157–165

Takken FLW, Goverse A (2012) How to build a pathogen detector: structural basis of NB-LRR function. Curr Opin Plant Biol **15**: 375–384

Tauzin AS, Giardina T (2014) Sucrose and invertases, a part of the plant defense response to the biotic stresses. Front Plant Sci **5**: 293

van Ooijen G, Mayr G, Kasiem MM, Albrecht M, Cornelissen BJ, Takken FL (2008) Structure-function analysis of the NB-ARC domain of plant disease resistance proteins. J Exp Bot **59**: 1383–1397

Wildermuth MC, Dewdney J, Wu G, Ausubel FM (2001) Isochorismate synthase is required to synthesize salicylic acid for plant defence. Nature **414**: 562–565

Williams SJ, Sohn KH, Wan L, Bernoux M, Sarris PF, Segonzac C, Ve T, Ma Y, Saucet SB, Ericsson DJ, (2014) Structural basis for assembly and function of a heterodimeric plant immune receptor. Science **344**: 299–303

Xu X, Liu X, Ge S, Jensen JD, Hu F, Li X, Dong Y, Gutenkunst RN, Fang L, Huang L, (2011) Resequencing 50 accessions of cultivated and wild rice yields markers for identifying agronomically important genes. Nat Biotechnol **30**: 105–111

Yamamoto E, Takashi T, Morinaka Y, Lin S, Wu J, Matsumoto T, Kitano H, Matsuoka M, Ashikari M (2010) Gain of deleterious function causes an autoimmune response and Bateson-Dobzhansky-Muller incompatibility in rice. Mol Genet Genomics **283**: 305–315

Yuan J, He SY (1996) The *Pseudomonas syringae* Hrp regulation and secretion system controls the production and secretion of multiple extracellular proteins. J Bacteriol **178**: 6399–6402

Zarza X, Atanasov KE, Marco F, Arbona V, Carrasco P, Kopka J, Fotopoulos V, Munnik T, Gómez-Cadenas A, Tiburcio AF, (2017) *Polyamine oxidase 5* loss-of-function mutations in *Arabidopsis thaliana* trigger metabolic and transcriptional reprogramming and promote salt stress tolerance. Plant Cell Environ **40**: 527–542

Zhang X, Bernoux M, Bentham AR, Newman TE, Ve T, Casey LW, Raaymakers TM, Hu J, Croll TI, Schreiber KJ, (2017) Multiple functional self-association interfaces in plant TIR domains. Proc Natl Acad Sci USA **114**: E2046–E2052

Zhang Z, Ersoz E, Lai C-Q, Todhunter RJ, Tiwari HK, Gore MA, Bradbury PJ, Yu J, Arnett DK, Ordovas JM, (2010) Mixed linear model approach adapted for genome-wide association studies. Nat Genet **42**: 355–360

CHAPTER 2

High ammonium suppresses NLR-mediated hybrid incompatibilities in *Arabidopsis thaliana* by NPR1 modulation

High ammonium suppresses NLR-mediated hybrid incompatibilities in *Arabidopsis thaliana* by *NPR1* modulation

Kostadin E. Atanasov[1] and Rubén Alcázar[1]

[1]Department of Biology, Healthcare & Environment. Section of Plant Physiology. Faculty of Pharmacy. University of Barcelona, Spain.

Published as: Thesis chapter.

*Supplemental data is included in Annex III (page 169).

RESUMEN

Arabidopsis es una planta generalmente autógama, aunque la polinización cruzada puede producirse hasta en un 3% de individuos en la naturaleza. Algunos de estos híbridos son incompatibles y muestran defectos en el crecimiento debido a interacciones epistásicas entre proteínas de la familia NLR (*Nucleotide Binding Leucine Rich Repeat*). Por otro lado, el nitrato y el amonio, después del carbono, son los elementos más importantes para el crecimiento y desarrollo vegetal. El amonio es la forma reducida del nitrógeno que más rápido se incorpora en la planta, y es esta la razón por la que gran parte de los fertilizantes usados en agricultura se basan en fórmulas de liberación más o menos rápida de amonio. No obstante, las dosis altas o acumulación de amonio pueden promover la susceptibilidad a patógenos, así como provocar efectos tóxicos en la planta disminuyendo su productividad. En este trabajo, hemos estudiado el efecto del amonio sobre la inmunidad vegetal y más específicamente, sobre las incompatibilidades híbridas. Los resultados obtenidos sugieren que altos niveles de amonio son capaces de atenuar el fenotipo híbrido incompatible, además de relacionarse con una mayor susceptibilidad a patógenos biotrofos como *Pseudomonas syringae DC3000 pv. tomate*. Finalmente, proponemos que el mecanismo por el que se atenúa la incompatibilidad híbrida mediado por el gen regulador de la respuesta inmunitaria sistémica, *NPR1*.

ABSTRACT

Arabidopsis is mainly a self-pollinator species, but 3 % outcrossing occurs in nature, which can lead to hybrid incompatibilities due to deleterious interactions involving NLR (*Nucleotide Binding Leucine Rich Repeat*) proteins. The incompatible phenotypes are shaped by the environment. Hence, higher temperature suppresses NLR-related hybrid incompatibility. From a plant nutrition point of view, NO_3^- and NH_4^+ are important elements for plant growth. Whereas NH_4^+ is the quickest way to assimilate nitrogen with limited metabolic costs, high levels of NH_4^+ can produce negative effects on plants. These are related to increased susceptibility to plant pathogens and toxicity related to NH_4^+ accumulation. In this work, we investigate the effects of NH_4^+ on the modulation of plant immunity and pathogen resistance using immune-related hybrids as model of study. We find that NH_4^+ attenuates hybrid incompatibility and we suggest that the systemic acquired resistance (SAR) master gene *NPR1* is involved in such effect.

Introduction

Plants are sessile organisms that lack an adaptive immune system (He and Wu, 2016). The main plant immune response relies on the existence of intracellular and membrane-associated receptors. Surface receptors or pattern recognition receptors (PRRs) can recognize pathogen-associated molecular patterns (PAMPs) that initiate pathogen triggered immunity (PTI). During the PTI response, the coordinated action of PRRs, their co-receptors and intracellular protein kinases trigger expression changes related with defense, propagating physiological processes that block pathogen penetration into the cell (Macho and Zipfel, 2014; Withers and Dong, 2017). Specialized biotrophic pathogens can deliver proteins into the host cell, known as effectors, that suppress PTI (Jones and Dangl, 2006). However, plants have a set of intracellular receptors that recognize effectors and initiate a robust response called effector-triggered immunity (ETI). These receptors are proteins carrying a *nucleotide binding domain* that binds ATP (NBD), *leucine-rich repeat domain* (LRR) and N-terminal *coiled-coil domain* (CC) or *Toll/interleukin-1* (TIR) (Hatsugai *et al.*, 2017). ETI also produces expression changes, massive production of reactive species of oxygen (ROS), stimulation of salicylic acid (SA) synthesis and eventually programmed cell death (PCD) at the infection sites, also known as the hypersensitive response (HR) (Vlot *et al.*, 2009). SA stimulates the expression of the pathogenesis-related protein 1 (*PR1*) and *Isochorismate synthase 1* (*ICS1*; *SALICYLIC ACID INDUCTION-DEFICIENT 2*, *SID2*), responsible for SA biosynthesis in the chloroplast. SA is also required for the signal transduction of the systemic acquired response (SAR) via *NON-EXPRESSOR OF PATHOGENESIS-RELATED 1* (NPR1). NPR1 signaling depends on the redox status of the cell. Hence, the accumulation of SA induces NPR1 monomerization, which is required for nuclear translocation and signaling (Kinkema *et al*., 2000; Mou, Fan, and Dong, 2003; Yan and Dong, 2014). NPR1 oligomerization is regulated by S-nitrosylation of certain Cys residues (e.g. Cys156), the activity of some thioredoxins (e.g. TRXH3 and TRXH5) and nitric oxide (NO) (Tada *et al*., 2008). Once in the nucleus, NPR1 recruits TGA transcription factors leading to expression changes of some NPR1 target genes (Jin *et al*., 2018; Johnson, Boden, and Arias, 2003).

Arabidopsis can grow in contrasted environments from sub-arctic and alpine to sub-desertic climates, being a basis for the study of natural variation and adaptation to

different habitats (Hoermiller *et al.,* 2018). Exploring the natural variation between accessions has revealed the occurrence of deleterious interactions between *Resistance* genes (*R*) from parental lineages, leading to constitutive activation of defense. Defense activation incurs into a cost for plant growth and reproduction, thus leading to the so-called immune-related hybrid incompatibilities (HI). Due to the high costs on fitness, hybrid incompatibilities have been proposed to be an incipient mechanism for speciation (Meinke *et al.*, 1998; Alcázar *et al.*, 2012; Provart *et al.*, 2016). One of the causes for speciation is geographical isolation, that implies genetic variation that in some cases can lead to molecular, spatial and/or anatomical incompatibilities at pre-zygotic or post-zygotic stages (Barnard-Kubow and Galloway, 2017; Bomblies, 2010; Haller *et al*., 2014; Pinheiro *et al.,* 2015; Schumer *et al.,* 2015). In the last Century, William Bateson (1909), Theodosius Dobzhansky (1932) and Herman Muller (1933), proposed a theory aimed at explaining how HI could occur. They suggested a speciation mechanism based on the accumulation of allelic variants in at least two loci from isolated populations. After time of divergence, when individuals from these populations mate again, an incompatible epistatic interaction between the diversified alleles triggers hybrid incompatibility (Bateson, 1909; Dobzhansky, 1951; Johnson, 2002; Muller, 1942). During the last decade, several cases of HI have been identified in *Arabidopsis* and in close related species (Bomblies *et al*., 2007; Case *et al.*, 2016; Mizuta *et al.*, 2010; Moyle and Nakazato, 2008; Okada *et al.*, 2017; Vaid and Laitinen, 2019). Most HI are associated with an autoimmune disease symptom, based on constitutive activation of ETI that leads to reproductive isolation (Alcázar *et al*. 2009, 2012; Bomblies *et al*. 2007; Bomblies 2010; Bomblies and Weigel 2007; Chae *et al*., 2014; Smith *et al.*, 2011; Sweigart and Willis 2012; Vaid and Laitinen 2019).

The first temperature-dependent hybrid incompatibility in *Arabidopsis* was reported between the accessions Umkirch-1 *(*Uk-1*)* and Umkirch-3 (Uk-3) (Bomblies *et al*., 2007; Chae *et al*., 2014). Uk-1 x Uk-3 F1 hybrids exhibit dwarfism and leaf necrosis at low temperature (14 ºC) (Bomblies *et al*., 2007). Authors described that incompatibility involved a two-way epistatic interaction between *DANGEROUS MIX 1 (DM1)* and *DANGEROUS MIX 2 (DM2)* loci. *DM1* from Uk-3 mapped to the *TIR-NB-LRR* locus *At5g41740 - At5g41750* and corresponds to *SUPPRESSOR OF SALICYLIC ACID INSENSITIVITY OF NPR1* 4 (*SSI4*). The *DM2* locus from the accession Uk-1 mapped to *RPP1* (*Recognition of Peronospora parasitica 1*) *At3g44630 - At3g446670*

locus of *TIR-NB-LRR* genes. More recently, by systematic analysis of several F1 populations, genomic regions have been identified that map to other *NLR* variants also leading to incompatibility with *DM2* (Chae *et al*., 2014).

Alcázar et al., 2009 reported a two-way recessive epistasic interaction between the *RPP1*-like haplotype of Landsberg *erecta* (L*e*r) (QTL3) and the Kashmir (Kas-2) allele of *Strubbelig-Receptor Family 3* (*SRF3*) (QTL4) leading to HI. L*e*r/Kas-2 incompatibility is temperature-dependent and leads to constitutive activation of defense in the absence of pathogens. Cell death, dwarfism, HR and sterility are all hallmarks of L*e*r/Kas-2 HI (Alcázar *et al.*, 2009, 2010, 2014). Causal loci for L*e*r/Kas-2 hybrid incompatibility was identified by quantitative trait of locus (*QTL*) analysis using a population of L*e*r/Kas-2 RILs (recombinant inbred lines). The QTL3 from L*er* overlaps with the *DM2* locus reported in other incompatibilities (Bomblies *et al*., 2007), although it is highly polymorphic between accessions. The causal *RPP1*-like L*e*r haplotype was found at a frequency of 30% in a local population of *A. thaliana* from Gorzów Wielkopolski (Poland) were L*e*r was originally collected in 1939 (Alcázar *et al*., 2009, 2014). Conversely, the incompatible *SRF3* Kas-2 allele is highly frequent in populations from central Asia, likely due to its contribution to enhanced basal disease resistance against bacterial pathogens (Alcázar *et al*., 2010). More recently, chemical and directed mutagenesis demonstrated that *RPP1*-like L*e*r incompatibility is fully suppressed by *R8* mutations, and partly suppressed by *R2*, *R3* and *R4* mutations. This suggests that *R2*-*R4* act additively to HI and *R8* is epistatic to other *RPP1*-like genes in the cluster. Remarkably, suppression of HI had no effect on disease resistance to a local *Hyaloperonospora arabidopsidis* isolate (Atanasov *et al*., 2018).

Interestingly, immune-related HI are influenced by the environment. As such, high temperature suppresses many HI (Bomblies *et al*., 2007). But not only temperature seems to influence the fitness outcome of HI. Here, we report that nutrient availability is an important aspect to be considered. After carbon, ammonium and nitrate (NH_4^+/NO_3^-) are the most important nutrients for plant growth. Their deficiency reduces dramatically crop production, whereas their overaccumulation can produce toxicity and negative effects on plant growth and yield (Li *et al*., 2014). NH_4^+ is quickly oxidized into NO_3^- by NH_4^+ oxidizing soil microbiota. The levels of NH_4^+ in forest soils are between 0.4 mM to 4 mM, whereas in an agriculture it ranges between 2 mM to 20 mM, or even higher concentrations under low NH_4^+ oxidizing conditions (Britto and Kronzucker,

2002a; Li *et al*., 2014). NH_4^+ soil pollution is mainly caused by human activity such as over-fertilization (Qu *et al.,* 2014), intensive cattle (Shen *et al*., 2016), industry and human organic waste (Umezawa *et al*., 2008).

NH_4^+ is not only important for plant growth but also for defense against pathogens. While nitrogen input increases plant growth and yield, it is also used by the pathogen itself in order to grow, establishing a competition for the nutrient (Tavernier *et al*., 2007). During pathogen attack, the availability of nutrients is essential to increase pathogenesis (Solomon *et al.,* 2003). To deal with this, plants relocate nutrients from the apoplast to make them less available for the pathogen at infection sites (Cao *et al.,* 2015; Schwachtje *et al.,* 2018). The global use of fertilizers based on the NH_4^+ can produce an imbalance between growth and appropriate activation of plant immune responses (Mur *et al*., 2017)**.**

In this study, we report that increasing the level of NH_4^+ is sufficient for suppression of L*er*/Kas-2 and Uk-1/Uk-3 HIs at 14 ºC – 16 ºC, both on soil and *in vitro* systems. We also established a hydroponic system suitable to test the effect of mineral nutrition on the plant immune system. In addition, we have measured pathogen growth when plants are irrigated with high levels of NH_4^+. We propose an *in vitro* Murashige and Skoog (MS) modified media, as tool for the study of the immune responses in pathogen-free systems. Finally, we find a link between immune-related HI and *NPR1*, through the finding of an intermediate HI phenotype by *NPR1* loss-of-function mutation.

Results

NH_4^+ attenuates the HI phenotypes of L*er*/Kas-2 NIL

- **Hydroponic system**

In the course of our experiments using a hydroponic system (**Figure 1**), we observed that L*er*/Kas-2 HI was suppressed at 14 ºC – 16 ºC when plants were grown using 0.5 x Murashige and Skoog (MS) solution, but not on 0.5 x Hoagland's solution (HS). To identify which component(s) in 0.5 x MS suppressed incompatibility, we cultivated plants in a hydroponic system and scaled down the concentration of each component present in 0.5 x MS to 0.5 x HS levels (**Annex III, Table 1**). We observed that reducing NH_4^+ from MS (186 mg/L) to HS levels (18 mg/L) restored HI (**Figure 2**). To determine the basal defense and oxidative stress status of L*er*/Kas-2 NIL in the different nutrient solutions, *PR1* and *GST1* expression analyses were performed in five-weeks old plants grown at 14 ºC – 16º C on 0.5x MS or 0.5x HS (**Figure 3**). L*er*/Kas-2 NIL plants cultivated on 0.5x MS or 0.5x MS supplemented with B6 vitamins exhibited much lower expression of *PR1* and *GST1* than L*er*/Kas-2 NIL grown on 0.5x HS or 0.5x HS supplemented with B6 vitamins (**Figure 3**). Lowering NH_4^+ levels in 0.5x MS triggered an increase in the expression of *PR1* and *GST1*. In contrast, lowering NO_3^- concentration did not produce such effect (**Figure 3**). We concluded that high NH_4^+ suppresses the autoimmune phenotype of the L*er*/Kas-2 NIL. Supplementation with Gamborg's B6 vitamins did not have any evident effect in the regulation of HI (**Figures 2 and 3**).

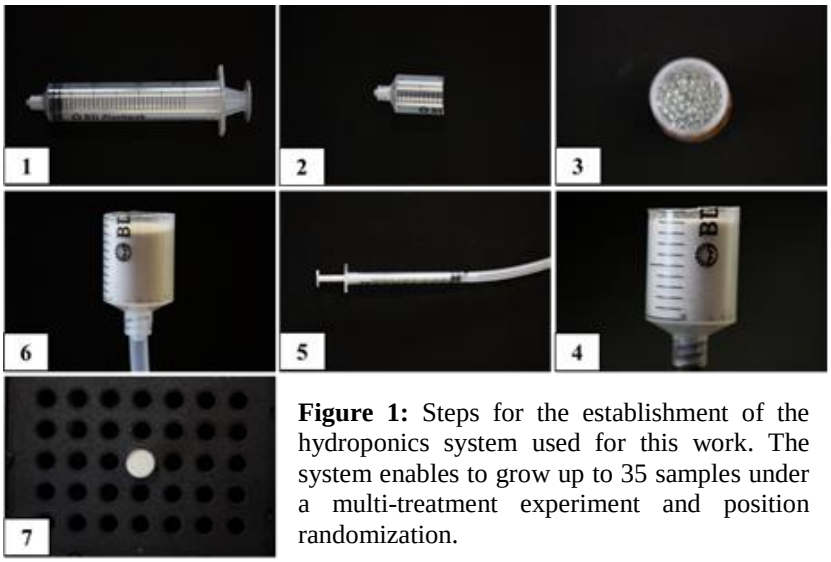

Figure 1: Steps for the establishment of the hydroponics system used for this work. The system enables to grow up to 35 samples under a multi-treatment experiment and position randomization.

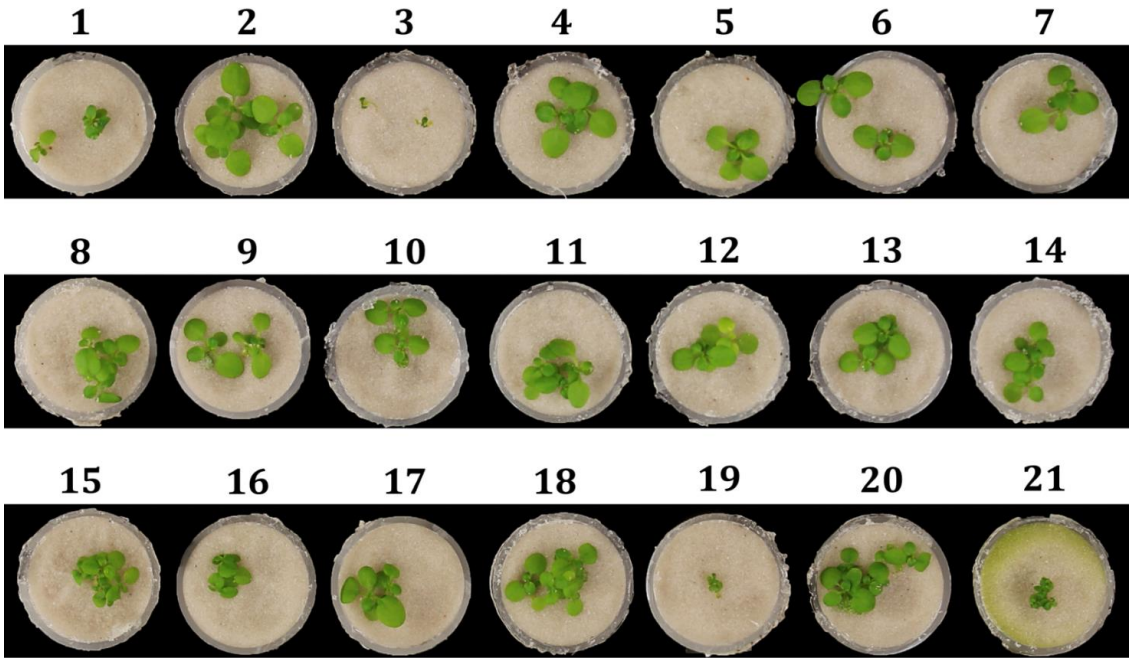

Figure 2: L*er*/Kas-2 NIL plants grown in a hydroponic system under long day conditions, 14ºC -16ºC (night/day), 70% RH. Numbers indicate individual nutrient modifications of the salt concentration (down to 0.5 x HS levels, see Table 1): 1) 1 mM NH_4NO_3 ; 2) 2 mM KNO_3; 3) 0 mM $CaCl_2$; 4) 0 mM KI; 5) 500 µM $MgSO_4 \cdot 7 \cdot H_2O$; 6) 1 mM KH_2PO_4; 7) 2 mM $Ca(NO_3)_2 \cdot 2 \cdot H_2O$; 8) 19 µM Fe-EDDHA; 9) 9 µM H_3BO_3; 10) 15 µM $MnSO_4 \cdot H_2O$; 11) 5µM $ZnSO_4 \cdot 7 \cdot H_2O$; 12) 5 µM $CuSO_4$; 13) 0.3 µM $CoCl_2$; 14) 0.9 µM $Na_2MoO_3 \cdot 2 \cdot H_2O$; 15) 0.5x HS +Gamborg B6 Vitamins; 16) 0.5x without Vit;17) 0.5x MS + Gamborg B6 Vitamins; 18) 0.5x MS without Vit; 19) dH_2O; 20) Commercial 0.5x MS-MES Including Gamborg B6 Vitamins; 21) Regular watering solution consisting of a 0.5x Hoagland & Arnon formulation.

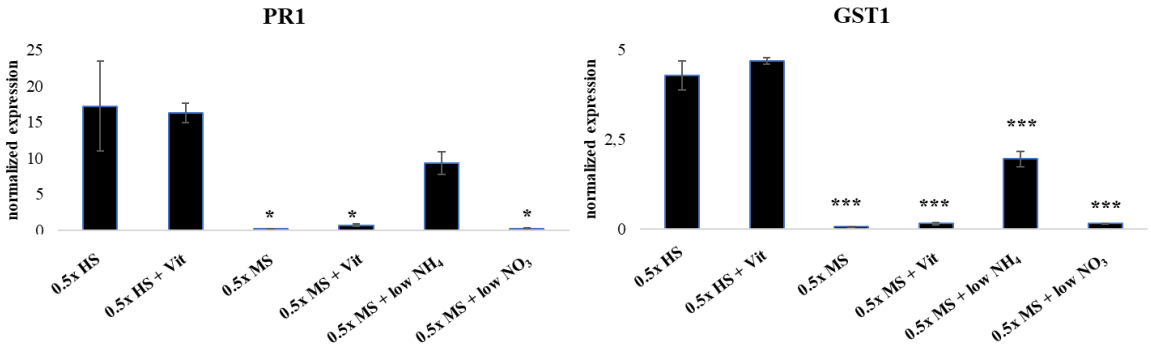

Figure 3: qRT-PCR gene expression analyses of five-weeks-old NIL plants grown in a hydroponic system under different nutrition media. Values are normalized to the housekeeping gene *ACTIN2*. Stars indicate significantly different values to 0.5 x HS (*** $p<0.001$; ** $p<0.01$; $p<0.05$) according to the T-Student test.

- **Soil conditions**

Given that high ammonium suppressed L*er*/Kas-2 HI in a hydroponic system, we asked whether this phenomenon also occurred in plants grown on soil. For this, we watered L*er*/Kas-2 NIL plants grown at 14 ºC – 16 ºC with 0.5x HS or 0.5x MS. We also included in this analysis the Uk-1/Uk-3 HI reported by Bomblies *et al*., 2007 (**Figure 4**). As shown in this figure, watering with 0.5x MS suppressed HI in L*er*/Kas-2 and Uk-1/Uk-3 hybrids. The projected leaf area of L*er*/Kas-2 NIL irrigated with conventional 0.5x MS in comparison with the 0.5x HS, was significantly higher and similar to the parental lines Kas-2 and L*er* (**Figure 5A)**. Similarly, when the incompatible Uk-1/Uk-3 hybrid was irrigated with 0.5x MS, it also restored growth to a similar degree as the parents (**Figure 5B**). We found that Col-0 accession exhibited less projected leaf area when watered with 0.5x MS than HS (**Figure 5**). This data might suggest that Col-0 is less tolerance to ammonium or other nutrient concentration present in MS. This effect was not observed in L*er*, Kas-2, Uk-1 or Uk-3 (**Figure 5**). No evident effects related with autoimmunity were observed in the parental lines L*er*, Kas-2, Uk-1, Uk-3 and Col-0 in either nutrient condition (**Figures 4 and 5**). Gene expression analyses in these genotypes evidenced the downregulation of *PR1*, *EDS1* and *GST1* expression in 0.5x MS irrigated L*er*/Kas-2 NIL plants compared with 0.5x HS treatment. The expression levels of *PR1*, *EDS1* and *GST1* resulted similar to the parental lines L*er* and Kas-2, as well the accession Col-0 (**Figure 6**).

An additional experiment was performed to determine whether increased ammonium or changes in the NH_4^+/NO_3^- ratio were causal for HI suppression. We watered plants with 0.5x HS supplemented with ammonium sulfate to reach an NH_4^+/NO_3^- ratio of 10:3 (10 mM of total NH_4^+; 3 mM of total NO_3^-) or NH_4^+/NO_3^- ratio of 1:2 (1.5 mM of total NH_4^+; 3 mM of total nitrate). In addition, we also watered with 0.5x MS supplemented with potassium nitrate to reach an NH_4^+/NO_3^- ratio of 1:3 (10.31 mM of total NH_4^+; 29.56 mM of total NO_3^-). HI suppression was observed when ammonium and nitrate were increased, maintaining 1/2 or 1/3 ratios. However, increasing the ammonium concentration to 10 mM was sufficient for suppression of HI. We quantified the extent of HI suppression by measuring the projected leaf area and trypan blue staining (**Annex III, Supplemental Figure S1)**. We concluded that increasing the ammonium concentration is sufficient for suppression of L*er*/Kas-2 HI.

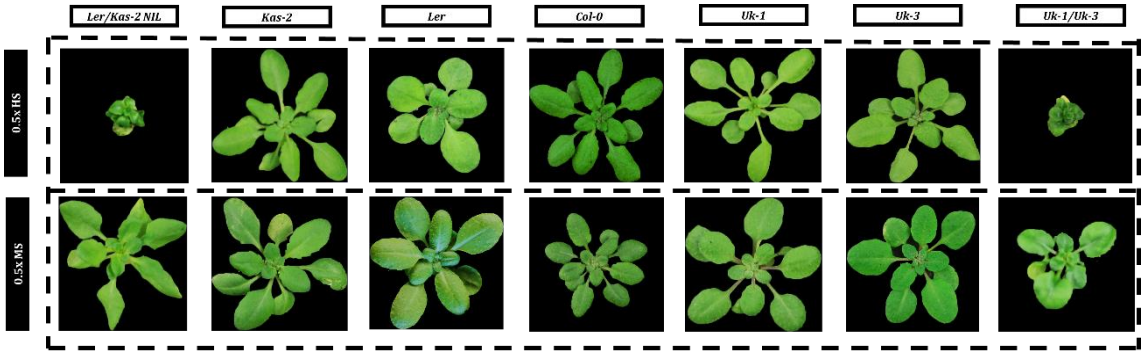

Figure 4: Phenotype of 5-week old parental lines and incompatible hybrids supplemented with 0.5x HS or 0.5 MS media and grown at low temperature (14 ºC – 16 ºC) under long day conditions and 70 % RH.

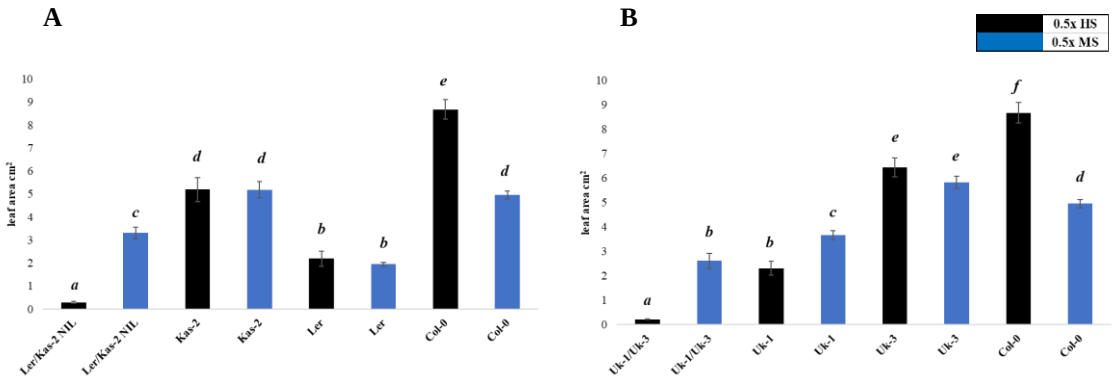

Figure 5: Leaf area measurements of five-weeks-old L*er*/Kas-2 hybrid and parental lines (A) or Uk-1/Uk-3 hybrid and parental lines (B) grown on soil at 14 ºC - 16 ºC and irrigated with 0.5 xMS or 0.5x HS media. Leaf surface analysis was determined using EasyLeafArea Software. Letters indicate significant differences according to a Student-Newman-Keuls test ($p<0.05$).

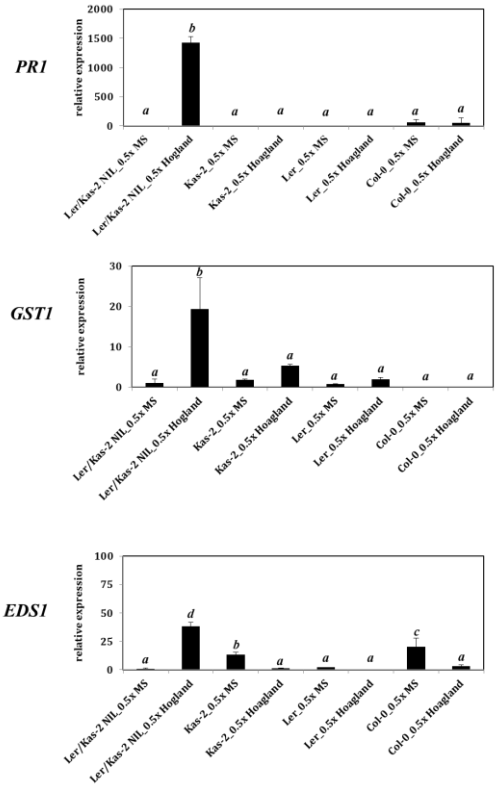

Figure 6: Quantitative gene expression analysis of *PR1*, *GST1* and *EDS1* genes. Values are relative to the L*er*/Kas-2 NIL genotype grown on soil and supplemented with 0.5x MS. Letters indicate significantly different values ($p<0.05$) according to the Student-Newman-Keuls (SNK) test.

Chlorophyll quantification as proxy for the determination of nitrogen assimilation status

We determined the chlorophyll (Chl) levels as marker for nitrogen assimilation to test whether differences could be found between treatments and genotypes. When we irrigated with 0.5x MS, we obtained an increase in Chl$_a$ and Chl$_b$ in almost all genotypes compared to 0.5x HS. Incompatible hybrids L*er*/Kas-2 NIL and Uk-1/Uk-3 also exhibited an increase in Chl content in response to 0.5x MS, whereas Col-0 exhibited an opposite behavior (**Figure 7)** consistent with a reduction of leaf area (**Figure 5**). These data point to the occurrence of natural variation for chlorophyll content related with nitrogen availability. However, we did not find evidence for impaired nitrogen assimilation in incompatible hybrids because increasing NH_4^+ availability also increased chlorophyll levels in L*er*/Kas-2 and Uk-1/Uk-3 hybrids (**Figure 7)**.

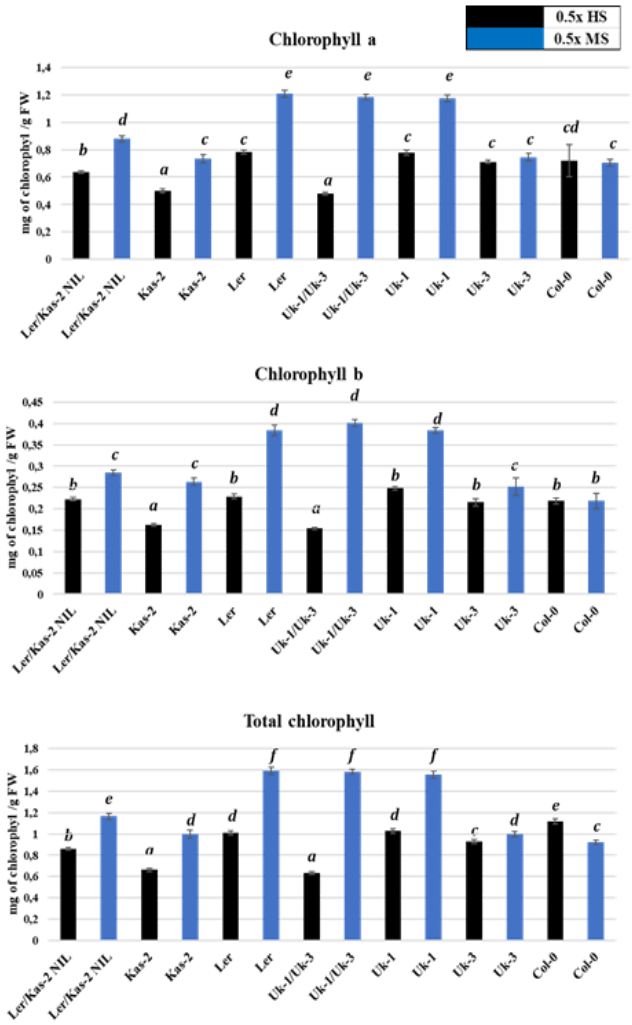

Figure 7*:* Chlorophyll *a*, *b* and total chlorophylls quantification. Letteres indicate different significant groups according to the Student-Newman-Keuls test ($p<0.05$).

Cell death determination by trypan blue staining

We determined the occurrence of cell death by trypan blue staining of leaves in the different genotypes and treatments detailed above (**Figure 8**). Microscope visualization evidenced the suppression of the cell death at low temperature (14 ºC – 16 ºC) in incompatible hybrids L*er*/Kas-2 but also Uk-1/Uk-3 irrigated with 0.5x MS. This data,

together with gene expression analyses and growth quantification, points to a full-suppression of incompatible phenotypes by MS treatment.

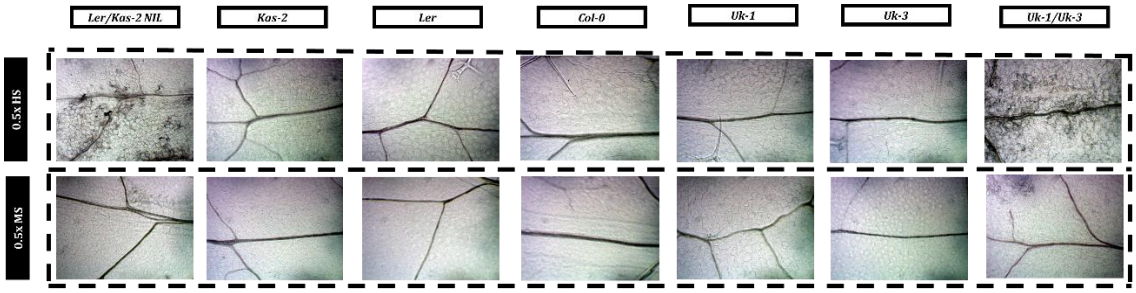

Figure 8: Trypan Blue staining of detached leaves from five-weeks-old plants grown on soil under low temperature (14 ºC – 16 ºC), long day conditions, 70% RH, and irrigated with half strength HS or MS solution..

Levels of ammonium and nitrate in soil

The striking effects of nitrogen availability on defense activation, prompted us to determine the NH_4^+ and NO_3^- levels in the MS and HS irrigated soil, and in soil from a natural population of *Arabidopsis* found in the natural Park of Collserola (Barcelona) and collected in the spring of 2017. Levels of NH_4^+ and NO_3^- from the soil irrigated with 0.5x MS were between 5 to 10 times higher than the 0.5x HS and natural soils (**Table 3; Supplemental Figure S3**). NH_4^+ values obtained were: 1047.5 µg NH_4^+ g^{-1} in 0.5x MS irrigated soil, 264.1 µg NH_4^+ g^{-1} in 0.5x HS irrigated soil and 142.6 µg NH_4^+ g^{-1} in natural soil. When we determined NO_3^- levels, they were about 10 times higher in 0.5 x MS than 0.5 x HS or natural soil. These correspond to NH_4^+/NO_3^- ratios of 1/17 (0.5x MS), 1/10 (forest soil) and 1/7 (0.5x HS). Again, we did not find a clear correlation between NH_4^+ / NO_3^- and the occurrence of HI in natural soils, Rather, high ammonium seems to be sufficient for HI suppression.

Overall, this and previous data suggest that the reduction of nitrate to ammonium is a key limiting factor in the suppression of HI. As such, when ammonium is directly added to the soil or media, it may be directly used for nitrogen metabolism whereas when provided in form of nitrate, it requires the action of two limiting enzymes (nitrate reductase and nitrite reductase) for nitrogen assimilation.

Analysis of hydrogen peroxide (H_2O_2), nitric oxide (NO) and nitrate reductase (NR) activities

It is known that reactive oxygen species (ROS) and reactive nitrogen species (RNS) participate during the plant immune response (Bellin *et al.*, 2013; Floryszak-Wieczorek and Arasimowicz-Jelonek, 2016; Gu *et al.*, 2017; Qi *et al.*, 2017; Torres, 2010; Wilkins *et al.*, 2011; Withers and Dong, 2017). We measured the levels of H_2O_2 and NO, and the activity of nitrate reductase, which is a source of NO through the reduction of NO_3^- to NH_4^+. The L*er*/Kas-2 NIL grown at 14-16 ºC did not exhibit higher H_2O_2 production than the parents, but their levels were reduced when L*er*/Kas-2 NIL plants were irrigated with 0.5x MS. Conversely, L*er*/Kas-2 NIL irrigated with 0.5x HS accumulated higher levels of NO than parental lines L*er* or Kas-2. Interestingly, NO levels in L*er*/Kas-2 NIL were reduced to similar levels of Kas-2 (isogenic background) when plants were irrigated with 0.5x MS (**Figure 9**).

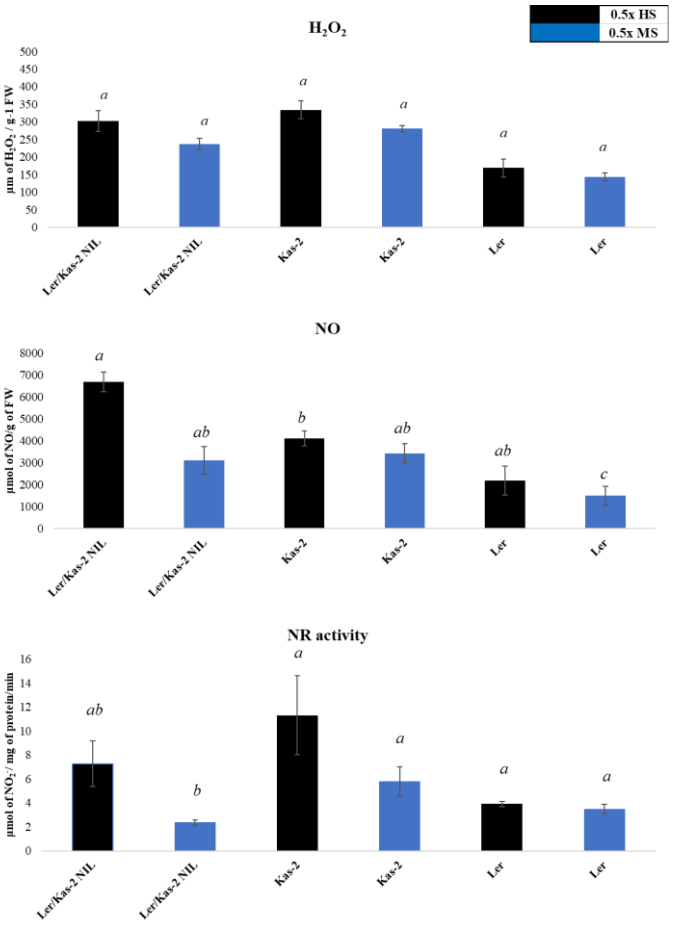

Figure 9: Quantification of the total H_2O_2 (A), nitric oxide (B) and NO_3^- reductase activity (C). NR activity values are expressed in kinetics units: 1 unit corresponds to 1 µmol of NO_2^- formed per minute and mg of protein. Letters indicate significant differences according to the Student-Newman-Keuls ($p<0.05$).

No striking differences were observed in NR activity between L*er*/Kas-2 NIL and other genotypes analyzed. However, this activity was clearly reduced when plants were irrigated with 0.5x MS (**Figure 9**). The Kas-2 accession also exhibited high NR activity,

but this was not related with hybrid incompatibility. Therefore, we also found natural variation for NR in *Arabidopsis* which was conditioned by nutrient availability. The reduced NR activity is also consistent with lower NO levels in the L*er*/Kas-2 NIL.

Analysis of the salicylic acid levels

Salicylic acid (SA) is one of the main plant compounds involved in defense (Dempsey and Klessig, 2017; Thomma *et al.*, 2011; Vlot *et al.*, 2009). Its accumulation is the key initiation factor for the systemic acquired response, known as SAR (Dempsey and Klessig, 2017; Fu and Dong, 2013). We determined total SA in rosette leaves of five-weeks old L*er*/Kas-2 NIL and Uk-1/Uk-3 hybrids and parents grown at low temperature and in both nutrient solutions. SA was quantified using the *Acinetobacter ADPWH_lux* system. Incompatible hybrids L*er*/Kas-2 NIL and Uk-1/Uk-3 irrigated with 0.5x HS accumulated high levels of total SA. Conversely, irrigation with 0.5x of MS lowered SA levels in both incompatible hybrids, although this response was stronger in L*er*/Kas-2 NIL than in Uk-1/Uk-3 (**Figure 10**). The levels of SA in Col-0 were significantly lower than other accessions. No clear differences in SA levels were detected by irrigation with 0.5x MS or 0.5x HS in Kas-2, L*er*, Uk-1, Uk-3 or Col-0. We concluded that the reduction of total SA in L*er*/Kas-2 NIL by 0.5x MS irrigation is due to suppression of HI.

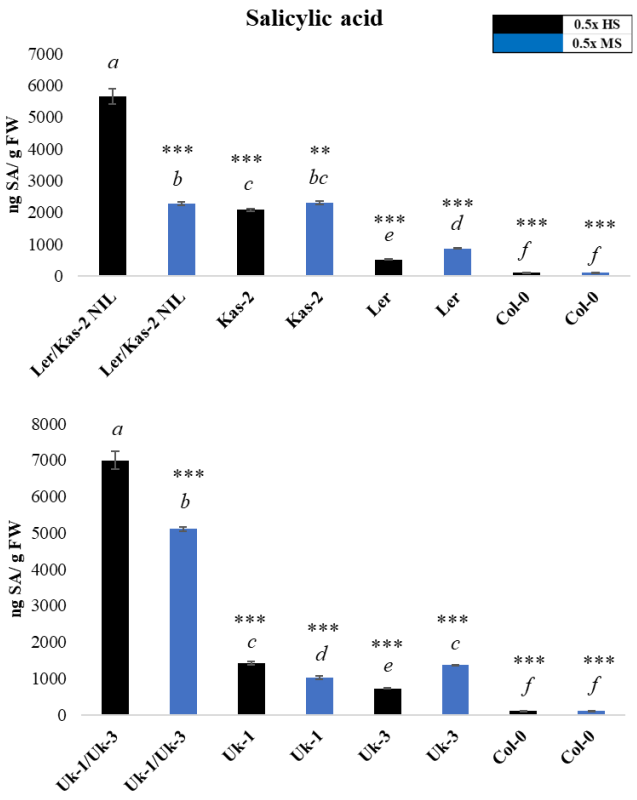

Figure 10: Total salicylic acid quantification of five-weeks old plants grown on soil at low temperature (14 ºC – 16 ºC) and irrigated with 0.5x HS or 0.5x MS. Letter indicate significant differences according to the Student-Newman-Keuls test (*** p<0.001; ** p<0.01; p<0.05).

Bacterial pathogen inoculation assays with *Pst* DC3000 pv. *tomato and Pst* DC3000 *hrcC*$^-$

In order to investigate the effect of plant nutrition on the plant immune response against biotrophic bacteria, we inoculated plants with *Pseudomonas syringae DC3000 pv. tomato* (*Pst DC3000*) and *Pst DC3000 hrcC*$^-$. Plants irrigated with 0.5x HS or 0.5x MS exhibited similar *Pst hrcC*$^-$ initial loading (3 hpi). However, differences were evident between 0.5x HS and 0.5x MS in plants spray-inoculated with the pathogenic *Pst DC3000* strain (**Figure 11A**).

When infection progressed for three days (3 dpi), we also observed evident bacterial growth differences between plants supplemented with 0.5x HS or 0.5x MS. For instance, genotypes irrigated with 0.5x MS exhibited similar bacterial growth as *Col eds1-2* in 0.5x HS. Autoimmune hybrids exhibited higher resistance against *Pst DC3000* in 0.5x HS treatment than in 0.5 x MS. The non-pathogenic *Pst hrcC*$^-$ strain did not grow in genotypes irrigated with 0.5x HS but exhibited some growth in 0.5x MS. Also, irrigation of L*er*/Kas-2 NIL and Uk-1/Uk-3 hybrids with 0.5 x MS suppressed resistance to *Pst DC3000* (**Figure 11B**). According to these data, we concluded that high nutrition facilitates higher bacterial loading (3 hpi) and more vigorous bacterial growth in the apoplast. This may result into higher levels of bacteria titers at 3 dpi. In addition, 0.5x MS attenuates HI phenotype of L*er*/Kas-2 and Uk-1/Uk-3 HI also at disease resistance against *Pst* DC3000.

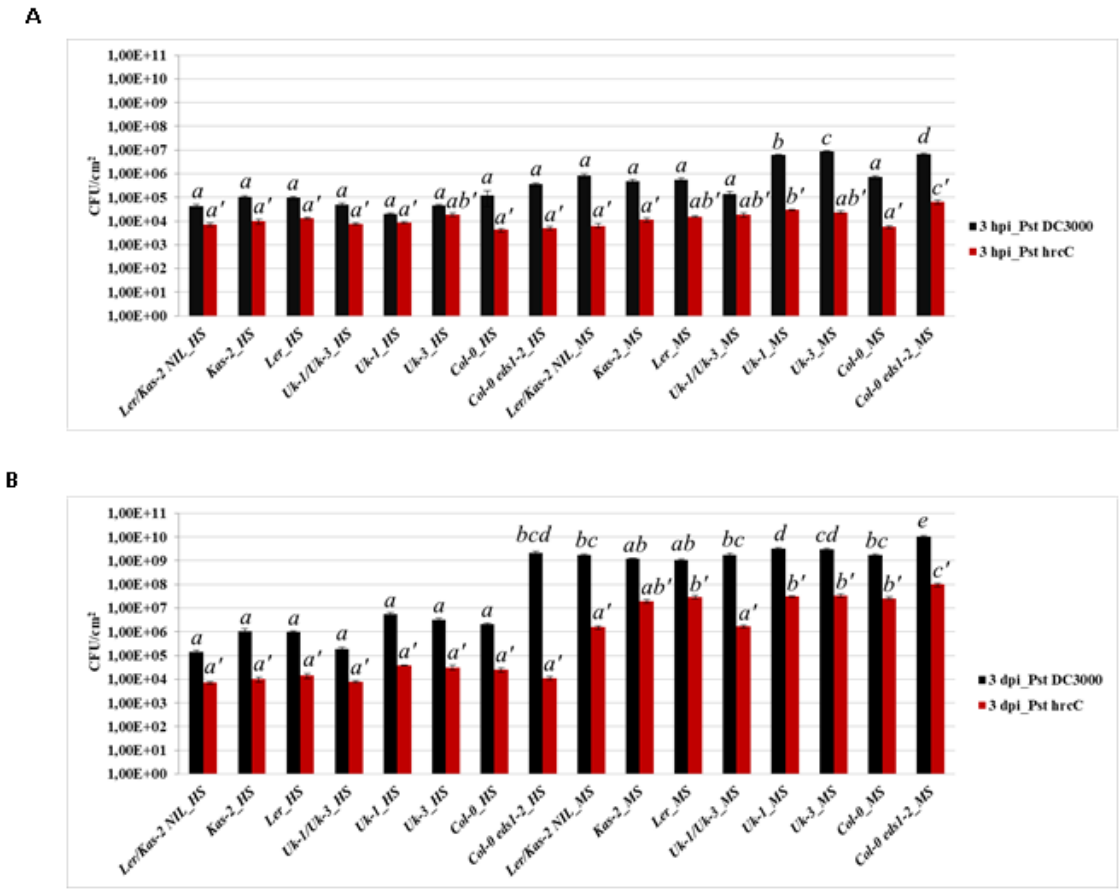

Figure 11: Disease resistance to *Pst DC3000 hrcC*$^-$ and *Pst DC3000*. Plants were irrigated with a half-strength Hoagland or Murashige and Skoog solutions. Inoculation was performed on five-weeks old plants grown at low temperature and then transferred at 20 ºC – 22 ºC to enable pathogen growth. **A)** Bacteria titers at 3 hours after spray-inoculation. **B)** Bacteria titers at 3 days after spray-inoculation. Student-Newman-Keuls test was applied to identify statistically significant differences ($p<0.05$).

Involvement of ROS and NOS on the occurrence of hybrid incompatibility

The L*er*/Kas-2 NIL does not show incompatible phenotypes when grown *in vitro* in 0.5x MS media. However, seedlings of L*er*/Kas-2 NIL grown at 14 ºC-16 ºC on 0.5x rMS (containing NH_4^+ down to 0.5x HS concentrations) reconstituted the HI phenotype (**Figure 12**) and cell death (**Figure 13**). In order to study the role of NOS and ROS on HI, five-days old seedlings grown on 0.5x rMS-MES were transferred to new 0.5x rMS-MES media containing 0.1 mM cPTIO (2-(4-carboxyphenyl)-4,4,5,5-tetramethylimidazoline-1-oxyl-3-oxide) or 0.1 mM DMTU (1,3-dimethyl-2-thiourea). Plants were incubated for 48 h and samples collected for gene expression analyses of defense-related genes. Results indicated a significant activation of defense responses

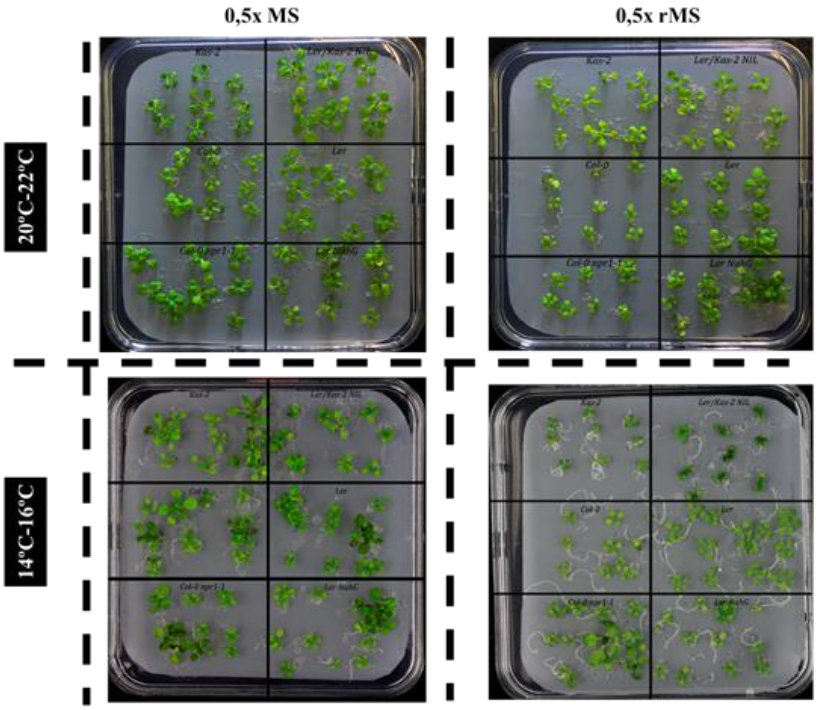

Figure 12: Twelve-days old *Arabidopsis thaliana* seedlings of L*er*/Kas-2 NIL, its parents (Ler and Kas-2), the *npr1-1* mutant and L*er* transformed with *NahG* (Salicylate hydroxylase) grown in vitro at 14 ºC – 16 ºC or 20 ºC – 22 ºC. Plants were grown on two different media: 0.5x rMS (MS with ammonium levels down to HS concentration) or 0.5x MS, both containing 1% of sucrose. The NIL phenotype is reconstituted in 0.5 x rMS at 14-16 ºC.

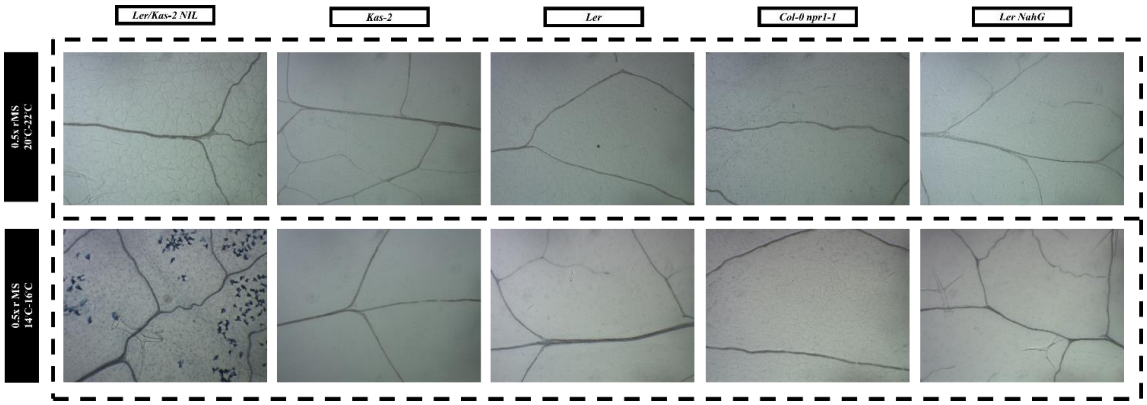

Figure 13: Trypan Blue staining of genotypes and treatments detailed in Figure 12.

when L*er*/Kas-2 NIL seedlings were grown on 0.5x rMS-MES (**Figure13; Annex III, Supplemental Figure S2**), with higher levels of *PR1*, *GST1* and *EDS1* expression than in 0.5 x MS (**Figure 14**). On other hand, when 0.5x rMS media was supplemented with the NO scavenger cPTIO or the ROS scavenger DMTU, we observed a decrease in the expression of these genes **(Figure 14)**. Seedlings treated with cPTIO exhibited less expression of *PR1*, *GST1* and *EDS1* than seedlings treated with DMTU (**Figure 14**). According to these data, we concluded that NO is important for L*er*/Kas-2 HI, and ROS might be a result of NO production. Finally, we also concluded that humidity has no effect on HI as previously suggested (Alcázar *et al*., 2009) (**Figure 11** and **Annex III, Supplemental Figure S2**).

Isolation of Ler/Kas-2 NIL in *npr1-1* background

The relevance of NO in L*er*/Kas-2 *HI* prompted us to investigate the potential role of *NPR1*. For this, we crossed L*er*/Kas-2 NIL with the Col-0 *npr1-1* mutant and isolated a quadruple homozygous mutant (**Figure 15**) from a segregating F2 population: *npr1-1* (Col-0/Col-0); *QTL3* (L*er*/L*er*); *QTL4* (Kas-2/Kas-2); *QTL5* (Kas-2/Kas-2). Growth of the L*er*/Kas-2 NIL carrying the *npr1-1* mutation was restored and cell death suppressed at 14 ºC – 16 ºC. We concluded that *NPR1* mutation partly suppressed hybrid incompatibility. We concluded that the involvement of NO on L*er*/Kas-2 HI is not exclusively mediated by *NPR1*.

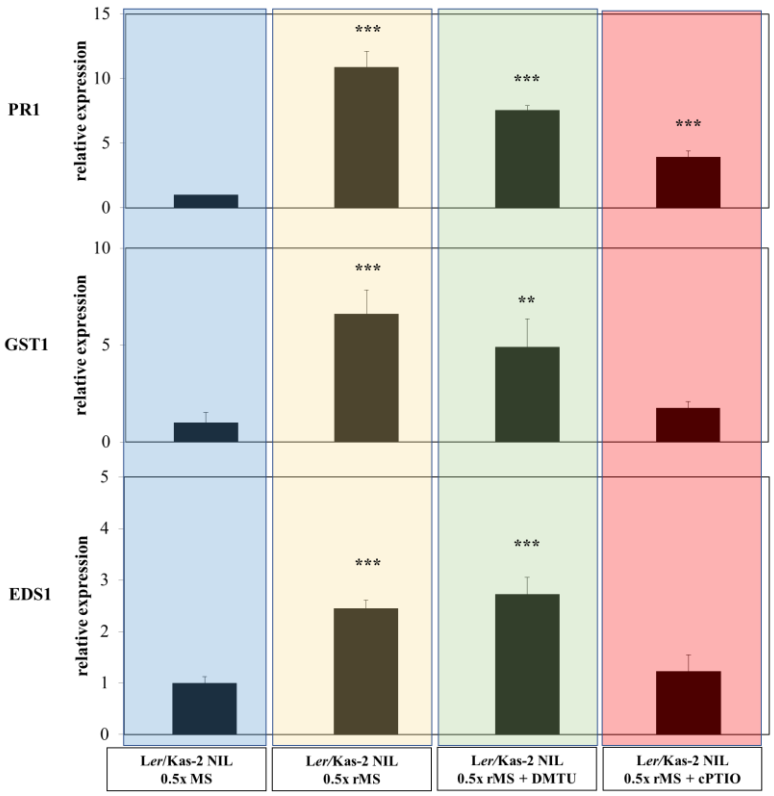

Figure 14: Quantitative gene expression analysis (RT-qPCR) of *PR1*, GST1 and *EDS1* genes in L*er*/Kas-2 NIL seedlings grown on 0.5x MS, 0.5x rMS or 0.5x rMS supplemented with DMTU or cPTIO at 14 ºC – 16 ºC. Values are relative the L*er*/Kas-2 NIL grown on 0.5x MS. Significant differences according to the t-Student test are highlighted with stars (*** p<0.001; ** p<0.01; * p<0.05).

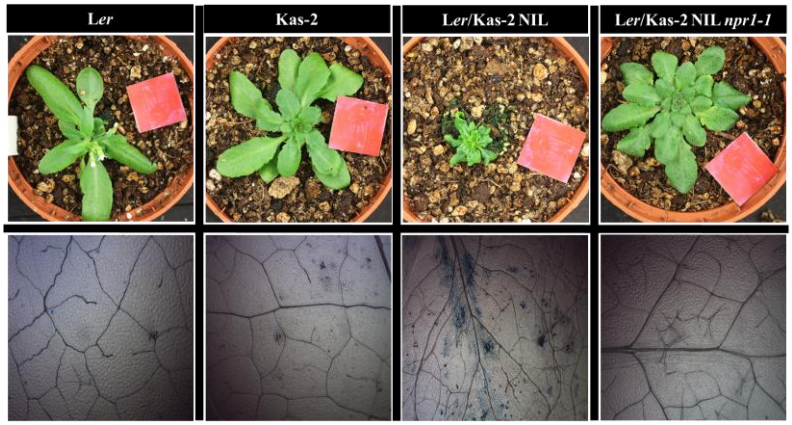

Figure 15: Pictures of five-weeks old plantlet basal rosette and the corresponding trypan blue stain for PCD detection. L*er*, Kas-2, L*er*/Kas-2 NIL and the quadruple homozygous mutant, L*er*/Kas-2 NIL *npr1-1*.

Discussion

Ammonium, as a fast nitrogen intake source for plants, can be found mainly in soil. The levels of NH_4^+ are highly variable due to leaching, nitrification or denitrification, presence of fertilizers, organic material under decomposition, soil pH, and anoxic conditions, among others (Britto and Kronzucker, 2002; Lee *et al.,* 2018). Human activity is also an important source of ammonia. Massive farming, farm-waste, fertilization of crop lands, organic material from food factories or even the chemical industry, represent global problems for the NH_4^+ environmental pollution (Lee *et al*., 2018; Shen *et al*., 2016) and has a direct relationship with the production of the hazardous gas N_2O (Huang *et al*., 2014).

In plants, NH_4^+ is fixed into amino acids via the g*lutamine synthase/glutamate synthase* GS/GOGAT cycle coupled to enzymatic activity of the *aspartate aminotransferase* (AAT) and *asparagine synthase* (AS) (Coruzzi, 2003). Glutamine (Gln) and, in less quantity asparagine (Asn), are transported to the shoot by the plant vascular system for its use in anabolic processes (Tischner, 2000). On other hand, the intake and utilization of nitrogen is more tedious and has important metabolic costs (Nunes-Nesi *et al.,* 2010). Nitrogen assimilation requires a reduction to NH_4^+ and later, fixation into Gln. In *Arabidopsis*, there are more than ten NO_3^- transporters (NRT) which are tissue specific and exhibit low or high affinity (Masclaux-Daubresse *et al*., 2010; Noguero and Lacombe, 2016; Wang *et al.,* 2012). Nitrate intake is performed in roots. It can be translocated to the shoot by xylem vessels or assimilated in root cells via NRT. In the cell, NO_3^- is reduced into nitrite (NO_2^-) by *nitrate reductase* (NR) which can also generate NO, a multitasked signaling gas (Domingos *et al*., 2015). NR activity is temperature dependent and negatively feed-back regulated by nitrite (Cheeseman and Tankou, 2004; Winck *et al*., 2015) (Ghosh *et al.,* 2000). However, NO_2^- is extremely toxic and it is converted into ammonium by the *nitrite reductase* (NiR) and finally, fixed into Gln and Asn (Stitt, 1999). In our research, we have demonstrated the importance of N on the immune system modulation (**Figure 11**). The importance of the NH_4^+/ NO_3^- ratio was demonstrated to play an important input signal in autoimmune mutant *suppressor of npr1-1, constitutive 1* (*SNC1*) and *nudix hydrolase homologues nudt6-2/nudt7 (AtNUDT6/7).* SNC1 is a TNL receptor involved in the SAR response (Wang *et al*., 2017). Low NH_4^+/NO_3^- ratio stimulates *snc1* autoimmunity whereas a

high ratio inhibits autoimmunity (Wang *et al*., 2013). On the other hand, *NUDT* codes for an *ADP-ribose/NADH pyrophosphohydrolase*. *AtNUDT6* positively regulates NPR1-dependent SA signaling, whereas *AtNUDT7* is a negative regulator of *EDS1* and hence, plant basal immunity (Fonseca and Dong, 2014; Ge *et al*., 2007; Ishikawa *et al*., 2010; Wang *et al*., 2017). It is thought that NUDT proteins can modulate AMP/ATP levels which are sensed by SnRK1 protein kinase regulating NR activity and *Gln synthase* (GS) (Moorhead *et al*., 2003). Nevertheless, it is still an issue of research the link between NUDT genes and the regulation of NR or GS activities in relation with defense.

In our study, we have used the incompatible lines L*er*/Kas-2 NIL and Uk-1/Uk-3, involving *TIR-NB-LRR* genes, to study the effects from N availability on the autoimmune response. Plants grown on soil and irrigated with 0.5x MS exhibited an attenuated phenotype of HI (**Figure 4** and **Figure 8**), with a partial growth recovery and higher leaf area (**Figure 6**), decreased expression of defense and oxidative stress-related marker genes (*PR1*, *EDS1* and *GST1*) and significantly lower levels of SA and cell death in comparison with the 0.5x HS treated group (**Figure 3** and **Figure 5**). We have also quantified NH_4^+ and NO_3^- levels in irrigated soil and compared them with a natural soil collected from a local population of *A. thaliana* in Collserola. The measured approximate ratios of NH_4^+/ NO_3^- in the 0.5x MS, 0.5x HS and natural soil were 1/20, 1/7, and 1/10, respectively. We consider that the two times lower ratio found in the 0.5x MS soil is due to ammonia oxidizing microbiota that oxidizes NH_4^+ to NO_3^- (Bothe *et al*., 2000). The discrepancy between our findings and the suggested ratio input-signal described by Wang *et al*., 2013, can be explained considering that these represent individual cases of autoimmunity (**Annex III, Supplemental Figure S1**).

The quick assimilation of NH_4^+ and its fixation into amino acids, nutritionally enriches plants compartments, such as the apoplastic space. Apoplastic nutrients are used by pathogens to grow. Pathogen-apoplastic growth is enhanced and can be related with higher disease (Schwachtje *et al*., 2018). By using a non-pathogenic mutant *Pst hrcC*$^-$ and the *Pst DC3000*, we observed higher levels of bacteria growth, not only at the final stage of infection (3 dpi) but also 3 h post infection (**Figure 11**). Higher bacterial loading at 3 hpi can be a consequence of higher bacteria entrance through stomata. This might be due to stomata aperture in a scenario of higher photosynthetic activity under optimal nutrient conditions provided by 0.5x MS (Geiger *et al*., 1999).

The temperature-dependent hybrid incompatibilities and their autoimmunity have direct impact on plant metabolism. Immune-system activation requires the usage of C, N and P for the synthesis of secondary metabolites involved in immune response against pathogens. Plants use carbohydrates for the synthesis of secondary compounds such as SA and for plant cell wall strengthening, contributing to metabolic costs on growth. When N assimilation and usage is limited, one of the first phenotypic indicators is the occurrence of chlorophyll loss. Chlorophyll quantification can be considered as a good indicator of N contents in leaves (Yu *et al*., 2014). Incompatible hybrid, irrigated with 0.5x HS solution exhibit total chlorophylls levels similar to the parental lines, and when they are irrigated with ammonia-rich media (0.5x MS), total chlorophyll levels increase similarly to the parents. Nevertheless, we have not observed such a response in the accessions Uk-3 and Col-0 (**Figure 7**). This may be due to differences in ammonia toxicity (Sarasketa *et al.,* 2014). In addition, N_2O and NO_2^- toxicity at root stage cannot be excluded. The immune-related HI phenotypes are unlikely to be due to limited N resources because the amino acid levels are not strikingly reduced bur rather increased probably due to proteolysis (Atanasov *et. al.,* 2017). As such, it seems that nutrition (high ammonium availability) suppresses defense activation, and all its associated phenotypes, rather than ameliorating growth defects with no changes on the immune status.

During the immune response, one of the main characteristics is the production of reactive species of oxygen. ROS can be produced by different ways. PAMP, MAMP (microbial associated molecular patterns) or DAMP (damage associated molecular patterns) recognition by immune receptors, stimulates specific plasma-membrane *NADPH oxidases* (RBOHs) to produce ROS. Two isoforms of RBOH proteins are described to play a role in the PTI response, the *respiratory burst oxidases homologs D* and *F* (Torres *et al.,* 2002). Also, ROS triggers defense related gene expression changes, hypersensitive response, stimulates SA and NO synthesis, among other immune-related processes (Torres, 2010). This study demonstrates that plant nutrition with high NH_4^+, e.g. 0.5x MS or 0.5x HS supplemented with ammonium (**Annex III, Supplemental Figure S1**), leads to lower expression of *PR1*, *GST1* and *EDS1* genes in incompatible hybrids (**Figure 5**). Conversely, irrigation with 0.5x HS media associates with higher production of H_2O_2 and NO. Nitric oxide production correlates with higher NR activity **(Figure 9)**. Treatment with the NO scavenger, cPTIO, decreases the expression of

defense marker genes whereas limited changes are observed with the H_2O_2 scavenger, DMTU (**Figure 14**). Hence, the production of RNS seems relevant for the HI phenotype. Pathogen colonization and PTI trigger hydrogen peroxide production, which in turns stimulates NO synthesis. However, not all pathogens trigger NO accumulation (Thalineau *et al*., 2016). We suggest that ROS and NO have different roles depending of the immune response. The produced nitric oxide, regulated via the storage molecule S-nitrosoglutathione (GSNO), is used as substrate for S-nitrosylation of NPR1 (Lindermayr *et al*., 2010). NPR1 oligomerizes in the cytoplasm and upon S-nitrosylation, a conformational change is induced delivering monomers that translocate into the nuclei, triggering SAR response gene-expression changes (Lindermayr *et al*., 2010; Mou *et al*., 2003; Tada *et al*., 2008). SA stimulates the synthesis of NO via nitric oxide synthase (Zottini *et al*., 2007) and in this complex signaling pathway, NO and SA, act synergistically upstream of NPR1 (El-Shetehy *et al*., 2015). In this study, we used the *npr1-1* allele which was identified by EMS mutagenesis by Cao et al., (Cao *et al*., 1997). *npr1-1* has a mutation in a highly conserved histidine residue (*H334Y*) in the ankyrin-repeat motif, which is necessary to interact with TGA transcription factors and trigger *PR* expression and SAR (Boyle *et al*., 2009; Cao *et al*., 1997). We have demonstrated that NPR1 is required for a complete HI phenotype and we suggest that this is due, at least partly, to the NO dependency of the L*er*/Kas-2 HI. The role of abiotic factors and their effects on plant immune response, is not fully understood. The *constitutive expressor of PR-1* mutant, *cpr1-1*, exhibits severe autoimmunity, PCD and dwarfism and is fully suppressed when is grown at 28 ºC (Wang *et al*., 2017). The *mitogen-activated protein kinase 4* (MPK4) is a negative regulator of the PTI, ETI and SAR (Bigeard *et al.*, 2015; Colcombet *et al.*, 2013; Petersen *et al*., 2000). Its mutant, *mpk4*, exhibits growth arrest and massive HR. The *mpk4* phenotype is suppressed increasing the temperature above 28 ºC or under high humidity, such as under *in vitro* conditions (Ichimura *et al*., 2006; Kong *et al*., 2012). The *sensitive to low humidity 1*, *slh1*, a TIR-NB-LRR receptor with a WRKY domain, has normal growth under *in vitro* but severe defense response when is transferred *ex vitro* (Noutoshi *et al*., 2005). It remains to be determined whether *in vitro* phenotypes are associated with nutrient compositions of the media.

Material and methods

Plant materials

L*e*r and Kas-2 accessions, Near Isogenic Line L*e*r/Kas-2 NIL and the NIL transformed with *SRF3*^{Ler} (*c*NIL) have been previously reported (Alcázar *et al*., 2010, 2009; Alcázar and Parker, 2011; Alcázar *et al*., 2012, 2014; Koornneef and Meinke, 2010). The Uk-1/Uk-3 incompatible hybrid was obtained by crossing Uk-1 and Uk-3 (Bomblies *et al*., 2007). Descents were selected according to the phenotype of strong HI (cell death, sterility and dwarfism). A stable F_5 population with homogeneous HI phenotype was used in this study. Immune related mutants, such as *eds1-2* Col-0 *(At3g48090)*, *npr1-1* Col-0 *(At1g64280)* and the L*e*r *NahG* transgenic line, were kindly provided by Prof. Dr. Jane E. Parker (Max Planck Institute for Plant Breeding Research, Cologne, Germany). The Col-0 (CS60000), Uk-1 (CS76620) and Uk-3 (CS28789) accessions were purchased from the Nottingham Arabidopsis Stock Center (NASC, http://arabidopsis.info/).

Hydroponic system

A hydroponic system was developed to test the effect of different nutrients on plant growth and disease resistance. A 30 ml Luer-Lok syringe (Becton Dickinson) was cut at 10 ml and the bench filled with a layer of 2.85-3.45 mm diameter glass beads (Carl Roth GmbH). The remaining volume was filled with Fontainebleau sand (VWR), which was washed ten times to ensure nutrient free conditions. A silicon tube was attached to the bottom of the syringe to remove, by aspiration, the excess of liquid in order to avoid anoxic conditions. The system was mounted into an Araponics box (http://www.araponics.com) placing the pots in vertical position **(Figure 1).** Four-days vernalized seeds were placed in the middle of the pot and grown under long day conditions (16h light, 8h dark) at a temperature of 14 ºC – 16 ºC, 70 % RH and 160 µmol photons $m^{-2} \cdot s^{-1}$ of light intensity. The effect on HI of macro/micronutrients and Gamborg B_6 Vitamins contained in Murashige & Skoog (MS) were tested individually, by scaling down to Hoagland's solution concentrations while maintaining the remaining nutrients at 0.5 x MS concentration (**Annex III, Table 1**). Plantlets were supplemented every two days with 1 ml of the specific nutrient solution and excess of media purged with the syringe (**Figure 1, step 5**).

Plant growth on soil

A mixture of peat moss : vermiculite : perlite (40:50:10) was used for plant growth on soil. Seeds were vernalized for at least 4 days on wet paper at 4ºC in the dark. Seeds were sown on pots containing 100 ml of substrate. Plants were grown for five weeks under long day conditions as detailed before. For treatments, plants were watered with different nutrient solutions: a traditional Hoagland and Arnon nutrient solution (Hoagland and Arnon, 1938) referred as 0.5x HS, 0.5x Murashige and Skoog (0.5x MS) solution, low NH_4^+ Murashige & Skoog (rMS), 0.5x HS solution supplemented with ammonium sulfate and 0.5x MS supplemented with potassium nitrate **(Annex III, Tables 2.1** and **2.2).**

Leaf area measurements

Shoots were detached, flattened and placed on a black surface including a 4 cm^2 scale for leaf area normalization. Pictures were captured with a Canon EOS 450D digital camera, using a Macro Lens (EFS 60mm f/2.8 USM). Leaf area measurements were performed using the Easy-Leaf-Area Software (Easlon and Bloom, 2014).

In vitro growth conditions and treatments

Two different Murashige & Skoog media were used in this study (MS and rMS) **(Annex III, Table 2.1)**. Both medias were supplemented with 1 % sucrose, 0.5 g/l of 2-(N-morpholino) ethanesulfonic acid (MES), 0.8 % plant agar and pH=5.8 adjusted with 1N KOH. Usually, seeds were placed on a sterilized nylon mesh (43 µm, Sefar Maissa, Spain) on top of the media, vernalized for at least four days and putted at light. Three days post-light growth, seedlings were transferred to a new plate and grown for 12 days more.

Treatments with cPTIO and DMTU

In vitro experiments were carried out to test the involvement of reactive nitrogen species (RNS) and ROS. The NO scavenger cPTIO [2-(4-carboxyphenyl)-4,4,5,5-tetramethylimidazoline-1-oxyl-3-oxide] (Sigma) and the H_2O_2 scavenger DMTU (1,3-dimethyl-2-thiourea) (Sigma) were used. Five-days old seedlings grown at 14 °C - 16 °C on 0.5x rMS-MES were transferred to new media containing 0.1 mM cPTIO or 0.1 mM

DMTU. Plantlets were incubated during 48 h and samples collected for RNA extraction and gene expression analyses.

Quantitative real-time PCR gene expression analysis (qRT-PCR)

Total RNA was extracted using TRI Reagent (Sigma-Aldrich) and the RNA dissolved in DEPC water (Sigma-Aldrich). Two micrograms of RNA were treated with DNase I (Invitrogen) and the cDNA synthesized using Superscript IV (Invitrogen) according to the manufacturer's instructions. qRT-PCR was performed using SYBR Green Master Mix kit (Bio-Rad) on a Roche Light Cycler 480 II device, following the following PCR conditions: 95 ºC for 15 sec (denaturing); 60 ºC for 15 sec (annealing) and 68 ºC for 1 min (extension). Standard curves were performed to calculate primer efficiencies. Primers and their sequences used for gene expression analyses are listed in **Annex III, Table 4.**

Chlorophyll quantification

Plant material was harvested and homogenized in mortar and pestle under liquid nitrogen. 200 mg of plant material was transferred into 1.5 ml Eppendorf tube and mixed with 1 ml of 80% Tris-buffered acetone (pH=7.8). Samples were incubated at 70 ºC for 10 minutes, cooled down on ice bath and the absorbance recorded at 663 nm (Chl *a*) and 645 nm (Chl *b*). Pigment quantification from at least five biological replicates was performed according to Porra, 2002.

Hydrogen peroxide quantification

Hydrogen peroxide (H_2O_2) was extracted and quantified by using a colorimetric method as described in Velikova *et al*., 2000. Plant material from the entire shoot was grinded in liquid nitrogen using mortar and pestle until a fine powder was obtained. Ten milligrams of the homogenized plant material were transferred to 1.5 ml tubes and mixed with 0.5 ml of fresh 0.1% (w/v) trichloroacetic acid (TCA). Samples were vortexed for 30 seconds, incubated on ice bath for 15 minutes and centrifuged at 15.000 *g* for 15 minutes at 4 ºC. The supernatant was transferred into a new tube and mixed with 0.5 ml 10 mM potassium dihydrogen phosphate buffer (pH=7.0). The reaction was started by the addition of 1 ml 1M KI and the absorbance measured during one min at

390 nm using an UV2310 Spectrophotometer (DINKO Industries). Standard curve was performed by preparing standard solutions of H_2O_2.

Nitric Oxide (NO) quantification

Nitric oxide (NO) quantification was performed following a modification of the protocol described by Zhou *et al.,* 2005. Twenty milligrams of homogenized plant material were mixed with 0.5 ml ice cold 50 mM acetic acid containing 4 % (w/v) zinc acetate (pH=3.6). Samples were incubated on ice for 15 min and centrifuged at 10.000 *g* for 15 min at 4 ºC. The supernatant was collected on a new tube and the pellet washed one more time. Both supernatants were treated with activated charcoal, centrifuged at 15.000 *g* for 15 minutes at 4 ºC. For this extract pool, one volume of Griess reagent (Sigma-Aldrich) was added to start the reaction. After 30 min of incubation at room temperature, the absorbance was determined at 540 nm. Standard curves were performed with increasing concentrations of $NaNO_2$.

Nitrate activity measurements

Nitrate reductase (NR) activity was measured according to the method described by Park et al., 2011. For NR activity analysis, we used at least five biological replicates from five-weeks old plants. The entire shoot was homogenized in liquid nitrogen and 20 mg mixed with an extraction buffer containing 100 mM potassium dihydrogen phosphate (pH=7.5), 5 mM magnesium acetate, 10 % (v/v) glycerol, 10% (w/v) polyvinylpyrrolidone (PVP), 0.1% (v/v) Triton X-100, 1 mM EDTA, 1 mM phenylmethyl sulfonyl fluoride (PMSF), 1 mM benzamidine and 1 mM 6-aminocaproic acid. After 15 min of centrifugation at 16.000 *g* at 4 ºC, the supernatant was immediately used for the determination of the enzymatic activity. 200 µl of crude extract were mixed with reaction buffer (50 mM KH_2PO_3 pH=7.5; 10 mM KNO_3 and 100 µM NADPH). The mixture was incubated for 15 min at room temperature and the reaction stopped by addition of 1% (w/v) sulphanilamide and Griess reagent. Samples were incubated at room temperature for one hour and the absorbance determined at 540 nm. A standard curve was determined with $NaNO_2$ and the activity normalized according to the total amount of protein quantified with Bradford Reagent (Bio-Rad) following manufacturer's instructions.

Salicylic acid quantification

Salicylic acid (SA) from plant material was traditionally analyzed by High Performance Liquid Chromatography (HPLC). During last two decades a variety of techniques has been appeared: Electrospray ionization (ESI) tandem mass spectrometry, colorimetric assay with titanium or iron dioxide nanoparticles, reverse iontophoretic detection and the biosensor system based on *Acinetobacter ADPWH_lux* (Chang *et al*., 2017; DeFraia *et al.,* 2008; González-Sánchez *et al.,* 2015; Pastor *et al*., 2012; Sánchez *et al.*, 2017; Tseng *et al*., 2014).

Extraction and quantification of SA was performed with a modified from DeFraia et al., (DeFraia *et al*., 2008). For in vitro plant material, samples were collected in 1.5 ml Eppendorf Safe Lock tubes (Eppendorf) containing a 0.2 cm diameter glass beads and immediately submerged in liquid nitrogen. Samples were homogenized with a Silamat S6 device (Ivoclar Vivadent) at maximum speed. 200 mg of plants grown on soil was homogenized using mortar and pestle in liquid nitrogen. 250 µl of 100 mM sodium acetate (pH=5.5) was added to the samples, vortexed and thawn on ice for 30 min. After centrifugation at 16.000 *g* for 15 min at 4 ºC, 200 µl of the supernatant was treated with 2U of β-glucosidase and incubated at 37 ºC for 1.5 h. Samples were then frozen for at least 3 h for enzymatic deactivation. Bacteria incubation was performed by adding 50 µl of *Acinetobacter ADPWH_lux* cell suspension (OD_{600}=0.4) to 200 µl of plant crude extract and incubated at 37 ºC for 1h. Standards of known SA concentrations and the negative control (L*er NahG* plant extract) were also included for data quantification and background subtraction.

***Pseudomonas syringae pv. tomato DC3000* (*Pst DC3000*) and *Pseudomonas syringae pv. tomato DC3000 hrcC*$^-$ (*Pst DC300 hrcC*$^-$) infections**

Pseudomonas syringae has more than 50 strains which can infect different plant species (Höfte and De Vos, 2006). *Pst DC3000* is a tomato biotrophic pathogen which can also infect *A. thaliana* and *Nicotiana benthamiana*. During the last decades, it has been widely used to study the *Arabidopsis* immune system providing to the research community a valuable knowledge about the molecular interaction that determinates the fate of resistance or susceptibility (Bektas and Eulgem, 2014; Carstens *et al.,* 2014; Nitta *et al*., 2014; Preiter *et al.,* 2005; Rico and Preston, 2008; Xin and He, 2013; Yang

et al., 2015; Zeng *et al.*, 2011). *Pst DC3000 hrcC*$^{-}$ is a type III secretion system (TTSS) mutant that induces a strong PTI response (Geeta and Mishra, 2018; Rathore and Ghosh, 2018; Rustagi *et al.*, 2018; Tiku, 2018).

To proceed with pathogen inoculation, *Pst DC3000* and *Pst DC3000 hrcC*$^{-}$ strains were inoculated in 5 ml NYGA liquid media (**Annex III, Table 5)** containing 50 µg/µl rifampicin. After an overnight culture at 28 ºC at 200 rpm, 1 ml of the culture was diluted to 50 ml fresh NYGA media containing the appropriate antibiotics. Cultures were incubated for one day more, under the same conditions and centrifuged for 15 min at 4.000 rpm. The pellet was resuspended on sterile 10 mM $MgCl_2$, adjusting the optical density to an $OD_{600\ nm}$ = 0.2 ($1 \cdot 10^8$ cfu·ml^{-1}). Before inoculation, plants were watered for 2 h and covered to increase the humidity. The bacteria were resuspended in a solution containing 10 mM $MgCl_2$ supplemented with 0.04 % of Silwet-77 (Lehle Seeds). Inoculation was performed by spraying.

Leaf bacterial recovery and bacterial growth curves.

Pst DC3000 and *Pst DC3000 hrcC*$^{-}$ were recovered from infected leaves at two different time points: three hours post-inoculation (T_{3hpi}) and three days post-inoculation (T_{3dpi}). We did at least five technical replicates. Each replicate consists of three 0.5 cm discs excised from the middle leaf-rib, from three individual plants. Leaf discs were incubated in 1 ml of sterile 10 mM $MgCl_2$ solution; 0.01% Silwet-77 for 1 h at 28 ºC shaking at 600 rpm. A serial dilution was performed and 5 µl droplets platted on NYGA solid media containing Rifa50, according to bacterial resistance. Plates were incubated at 28 ºC for 48 h and colonies counted for bacterial quantification. Values of bacterial growth curves were reported in cfu * cm^2.

Trypan blue staining

Generally, we used fully extended leaves from five-weeks old plants grown on soil under low temperature, or either, from twelve-days old seedlings grown in vitro. Trypan blue staining was based on Kock and Slusarenko (Koch and Slusarenko, 1990). Five leaves from at least three plants were detached and immersed into trypan blue solution (0.025 % w/v Trypan blue, 8% phenol v/v, 8% lactic acid v/v, 67% ethanol v/v and 17% of water v/v). Samples were heated at 95 ºC for 5 min, incubated at room temperature and washed one time with distilled water. De-staining was performed by adding chloral

hydrate solution (5:2 w/v) and incubated for two days in the dark shaking at 50 rpm. Finally, preparations were mounted in 70% glycerol and images taken with a Moticam 5.0 MP camera in a Motic BA310 Microscope and (MoticEurope).

Crosses, mapping and sequencing

Emasculated flowers from adult L*er*/Kas-5 NIL plants were pollinated with Col-0 *npr1-1* mutant. We obtained 38 F1 seeds from two successful crosses (L*er*/Kas-2/Col-0 *npr1-1*). After two weeks of maturation to break dormancy, seeds were imbibed in distilled water and vernalized for four days. Plants were cultivated for five weeks on soil at low temperature (14 ºC – 16 ºC) and once no HI was observed, the temperature was changed to 20 ºC – 22 ºC to promote flowering and seed set. L*er*/Kas-2/Col-0 *npr1-1 F2* generation was grown at low temperature and HI segregation determined.

Genomic DNA extraction

We extracted gDNA from Ler/Kas-2/Col-0 *npr1-1 F2* plants according to the modified protocol of Dellaporta (Dellaporta *et al.,* 1983; Weigel and Glazebrook, 2009) Solutions used for gDNA extraction are described in **Annex III, Table 6**. Two fully expanded leaves were detached from four-weeks old plants grown under low temperature, long day conditions and 70% RH. Plant material was introduced in 96 collection microtubes (Qiagen) sealed with silicon caps, submerged in liquid nitrogen and homogenized in Qiagen TissueLyser II for 10 sec at frequency of 30 cycles per second. 300 µl of EB1 was added and samples homogenized once more. 20 µl of 20 % SDS was added to the samples, quickly mixed and incubated at 65 ºC for 10 min, mixed with 80 µl 5 M KAc and incubated for 15 min on ice. Samples were centrifuged at 4.000 rpm for 5 min, and 200 µl of the supernatant transferred in a new 96 well collection rack. 20 µl of 3 M NaAc and 220 µl of IPA was added and mixed with the crude extract. Samples were centrifuged at 4.000 rpm for 10 minutes and the supernatant carefully discarded. The pellet was dissolved in 200 µl of EB2 and mixed with 20 µl of 3M NaAc and 450 µl of 96 % EtOH. Samples were centrifuged at 4.000 rpm for 10 min and pellet washed at least one time with 70 % EtOH. Finally, the pellet was air-dried for 15 min and dissolved in 100 µl of $_{dd}H_2O$.

PCR marker amplification and CAPS genotyping

PCR markers covered four different genomic regions: *QTL3* (*F9K21*), *QTL4* (*F4C21.22*), *QTL5* (*MVA3*) and chromosome 1 (*F11P17* and *F5I14*). Cleaved Amplified Polymorphic Sequences (CAPS) genotyping (Konieczny and Ausubel, 1993) and markers were designed according to Hou *et al.*, 2010. PCR products were loaded on 2-3 % agarose gel with 0.04 % Ethidium bromide (EtBr). Gels were captured using a UV transilluminator (VilberLourmat), EOS 1300D camera and EOS Utility 3.0 software (Canon). Marker sequences, PCR conditions and enzymes used are described in **Annex III, Table 7**.

SANGER sequencing

NPR1 was amplified using specific markers and the PCR program described in **Annex III, Table 8**. 5 µl of the PCR product were transferred into a new tube and mixed with 2 µl of ExoSAP (0.35µl Antarctic phosphatase; 0.35 µl Exonuclease I, 0.75 µl Antarctic phosphatase buffer and 0.55 µl of $_{dd}H_2O$). The mixture was incubated at 37 ºC for 30 min and the enzyme deactivated at 80 ºC for 15 min. The reaction product was dried for 15 min at 80ºC and 1 µl of 1:20 diluted *NPR1_Fwd_v2* or *NPR1_Rev_v2* primer, added to each tube. The sample was dried for 15 min at 80ºC and kept at -20 ºC until SANGER sequencing. Sequence alignment was performed by using CodonCode Aligner v8.0.2 software (LI-COR, Inc.).

Nitrate and ammonium quantification from soil

Soil from plants irrigated with 0.5x HS or 0.5x MS was collected for NH_4^+ and free NO_3^-quantification. To compare nitrogen concentration with natural soil, we also collected soil from Parc Natural de Collserola, Barcelona, in April 2017. For NH_4^+ quantification, soil was mixed with 1% K_2SO_4 solution (1:10) and incubated 16 h at 4 ºC in the dark. Samples were filtered through a Whatman-40 paper and later, through 0.22 µm nylon filter. Colorimetric quantification was performed according to the Berthelot reaction method based on phenol hypochlorite assay producing a yellow indophenol solution under acidic conditions (Gordon *et al.*, 1978). Nitrate quantification was carried out by mixing soil with distilled water in a ratio of 1:10. Samples were incubated for 16 h at 4 ºC in the dark. Preparations were first filtered through Whatman-40 and after, through 0.22 µm nylon filter. Nitrate content was analyzed by using an

Ionic Chromatograph DIONEX DX-300 with electronic suppression, AS11-HC column (4·250 mm) under the flow of 1 ml·min^{-1} of 15 mM NaOH (isocratic). Detection was carried out by electrical conductivity (μS·cm^{-1}).

CHAPTER 3

Genome Wide Association Mapping for the Tolerance to the Polyamine Oxidase Inhibitor Guazatine in *Arabidopsis thaliana*

Genome Wide Association Mapping for the Tolerance to the Polyamine Oxidase Inhibitor Guazatine in *Arabidopsis thaliana*

Kostadin E. Atanasov[1], Luis Barboza-Baquero[2], Antonio F. Tiburcio[1] and Rubén Alcázar[1]

[1]Laboratory of Plant Physiology, Department of Natural Products, Plant Biology and Soil Science, Faculty of Pharmacy. University of Barcelona, Spain.

[2]Centro para Investigaciones en Granos y Semillas, Universidad de Costa Rica, San José, Costa Rica.

Published as: Research publication in Frontiers in Plant Sci. 05 April 2016.
DOI: 10.3389/fpls.2016.00401

*Supplemental data is included in Annex IV (page 179).

SPANISH SUMMARY

La Guazatina es un inhibidor potente de las poliamino-oxidasas. En agricultura, es usada como fungicida de contacto al demostrarse eficaz como tratamiento postcosecha en cereales y cítricos, protegiéndolos de enfermedades que deterioran el producto. La composición de la guazatina es compleja: consiste en una mezcla sintética de poliaminas guaniladas (poliaminoguanidinas). En este trabajo hemos estudiado el efecto de la exposición a la guazatina en *Arabidopsis thaliana*. Describimos que concentraciones micromolares son capaces de inhibir el crecimiento de las plántulas de *Arabidopsis* e inducir clorosis en ellas, con un efecto prácticamente neutro sobre la germinación. Para llevar a cabo este estudio, hemos analizado las variaciones cuantitativas, frente a la guazatina, en 107 "accessions" de *Arabidopsis thaliana* escogidos al azar. Los datos obtenidos nos han permitido aplicar un estudio de asociación del genoma completo (GWAS) e identificar un locus en el cromosoma 1 que se asocia con la tolerancia a la guazatina. En el locus seleccionado para su estudio y validación, encontramos el gen candidato de la clorofilasa 1 (*CLH1*). Así mismo, decidimos incluir su gen parálago de la clorofilasa 2 (*CHL2*). El análisis independiente de los mutantes con pérdida de función o con baja expresión, *clh1-2*, *clh1-3*, *clh2-3*, *clh2-2* y del doble mutante *clh1-2/clh2-3*, nos indica que tanto el gen de la *CLH1* como el gen que codifica para la CLH2 se relacionan con una mayor tolerancia a la guazatina en *Arabidopsis*. A continuación, describimos un mecanismo basado en la variabilidad natural entre poblaciones de *Arabidopsis* que es capaz de solventar la toxicidad inducida por el antifúngico guazatina.

frontiers in Plant Science

ORIGINAL RESEARCH
published: 05 April 2016
doi: 10.3389/fpls.2016.00401

Genome Wide Association Mapping for the Tolerance to the Polyamine Oxidase Inhibitor Guazatine in *Arabidopsis thaliana*

Kostadin E. Atanasov[1], *Luis Barboza-Barquero*[2], *Antonio F. Tiburcio*[1] *and Rubén Alcázar*[1]*

[1] *Laboratory of Plant Physiology, Department of Natural Products, Plant Biology and Soil Science, Faculty of Pharmacy, University of Barcelona, Barcelona, Spain,* [2] *Centro para Investigaciones en Granos y Semillas, Universidad de Costa Rica, San José, Costa Rica*

Guazatine is a potent inhibitor of polyamine oxidase (PAO) activity. In agriculture, guazatine is used as non-systemic contact fungicide efficient in the protection of cereals and citrus fruits against disease. The composition of guazatine is complex, mainly constituted by a mixture of synthetic guanidated polyamines (polyaminoguanidines). Here, we have studied the effects from exposure to guazatine in the weed *Arabidopsis thaliana*. We report that micromolar concentrations of guazatine are sufficient to inhibit growth of *Arabidopsis* seedlings and induce chlorosis, whereas germination is barely affected. We observed the occurrence of quantitative variation in the response to guazatine between 107 randomly chosen *Arabidopsis* accessions. This enabled us to undertake genome-wide association (GWA) mapping that identified a locus on chromosome one associated with guazatine tolerance. *CHLOROPHYLLASE 1* (*CLH1*) within this locus was studied as candidate gene, together with its paralog *(CLH2)*. The analysis of independent *clh1-2*, *clh1-3*, *clh2-3*, *clh2-2,* and double *clh1-2 clh2-3* mutant alleles indicated that *CLH1* and/or *CLH2* loss-of-function or expression down-regulation promote guazatine tolerance in *Arabidopsis*. We report a natural mechanism by which *Arabidopsis* populations can overcome toxicity by the fungicide guazatine.

Keywords: guazatine, polyaminoguanidines, GWAS, natural variation, population genetics

OPEN ACCESS

Edited by:
Riccardo Angelini,
Roma Tre University, Italy

Reviewed by:
Günther F. E. Scherer,
Leibniz Universität Hannover, Germany
Autar Krishen Mattoo,
United States Department of Agriculture, USA
Manuela Cervelli,
Roma Tre University, Italy

***Correspondence:**
Rubén Alcázar
ralcazar@ub.edu

Specialty section:
This article was submitted to Plant Physiology, a section of the journal Frontiers in Plant Science

Received: *11 December 2015*
Accepted: *14 March 2016*
Published: *05 April 2016*

Citation:
Atanasov KE, Barboza-Barquero L, Tiburcio AF and Alcázar R (2016) Genome Wide Association Mapping for the Tolerance to the Polyamine Oxidase Inhibitor Guazatine in Arabidopsis thaliana. Front. Plant Sci. 7:401. doi: 10.3389/fpls.2016.00401

INTRODUCTION

Arabidopsis thaliana (thereafter referred to as *Arabidopsis*) is a small weed mainly distributed in the northern hemisphere. It grows in open or recently disturbed habitats and its spread was facilitated by the expansion of agriculture (François et al., 2008). *Arabidopsis* exhibits extensive natural variation for different developmental, abiotic and biotic stress resistance traits (Koornneef et al., 2004; Alonso-Blanco et al., 2009; Atwell et al., 2010). Understanding the genetic bases for such variation enables the identification of potential mechanisms underlying local adaptation. Here, we have used genome-wide association studies (GWAS) to identify genes contributing to the natural variation in guazatine tolerance observed in this species. Multiple recombination events in the genetic history of populations produce close linkage disequilibrium (LD) of markers with causal loci for certain phenotypes. Such associations can be detected through GWAS. These type of approaches require the genetic

validation of associations and have some limitations compared to, for example, QTL mapping (Korte and Farlow, 2013). In *Arabidopsis*, GWAS has been successfully applied to uncover the genetics of multiple traits (Atwell et al., 2010; Baxter et al., 2010; Li et al., 2010; Chan et al., 2011; Chao et al., 2012; Filiault and Maloof, 2012). Furthermore, the use of natural variation as source of genetic variability enables the analysis of how naturally occurring alleles evolve and may be selected (Alonso-Blanco et al., 2009).

Guazatine is a non-systemic, contact-based, aliphatic nitrogen fungicide used in agriculture that protects cereals against different diseases such as common bunt (*Tilletia* ssp.), common root rot (*Helminthosporium*), seedling blight (*Fusarium* ssp.), glume blotch (*Septoria*), and smut (*Ustilago;* Dreassi et al., 2007). In citrus fruits, guazatine also protects from infection by sour rot (*Geotrichum candidum*), green mold (*Penicillium digitatum*), and blue mold (*Penicillium italicum;* Wild, 1983). The mode of action of guazatine, at least in the ascomycete *Alternaria*, is inhibition of lipid biosynthesis and membrane destabilization (Yagura et al., 1984). The composition of guazatine is complex and constituted by a mixture of guanidated polyamines (PAs) referred to as polyaminoguanidines (PAGs). Most abundant PAGs in guazatine are diamines [octamethylenediamine H_2N-$(CH_2)_8$-NH_2] and triamines [iminodi(octamethylene)diamine H_2N-$(CH_2)_8$-NH-$(CH_2)_8$-NH_2], but also guanidated tetramines and carbamonitrile. In plants, guazatine is a potent inhibitor of PA oxidase activity (PAO) that has been extensively used to block PA oxidation or PA back-conversion in different species, thus contributing to decipher the biological functions of PAO in plants in relation to H_2O_2 production and ROS signaling (Federico et al., 2001; Yoda et al., 2006; Marina et al., 2008; Moschou et al., 2008; Fincato et al., 2011; Agudelo-Romero et al., 2014). The long alkyl chains, secondary amino groups and guanidine groups of PAGs constitute the structural requirements for the inhibition of PAO activity by guazatine (Cona et al., 2004). Despite its use in agriculture as fungicide, little is known about the physiological effects from long-term exposure to guazatine in weeds, such as *Arabidopsis*. We find that guazatine concentrations as low as 2.5 μM inhibit *Arabidopsis* shoot and root growth, and reduce total chlorophyll levels. We identified the occurrence of quantitative variation in response to guazatine in 107 natural *Arabidopsis* accessions from Europe and America. We performed genome-wide association mapping to determine the genetic bases for the variation observed. GWAS identified associations between guazatine tolerance and allelic variation at *CHLOROPHYLLASE 1* (*CLH1*), encoding an enzyme that catalyzes the hydrolysis of the ester bond of chlorophyll producing chlorophyllide and phytol (Hörtensteiner, 2006). *CLH1* and its paralog *CLH2*, were further validated for this association. The isolation and analysis of *chl1-2, clh1-3*, *chl2-2, clh2-3,* and double *clh1-2 clh2-3* mutant alleles confirmed that *CLH1* or *CLH2* loss-of-function promote guazatine-tolerance in *Arabidopsis*. We conclude that a natural mechanism occurs which provides tolerance to guazatine in natural populations, involving enzymes in the chlorophyll degradation pathway.

MATERIALS AND METHODS

Plant Materials and Growth Conditions

Accessions used in this work were obtained from the Nottingham *Arabidopsis* Stock Centre (NASC, www.arabidopsis.info) or kindly provided by Prof. Maarten Koornneef (Max Planck Institute for Plant Breeding Research, Cologne, Germany). A complete list of *Arabidopsis* accessions, origins and accession numbers is detailed in **Table S1**. Seed sterilization was performed by vigorous shaking of seeds in an aqueous solution containing 30% sodium hypochlorite supplemented with 0.5% TritonX-100 for 10 min, followed by three washes with sterile deionized H_2O. For *in vitro* culture, sterilized seeds were sown on Growth Media (GM: 0.5 x Murashige & Skoog supplemented with vitamins, 1% sucrose, 0.8% Plant Agar (Duchefa Biochemie), pH 5.7 adjusted with KOH). Seeds were stratified in the dark at 4°C during 2–4 days. Seedlings were grown under 12 h dark/12 h light cycles at 20/22°C, 100–125 μmol photons m^{-2} s^{-1} of light intensity.

Isolation and Characterization of *clh1-2*, *clh1-3*, *clh2-2*, *clh2-3* Double *clh1-2 clh2-3* Mutants

clh1 and *clh2* T-DNA insertion mutants were obtained from NASC (*clh1-2*, N653869; *clh1-3*, N871333; *clh2-2*, N827897; and *clh2-3*, N668619). Confirmation of the T-DNA insertion position and isolation of homozygous lines was performed by PCR-based genotyping and sequencing from genomic DNA, using T-DNA (LB) primer (5′-GCGTGGACCGCTTGC TGCAACT) and gene specific primers: *clh1-2* (Fwd: 5′-TTTGTTAGTTCCTGCGACTGG and Rev: 5′-AGAGAGAGA GACGGAGGTTGG), *clh1-3* (Fwd: 5′-CACATACAACCGGCC ATAAAC and Rev: 5′-GAAAAATCAACATTCTCCCCC), *clh2-3* (Fwd: 5′-CGGATAATCTCCTTCCTCCAC and Rev: 5′-ACA AAGCCCATTCCTTGTACC), *clh2-2* (Fwd: 5′-GAGGGTGGA GAGAATTTGAGG and Rev: 5′ GTCGCCTTAAAGAAATTT GGG). Genomic DNA was extracted using DNeasy plant mini Kit (Qiagen) according to manufacturer's instructions. PCR conditions were as follows: 95°C 5 min, 30 cycles (95°C 15 s, 55°C 45 s, 72°C 2 min), 72°C 10 min.

The double homozygous *clh1-2 clh2-3* mutant was isolated by genotyping 48 F_2 plants derived from the cross of the respective parental lines with primers described above. Expression of *CLH1* and *CLH2* was determined by RT-PCR. Briefly, total RNA isolated from 7-days old seedlings was extracted using TRIzol reagent (Invitrogen). Two micrograms of RNA was treated with DNAse I (Invitrogen) and first strand cDNA synthesized using Superscript II (Invitrogen) and oligo dT. One microliter of cDNA was used for PCR amplification of *CLH1* (Fwd: 5′-TTACATTCT TGTAGCCCCAC, Rev: 5′-GCGACTGGATCAATTCCTAT) or *CLH2* (Fwd: GCTTATGTTGCATGTCTCT, Rev: CGAGGAGTA CCCAAATTTCT) with LA Taq DNA polymerase (Takara) using the following PCR conditions: 95°C 5 min, 30 cycles (95°C 15 s, 55°C 45 s, 68°C 1 min), 68°C 10 min.

Guazatine Treatments

Guazatine acetate was obtained from KenoGard (Stockholm). Sterilized seeds of *Arabidopsis* accessions were sown directly

on GM supplemented with or without 2.5 μM guazatine. Chlorophyll levels were determined 16 days after germination.

clh mutants were germinated and grown on a nylon mesh (43 μm) placed on top of the GM media. Four days after germination, the nylon mesh was transferred to GM supplemented with 5 μM guazatine. Samples for chlorophyll extraction were harvested 12 days after guazatine treatment.

Quantification of Chlorophyll Levels

Seedlings were harvested individually, weighted and placed in 2 ml tubes (Eppendorf safe-lock) in the presence of 100 μl of borosilicate beads (Ø 4 mm), submerged in liquid nitrogen and homogenized with Star-Beater device (VWR International). Buffered acetone (acetone/Tris-HCl 80:20 vol, pH 7.8) was added in a ratio of 1 ml per 20 mg fresh weight (FW). Samples were incubated in the dark at 70°C during 10 min and centrifuged at 12,000 rpm for 1 min. Chlorophylls were determined using UV2310 Spectrophotometer (DINKO Industries) at 663 nm for chlorophyll A and 645 nm for chlorophyll B. Chlorophyll levels were calculated according to Porra (2002).

Transmission Electron Microscopy

Fifteen randomly chosen leaf segments from guazatine-treated and untreated leaves, were cut into pieces of 5 mm length and fixed in a solution of 2% glutaraldehyde in 2.5% cacodylate buffer pH 7.4 (CB) at 4°C. The segments were washed five times for 10 min in CB and post-fixed for 2 h 15 min in a solution of 1% OsO_4 and 0.8% FeCNK (w/v). After five additional washes with distilled H_2O at 4°C, samples were dehydrated in acetone and embedded in Spurr Low-Viscosity Embedding kit (Sigma-Aldrich). Serial ultrathin sections (60–70 nm) were obtained using an ultramicrotome (Reichert-Jung, Wien, Austria), collected on 200 mesh uncoated copper grids and stained with 2% uranyl acetate and Reynolds lead citrate. Samples were observed under a TEM Bioscan Gatan, JEOL 1010 at the Scientific and Technological Centers (CCiT) of the University of Barcelona.

GWA Mapping

GWAS was performed using the GWAPP web interface (Seren et al., 2012). Mean chlorophyll values of 107 *Arabidopsis* accessions grown under control and guazatine conditions (as indicated above), were transformed using the square root. GWAS was conducted using the accelerated mixed model (AMM), and linear regression (LM; Seren et al., 2012). To correct for multiple testing, a Bonferroni correction with a threshold of 0.5 was performed. *P*-value bias due to population stratification was evaluated with Q–Q plots. The LD was visualized in the flanking region of the *CLH1* gene (between 6.74 and 6.87 Mb on chromosome 1).

Root and Biomass Measurements

For root measurements, 4-days old seedlings germinated on GM were transferred into GM plates containing 1.5 μM guazatine. Plates were placed vertically and root measurements determined after 12 days of guazatine treatment using the SmartRoot software (Lobet et al., 2011).

Quantification of Free PAs

PAs from plant material were extracted using 5% (v/v) perchloric acid (PCA, 1 ml per 200 mg of fresh weight). Samples were vortexed vigorously, incubated on ice during 5 min and centrifuged at 16,000 g 10 min at 4°C. 200 μl of the PCA supernatant were taken for dansyl derivatization and detection according to Marcé et al. (1995).

Expression Analyses

The expression of *CLH1* (*At1g19670*) and *CLH2* (*At5g43860*) in *Arabidopsis* accessions was obtained from microarray data deposited in Genevestigator under experiment IDs AT-00283 and AT-00407 (Hruz et al., 2008). Expression values from three independent biological replicates were normalized to *UBIQUITIN 10* (*AT4G05320*) and expressed relative to Col-0 accession.

Phylogenetic and Statistical Analyses

DNA sequences were obtained from the 1001 Genomes project (www.1001genomes.org). NJ tree was computed using MEGA6.06. Statistical analyses were performed using *SPSS* software v.22 (IBM *SPSS Statistics*, IBM, Chicago, IL).

RESULTS

Effects of Long-Term Exposure to Guazatine in *Arabidopsis*

Due to the use of polyaminoguanidines (guazatine) as fungicide in agriculture, we studied the effects of guazatine treatment in germination and growth of the weed *Arabidopsis*. Exposure of *Arabidopsis* (Col-0) to increasing concentrations of guazatine from 0 to 25 μM did not affect germination (**Figure 1A**). Conversely, treatment with guazatine inhibited growth of *Arabidopsis* seedlings, produced chlorosis and affected chloroplast integrity (**Figures 1A–C**). Accumulation of osmophilic bodies that resembled plastoglobules was observed in chloroplasts of guazatine-treated leaves (**Figure 1C**). Guazatine concentrations as low as 2.5 μM were sufficient to inhibit growth in different *Arabidopsis* accessions, whereas chlorosis exhibited a dose-dependent response depending on the accession (**Figures 1A,B**). We concluded that long-term exposure to μM concentrations of guazatine is detrimental for *Arabidopsis* growth and reduces chlorophyll levels, for which quantitative variation between accessions was observed.

Quantitative Variation of Chlorophyll Levels in Response to Guazatine in 107 *Arabidopsis* Accessions

We selected 2.5 μM for the quantitative analysis of the natural variation in response to guazatine in 107 *Arabidopsis* accessions originally collected from worldwide. Higher concentrations were lethal for most natural accessions, whereas 2.5 μM guazatine was optimal to generate a large degree of phenotypic variation (**Figures 2A,B** and **Table S1**). We determined total chlorophyll levels as proxy for the quantification of guazatine tolerance traits. Quantification of chlorophyll in guazatine treated and untreated seedlings evidenced the occurrence of quantitative

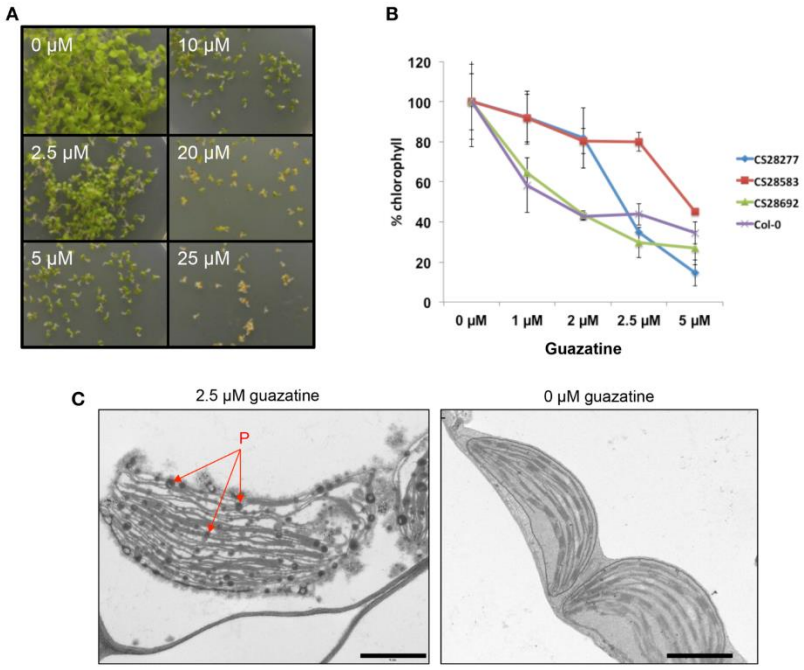

FIGURE 1 | Effects of guazatine treatment in *Arabidopsis* germination, growth and chlorophyll content. (A) Phenotype of 12-days-old *Arabidopsis* seedlings germinated and grown under different concentrations of guazatine from 0 to 25 µM. **(B)** Quantitation of chlorophyll loss by guazatine treatment in four genetically different accessions (CS28277, Ge-1; CS28583, Old-1; CS28692, Rou-0; Col-0). Values are normalized to chlorophyll levels at 0 µM guazatine for every genotype and expressed as %. Values are the mean from at least five independent biological replicates ±SD. **(C)** TEM images of 12-days-old wild-type Col-0 seedlings treated with 2.5 µM guazatine (+) or 0 µM guazatine (–). P, plastoglobules. Scale bar: 1 µM.

variation for this trait, with some accessions exhibiting high sensitivity and others increased tolerance to the fungicide (**Figure 2B**). Guazatine resistant and sensitive accessions were evenly distributed in populations from Austria, Czech Republic, France, Germany, The Netherlands, Portugal, UK and USA, with a high frequency of guazatine tolerance in accessions from Germany. We concluded that guazatine tolerant and sensitive accessions are not geographically restricted. Their distributions do not exhibit evident population patterns, although the frequencies of tolerant and sensitive accessions vary between populations (**Figure 2B**).

GWAS Analysis for Chlorophyll Levels in Response to Guazatine

GWAS was conducted to identify genetic factors underlying the response to guazatine in *Arabidopsis* natural populations using chlorophyll levels. The GWAS profiles showed a complex regulation of guazatine tolerance using both the accelerated mixed model (AMM) and linear regression (LM) methods (**Figures 3A,B;** Seren et al., 2012). Confounding due to population structure between both methods was assessed using Q–Q plots (**Figure S1**). The AMM method presented lower deviation from the identity line than the LM method, indicating an efficient control for population structure (**Figure S1**). Several strong associations were identified on the top of chromosome one between 6.74 and 6.87 Mb (**Figure 3B**) using the LM method. Remarkably, this association was absent under control conditions (**Figure S2**). The difference between methods seems to be due to the correction for population structure. The risk of *P*-value overcorrection is absent in the LM method when applied to traits correlated with population structure. Considering the advantages and disadvantages of both methods, we investigated potential gene candidates obviously associated with the variation of chlorophyll content within the associated region. *CHLOROPHYLLASE 1* (*CLH1, At1g19670*), involved in the chlorophyll degradation pathway (Hörtensteiner, 2006), is located in the associated region on chromosome one (**Figure 3C**). Pairwise linkage disequilibrium (LD) between SNPs for this region indicated LD values higher than 0.4 near *CLH1* (**Figure 3D**), denoting strong LD. The *CLH1* gene has one gene paralog, *CLH2* (*At5g43860*), located on chromosome 5 for which associations could not be detected regardless of the method (**Figures 3A,B** and **Figure S3**). We concluded that *CLH1* was an obvious candidate for gene validation studies.

Characterization of *clh1* and *clh2* Mutants in Response to Guazatine Treatment

We isolated *clh1* (*clh1-2* and *clh1-3*) and *clh2* (*clh2-2* and *clh2-3*) T-DNA insertion mutants that exhibited reduced or no

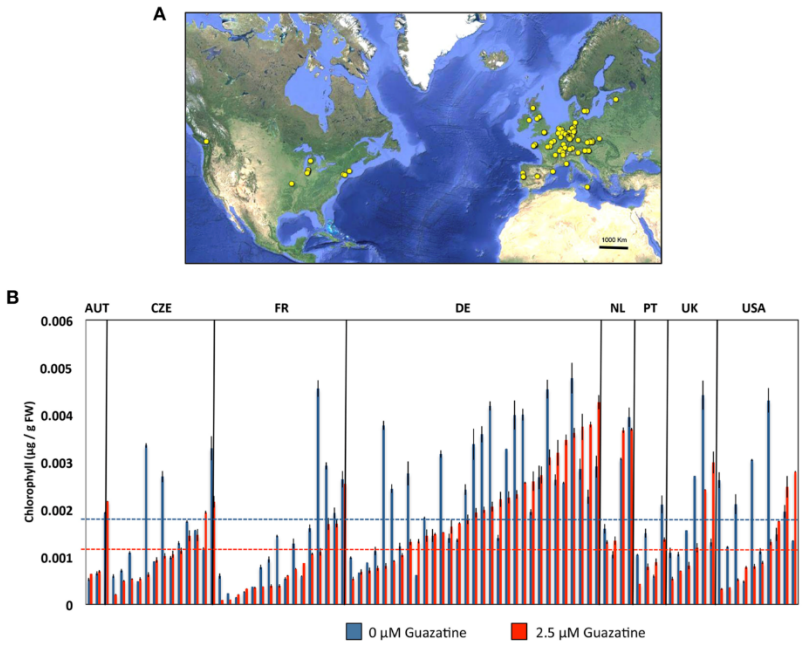

FIGURE 2 | (A) Geographical distribution of *Arabidopsis* accessions used in this work. The origins of accessions are indicated in yellow spots and detailed in **Table S1**. **(B)** Levels of chlorophylls in *Arabidopsis* accessions grown in the presence of 2.5 or 0 µM guazatine for 12 days. Accessions were sorted according to populations and guazatine tolerance. Only populations for which four or more individuals were available are shown. Values are the mean of at least five biological replicates ± SD.

expression of *CLH1* and *CLH2* genes, respectively, (**Figure S4**). In agreement with that previously reported for *clh1-1*, *clh2-1,* and *clh2-2*, mutants (Schenk et al., 2007), *clh1-2*, *clh1-3,* and *clh2-3* in this work did not show visually evident phenotypes on development or natural senescence differing from wild-type plants. We tested the tolerance of these genotypes to 5 µM guazatine, which is twice the concentration at which most *Arabidopsis* wild-type accessions, including Col-0, exhibited susceptibility (**Figure 1B**). Remarkably, loss of chlorophyll and growth inhibition induced by 5 µM guazatine treatment was significantly attenuated in *clh1-2, clh1-3*, *clh2-2,* and *clh2-3* seedlings compared to the wild-type (**Figures 4A,B**). This indicated that *CLH1* and/or *CLH2* loss-of-function or expression down-regulation enhances guazatine tolerance. The double *clh1-2 clh2-3* mutant exhibited higher chlorophyll and biomass in the presence of guazatine than single *clh1-2, clh1-3,* or *clh2-2, clh2-3* mutants, which is consistent with an additive effect by individual mutations (**Figures 4A,B**). In the root system, we observed that guazatine concentrations as low as 1.5 µM inhibited primary root elongation in wild-type *Arabidopsis* seedlings and this response was attenuated in *clh1-2 and clh1-3* but not so significantly in *clh2-2 or clh2-3* (**Figure 4C** and **Figure S5**). The lower dosage required for root growth inhibition might be due to direct uptake by root cells without the need of transport. The double *clh1-2 clh2-3* responded similarly to *clh1* loss of function (**Figure 4C**). We concluded that *CLH1* and/or *CLH2* loss-of-function or their down-regulation promote guazatine tolerance in *Arabidopsis*.

Polyamine Levels in Response to Guazatine Treatment

Free putrescine (Put), spermidine (Spd) and spermine (Spm) levels were quantified in *clh1-2, clh1-3, clh2-2, clh2-3,* double *clh1-2 clh2-3* and wild-type seedlings treated or not with 5 µM guazatine during 16 days. Free Put levels accumulated up to 6.7-fold in guazatine-treated seedlings compared to untreated controls (**Figure 5**). No evident differences in Put levels were apparent between *clh1-2, clh1-3, clh2-2, clh2-3* or double *clh1-2 clh2-3* mutants and the wild-type (**Figure 5**). The levels of free Spd did not change in response to guazatine treatment, whereas those of free Spm were slightly reduced in all genotypes tested (**Figure 5**). We concluded that guazatine leads to accumulation of free Put and slight reduction of Spm, and this response was similar in *clh1*, *clh2* and wild-type plants. Therefore, *CLH1* and *CLH2* mutations do not affect PA responsiveness to guazatine.

Natural Allelic Variation at *clh1* and *clh2*

The sequence of *CLH1* and *CLH2* genes from 53 accessions used in this study (**Table S1**) was obtained from the 1001 genomes project (www.1001genomes.org) and used to construct *CLH1* and *CLH2* phylogenies (**Figure 6**). *CLH1* alleles from

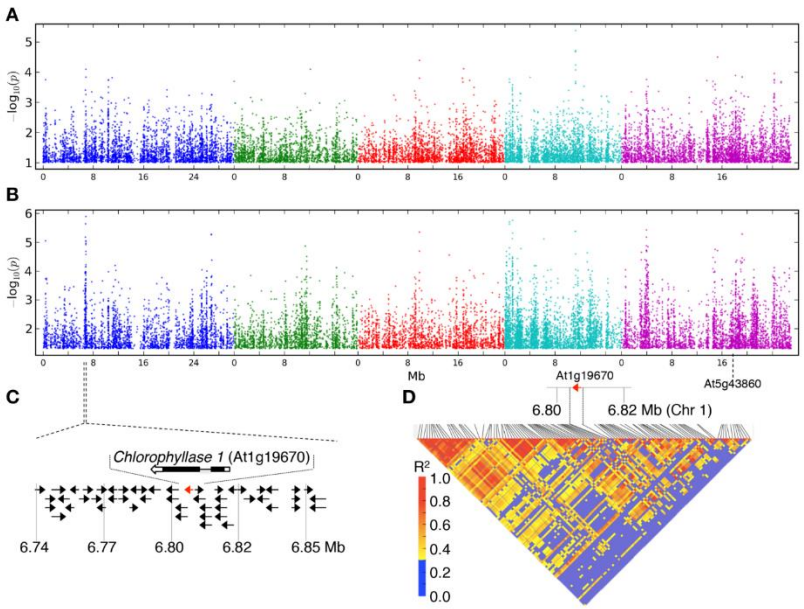

FIGURE 3 | GWA mapping for guazatine tolerance in 107 *Arabidopsis* accessions. GWA mapping profiles using the **(A)** accelerated mixed model (AMM) and **(B)** linear regression (LM) methods. Chromosomes are shown in different colors. **(C)** Schematic representation of the *CLH1* flanking region. **(D)** LD triangle plot for the *CLH1* genomic region.

guazatine tolerant accessions were found in different branches of the *CLH1* tree. However, we observed that 10 out of the 22 guazatine tolerant accessions analyzed in this phylogeny, clustered together in the same branch of the tree (clade III), which indicated that they carry similar *CLH1* alleles. Guazatine tolerant accessions in this clade belonged to populations from Germany (Kl-5, Mnz-0, Do-0, and Ga-0), Austria (Gr-1 and Gr-5), Italy (Sei-0), Czech Republic (Da1-12) and Sweden (Lom1-1). Most guazatine tolerant accessions in this *CLH1* clade did not cluster together in the *CLH2* phylogeny, for which variation was higher (**Figure 6**). Hence, the *CLH1* clade III was not likely due to simple genetic relationship between accessions, except for Gr-1 and Gr-5. Because of the contribution of both *CLH1* and *CLH2* genes to guazatine tolerance, and the high diversity of *CLH2* alleles detected that does not correlate with *CLH1* phylogeny, we could not identify straightforward associations between specific *CLH1* polymorphism(s) and guazatine tolerance traits by simple comparison between tolerant and sensitive variants.

CLH1 and *CLH2* expression was studied in 11 natural accessions that showed contrasted guazatine-tolerance traits (**Figure 7**). This analysis evidenced the absence of variation in *CLH1* and *CLH2* transcript levels between the accessions. Therefore, changes in *CLH1* and *CLH2* expression are unlikely to underlie guazatine tolerance in *Arabidopsis* natural populations. Rather, we suggest that non-synonymous substitutions in the coding sequence of CLH1 and CLH2 may cause the quantitative variation observed (**Figure 7**).

Overall, we report that genetic variation at both *CLH1* and *CLH2* genes conditions guazatine tolerance in *Arabidopsis*. The occurrence of multiple (rare) *CLH2* alleles contributing to guazatine tolerance may limit the identification of associations between *CLH2* and guazatine tolerance by GWAS, which was validated by mutant analysis.

DISCUSSION

In this work, we report the deleterious effects derived from the exposure to low (2.5 μM) concentrations of guazatine in *Arabidopsis* seedlings, the occurrence of extensive natural variation for guazatine tolerance traits in a set of 107 accessions, and the identification of genes involved in this response by GWA mapping. Guazatine is used in agriculture as fungicide recommended for cereals and citrus fruits. We have observed that treatment of the weed *Arabidopsis* with micromolar concentrations of guazatine inhibits growth, primary root elongation and depletes chlorophyll levels (**Figures 1**, **4**). Due to these effects, we conclude that guazatine may be used as herbicide. The 107 accessions selected were sufficient to perform GWA mapping for guazatine tolerance traits and identify *CLH1* as candidate gene (**Figure 3C**), that together with *CLH2*, were further validated using loss-of-function mutants.

The identification of *CLH* genes underlying guazatine-tolerance traits indicates the involvement of chlorophyll

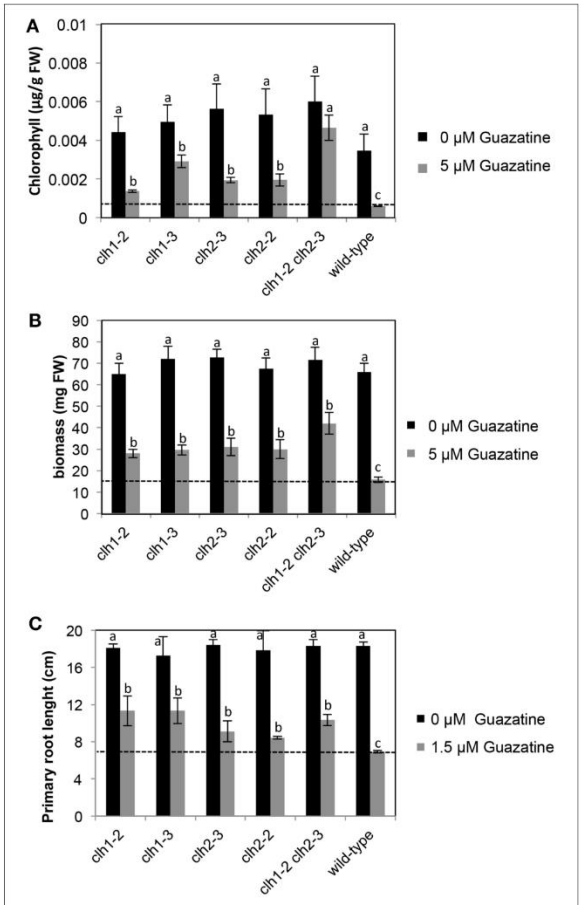

FIGURE 4 | Chlorophyll levels (A), biomass (B) and primary root length (C) in *clh*, *clh2* and double *clh1 clh2* mutants grown in the presence of 5 or 0 µM guazatine. Values are the mean of at least five biological replicates ±SD. Letters indicate values that are significantly different according to Student-Newman-Keuls test at $P < 0.05$.

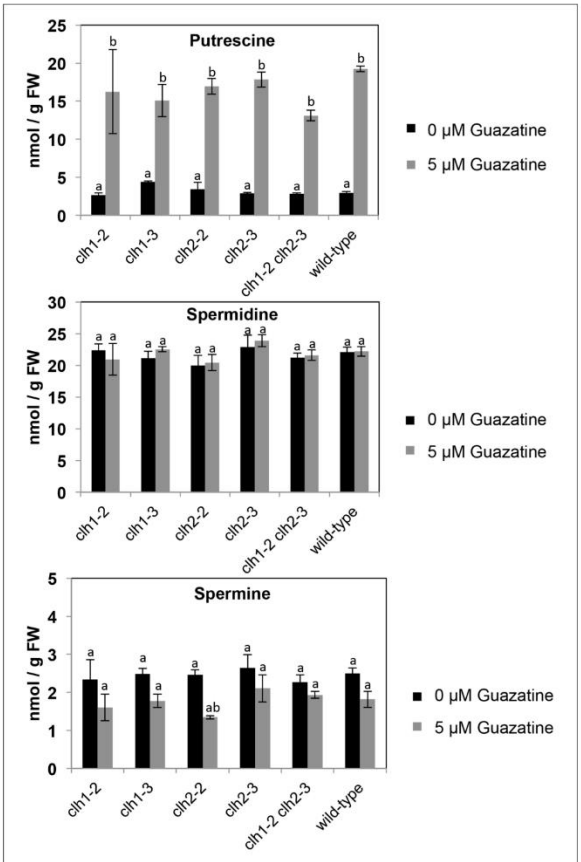

FIGURE 5 | Levels of free puterscine, spermidine, and spermine in *clh1*, *clh2* and double *clh1 clh2* mutants grown in the presence of 5 or 0 µM guazatine. Values are the mean of at least five biological replicates ± SD. Letters indicate values that are significantly different according to Student-Newman-Keuls test at $P < 0.05$.

degradation pathways in this response. *Arabidopsis* carries two *CLH* coding genes (*CLH1* and *CLH2*; Benedetti, 1998; Tsuchiya et al., 1999; Benedetti and Arruda, 2002) but associations with guazatine tolerance were only detected for *CLH1* (**Figure 3**). Because *CLH2* exhibits higher allelic diversity (**Figure 6**), we reason that the occurrence of multiple, low frequent *CLH2* alleles contributing to guazatine tolerance, might affect the identification of this locus by GWAS. Furthermore, predominant activity of CLH1 over CLH2 in *Arabidopsis* has been reported (Schenk et al., 2007). Interestingly, no variation in *CLH1* and *CLH2* expression was evidenced in *Arabidopsis* accessions differing in their tolerance to guazatine (**Figure 7**). We suggest that SNPs leading to non-synonymous substitutions in the coding sequence of *CLH1* and *CLH2* may underlie the naturally occurring variation observed, which is compatible with GWAS analysis.

CLH and pheophytinase (PPH) activities catalyze the cleavage of the lipophilic phytol chain of chlorophyll to produce chlorophyllide, a more hydrophilic derivative (Hörtensteiner, 2006). However, the biological assessment of *CLH* function in *Arabidopsis* indicated that *CLH1* and *CLH2* are not involved in senescence-related chlorophyll breakdown (Schenk et al., 2007; Hu et al., 2015). In *Arabidopsis*, PPH is localized in chloroplasts (Schelbert et al., 2009) whereas CLH1 and CLH2 are not plastidial proteins (Schenk et al., 2007). CLH1 is located in the ER and tonoplast of plant cells (Hu et al., 2015). Because of the CLH1 localization, chlorophyll could only be substrate of CLH activity upon release of chlorophyll from the thylakoid membranes. This may be caused by different types of abiotic and biotic stresses that damage plant tissues (Karpinski et al., 2003), or the use of guazatine (**Figure 1C**). In high amounts, some tetrapyrroles can generate ROS and induce cell death (Kruse et al., 1995; Meskauskiene et al., 2001; Hörtensteiner, 2006; Hirashima et al., 2009). Hu et al. (2015)

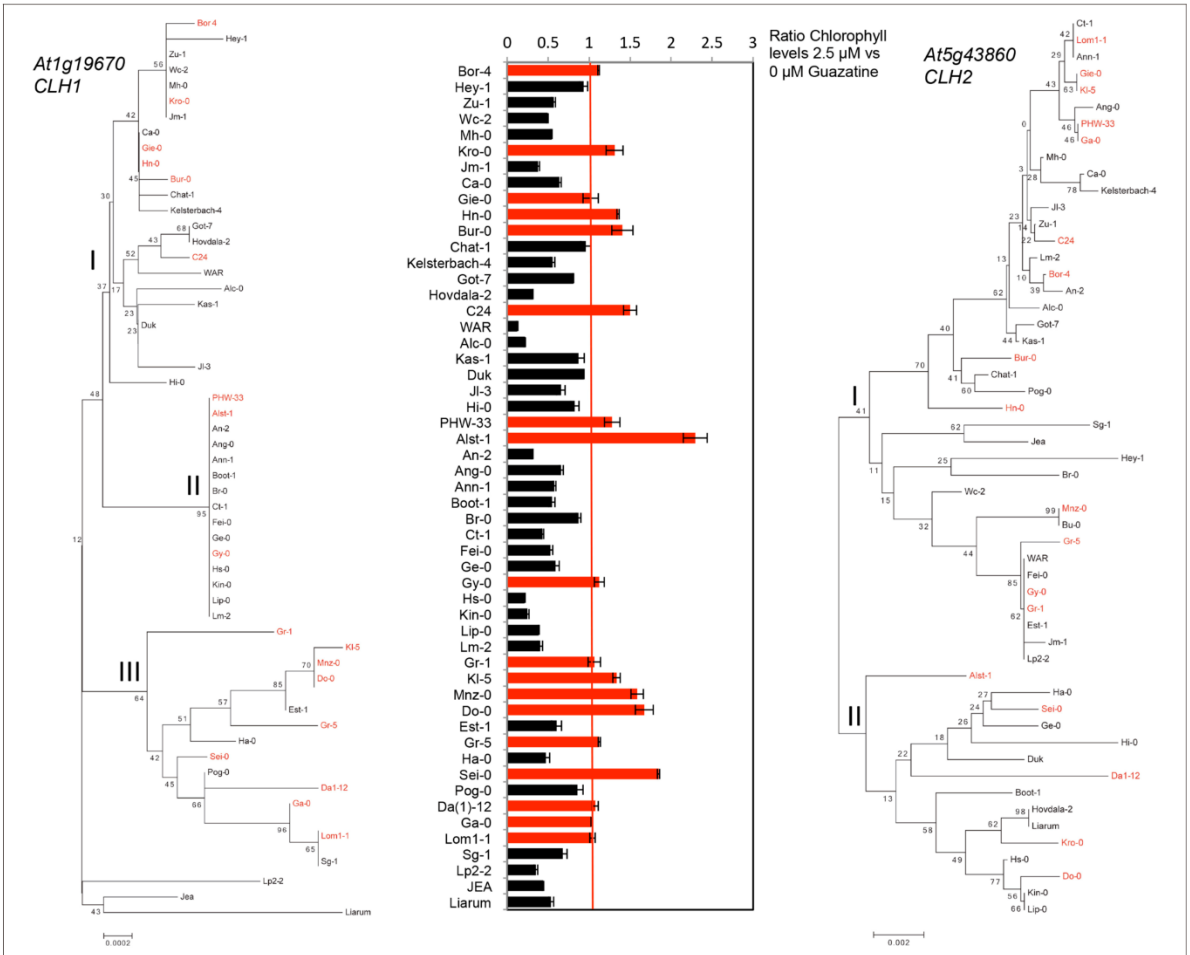

FIGURE 6 | Neighbor-Joining (NJ) tree of *At1g19670* (*CLH1*) and (*At5g43860*) *CLH2* genes. Bootstrap values for different nodes are indicated (% from 1000 replicates). Alleles from guazatine-tolerant accessions are highlighted in red.

suggested that CLH and chlorophyll constitute a binary defense system effective against certain chewing herbivores, due to the inducible production of chlorophyllide upon attack, which is toxic for *Spodoptera litura* larvae. Similarly, accumulation of chlorophyllide is a defense mechanism against infection by the necrotrophic fungus *Alternaria brassicicola* in *Arabidopsis* (Kariola et al., 2005). Yagura et al. (1984) reported that the fungal activity of guazatine is due to alterations in membrane integrity, permeability and composition. In *Arabidopsis*, the physiological effects of guazatine application have been less studied. Its use as PAO inhibitor does not require long-term exposure and, for PAO inhibition, guazatine is frequently added to protein extracts for *in vitro* enzymatic reactions. In this work, we report that long-term exposure to guazatine induces membrane damage in *Arabidopsis*, which was evidenced in the alteration of chloroplast integrity followed by chlorophyll degradation. Accumulation of osmophilic bodies, which resembled plastoglobules, was evidenced in guazatine-treated leaves (**Figure 1C**). Such particles accumulate in response to different stresses and senescence, in parallel to the break-down of thylakoid integrity (Austin et al., 2006). Interestingly, guazatine toxicity is not evident in monocots like oat (Capell et al., 1993). For auxinic herbicides, selectivity between dicots and monocots is due to differences in auxin translocation, degradation, perception, and vascular physiology (Gauvrit and Gaillardon, 1991; Monaco et al., 2002; Kelley and Reichers, 2007). Similar mechanisms may underlie guazatine selectivity between dicots and monocots. However, within-species variation in *Arabidopsis* can be explained by genetic determinisms involving natural variation at *CLH1* and *CLH2* genes.

CLH1 and/or *CLH2* loss-of-function or expression down-regulation attenuate guazatine toxicity in *Arabidopsis*. We suggest

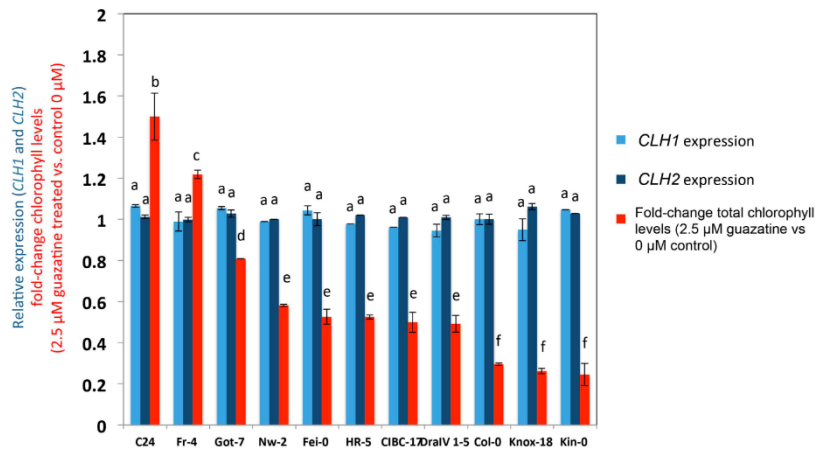

FIGURE 7 | Gene expression analyses of *CLH1* and *CLH2* and guazatine tolerance. Expression values in different accessions were obtained from Genevestigator (Hruz et al., 2008). Values were obtained from biological triplicates, normalized to *UBIQUITIN 10* as housekeeping gene, and expressed relative to Col-0 ± SD. Guazatine tolerance was measured by calculating the fold-change of total chlorophyll levels in 2.5 µM guazatine-treated seedlings vs. untreated control (see Materials and Methods). Letters indicate values that are significantly different according to Student-Newman-Keuls test at $P < 0.05$.

that loss of CLH activity limits chlorophyll degradation under stress conditions that damage the integrity of chloroplast membranes. This would prevent ROS generation and cell death induced by CLH enzymatic activity. Interestingly, no significant differences were observed between the PA profiles of wild-type, *clh1* and *clh2* mutants treated with guazatine. These observations suggest that guazatine effects under long-term exposure of *Arabidopsis* seedlings is not due to its activity as PAO inhibitor, but to other mechanisms involving oxidative stress and/or membrane damage.

PAs in the chloroplast are found as free or conjugated forms, the latter forms produced by transglutaminase activities that bind polyamines to stromal and thylakoid proteins (Kotzabasis et al., 1993; Del Duca et al., 1994; Della Mea et al., 2004; Ioannidis et al., 2009; Hamdani et al., 2011). PAs in the photosynthetic apparatus are beneficial and protect against photoinhibition and ROS production (Navakoudis et al., 2003; Demetriou et al., 2007; Hamdani et al., 2011; Yaakoubi et al., 2014). Surprisingly, guazatine application in osmotically stressed oat leaves resulted beneficial and enhanced Spd and Spm levels, which led to the prevention of chlorophyll loss and senescence (Capell et al., 1993). This contrasts with the effects observed in *Arabidopsis*, in which Put accumulated but Spd or Spm increases were absent (**Figure 5**). Guazatine application to *Vitis vinifera* also induced Put accumulation with no concomitant changes in the levels of Spd or Spm (Agudelo-Romero et al., 2014). In this case, the raise in Put levels was likely due to activation of ABA pathway and increased expression of *Arginine Decaborxylase (ADC)*, encoding the first biosynthetic step in the ADC pathway to Put biosynthesis (Agudelo-Romero et al., 2014). We conclude that PA profiles by guazatine treatment vary between species, which may be related to the predominance of terminal catabolism and/or PA back-conversion pathways between species.

Overall, we report natural mechanisms by which *Arabidopsis* populations can overcome toxicity by polyaminoguanidine-based fungicides used in agriculture, which might be the result of local adaptation processes.

AUTHOR CONTRIBUTIONS

KA performed all the experimental research. LB performed the GWAS analyses. KA, AT and RA planned the experiments. RA analyzed the data and wrote the paper with contributions from all authors.

ACKNOWLEDGMENTS

RA acknowledges funding support from the Ramón y Cajal Program (RYC-2011-07847) of the Ministerio de Ciencia e Innovación (Spain), the BFU2013-41337-P grant of the Programa Estatal de Fomento de la Investigación Científica y Técnica de Excelencia (Ministerio de Economía y Competitividad, Spain) co-financed by FEDER (Fondo Europeo de Desarrollo Regional), and the Marie Curie Career Integration Grant (DISEASENVIRON, PCIG10-GA-2011-303568) of the European Union. A.F.T. acknowledges funding support the Spanish Ministerio de Ciencia e Innovación (BIO2011-29683). RA and AT are members of the Grup de Recerca Consolidat 2014 SGR-920 of the Generalitat de Catalunya, Spain. We thank Prof. Maarten Koornneef for *Arabidopsis* accessions, support, and scientific inspiration on the occasion of his retirement.

SUPPLEMENTARY MATERIAL

The Supplementary Material for this article can be found online at: http://journal.frontiersin.org/article/10.3389/fpls.2016.00401

Figure S1 | Quantile-Quantile (Q–Q) plots for GWAS analysis of chlorophyll levels in response to guazatine using AMM and LM methods.

Figure S2 | Genome wide association mapping profile for chlorophyll levels under control conditions (0 μM guazatine) in 107 *Arabidopsis* accessions analyzed with the AMM and LM methods.

Figure S3 | Detailed view of the genome wide association mapping profile for guazatine tolerance in 107 *Arabidopsis* accessions analyzed with the AMM and LM methods in the *CLH1* (*At1g19670*) and *CLH2* (*At5g43860*) loci.

Figure S4 | Schematic representation of 5′ and 3′ UTRs (white), exons (black), introns (lines), and promoter region (gray) in *CLH1* (*At1g19670*) and *CLH2* (*At5g43860*) genes. The position of T-DNA insertion in *clh1-2*, *clh1-3*, *clh2-2,* and *clh2-3* is indicated. The expression of *CLH1* and *CLH2* in 7-days-old *clh1* and *clh2* seedlings, respectively, was determined by RT-PCR using gene-specific primers and *ACTIN2* as housekeeping control.

Figure S5 | Root phenotype of *clh1-2*, *clh1-3*, *clh2-2*, *clh2-3* and double *clh1-2 clh2-3* 16-days-old seedlings. Seedlings were germinated and grown in the absence of guazatine during 4 days, and then transferred to vertical plates containing 1.5 μM guazatine. Pictures were taken 12 days after treatment.

Table S1 | List of *Arabidopsis thaliana* accessions used in this work.

REFERENCES

Agudelo-Romero, P., Ali, K., Choi, Y. H., Sousa, L., Verpoorte, R., Tiburcio, A. F., et al. (2014). Perturbation of polyamine catabolism affects grape ripening of *Vitis vinifera* cv. *Trincadeira*. *Plant Physiol. Biochem.* 74, 141–155. doi: 10.1016/j.plaphy.2013.11.002

Alonso-Blanco, C., Aarts, M. G. M., Bentsink, L., Keurentjes, J. J. B., Reymond, M., Vreugdenhil, D., et al. (2009). What has natural variation taught us about plant development, physiology, and adaptation? *Plant Cell* 21, 1877–1896. doi: 10.1105/tpc.109.068114

Atwell, S., Huang, Y. S., Vilhjálmsson, B. J., Willems, G., Horton, M., Li, Y., et al. (2010). Genome-wide association study of 107 phenotypes in *Arabidopsis thaliana* inbred lines. *Nature* 465, 627–631. doi: 10.1038/nature08800

Austin, J. R. I. I., Frost, E., Vidi, P.-A., Kessler, F., and Staehlin, L. A. (2006). Plastoglobules are lipoprotein subcompartments of the chloroplast that are permanently coupled to thylakoid membranes and contain biosynthetic enzymes. *Plant Cell* 18, 1693–1703. doi: 10.1105/tpc.105.039859

Baxter, I., Brazelton, J. N., Yu, D., Huang, Y. S., Lahner, B., Yakubova, E., et al. (2010). A coastal cline in sodium accumulation in *Arabidopsis thaliana* is driven by natural variation of the sodium transporter AtHKT1;1. *PLoS Genet.* 6:e1001193. doi: 10.1371/journal.pgen.1001193

Benedetti, C. E. (1998). Differential expression of a novel gene in response to coronatine, methyl jasmonate, and wounding in the *coi1* mutant of *Arabidopsis*. *Plant Physiol.* 116, 1037–1042. doi: 10.1104/pp.116.3.1037

Benedetti, C. E., and Arruda, P. (2002). Altering the expression of the chlorophyllase gene *ATHCOR1* in transgenic *Arabidopsis* caused changes in the chlorophyll-to-chlorophyllide ratio. *Plant Physiol.* 128, 1255–1263. doi: 10.1104/pp.010813

Capell, T., Campos, J. L., and Tiburcio, A. F. (1993). Antisenescence properties of guazatine in osmotically stressed oat leaves. *Phytochemistry* 32, 785–788. doi: 10.1016/0031-9422(93)85205-6

Chan, E. K. F., Rowe, H. C., Corwin, J. A., Joseph, B., and Kliebenstein, D. J. (2011). Combining genome-wide association mapping and transcriptional networks to identify novel genes controlling glucosinolates in *Arabidopsis thaliana*. *PLoS Biol.* 9:e1001125. doi: 10.1371/journal.pbio.1001125

Chao, D.-Y., Silva, A., Baxter, I., Huang, Y. S., Nordborg, M., Danku, J., et al. (2012). Genome-wide association studies identify heavy metal ATPase3 as the primary determinant of natural variation in leaf cadmium in *Arabidopsis thaliana*. *PLoS Genet.* 8:e1002923. doi: 10.1371/journal.pgen.1002923

Cona, A., Manetti, F., Leone, R., Corelli, F., Tavladoraki, P., Polticelli, F., et al. (2004). Molecular basis for the binding of competitive inhibitors of maize polyamine oxidase. *Biochemistry* 43, 3426–3435. doi: 10.1021/bi036152z

Del Duca, S., Tidu, V., Bassi, R., Esposito, C., and Serafmi-Fracassini, D. (1994). Identification of chlorophyll-a/b proteins as substrates of transglutaminase activity in isolated chloroplasts of *Helianthus tuberosus* L. *Planta* 193, 283–289. doi: 10.1007/BF00192542

Della Mea, M., Di Sandro, A., Dondini, L., Del Duca, S., Vantini, F., Bergamini, C., et al. (2004). A Zea mays 39-kDa thylakoid transglutaminase catalyses the modification by polyamines of light-harvesting complex II in a light-dependent way. *Planta* 219, 754–764. doi: 10.1007/s00425-004-1278-6

Demetriou, G., Neonaki, C., Navakoudis, E., and Kotzabasis, K. (2007). Salt stress impact on the molecular structure and function of the photosynthetic apparatus–the protective role of polyamines. *Biochim. Biophys. Acta* 1767, 272–280. doi: 10.1016/j.bbabio.2007.02.020

Dreassi, E., Zizzari, A. T., D'Arezzo, S., Visca, P., and Botta, M. (2007). Analysis of guazatine mixture by LC and LC-MS and antimycotic activity determination of principal components. *J. Pharm. Biomed. Anal.* 43, 1499–1506. doi: 10.1016/j.jpba.2006.10.029

Federico, R., Leone, L., Botta, M., Binda, C., Angelini, R., Venturini, G., et al. (2001). Inhibition of pig liver and *Zea mays* L. polyamine oxidase: a comparative study. *J. Enzyme Inhib.* 16, 147–155. doi: 10.1080/14756360109162364

Filiault, D. L., and Maloof, J. N. (2012). A genome-wide association study identifies variants underlying the *Arabidopsis thaliana* shade avoidance response. *PLoS Genet.* 8:e1002589. doi: 10.1371/journal.pgen.1002589

Fincato, P., Moschou, P. N., Spedaletti, V., Tavazza, R., Angelini, R., Federico, R., et al. (2011). Functional diversity inside the *Arabidopsis* polyamine oxidase gene family. *J. Exp. Bot.* 62, 1155–1168. doi: 10.1093/jxb/erq341

François, O., Blum, M. G. B., Jakobsson, M., and Rosenberg, N. A. (2008). Demographic history of european populations of *Arabidopsis thaliana*. *PLoS Genet.* 4:e1000075. doi: 10.1371/journal.pgen.1000075

Gauvrit, C., and Gaillardon, P. (1991). Effect of low temperatures on 2,4-D behaviour in maize plants. *Weed Res.* 31, 135–142. doi: 10.1111/j.1365-3180.1991.tb01752.x

Hamdani, S., Gauthier, A., Msilini, N., and Carpentier, R. (2011). Positive charges of polyamines protect PSII in isolated thylakoid membranes during photoinhibitory conditions. *Plant Cell Physiol.* 52, 866–873. doi: 10.1093/pcp/pcr040

Hirashima, M., Tanaka, R., and Tanaka, A. (2009). Light-independent cell death induced by accumulation of pheophorbide a in *Arabidopsis thaliana*. *Plant Cell Physiol.* 50, 719–729. doi: 10.1093/pcp/pcp035

Hörtensteiner, S. (2006). Chlorophyll degradation during senescence. *Annu. Rev. Plant Biol.* 57, 55–77. doi: 10.1146/annurev.arplant.57.032905.105212

Hruz, T., Laule, O., Szabo, G., Wessendorp, F., Bleuler, S., Oertle, L., et al. (2008). Genevestigator V3: a reference expression database for the meta-analysis of transcriptomes. *Adv. Bioinformatics* 2008:420747. doi: 10.1155/2008/420747

Hu, X., Makita, S., Schelbert, S., Sano, S., Ochiai, M., Tsuchiya, T., et al. (2015). Reexamination of chlorophyllase function implies its involvement in defense against chewing herbivores. *Plant Physiol.* 167, 660–670. doi: 10.1104/pp.114.252023

Ioannidis, N. E., Ortigosa, S. M., Veramendi, J., Pintó-Marijuan, M., Fleck, I., Carvajal, P., et al. (2009). Remodeling of tobacco thylakoids by over-expression of maize plastidial transglutaminase. *Biochim. Biophys. Acta* 1787, 1215–1222. doi: 10.1016/j.bbabio.2009.05.014

Kariola, T., Brader, G., Li, J., and Palva, E. T. (2005). Chlorophyllase 1, a damage control enzyme, affects the balance between defense pathways in plants. *Plant Cell* 17, 282–294. doi: 10.1105/tpc.104.025817

Karpinski, S., Gabrys, H., Mateo, A., Karpinska, B., and Mullineaux, P. M. (2003). Light perception in plant disease defence signalling. *Curr. Opin. Plant Biol.* 6, 390–396. doi: 10.1016/S1369-5266(03)00061-X

Kelley, K. B., and Reichers, D. E. (2007). Recent developments in auxin biology and new opportunities for auxinic herbicide research. *Pesticide Biochem. Physiol.* 89, 1–11. doi: 10.1016/j.pestbp.2007.04.002

Koornneef, M., Alonso-Blanco, C., and Vreugdenhil, D. (2004). Naturally occurring genetic variation in *Arabidopsis thaliana*. *Annu. Rev. Plant Biol.* 55, 141–172. doi: 10.1146/annurev.arplant.55.031903.141605

Korte, A., and Farlow, A. (2013). The advantages and limitations of trait analysis with GWAS: a review. *Plant Methods* 9:29. doi: 10.1186/1746-4811-9-29

Kotzabasis, K., Fotinou, C., Roubelakis-Angelakis, K. A., and Ghanotakis, D. (1993). Polyamines in the photosynthetic apparatus: photosystem II highly resolved subcomplexes are enriched in spermine. *Photosyn. Res.* 38, 83–88. doi: 10.1007/BF00015064

Kruse, E., Mock, H. P., and Grimm, B. (1995). Coproporphyrinogen III oxidase from barley and tobacco–sequence analysis and initial expression studies. *Planta* 196, 796–803. doi: 10.1007/BF01106776

Li, Y., Huang, Y., Bergelson, J., Nordborg, M., and Borevitz, J. O. (2010). Association mapping of local climate-sensitive quantitative trait loci in *Arabidopsis thaliana*. *Proc. Natl. Acad. Sci. U.S.A.* 107, 21199–21204. doi: 10.1073/pnas.1007431107

Lobet, G., Pagès, L., and Draye, X. (2011). A novel image-analysis toolbox enabling quantitative analysis of root system architecture. *Plant Physiol.* 157, 29–39. doi: 10.1104/pp.111.179895

Marcé, M., Brown, D. S., Capell, T., Figueras, X., and Tiburcio, A. F. (1995). Rapid high-performance liquid chromatographic method for the quantitation of polyamines as their dansyl derivatives: application to plant and animal tissues. *J. Chromatogr. B Biomed. Appl.* 666, 329–335. doi: 10.1016/0378-4347(94)00586-T

Marina, M., Maiale, S. J., Rossi, F. R., Romero, M. F., Rivas, E. I., Gárriz, A., et al. (2008). Apoplastic polyamine oxidation plays different roles in local responses of tobacco to infection by the necrotrophic fungus *Sclerotinia sclerotiorum* and the biotrophic bacterium *Pseudomonas viridiflava*. *Plant Physiol.* 147, 2164–2178. doi: 10.1104/pp.108.122614

Meskauskiene, R., Nater, M., Goslings, D., Kessler, F., op den Camp, R., and Apel, K. (2001). FLU: a negative regulator of chlorophyll biosynthesis in *Arabidopsis thaliana*. *Proc. Natl. Acad. Sci. U.S.A.* 98, 12826–12831. doi: 10.1073/pnas.221252798

Monaco, T. J., Weller, S. C., and Ashton, F. M. (2002). *Weed Science: Principles and Practices*. New York, NY: Wiley-Blackwell.

Moschou, P. N., Sanmartin, M., Andriopoulou, A. H., Rojo, E., Sanchez-Serrano, J. J., and Roubelakis-Angelakis, K. A. (2008). Bridging the gap between plant and mammalian polyamine catabolism: a novel peroxisomal polyamine oxidase responsible for a full back-conversion pathway in *Arabidopsis*. *Plant Physiol.* 147, 1845–1857. doi: 10.1104/pp.108.123802

Navakoudis, E., Lütz, C., Langebartels, C., Lütz-Meindl, U., and Kotzabasis, K. (2003). Ozone impact on the photosynthetic apparatus and the protective role of polyamines. *Biochim. Biophys. Acta* 1621, 160–169. doi: 10.1016/S0304-4165(03)00056-4

Porra, R. J. (2002). The chequered history of the development and use of simultaneous equations for the accurate determination of chlorophylls a and b. *Photosyn. Res.* 73, 149–156. doi: 10.1023/A:1020470224740

Schelbert, S., Aubry, S., Burla, B., Agne, B., Kessler, F., Krupinska, K., et al. (2009). Pheophytin pheophorbide hydrolase (pheophytinase) is involved in chlorophyll breakdown during leaf senescence in *Arabidopsis*. *Plant Cell* 21, 767–785. doi: 10.1105/tpc.108.064089

Schenk, N., Schelbert, S., Kanwischer, M., Goldschmidt, E. E., Dörmann, P., and Hörtensteiner, S. (2007). The chlorophyllases AtCLH1 and AtCLH2 are not essential for senescence-related chlorophyll breakdown in *Arabidopsis thaliana*. *FEBS Lett.* 581, 5517–5525. doi: 10.1016/j.febslet.2007.10.060

Seren, Ü., Vilhjálmsson, B. J., Horton, M. W., Meng, D., Forai, P., Huang, Y. S., et al. (2012). GWAPP: a Web application for genome-wide association mapping in *Arabidopsis*. *Plant Cell* 24, 4793–4805. doi: 10.1105/tpc.112.108068

Tsuchiya, T., Ohta, H., Okawa, K., Iwamatsu, A., Shimada, H., Masuda, T., et al. (1999). Cloning of chlorophyllase, the key enzyme in chlorophyll degradation: finding of a lipase motif and the induction by methyl jasmonate. *Proc. Natl. Acad. Sci. U.S.A.* 96, 15362–15367. doi: 10.1073/pnas.96.26.15362

Wild, B. L. (1983). Double resistance by citrus green mould *Penicillium digitatum* to the fungicides guazatine and benomyl. *Ann. Appl. Biol.* 103, 237–241. doi: 10.1111/j.1744-7348.1983.tb02760.x

Yaakoubi, H., Hamdani, S., Bekalé, L., and Carpentier, R. (2014). Protective action of spermine and spermidine against photoinhibition of photosystem I in isolated thylakoid membranes. *PLoS ONE* 9:e112893. doi: 10.1371/journal.pone.0112893

Yagura, Y., Kirinuki, T., and Matsunaya, S. (1984). Mode of action of the fungicide guazatine in *Alternaria kikuchiana*. *J. Pestic. Sci.* 9, 425–431. doi: 10.1584/jpestics.9.425

Yoda, H., Hiroi, Y., and Sano, H. (2006). Polyamine oxidase is one of the key elements for oxidative burst to induce programmed cell death in tobacco cultured cells. *Plant Physiol.* 142, 193–206. doi: 10.1104/pp.106.080515

Conflict of Interest Statement: The authors declare that the research was conducted in the absence of any commercial or financial relationships that could be construed as a potential conflict of interest.

The reviewer, MC and handling Editor declared their shared affiliation, and the handling Editor states that the process nevertheless met the standards of a fair and objective review.

General discussion

Plants are fascinating organisms. They were the first to colonize hostile lands on the primitive Earth and to transform this sterile habitat into a fruitful ecosystem. This was possible because evolution is the main process providing the capacity to adapt survive and reproduce under adverse conditions. Evolution is mainly driven by natural selection, but genetic variation is also conditioned by genetic drift, gene flow and demography. Biotic and abiotic stresses are important natural selection forces for this continued adaptive process (Brockhurst *et al*., 2014). In plants, natural variation can be considered as the genetic and phenotypic diversity caused by the spontaneous occurrence of genomic variants which are contributed, at least partly, by evolutionary forces. Genetic variation is also a source of complex processes such as speciation (Alonso-Blanco *et al*., 2009). Speciation is a continuous process and immune-related hybrid incompatibilities are likely to be in this continuum between interbreeding and complete isolation.

The main core of this thesis deals with the need to investigate the molecular and genetic mechanisms underlying the immune-related hybrid-incompatibility (HI) between two natural populations of *A. thaliana* in North Europe (L*e*r) and Central Asia (Kas-2), as well, the environmental factors modulating the self-activation of the immune response (*see* **Chapters 1** and **2**).

Incompatible hybrids are in principle purged by selection because in a geological time-scale, the probability to acquire loss-of-function mutations is considered extremely low, and the direct impact on growth and fitness acts as a barrier. Plant breeders have faced HI in food-cultivars, ornamental plants, and others plant species. There is the need to provide solutions to overcome this issue. Chemical mutagenesis with ethyl methanesulfonate (EMS), and more recently, the *clustered regularly interspaced short palindromic repeats* (CRISPR/Cas9) gene edition technique, have been useful to revert HI at a genetic level.

Deleterious recessive epistasic-interaction between L*e*r TNL receptor, *Recognition of Peronospora parasitica 1-like* (*RPP1-like*) haplotype, and the Kas-2 immune-kinase receptor, *Strubbelig-receptor family 3 (SRF3*), produce autoimmune hybrids with severe growth defects (dwarfism), massive cell death, and sterility. The autoimmune phenotype is temperature dependent and occurs when plants are grown at 14 ºC – 16 ºC, which is the average temperature for most *Arabidopsis* populations in the wild. However, when

temperature is slightly increased to just 20 ºC – 22 ºC, the incompatibility is suppressed, and growth is recovered.

In this work, we performed an EMS mutagenesis on L*er*/Kas-2 NIL seeds, collected 200 M1 pools of around 100 plants each, and screened for suppressors of incompatibility (growth) at 14 ºC – 16 ºC. Plants with fully restored growth and ameliorated fitness were selected for further analyses. Twenty suppressors of the L*er*/Kas-2 incompatibility (*sulki*) were isolated, backcrossed five times with the parental L*er*/Kas-2 NIL line, and mutations identified by whole genome sequencing (Illumina), and further confirmed by SANGER sequencing (*see* **Chapter 1**). Eleven *sulki* mutants were intragenic and contained non-synonymous substitutions in *R8* and *R3* genes within the *RPP1-like* L*er* haplotype. For the *R8* L*er*, we identified ten allelic suppressors (*sulki1-1* to *sulki1-10*). Nine of them contained G/C to A/T – mutations expected for EMS treatment, whereas *sulki1-7* carried a 8-nucleotide deletion. Mutations were found within the *Toll/Interleukin* (TIR) *domain* (*sulki1-1*), the *nucleotide binding* (NB) domain (*sulki1-2*, *sulki1-3*, *sulki1-4*, *sulki1-5*, and *sulki1-6*), the splicing donor site preceding the *leucine rich-repeats* (LRR) domain (*sulki1-7*) and the LRR domain (*sulki1-8*, *sulki1-9*, and *sulki1-10*) (*see* **Chapter 1**; **Figure 1A**, and **Figure. 2**). The mutations were found in NLR conserved domains, which highlight the importance of these motifs for the normal L*er* *R8* gene function. In addition, we found a suppressor *sulki2-1*, within the TIR domain of L*er* *R3* gene which produced a partial suppression of the incompatibility.

Mutations in both *R3* and *R8* proteins exhibited a dominant inheritance pattern. In addition to restore growth, cell death was also suppressed (*see* **Chapter 1**; **Annex II, Supplemental Figure S1**), and the expression of immune-related and oxidative stress genes (*PR1*, *GST1*, and *EDS1*) significantly reduced compared to the NIL. *sulki2-1* expression of these genes was slightly higher than the *sulki1*, but much lower than the NIL. (*see* **Chapter 1**; **Figure 3**).

The identity of causal genes was corroborated with allelism studies. Single mutants for each of the L*er* *RPP1-like* genes were obtained by CRISPR/Cas9. Frameshift mutations on *R2*, *R3*, *R4* and *R8* genes were identified (*see* **Chapter 1**; **Figure 4A**, **Annex II, Supplemental Figure S4**). CRISPR/Cas9 mutants, referred to as *r2*, *r3*, *r4* and *r4*, exhibited different degrees of HI suppression. *r8* mutants exhibited complete HI

suppression, whereas *r3*, *r2* and *r4* showed partial suppression of HI (*see* **Chapter 1**; **Figure 4B**; **Annex II, Supplemental Figures S3, S5A-C, and S7**).

A recent publication from Jones *et al.,* suggested that some *NLR* proteins require oligomerization for triggering cell death (Jones *et al.,* 2016). We have observed a complex interrelationship between *R* genes within the *RPP1-like* L*e*r haplotype based on an additive contribution of *R2*, *R3* and *R4* to HI in epistasis with *R8*. Previous publications from Alcázar *et al*. (2014), and Stuttmann *et al*. (2016), anticipated a role for *R8* and *R3* on immune-related hybrid incompatibility. Whether or not *R8* and *R3* proteins homo or heterodimerize, remains a question.

It is generally assumed that defense activation incurs into a metabolic cost, which is translated into growth inhibition. We investigated the metabolic costs of maintaining an activated immune response in the NIL, and compared it with L*e*r, Kas-2 and some *sulki1* mutants (*sulki1-1*, *sulki1-7*, *sulki1-8*, and *sulki1-9*) grown at 14 ºC – 16 ºC. The approach carried out was based on global polar-fraction metabolomic-profiling by Gas-Chromatography coupled to Mass-Spectrometer (GC-MS/MS). *Sulki1* mutations reverted most of the metabolites which were altered in the NIL. However, parental lines, *sulki* and NIL were differentiated in Principal Component Analysis (PCA) suggesting a characteristic genotype-based metabolite profile (*see* **Chapter 1**; **Figure 7A**). Indeed, some of the metabolites were not reverted by *sulki1* mutations and exhibited a characteristic profile in these genotypes (e.g. Glucose, Fructose, Dehydroascorbate, Aspartate, Glutamate, Citrate, and Alanine, among others) (*see* **Chapter 1**; **Figure 7B**). Moreover, some metabolite levels were intermediate between the incompatible NIL line and the parents, L*e*r and Kas-2. These results are in agreement with RNAseq data that demonstrates the dependency of some, but not all, gene expression sectors on *R8*. According to the metabolite profiling, we suggest that autoimmunity produces accumulation of certain amino acids due to the higher ratio of proteolysis. Also, immune activation induces oxidative stress and for this reason, antioxidative metabolites such as ascorbate are depleted possibly by exhausting usage of the gluthatione-ascrobate cycle. Enhanced lipid peroxidation was manifested in the autoimmune NIL line, which accumulates Phosphatidic acid, ethanolamine and Glycerol. Some sugar metabolites were accumulated in the NIL (Glucose-6P and Sucrose), meanwhile others were similar to the parental lines, L*e*r and Kas-2, but increased in *sulki* (fructose and glucose) (*see* **Chapter 1**; **Figure 7C**). For this reason,

we asked whether the metabolic cost was determined by the carbohydrate limitations. Starch levels quantification and apoplastic invertase activity measurements were carried out, at two crucial anabolic/catabolic stages (at the end of the day and night) (*see* **Chapter 1**; **Annex II, Supplemental Figure S8** and **S9**). Our data prompted us to suggest that there is no metabolic cost for any specific metabolite that explains the NIL phenotype. Rather, the primary metabolism adapts to the activation of defense responses which requires secondary compounds biosynthesis, as well, to maintain and renew, plant structures (e.g. plant cell wall). In this regard, we speculate that NIL dwarfism is due to alterations in the cell wall composition that do not enable proper cell expansion. In this regard, it is interesting that Uk-1/Uk-3 incompatible hybrids do not exhibit lower cell death division or cell number per leaf area (Bomblies *et al*., 2007). Interestingly, *sulki* mutants accumulate higher levels of starch, glucose and fructose possibly by due to gene expression differences observed in these genotypes, which belong to *R8*-independent gene expression sectors (*see* **Chapter 1**; **Figure 6**).

The *RPP1-like* L*e*r haplotype is found in 30% of individuals collected from a local population in Gorzów (Poland) (Alcázar *et al*., 2014). The cluster contains a set of eight genes belonging to the *TIR-NB-LRR* family and their sequence is homolog to *RPP1*, which can recognize *Hpa* effectors. However, we hypothesized that the high frequency found in this local population was due to its contribution to the recognition of local *Hpa* isolates, providing pathogen resistance. For this reason, we cloned the *Hpa Gw* effector *ATR1-δ51* (lacking the secretory signal peptide) and co-infiltrated with single constructs of *RPP1-like* genes in order to identify whether any combination triggered cell death in *N. tabacum*. We tested *R2, R3, R4* and *R8*, but excluded *R1, R5, R6* and *R7* because they contain early stop codons within their sequence. The results we obtained indicated no induction of hypersensitive response (HR) in any combination tested, whereas *R3* alone was sufficient to induce cell death (*see* **Chapter 1**, **Figure 8A-B**). We speculate that the high frequency of the *RPP1-like* L*e*r haplotype in Gorzów might be due to a beneficial effect of *R3* in providing broad range disease resistance, as *R3* overexpression triggers resistance against pathogenic bacteria and oomycetes (Alcázar *et al.*, 2014).

Sequencing of the *ATR1* from *Hpa Gw* and the corresponding phylogenetic analysis with other well characterized *Hpa* isolates, has revealed higher relationship with Cala2 and Emwa1 than other isolates, such as Emco5, Noks1, Maks2, Hiks1, Wako5, and Emoy2 (*see* **Chapter 1**, **Annex II, Supplemental Figure 10**). Moreover, the

examination of disease susceptibility among 40 Gw accessions (containing or lacking the *RPP1-like* cluster), as well, T-DNA insertional Col-0 mutants of *RPP1* genes, supports the conclusion that L*er* *RPP1-like* haplotype is not casual for *Hpa Gw* resistance (*see* **Chapter 1**; **Annex II, Supplemental Figure 11**, **12** and **Supplemental Table S5**). Furthermore, L*er*/Kas-2 NIL suppressors *Cas9-r2*, *Cas9-r3*, *Cas9-r4*, *Cas9-r8*, *sulki1* alleles, *sulki2-1*, the *R3-R8* intergenic deletion contained in the *nde1-3*, and also *eds1* were all resistant to *Hpa Gw*.

Because TNL signaling is EDS1 dependent, we suggest the contribution of CNL loci providing resistance to *Hpa Gw* (*see* **Chapter 1**; **Annex II, Supplemental Figure 11**). To identify loci contributing to *Hpa* Gw resistance, we performed QTL mapping using a L*er*/Sha RIL population and identified a major effect QTL on chromosome 1, spanning a 2.83 Mb region which contains several *CNL* genes. Among these, *RPP7* (*At1g58602*) confers resistance against the *Hpa* isolate Hiks1 in a SA and EDS1 independent manner (*see* **Chapter 1**; **Figure 9**). In addition to the QTL analysis, we infected a set of 288 *Arabidopsis* accessions with *Hpa* Gw, for GWAS mapping. The association study highlighted a region encoding an *F-box* protein (*At3g24580*) of unknown function. Nevertheless, no genetic variation for this gene was observed, among the inoculated Gw accessions containing or not the L*er* *RPP1-like* haplotype. The results suggest that this gene acts in epistasis with other unidentified loci, or in other words, its phenotype is background dependent.

Based on climate change predictions, temperatures in the Northern Hemisphere will increase at least 2 ºC during this century (Moore, 2008). We have described that the HI between L*er* and Kas-2 accessions is temperature dependent (14 º - 16 ºC) and increasing the temperature above 16 ºC, such as 20 ºC – 22 ºC, abolishes HI. Therefore, climate change might also affect the fate of HI in natural populations in the coming decades.

Considering that *Arabidopsis* expanded with agriculture, and one of the main impacts of human activity is soil pollution with sources of nitrogenated compounds, we decided to further study how ammonium and nitrate can modulate plant immune responses using the HI model (*see* **Chapter 2**).

We found that only increasing the ammonium concentration on soil is sufficient to suppress HI phenotype, not only in the L*er*/Kas-2 NIL but also in Uk-1/Uk-3 (*see*

Chapter 2; **Figure 2**, **4, and 5**; **Annex III, Supplemental Figure S1**). Increases of ammonium in watering solution by supplementing 0.5x HS media or by irrigating plants directly with 0.5x MS, abolished plant cell death, restored plant growth and improved plant fitness to L*e*r, Kas-2, Uk-1 and Uk-3 parental levels (*see* **Chapter 2**; **Figure 3**, **5**, **6**, and **8**). In contrast with (Wang *et al*., 2013) who suggested the importance of the ammonium/nitrate ratio on modulation of *snc1* autoimmunity, here we report that such ratio does not condition L*e*r/Kas-2 and Uk-1/Uk-3 HIs. High ammonium is sufficient to suppress autoimmunity regardless of the ratio (*see* **Chapter 2**; **Annex III, Supplemental Figure S1**).

The quantification of hydrogen peroxide (H_2O_2), nitric oxide (NO) and *nitrate reductase* activity (NR) suggested the modulation of HI by NO (*see* **Chapter 2**; **Figure 9**). We also analyzed the origin of the NO, an immune-related multitask signaling gas, by measuring the *nitrate reductase* activity on plantlets. Our results revealed an increased NR activity on NIL, Kas-2 and L*e*r plants when were watered with 0.5x HS solution (*see* **Chapter 2**; **Figure 9**). To confirm the importance of NO in the L*e*r/Kas-2 incompatibility, we performed in vitro experiment in which seedlings were grown on reconstituted 0.5x MS media at 14 ºC – 16ºC for five days, and then treated for 48 h with the RNS scavenger, cPTIO, or the ROS scavenger DMTU (*see* **Chapter 2**). Gene expression analysis demonstrated a strong reduction of *PR1*, *GST1*, and *EDS1* expression upon cPTIO treatment (*see* **Chapter 2**; **Figure 14**). These results suggested a key role for NO governing autoimmunity.

The main source of NO is nitrate reduction to nitrite by *NR* activity in roots. Nitrite is quickly converted into ammonium by the *nitrite reductase* (NiR) and ammonium is fixed into amino acids through the GS/GOGAT cycle. We performed pathogen inoculations with strains *PstDC3000* and *Pst DC3000 hrcC*$^-$ with the aim to investigate whether high ammonium based-nutrition affects plant resistance. Our results evidenced higher pathogen growth for both strains when plants were irrigated with 0.5x MS (*see* **Chapter 2**; **Figure 11**). The increased susceptibility in the ammonium-supplemented conditions can be due to the increase of total free amino acids, which concentration can be increased in the apoplastic space, and possibly used by the pathogens to grow (Schwachtje *et al*., 2018).

Incompatible hybrids grown on soil and irrigated with 0.5x MS media were also able to accumulate higher levels of chlorophylls (*see* **Chapter 2**; **Fig. 7**). This might correlate with higher photosynthetic activity which leads to the opening of stomata (Lawson, 2009) facilitating *Pseudomonas* invasion. This might explain the differences in the bacterial loading (3 hpi) between 0.5x HS and 0.5x MS treatments. (Gupta *et al*., 2013) have also reported the importance of nitrogen forms of nutrition in the resistance to *Pseudomonas syringae* pv. *phaseolicola* in tobacco.

Finally, we asked how NO could regulate the plant immune response in the immune-related HI. We focused on the master gene regulator of the SAR response, *NPR1*. NPR1 can be found in the cytoplasm in an oligomeric form, whereas its activation by conformational changes, delivers monomers that translocate into the nuclei and interact with several TGA transcription factors initiating immune-resistance gene expression. *NPR1* activation is produced when SA levels increase and induce NO-mediated *S*-nitrosylation of certain cysteine residues (Withers and Dong, 2017).

To confirm the importance of NPR1 in HI, we isolated L*er*/Kas-2 NIL plants carrying *npr1-1* mutation. The L*er*/Kas-2 NIL *npr1-1* partly suppressed HI and the mutant phenotype resembled to 0.5x MS irrigated NIL plants (*see* **Chapter 2**; **Figure 15**).

Overall, *Arabidopsis* incompatible-hybrids seem to be favored somehow by ammonium land pollution which has an origin from the global fertilization, farming, food waste and industry, among others. Hence, temperature change, and soil pollution might condition the outcome of HI in wild populations. Here we speculate that climate change due to human activity will have a relevant impact on speciation genetics. However, as many evolutionary processes, this impact will be difficult to quantify and demonstrate.

In the context of my PhD I was trained on the genetics of natural variation. One of the interests of the lab was to apply GWAS mapping on primary metabolism, and with a focus on the nitrogen metabolism of polyamines. Polyamines (PAs) are small aliphatic polycationic molecules present in all living organisms, with important functions in several physiological processes such as abiotic stress response, development, vascular system and reproduction. Recently, they have also been reported to participate in the plant immune response (Tiburcio *et al.,* 2014). In *Arabidopsis* the main PAs are Putrescine (Put), Spermidine (Spd), Spermine (Spm), and Thermosperimine (tSpm). However, *Arabidopsis* lacks some PAs such as the Cadaverine (Cad), long chain PAs,

and other forms of the PAs mentioned above, for example Homospermidine, Norspermidine, Homospermine, and Norspermine. By other hand, synthetic mixtures of long chain polyamines have been used as fungicides and herbicides in certain plant species.

Due to the relevance of herbicides and fungicides in agriculture, and the polyamine-based formulation for some of them, we investigated the natural variation for the resistance against the herbicide/fungicide guazatine (*see* **Chapter 3**). Guazatine is a non-systematic repellent and contact fungicide, containing a complex mixture of guanidated polyamines or polyaminoguanidines. Guazatine has been used on seeds (e.g. wheat) to prevent seed-borne diseases and in post-harvesting treatments of fruits (e.g. citrus and watermelons).

Guazatine has been described to be a potent polyamine oxidase (PAO) inhibitor. Depending on the species, PAO enzymes catalyze the back conversion or oxidation of PAs into their aldehyde forms, releasing in both cases hydrogen peroxide (H_2O_2). The H_2O_2 produced by PAO activity can induce HR in tobacco (Yoda *et al.,* 2003). Therefore, PAOs are candidates to be implied in the generation of ROS during defense (Yoda *et al.,* 2006).

We did not observe germination defects using guazatine concentrations from 0 µM to 25 µM, whereas 2.5 µM was sufficient to induce deleterious measurable quantitative effects on seedlings, affecting their growth. 2.5 µM of guazatine produced different degrees of chlorosis and the mechanism underlying this phenotype was likely to involve plastid membrane integrity disruption. The first report referring to guazatine uses as fungicide suggests that its effect is based on the plasma membrane disruption. Our analyses also corroborate this finding, but in its use as herbicide (*see* **Chapter 3**; **Figure 1A-C**).

We measured chlorosis in a set of 107 Arabidopsis accessions treated with guazatine for 16 days. Chlorophylls were extracted by using acetone-tris buffered solution and we calculated chlorophylls according to Porra (Porra, 2002), which consist on an easy, robust and quick method for chlorophyll quantification. As was expected, *Arabidopsis* accessions exhibited different degrees of tolerance to the noxious compound. Accessions used in this study were collected from worldwide (*see* **Chapter 3**; **Figure 2A**). Interestingly, no geographical distribution was observed in terms of tolerance to

guazatine. However, higher allele frequency of tolerant accessions was observed in German populations. Nevertheless, the lack of population patterns behind the observed response and the homogeneous distribution of frequencies, encouraged us to suggest that tolerant accessions are not geographical restricted and hence, they have not been originated by natural selection or bottleneck events.

GWAS was carried out by applying two mapping statistical methods; linear model (LM) and accelerated mixed model (AMM). Both methods provided us an output data suggesting a complex regulation by which tolerance to guazatine can be achieved in different natural populations. However, results from both mapping methods differed. For the LM model, several associations were identified within the spanning genomic region between 6.74 Mb and 6.87 Mb (*see* **Chapter 3**; **Figure 3A-C**). This association was less clear when we carried out an AMM mapping. We argue that these differences are due to the correction for population structure. In addition, the AMM method reestimates P-values for the most significant SNPs by using an exact inference statistic and has demonstrated an efficient population structures control, with a lower deviation from the identity line than LM approach. On the other hand, LM method is less strict and has no P-value overcorrection when is applied to traits with population structure. Surprisingly, LM method provided the strongest association. The selected gene candidate within the region 6.74 - 6.87 Mb, encodes for *Chlorophyllase 1* (*CLH1*: *Atg19670*). CLH1 was initially suggested to participate in the chlorophyll degradation pathway. In this catabolic process, CLH hydrolyzes chlorophyll ester bonds and produces chlorophyllide and phytol groups. Moreover, pairwise linkage disequilibrium (LD) values between SNPs on this region were near 0.4, indicating strong LD (*see* **Chapter 3**; **Figure 3D**). *CLH1* has an orthologue gene, the *Chlorophyllase 2* (*CLH2*; *At5g43860*). However, no association was found for *CLH2* in this GWAS analysis, but we included both genes for the molecular gene function validation. We isolated *clh1-2* and *clh1-3* mutant alleles for *CLH1*, and *clh2-2* and *clh2-3* mutant alleles for *CLH2* gene, as well the double mutant, *clh1-2 clh2-3*.

The loss-of function mutants were exposed to a two-times higher concentration of guazatine (5 µM), a concentration to which almost all-natural accessions exhibit sensitivity. Single mutants, *clh1-2*, *clh1-3*, *clh2-2* and *clh2-3*, revealed higher tolerance to 5 µM guazatine in comparison with the wild-type Col-0, whereas the double mutant *clh1-2 clh2-3* exhibited higher tolerance than single mutants (*see* **Chapter 3**; **Figures**

4A-B). Primary root elongation analysis at 1.5 µM of guazatine, evidenced an inhibition of the primary root growth in the wild-type, *clh2-2* and *clh2-3*, but higher tolerance in *clh1-2*, *clh1-3* mutants (*see* **Chapter 3**; **Figure 4C**). No differences in PA contents were detected between *clh* mutants and wild-type in the presence or absence of guazatine (*see* **Chapter 3**). We concluded that higher tolerance to guazatine in *clh* mutants is not related with differences in polyamines levels (*see* **Chapter 3**; **Figure 5**). The data indicated an additive effect of *CLH1* and *CLH2* genes to guazatine tolerance, with a major contribution of *CLH1*.

Analysis of natural allelic variation on *CLH1* and *CLH2* genes was carried out by constructing a neighbor-joining (NJ) tree. Guazatine tolerant accessions mostly localized in different branches of the *CLH1* phylogeny and clustering did not correlate with the associated SNP candidate to modulate guazatine tolerance or sensitivity. However, ten tolerant accessions grouped to same clade of the *CLH1* NJ tree. These accessions belong to populations from Central/North Europe (Germany, Czech Republic, Austria and Sweden) and South Europe e.g. Italy (*see* **Chapter 3**; **Figure 6**). In addition, the sequence and phylogenetic analysis for *CLH2* revealed higher allelic diversity (*see* **Chapter 3**; **Figure 6**). No expression changes for *CLH1* and *CLH2* were detected between accessions that correlated with their tolerance (*see* **Chapter 3**; **Figure 7**), reinforcing the possibility of multiple independent mutations providing tolerance to guazatine. The occurrence of multiple allelic forms with a similar loss-of-function effect on *CLH2* might underlie the absence of clear associations with conserved causal SNP at this locus.

Guazatine acetate was widely used in Europa and other countries since the 70s, to prevent fruit and seed degradation. The normative of EC 2015/1910 establishes a maximum residue level of 0.05 $mg \cdot Kg^{-1}$, for every producer and importer in European Union (EU). So, the use of guazatine is almost forbidden. Nevertheless, its usage may remain in other countries that are no exporting to the EU or in inner markets. Nevertheless, it is intriguing the occurrence of natural variation for the tolerance against this herbicide and fungicide. *A. thaliana* is a ruderal plant that has a direct association with human activity and hence, agriculture. Guazatine was used as pesticide for decades in Europe and other countries such as the U.S.A and Australia. During the time of guazatine utilization, it was delivered to the wild exposing *Arabidopsis* and other plants. Herbicide resistance becomes more and more frequent in different plant species (Heap,

2014). Persistent application with sub-lethal doses, introduce a selective pressure and alleles that cause physiological adaptation can be fixed in few generations (Busi *et al.*, 2013). However, we have not detected a clear geographical pattern that supports such hypothesis, although some intriguing patterns are revealed. In our study, the higher frequency of guazatine-tolerant accessions from Germany, can be a consequence of the local persistent use of the pesticide, although we miss local data to corroborate what it might be a mere coincidence. Nevertheless, why these individuals would still persist if the local selective force is absent? It seems rather that *CLH* variation contributes to other naturally-relevant traits and, as secondary effect, it also influences herbicide resistance.

Resistance to pesticides and herbicides involve two main mechanisms of adaptation: target site and non-target site (Ghanizadeh and Harrington, 2017). Target site mechanisms involve gene amplification/overexpression of the herbicide/pesticide target-protein or structural modification of the target (Devine and Shukla, 2000; Gaines *et al*., 2009). Non-target site (NTS) mechanisms are more complex and assume plant stress response adaptation over time (Délye, 2013). NTS mechanism involve a complex interaction between alleles in such a way that appropriate alleles are inherited and accumulated because they provide fitness advantage, meanwhile other individuals from the population are purged by selection (Délye, 2013; Yoshida, 2005). Changes in gene expression patterns or epigenetics (Guerra *et al*., 2015; Sadakierska-Chudy and Filip, 2014), fitness alteration and allele frequency changes are also mechanism underlying NTS herbicide mode of resistance (Orr, 2009; Vila-Aiub *et al.,* 2015).

When guazatine disrupts chloroplast membrane and thylakoids, chlorophyll is released in the cytosol and becomes substrate of *CLH* enzymes which catabolize chlorophyll to chlorophyllide and other more hydrophilic derivates. The products of this reaction have been suggested to be a source of ROS. Chlorophyllide has been shown to protect against chewing herbivores such as *Spodoptora litura* or necrotrophic fungus as *Alternaria brassicicola*. According to this, *CLH* and chlorophyll have been suggested to act as a binary defense system that remains inactive upon cell structure disruption. Nevertheless, it is not yet studied whether guazatine also provides higher resistance to herbivores such as caterpillars, grasshopper and worms.

Future perspectives

Recently, there is a growing interest to investigate plants in their habitats, and more specifically the study of the rhizosphere, phylosphere and the interplay microbiota-plant growth and health. Soil microbiota plays a key role in plant immunity, pathogen resistance, water availability, nutrient assimilation, turnover and competition. It was suggested that the small microbiota community interacting with plants, in comparison with the huge quantity of taxa found in soil, can be explained by the host genotype and has an effect on plant health (Haney *et al.*, 2015; Philippot *et al.*, 2013; Wagner *et al*., 2016). Lebeis et al., suggested that SA plays a role on the root-microbiome community composition (Lebeis *et al*., 2015). Castrillo *et al*., have demonstrated that root microbiota drives phosphate integration and immune response during phosphate starvation by regulating the master transcriptional phosphate response factor, *PHR1*, prioritizing phosphate intake than defense (Castrillo *et al*., 2017). Zamioudis *et al*., have demonstrated the induction of the transcription factor *MYB72* by rhizobacteria VOCs and photosynthetic related signals, enhancing iron-assimilation and inducing systematic resistance in plant (Zamioudis *et al*., 2015). *MYB72* has also been reported to regulate coumarin scopoletin root exudate, which is an iron-mobilizing phenolic compound that shapes root microbiota and improves plant growth and resistance (Stringlis *et al*., 2018). Root exudates composition, such as carbohydrates, amino acids, and organic compounds (e.g. coumarin, rosmarininc acid), is genotype and environmentally dependent and shape the root microbiome (Corral-Lugo *et al*., 2016; Philippot *et al*., 2013). However, little is known about the role of root microbiota, soil physicochemical composition and the source of nitrogen (ammonium and nitrate), and their role in the plant immune response. In this regard, future studies should address the study of defense responses in combination with the study of microbial populations in roots and the nutrient compositions of soils.

Conclusions

The main objective of this PhD thesis work has been the investigation of the genetic mechanisms and effects of nutrition on hybrid incompatibility between accessions L*er* and Kas-2 (*see* **Chapters 1** and **2**). Also, natural variation against pesticide tolerance was investigated to identify genes underlying such effect in different *Arabidopsis* accessions.

Based on the results reported in the three Chapters the main conclusions are listed below:

Chapter 1

I. Suppression of hybrid incompatibilities can be achieved in plants with no deleterious effects on plant growth or disease resistance against pathogens. This is concluded from the analysis of intragenic *RPP1-like* HI suppressors that were analyzed in terms of growth, metabolic costs, gene expression and resistance to *Pseudomonas syringae* and to a local *Hyaloperonospora arabidopsidis* (*Hpa*) (Gw) isolate.

II. The contribution of the *RPP1-like* genes in the L*er*/Kas-2 incompatibility is additive and epistasic between them. *RPP1-like R8* plays an essential role because mutations fully suppress HI. *RPP1-like R3* overexpression triggers plant cell death, but loss-of-function mutations only partly suppress HI, similarly to *RPP1-like R2* and *R4*. We hypothesize that *RPP1-like R3* is beneficial in terms of broad-sense disease resistance.

III. Through GWAS and QTL mapping we identified new candidate loci underlying *Hpa* Gw disease resistance. One locus maps to the CC-NB-LRR gene *RPP7*, and the other locus maps to an F-box protein of unknown biological function. *Hpa* Gw resistance is independent of the *RPP1-like* L*er* gene cluster, *EDS1* and SA, consistent with the involvement of CC-NB-LRR proteins in *Hpa* Gw recognition.

IV. Analysis of *sulki1* global gene expression and primary metabolism reveals that some gene expression sectors and metabolic hallmarks of HI are dependent on *RPP1-like R8*, but others are governed by other *RPP1-like* cluster genes (*R2*, *R3*, or *R4*).

Chapter 2

I. Increases in ammonium attenuate plant hybrid incompatibilities in terms of growth, cell death, and gene expression. Nitrate reduction to ammonium by the nitrate reductase and nitrite reductase enzymatic activities generates NO, which contributes to HI probably through RNS generation. H_2O_2 inhibition has a lower effect on suppression of HI than NO inhibition, based on gene expression analysis.

II. Immune activation in incompatible hybrids has no evident metabolic costs on nitrogen metabolism. Incompatible hybrids exhibit the same chlorophyll levels than the parental lines. Nevertheless, an ammonium increase is related with higher pathogen infection possibly due to higher initial bacterial loading, apoplastic nutrient enrichment or more opened stomata.

III. *NPR1*, a systemic acquired resistance (SAR) master gene, is required for L*er*/Kas-2 hybrid incompatibility. *NPR1* loss-of-function mutations partly suppress HI.

IV. Nutrient composition of the *in vitro* media might interfere with the NLR-triggered immune response, in particular high concentration of NH_4^+ in Murashige & Skoog-based media.

Chapter 3

I. There is natural variation for the tolerance to guazatine. The genetic mechanism behind implies allelic variation at Clorophyllase (*CLH1* and *CLH2*) genes. This association was validated through the use of *clh* loss-of-function mutants.

II. Tolerance to guazatine is acquired through evolutionarily independent events in geographically separated accessions.

III. We propose a model in which chlorophyllase degrades chlorophyll to chlorophyllide when the chloroplast membrane is compromised by guazatine treatment, generating ROS and leading to toxicity.

IV. We did not find a clear correlation between guazatine tolerance and population structure, although the frequency of tolerant alleles was higher in accessions from Germany.

General references

Al-Shehbaz, **I. A**., **and O'Kane, S. L.** (2002). Taxonomy and phylogeny of *Arabidopsis* (Brassicaceae). The Arabidopsis Book, 1, e0001.

Albert, **M**. (2013). Peptides as triggers of plant defence. J Exp Bot. 64, 5269–5279

Alcázar, R., García, A. V, Kronholm, I., de Meaux, J., Koornneef, M., Parker, J. E., and Reymond, M. (2010). Natural variation at *Strubbelig Receptor Kinase 3* drives immune-triggered incompatibilities between *Arabidopsis thaliana* accessions. Nature Genet, 42, 1135–1139.

Alcázar, R., García, A. V, Parker, J. E., and Reymond, M. (2009). Incremental steps toward incompatibility revealed by *Arabidopsis* epistatic interactions modulating salicylic acid pathway activation. Proc. Natl. Acad. Sci, 106, 334–339.

Alcázar, R., Marco, F., Cuevas, J. C., Patron, M., Ferrando, A., Carrasco, P., Altabella, T. (2006). Involvement of polyamines in plant response to abiotic stress. Biotechnol Lett, 28, 1867–1876.

Alcázar, R., and Parker, J. E. (2011). The impact of temperature on balancing immune responsiveness and growth in *Arabidopsis*. Trends Plant Sci, 16, 666–675.

Alcázar, R., Pecinka, A., Aarts, M. G. M., Fransz, P. F., and Koornneef, M. (2012, April 1). Signals of speciation within *Arabidopsis thaliana* in comparison with its relatives. Curr Opin Plant Biol, 15, 205-211.

Alcázar, R., von Reth, M., Bautor, J., Chae, E., Weigel, D., Koornneef, M., and Parker, J. E. (2014). Analysis of a plant complex resistance gene locus underlying immune-related hybrid incompatibility and its occurrence in nature. PLoS Genet, 10, e1004848.

Ali, M. A., Anjam, M. S., Nawaz, M. A., Lam, H. M., and Chung, G. (2018). Signal transduction in plant–nematode interactions. Int J Mol Sci. 19: e1648.

Almli, L. M., Duncan, R., Feng, H., Ghosh, D., Binder, E. B., Bradley, B., Epstein, M. P. (2014). Correcting systematic inflation in genetic association tests that consider interaction effects application to a genome-wide association study of posttraumatic stress disorder. JAMA Psychiatry, 71, 1392–1399.

Alonso-Blanco, C., Aarts, M. G. M., Bentsink, L., Keurentjes, J. J. B., Reymond, M., Vreugdenhil, D., and Koornneef, M. (2009). What has natural variation taught us about plant development, physiology, and adaptation? Plant Cell, 21, 1877–1896.

An, C., Wang, C., and Mou, Z. (2017). The *Arabidopsis* Elongator complex is required for nonhost resistance against the bacterial pathogens *Xanthomonas citri* subsp. *citri* and *Pseudomonas syringae* pv. *phaseolicola* NPS3121. New Phytol, 214, 1245–1259.

Asai, S., Furzer, O. J., Cevik, V., Kim, D. S., Ishaque, N., Goritschnig, S., Jones, J. D. G. (2018). A downy mildew effector evades recognition by polymorphism of expression and subcellular localization. Nature Commun, 9, 5192.

Atanasov, K. E., Liu, C., Arafaty, N., and Tiburcio, Antonio Fernández and Alcázar, R. (2019). Immune gene expression triggered by polyamines. *In Preparation*.

Atanasov, K. E., Liu, C., Erban, A., Kopka, J., Parker, J. E., and Alcázar, R. (2018). NLR mutations suppressing immune hybrid incompatibility and their effects on disease resistance. Plant Physiol, 177, pp.00462.2018.

Atwell, S., Huang, Y. S., Vilhjálmsson, B. J., Willems, G., Horton, M., Li, Y., Nordborg, M. (2010). Genome-wide association study of 107 phenotypes in a common set of *Arabidopsis thaliana* inbred lines. Nature, 465, 627–631.

Baack, E., Melo, M. C., Rieseberg, L. H., and Ortiz-Barrientos, D. (2015). The origins of reproductive isolation in plants. New Phytol, 207, 968-984.

Bailey, K., Çevik, V., Holton, N., Byrne-Richardson, J., Sohn, K. H., Coates, M., Tör, M. (2011). Molecular Cloning of *ATR5* Emoy2 from *Hyaloperonospora arabidopsidis*, an avirulence determinant that triggers *RPP5*-mediated defense in *Arabidopsis*. Mol Plant Microbe Interact., 24, 827–838.

Barnard-Kubow, K. B., and Galloway, L. F.

(2017). Variation in reproductive isolation across a species range. Ecol. Evol, *7*, 9347–9357.

Barrett, S. C. H. (2002). The evolution of plant sexual diversity. Nat Rev Genet, 3, 274-284.

Bartels, S., Anderson, J. C., Gonzalez Besteiro, M. A., Carreri, A., Hirt, H., Buchala, A., Ulm, R. (2009). *Map kinase Phosphatase1* and protein *tyrosine phosphatase1* are repressors of salicylic acid synthesis and *SNC1*-mediated responses in *Arabidopsis*. Plant Cell, 21, 2884–2897.

Bartels, Sebastian, Lori, M., Mbengue, M., Verk, M. Van, Klauser, D., Hander, T., Boller, T. (2013). The family of peps and their precursors in *Arabidopsis*: Differential expression and localization but similar induction of pattern-Triggered immune responses. J Exp Bot, 64, 5309–5321.

Bateson, W. (1909). Darwin and modern science, ed Seward AC. Cambridge University Press, 85–101.

Bayer, P. E., Golicz, A. A., Tirnaz, S., Chan, C. K. K., Edwards, D., and Batley, J. (2018, May 31). Variation in abundance of predicted resistance genes in the *Brassica oleracea* pangenome. Plant Biotechnol J, 17:789-800.

Bechsgaard, J. S., Castric, V., Charlesworth, D., Vekemans, X., and Schierup, M. H. (2006). The transition to self-compatibility in *Arabidopsis thaliana* and evolution within S-haplotypes over 10 Myr. Mol Biol Evol, 23, 1741–1750.

Begum, H., Spindel, J. E., Lalusin, A., Borromeo, T., Gregorio, G., Hernandez, J., McCouch, S. R. (2015). Genome-wide association mapping for yield and other agronomic traits in an elite breeding population of tropical rice (*Oryza sativa*). Plos One, 10, e0119873.

Beilstein, M. A., Nagalingum, N. S., Clements, M. D., Manchester, S. R., and Mathews, S. (2010). Dated molecular phylogenies indicate a miocene origin for *Arabidopsis thaliana*. Proc. Natl. Acad. Sci, 107, 18724–18728.

Bektas, Y., and Eulgem, T. (2014). Synthetic plant defense elicitors. Front Plant Sci, 5: 804.

Bellin, D., Asai, S., Delledonne, M., and Yoshioka, H. (2013). Nitric oxide as a mediator for defense responses. Mol Plant icrobe Interact, 26, 271–277.

Belmont, J. W., Boudreau, A., Leal, S. M., Hardenbol, P., Pasternak, S., Wheeler, D. A., Stewart, J. (2005). A haplotype map of the human genome. Nature, 437, 1299–1320.

Benajmini, Y., Hochberg, Y., Benjamini, Y., and Hochberg, Y. (1995). Controlling the false discovery rate: A practical and powerful approach to multiple testing tuthor (s): Yoav Benjamini and Yosef Hochberg Source: Journal of the Royal Statistical Society. Series B (Methodological), *J* R Statist Soc *B*, 57, 289–300.

Bi, D., Cheng, Y. T., Li, X., and Zhang, Y. (2010). Activation of plant immune responses by a gain-of-function mutation in an atypical receptor-like kinase. Plant Physiol, 153, 1771–1779.

Bigeard, J., Colcombet, J., and Hirt, H. (2015). Signaling mechanisms in pattern-triggered Immunity (PTI). Mol Plant, 8, 521–539.

Bischoff, K. L. (2016). Glucosinolates. Nutraceuticals, 7, 551–554.

Blackman, B. K. (2017). Changing responses to changing seasons: natural variation in the plasticity of flowering time. Plant Physiol, 173, 16–26.

Boero, F. (2015). From Darwin's origin of species toward a theory of natural history. F1000Prime Reports, 7, 49.

Bomblies, K. (2010). Doomed lovers: mechanisms of isolation and incompatibility in plants. Annu Rev Plant Biol, 61, 109–124.

Bomblies, K., Lempe, J., Epple, P., Warthmann, N., Lanz, C., Dangl, J. L., and Weigel, D. (2007). Autoimmune response as a mechanism for a Dobzhansky-Muller-type incompatibility syndrome in plants. PLoS Biology, 5, e236.

Bomblies, K., and Weigel, D. (2007). *Arabidopsis* a model genus for speciation. Curr Opin Genet Dev, 17:500-504

Bomblies, K., and Weigel, D. (2007). Hybrid

necrosis: autoimmunity as a potential gene-flow barrier in plant species. Nat Rev Genet, 8, 382–393.

Bomblies, K., Yant, L., Laitinen, R. A., Kim, S. T., Hollister, J. D., Warthmann, N., Weigel, D. (2010). Local-scale patterns of genetic variability, outcrossing, and spatial structure in natural stands of *Arabidopsis thaliana*. PLoS Genet, 6, e1000890.

Botella, M. A., Parker, J. E., Frost, L. N., Bittner-Eddy, P. D., Beynon, J. L., Daniels, M. J., Jones, J. D. (1998). Three genes of the *Arabidopsis RPP1* complex resistance locus recognize distinct *Peronospora parasitica* avirulence determinants. Plant Cell, 10, 1847–1860.

Bothe, H., Jost, G., Schloter, M., Ward, B. B., and Witzel, K. P. (2000). Molecular analysis of ammonia oxidation and denitrification in natural environments. FEMS Microbiol Rev, 24,673-90

Bowling, S. A., Clarke, J. D., Liu, Y., Klessig, D. F., and Dong, X. (1997). The *cpr5* mutant of *Arabidopsis* expresses both NPR1-dependent and NPR1-independent resistance. Plant Cell, 9, 1573–1584.

Bowling, S. A., Guo, A., Cao, H., Gordon, A. S., Klessig, D. F., and Dong, X. (1994). A mutation in *Arabidopsis* that leads to constitutive expression of systemic acquired resistance. Plant Cell, 6, 1845–1857.

Boyle, P., Su, E. Le, Rochon, A., Shearer, H. L., Murmu, J., Chu, J. Y., Després, C. (2009). The *BTB*/*POZ* Domain of the *Arabidopsis* disease resistance protein *NPR1* interacts with the repression domain of *TGA2* to negate its function. Plant Cell, 21, 3700–3713.

Briskine, R. V., Paape, T., Shimizu-Inatsugi, R., Nishiyama, T., Akama, S., Sese, J., and Shimizu, K. K. (2017). Genome assembly and annotation of *Arabidopsis halleri*, a model for heavy metal hyperaccumulation and evolutionary ecology. Mol Ecol Resour, 17, 1025–1036.

Britto, D. T., and Kronzucker, H. J. (2002). NH4+ toxicity in higher plants: a critical review. Journal of Plant Physiol, 159, 567–584.

Brockhurst, M. A., Chapman, T., King, K. C., Mank, J. E., Paterson, S., and Hurst, G. D. D. (2014). Running with the Red Queen: the role of biotic conflicts in evolution. Proc R Soc Lond, 281, pii: 20141382.

Brodersen, P., Petersen, M., Pike, H. M., Olszak, B., Skov, S., Ødum, N., Mundy, J. (2002). Knockout of *Arabidopsis* accelerated-cell-death11 encoding a sphingosine transfer protein causes activation of programmed cell death and defense. Genes Dev, 16, 490–502.

Brutus, A., Sicilia, F., Macone, A., Cervone, F., and De Lorenzo, G. (2010). A domain swap approach reveals a role of the plant wall-associated kinase 1 (*WAK1*) as a receptor of oligogalacturonides. Proc. Natl. Acad. Sci, 107, 9452–9457.

Buchala, A., Gonzalez Besteiro, M. A., Ulm, R., Metraux, J.-P., Peck, S. C., Bartels, S., Anderson, J. C. (2009). MAP kinase phosphatase1 and protein tyrosine phosphatase1 are repressors of salicylic acid synthesis and SNC1-mediated responses in *Arabidopsis*. Plant Cell, 21, 2884–2897.

Busi, R., Neve, P., and Powles, S. (2013). Evolved polygenic herbicide resistance in *Lolium rigidum* by low-dose herbicide selection within standing genetic variation. Evol. Appl, 6, 231–242.

Cai, G., Yang, Q., Yi, B., Fan, C., Edwards, D., Batley, J., and Zhou, Y. (2014). A complex recombination pattern in the genome of allotetraploid *Brassica napusas* revealed by a high-density genetic map. PLoS ONE, 9, e109910.

Cao, H., Glazebrook, J., Clarke, J. D., Volko, S., and Dong, X. (1997). The *Arabidopsis* NPR1 Gene that controls systemic acquired resistance encodes a novel protein containing ankyrin repeats. Cell, 88, 57–63.

Cao, J., Cheng, C., Yang, J., and Wang, Q. (2015). Pathogen infection drives patterns of nutrient resorption in citrus plants. Sci. Rep, 5, 14675.

Carstens, M., McCrindle, T. K., Adams, N., Diener, A., Guzha, D. T., Murray, S. L., Ingle, R. A. (2014). Increased resistance to biotrophic pathogens in the *Arabidopsis* constitutive

induced resistance 1 mutant is EDS1 and PAD4-dependent and modulated by environmental temperature. PLoS ONE, 9, e109853.

Case, A. L., Finseth, F. R., Barr, C. M., and Fishman, L. (2016). Selfish evolution of cytonuclear hybrid incompatibility in *Mimulus*. Proc R Soc Lond, 14, 283(1838).

Casey, L. W., Lavrencic, P., Bentham, A. R., Cesari, S., Ericsson, D. J., Croll, T., Williams, S. J. (2016). The CC domain structure from the wheat stem rust resistance protein Sr33 challenges paradigms for dimerization in plant *NLR* proteins. Proc. Natl. Acad. Sci, 113, 12856–12861.

Castrillo, G., Teixeira, P. J. P. L., Paredes, S. H., Law, T. F., De Lorenzo, L., Feltcher, M. E., Dangl, J. L. (2017). Root microbiota drive direct integration of phosphate stress and immunity. Nature, 543, 513–518.

Césari, S., Kanzaki, H., Fujiwara, T., Bernoux, M., Chalvon, V., Kawano, Y., Kroj, T. (2014). The *NB-LRR* proteins *RGA4* and *RGA5* interact functionally and physically to confer disease resistance. The EMBO Journal, 33, 1941–1959.

Chae, E., Bomblies, K., Kim, S. T., Karelina, D., Zaidem, M., Ossowski, S., Weigel, D. (2014). Species-wide genetic incompatibility analysis identifies immune genes as hot spots of deleterious epistasis. Cell, 159, 1341–1351.

Chandra Ghosh, S., Asanuma, K., Kusutani, A., and Toyota, M. (2000). Effects of temperature at different growth stages on nonstructural carbohydrate, nitrate reductase activity and yield of potato. Control in Biol, 38:197-206

Chang, C., Bowman, J. L., and Meyerowitz, E. M. (2016). Field guide to plant model systems. Cell, 167, 325-339.

Chang, H. X., Brown, P. J., Lipka, A. E., Domier, L. L., and Hartman, G. L. (2016). Genome-wide association and genomic prediction identifies associated loci and predicts the sensitivity of tobacco ringspot virus in soybean plant introductions. BMC Genomics, 17, 153.

Chang, Y.-H., Huang, C.-W., Fu, S.-F., Wu, M.-Y., Wu, T., and Lin, Y.-W. (2017). Determination of salicylic acid using a magnetic iron oxide nanoparticle-based solid-phase extraction procedure followed by an online concentration technique through micellar electrokinetic capillary chromatography. J. Chromatogr. A, 1479, 62–70.

Charlesworth, D., and Vekemans, X. (2005). How and when did *Arabidopsis thaliana* become highly self-fertilising. Bioessays, 27, 472-476.

Cheeseman, J. M., and Tankou, S. K. (2004). Nitrate reductase and growth of *Arabidopsis thaliana* in solution culture. Plant and Soil, 266; 143.

Chen, C., Chen, H., Lin, Y. S., Shen, J. B., Shan, J. X., Qi, P., Lin, H. X. (2014). A two-locus interaction causes interspecific hybrid weakness in rice. Nature Commun, 5, 3357.

Chen, C., E, Z., and Lin, H. X. (2016). Evolution and Molecular Control of Hybrid Incompatibility in Plants. Front Plant Sci, 7, 1208.

Chen, H. F., Wang, H., and Li, Z. Y. (2007). Production and genetic analysis of partial hybrids in intertribal crosses between Brassica species (*B. rapa*, *B. napus*) and *Capsella bursa-pastoris*. Plant Cell Reports, 26, 1791–1800.

Chen, Z. J. (2010). Molecular mechanisms of polyploidy and hybrid vigor. Trends Plant Sci, 15, 57–71

Cheng, Y. T., Li, Y., Huang, S., Huang, Y., Dong, X., Zhang, Y., and Li, X. (2011). Stability of plant immune-receptor resistance proteins is controlled by *SKP1-CULLIN1-F-box* (SCF)-mediated protein degradation. Proc. Natl. Acad. Sci, 108, 14694–14699.

Chern, M., Canlas, P. E., and Ronald, P. C. (2008). Strong suppression of systemic acquired resistance in *Arabidopsis* by NRR is dependent on its ability to interact with NPR1and its putative repression domain. Mol Plant, 1, 552–559.

Choi, H. W., and Klessig, D. F. (2016). DAMPs, MAMPs, and NAMPs in plant innate immunity. BMC Plant Biol, 16, 232.

Claverie, J., Balacey, S., Lemaître-Guillier, C., Brulé, D., Chiltz, A., Granet, L., Poinssot, B.

(2018). The cell wall-derived xyloglucan is a new DAMP triggering plant immunity in Vitis vinifera and *Arabidopsis thaliana*. Front Plant Sci, 9, 1725.

Colcombet, J., Berriri, S., and Hirt, H. (2013). Constitutively active *MPK4* helps to clarify its role in plant immunity. Plant Signal Behav, 8, e22991.

Coluccio, M. P., Sanchez, S. E., Kasulin, L., Yanovsky, M. J., and Botto, J. F. (2011). Genetic mapping of natural variation in a shade avoidance response: ELF3 is the candidate gene for a QTL in hypocotyl growth regulation. J Exp Bot. 62, 167–176.

Corral-Lugo, A., Daddaoua, A., Ortega, A., Espinosa-Urgel, M., and Krell, T. (2016). Rosmarinic acid is a homoserine lactone mimic produced by plants that activates a bacterial quorum-sensing regulator. Science, 9, ra1

Coruzzi, G. M. (2003). Primary N-assimilation into amino Acids in *Arabidopsis*. The Arabidopsis Book, 2, e0010.

Daire, X., Noirot, E., Darblade, B., Héloir, M.-C., Lemaître-Guillier, C., Poinssot, B., Granet, L. (2018). The cell wall-derived xyloglucan is a new DAMP triggering plant immunity in *Vitis vinifera* and *Arabidopsis thaliana*. Front Plant Sci, 9, 1725.

Dangl, J. L., and Jones, J. D. G. (2001). Plant pathogens and integrated defence responses to infection. Nature, 411, 826–833

Dangl, J. L., and McDowell, J. M. (2006). Two modes of pathogen recognition by plants. Proc. Natl. Acad. Sci, 103, 8575–8576.

Day, B., Dahlbeck, D., and Staskawicz, B. J. (2006). NDR1 Interaction with RIN4 Mediates the differential activation of multiple disease resistance pathways in *Arabidopsis*. Plant Cell, 18, 2782–2791.

DeFraia, C. T., Schmelz, E. A., and Mou, Z. (2008). A rapid biosensor-based method for quantification of free and glucose-conjugated salicylic acid. Plant Methods, 4, 28.

Dellaporta, S. L., Wood, J., and Hicks, J. B. (1983). A plant DNA minipreparation: Version II. Plant Mol Biol Reporter, 1, 19–21.

Délye, C. (2013). Unravelling the genetic bases of non-target-site-based resistance (NTSR) to herbicides: A major challenge for weed science in the forthcoming decade. Pest Manag Sci, 69, 176–187.

Dempsey, D'Maris Amick, and Klessig, D. F. (2017). How does the multifaceted plant hormone salicylic acid combat disease in plants and are similar mechanisms utilized in humans? BMC Biol, 15, 23.

Dempsey, D'Maris Amick, Vlot, A. C., Wildermuth, M. C., and Klessig, D. F. (2012). Salicylic acid biosynthesis and metabolism. The Arabidopsis Book, 9, e0156.

Devine, M. D., and Shukla, A. (2000). Altered target sites as a mechanism of herbicide resistance. Crop Protection, 19, 881–889.

Devlin, B., and Risch, N. (1995). A comparison of linkage disequilibrium measures for fine-scale mapping. Genomics, 29, 311–322.

Dobzhansky, T. (1951). Genetics and the origin of species. Columbia University Press. New York, NY.

Domingos, P., Prado, A. M., Wong, A., Gehring, C., and Feijo, J. A. (2015). Nitric oxide: A multitasked signaling gas in plants. Mol Plant, 8, 506–520.

Douglas, G. M., Gos, G., Steige, K. A., Salcedo, A., Holm, K., Josephs, E. B., Wright, S. I. (2015). Hybrid origins and the earliest stages of diploidization in the highly successful recent polyploid *Capsella bursa-pastoris*. Proc. Natl. Acad. Sci, 112, 2806–2811.

Dyrka, W., Lamacchia, M., Durrens, P., Kobe, B., Daskalov, A., Paoletti, M., Saupe, S. J. (2014). Diversity and variability of NOD-like receptors in fungi. Genome Biol Evol, 6, 3137–3158.

Easlon, H. M., and Bloom, A. J. (2014). Easy leaf area: Automated digital image analysis for rapid and accurate measurement of leaf area. Applications in Plant Scis, 2, 1400033.

El-Shetehy, M., Wang, C., Shine, M. B., Yu, K., Kachroo, A., and Kachroo, P. (2015). Nitric

oxide and reactive oxygen species are required for systemic acquired resistance in plants. Plant Signal Behav, 10, e998544.

Elven, R., D. F. Murray, V. Y. Razzhivin, and B. A. Y. (2007). Panarctic flora checklist. National centre for biosystematics, University of Oslo, Oslo, (http://panarcticflora.org)/

Fan, W., and Dong, X. (2002). In vivo interaction between NPR1 and transcription factor TGA2 leads to salicylic acid-mediated gene activation *in Arabidopsis*. Plant Cell, 14, 1377–1389.

Filiault, D. L., Wessinger, C. A., Dinneny, J. R., Lutes, J., Borevitz, J. O., Weigel, D., Maloof, J. N. (2008). Amino acid polymorphisms in *Arabidopsis* phytochrome B cause differential responses to light. Proc Natl Acad Sci U S A; 105, 3157–3162.

Fischer, S., Spielau, T., and Clemens, S. (2017). Natural variation in *Arabidopsis thaliana* Cd responses and the detection of quantitative trait loci affecting Cd tolerance. Sci. Rep, 7, 3693.

Fishman, L., and Sweigart, A. L. (2018). When two rights make a wrong: The evolutionary genetics of plant hybrid incompatibilities. Annu Rev Plant Biol, 69, 707–731.

Floryszak-Wieczorek, J., and Arasimowicz-Jelonek, M. (2016). Contrasting regulation of NO and ROS in potato defense-associated metabolism in response to pathogens of different lifestyles. PLoS One, 11, e0163546.

Fonseca, J. P., and Dong, X. (2014). Functional characterization of a Nudix hydrolase *AtNUDX8* upon pathogen attack indicates a positive role in plant immune responses. PLoS One, 9, e114119.

Fu, Z. Q., and Dong, X. (2013). Systemic acquired resistance: Turning local infection into global defense. Annu Rev Plant Biol, 64, 839–863.

Gaines, T. A., Zhang, W., Wang, D., Bukun, B., Chisholm, S. T., Shaner, D. L., Westra, P. (2009). Gene amplification confers glyphosate resistance in *Amaranthus palmeri*. Proc. Natl. Acad. Sci, 107, 1029–1034.

Gantner, J., Ordon, J., Kretschmer, C., Guerois, R., and Stuttmann, J. (2019). An *EDS1-SAG101* complex functions in TNL-mediated immunity in *Solanaceae*. BioRxiv, 1, 511956.

Gao, M., Wang, X., Wang, D., Xu, F., Ding, X., Zhang, Z., Zhang, Y. (2009). Regulation of cell death and innate immunity by two receptor-like kinases in *Arabidopsis*. Cell Host Microbe, 6, 34–44.

Ge, X., Li, G.-J., Wang, S.-B., Zhu, H., Zhu, T., Wang, X., and Xia, Y. (2007). *AtNUDT7*, a negative regulator of basal immunity in *Arabidopsis*, modulates two distinct defense response pathways and is involved in maintaining redox homeostasis. Plant Physiol, 145, 204–215.

Geeta, and Mishra, R. (2018). Fungal and Bacterial Biotrophy and Necrotrophy. In Molecular Aspects of Plant-Pathogen Interaction (pp. 21–42). Singapore: Springer Singapore.

Geiger, M., Haake, V., Ludewig, F., Sonnewald, U., and Stitt, M. (1999). The nitrate and ammonium nitrate supply have a major influence on the response of photosynthesis, carbon metabolism, nitrogen metabolism and growth to elevated carbon dioxide in tobacco. Plant Cell Environ, 22, 1177–1199.

Ghanizadeh, H., and Harrington, K. C. (2017). Perspectives on non-target site mechanisms of herbicide resistance in weedy plant species using evolutionary physiology. AoB Plants, 9, plx035

Gimenez-Ibanez, S., Hann, D. R., Ntoukakis, V., Petutschnig, E., Lipka, V., and Rathjen, J. P. (2009). *AvrPtoB* Targets the LysM Receptor Kinase *CERK1* to Promote Bacterial Virulence on Plants. Current Biol, 19, 423–429.

Glazebrook, J. (2005). Contrasting mechanisms of defense against biotrophic and necrotrophic pathogens. Annu Rev Phytopathol, 43, 205–227.

Gong, C., Cao, S., Fan, R., Wei, B., Chen, G., Wang, X., Zhang, X. (2013). Identification and phylogenetic analysis of a CC-NBS-LRR encoding gene assigned on chromosome 7B of wheat. Int J Mol Sci, 14, 15330–15347.

González-Sánchez, M. I., Lee, P. T., Guy, R. H., and Compton, R. G. (2015). In situ detection of salicylate in *Ocimum basilicum* plant leaves via reverse iontophoresis. Chemical Commun, 51, 16534–16536.

Gordon, S. A., Fleck, A., and Bell, J. (1978). Optimal conditions for the estimation of ammonium by the Berthelot reaction. Annals of Clinical Biochemistry: Ann. Clin. Biochem, 15, 270–275.

Goritschnig, S., Krasileva, K. V., Dahlbeck, D., and Staskawicz, B. J. (2012). Computational prediction and molecular characterization of an oomycete effector and the cognate *Arabidopsis* resistance gene. PLoS Genet, 8, e1002502.

Gou, M., and Hua, J. (2012). Complex regulation of an R gene *SNC1* revealed by autoimmune mutants. Plant Signal Behav, 7, 213–216.

Grant, M. R., Godiard, L., Straube, E., Ashfield, T., Lewald, J., Sattler, A., Dangl, J. L. (1995). Structure of the *Arabidopsis* RPM1 gene enabling dual specificity disease resistance. Science, 269, 843–846.

Gu, Y., Zavaliev, R., and Dong, X. (2017). Membrane trafficking in plant immunity. Mol Plant, 10, 1026–1034.

Guerra, D., Crosatti, C., Khoshro, H. H., Mastrangelo, A. M., Mica, E., and Mazzucotelli, E. (2015). Post-transcriptional and post-translational regulations of drought and heat response in plants: a spider's web of mechanisms. Front Plant Sci, 6, 57.

Guo, Y.-L., Bechsgaard, J. S., Slotte, T., Neuffer, B., Lascoux, M., Weigel, D., and Schierup, M. H. (2009). Recent speciation of *Capsella rubella* from *Capsella grandiflora*, associated with loss of self-incompatibility and an extreme bottleneck. Proc. Natl. Acad. Sci, 106, 5246–5251.

Gupta, K. J., Brotman, Y., Segu, S., Zeier, T., Zeier, J., Persijn, S. T., Mur, L. A. J. (2013). The form of nitrogen nutrition affects resistance against *Pseudomonas syringae* pv. *phaseolicola* in tobacco. J Exp Bot, 64, 553–568.

Gurung, S., Mamidi, S., Bonman, J. M., Xiong, M., Brown-Guedira, G., and Adhikari, T. B. (2014). Genome-wide association study reveals novel quantitative trait loci associated with resistance to multiple leaf spot diseases of spring wheat. PLoS One, 9, e108179.

Gust, A. A. (2015). Peptidoglycan Perception in Plants. PLoS Pathog, 11, e1005275.

Haller, B. C., de Vos, J. M., Keller, B., Hendry, A. P., and Conti, E. (2014). A tale of two morphs: modeling pollen transfer, magic traits, and reproductive isolation in parapatry. PloS One, 9, e106512.

Hamada, M., Shoguchi, E., Shinzato, C., Kawashima, T., Miller, D. J., and Satoh, N. (2013). The Complex NOD-Like receptor repertoire of the coral *Acropora digitifera* includes novel domain combinations. Mol Biol Evol, 30, 167–176.

Haney, C. H., Samuel, B. S., Bush, J., and Ausubel, F. M. (2015). Associations with rhizosphere bacteria can confer an adaptive advantage to plants. Nature Plants, 1, 15051.

Hatsugai, N., Igarashi, D., Mase, K., Lu, Y., Tsuda, Y., Chakravarthy, S., Katagiri, F. (2017). A plant effector-triggered immunity signaling sector is inhibited by pattern-triggered immunity. The EMBO Journal, 36, 2758–2769.

He, K., and Wu, Y. (2016). Receptor-like kinases and regulation of plant innate immunity. In Enzymes, 40, 105–142.

He, Kai, Gou, X., Yuan, T., Lin, H., Asami, T., Yoshida, S., Li, J. (2007). BAK1 and BKK1 regulate brassinosteroid-dependent growth and brassinosteroid-independent cell-death pathways. Current Biol, 17, 1109–1115.

Heap, I. (2014). Global perspective of herbicide-resistant weeds. Pest Manag Sci, 70, 1306-1315.

Heil, M., Ibarra-Laclette, E., Adame-Álvarez, R. M., Martínez, O., Ramirez-Chávez, E., Molina-Torres, J., and Herrera-Estrella, L. (2012). How plants sense wounds: damaged-self recognition is based on plant-derived elicitors and induces octadecanoid signaling. PloS One, 7, e30537.

Henderson, I. R., and Salt, D. E. (2017). Natural genetic variation and hybridization in plants. J Exp Bot, 68, 5415–5417.

Henry, E., Yadeta, K. A., and Coaker, G. (2013, September). Recognition of bacterial plant pathogens: Local, systemic and transgenerational immunity. New Phytol, 199, 908-915.

Hoagland, D. R., and Arnon, D. I. (1938). The water-culture method for growing plants without soil. Water culture method for growing plants without soil. Berkeley, Calif.: University of California, College of Agriculture, Agricultural Experiment Station.

Hoermiller, I. I., Ruschhaupt, M., and Heyer, A. G. (2018). Mechanisms of frost resistance in Arabidopsis thaliana. Planta, 248, 827–835.

Höfte, M., and De Vos, P. (2006). Plant pathogenic *Pseudomonas* species. In Plant-Associated Bacteria (Gnanamanickam, S.S, ed), pp. 507–533. Dordrecht: Springer Netherlands.

Hohmann, N., Schmickl, R., Chiang, T. Y., Lučanová, M., Kolář, F., Marhold, K., and Koch, M. A. (2014). Taming the wild: Resolving the gene pools of non-model *Arabidopsis* lineages. BMC Evol Biol, 14, 1–21.

Hohmann, N., Wolf, E. M., Lysak, M. A., and Koch, M. A. (2015). A time-calibrated road Map of Brassicaceae species radiation and evolutionary history. Plant Cell, 27, 2770-2784.

Holbein, J., Grundler, F. M. W., and Siddique, S. (2016). Plant basal resistance to nematodes: An update. J Exp Bot, 67, 2049-2061.

Horton, M. W., Bodenhausen, N., Beilsmith, K., Meng, D., Muegge, B. D., Subramanian, S., Bergelson, J. (2014). Genome-wide association study of *Arabidopsis thaliana* leaf microbial community. Nature Commun, 5, 5320.

Horton, M. W., Hancock, A. M., Huang, Y. S., Toomajian, C., Atwell, S., Auton, A., Bergelson, J. (2012). Genome-wide patterns of genetic variation in worldwide *Arabidopsis thaliana* accessions from the RegMap panel. Nature Genet, 44, 212–216.

Hou, S., Wang, X., Chen, D., Yang, X., Wang, M., Turrà, D., Zhang, W. (2014). The secreted peptide PIP1 amplifies immunity through receptor-like kinase 7. PLoS Pathog, 10, e1004331.

Hou, S., Yang, Y., Wu, D., and Zhang, C. (2011). Plant immunity: evolutionary insights from *PBS1*, *Pto*, and *RIN4*. Plant Signal Behav, 6, 794–799.

Hou, X., Li, L., Peng, Z., Wei, B., Tang, S., Ding, M., Qu, L. J. (2010). A platform of high-density INDEL/CAPS markers for map-based cloning in *Arabidopsis*. Plant Journal, 63, 880–888.

Huang, S., Yuan, S., Guo, L., Yu, Y., Li, J., Wu, T., Xu, A. (2008). Genomic analysis of the immune gene repertoire of amphioxus reveals extraordinary innate complexity and diversity. Genome Res, 18, 1112–1126.

Huang, T., Gao, B., Hu, X.-K., Lu, X., Well, R., Christie, P., Ju, X.-T. (2014). Ammonia-oxidation as an engine to generate nitrous oxide in an intensively managed calcareous fluvo-aquic soil. Sci. Rep, 4, 3950.

Huffaker, A., and Ryan, C. A. (2007). Endogenous peptide defense signals in *Arabidopsis* differentially amplify signaling for the innate immune response. Proc. Natl. Acad. Sci, 104, 10732–10736.

Hunter, B., and Bomblies, K. (2010). Progress and promise in using *Arabidopsis* to study adaptation, divergence, and speciation. The Arabidopsis Book, 8, e0138.

Huot, B., Yao, J., Montgomery, B. L., and He, S. Y. (2014, August 1). Growth-defense tradeoffs in plants: A balancing act to optimize fitness. Mol Plant, 7, 1267-1287.

Ichimura, K., Casais, C., Peck, S. C., Shinozaki, K., and Shirasu, K. (2006). MEKK1 is required for MPK4 activation and regulates tissue-specific and temperature-dependent cell death in *Arabidopsis.* J Biol Chem, 281, 36969–36976.

Igic, B., Kohn, J., Slotte, T., Neuffer, B., Lascoux, M., Weigel, D.,and Schierup, M. H. (2009). Evolutionary relationships among self-incompatibility RNases. Proc. Natl. Acad. Sci, 98, 13167–13171.

Ishikawa, K., Yoshimura, K., Harada, K., Fukusaki, E., Ogawa, T., Tamoi, M., and Shigeoka, S. (2010). AtNUDX6, an ADP-ribose/NADH pyrophosphohydrolase in *Arabidopsis*, positively regulates NPR1-dependent salicylic acid signaling. Plant Physiol, 152, 2000–2012.

Iwano, M., Ito, K., Shimosato-Asano, H., Lai, K.-S., and Takayama, S. (2014). Self-

Incompatibility in the *Brassicaceae*. In Sexual Reproduction in Animals and Plants, pp. 245–254. Tokyo: Springer Japan.

Jambunathan, N., Siani, J. M., and McNellis, T. W. (2001). A humidity-sensitive Arabidopsis copine mutant exhibits precocious cell death and increased disease resistance. Plant Cell, 13, 2225–2240.

Jarne, P., and Charlesworth, D. (1993). The evolution of the selfing rate in functionally hermaphrodite plants and animals. Rev Ecol Sys, 24, 441–466.

Jeuken, M. J. W., Zhang, N. W., McHale, L. K., Pelgrom, K., den Boer, E., Lindhout, P., Niks, R. E. (2009). Rin4 causes hybrid necrosis and race-specific resistance in an interspecific lettuce hybrid. Plant Cell, 21, 3368–3378.

Jiménez-Quesada, M. J., Traverso, J. Á., and Alché, J. de D. (2016). NADPH Oxidase-dependent superoxide production in plant reproductive tissues. Front Plant Sci, 7, 359.

Jin, H., Choi, S.-M., Kang, M.-J., Yun, S.-H., Kwon, D.-J., Noh, Y.-S., and Noh, B. (2018). Salicylic acid-induced transcriptional reprogramming by the HAC–NPR1–TGA histone acetyltransferase complex in *Arabidopsis*. Nucleic Acids Res, 46, 11712–11725.

Johnson, C., Boden, E., and Arias, J. (2003). Salicylic acid and NPR1 induce the recruitment of trans-activating TGA factors to a defense gene promoter in *Arabidopsis*. Plant Cell, 15, 1846–1858.

Johnson, N. A. (2002). Sixty years after "Isolating mechanisms, evolution and temperature": Muller's legacy. Genetics, 161, 939–944.

Johnston, J. S., Pepper, A. E., Hall, A. E., Chen, Z. J., Hodnett, G., Drabek, J., Price, H. J. (2005a). Evolution of genome size in Brassicaceae Ann Bot, 95, 229-35.

Johnston, M. O. (1998). Evolution of intermediate selfing rates in plants: pollination ecology versus deleterious mutations. Genetica 102, 267–278.

Jones, J. D. G., and Dangl, J. L. (2006). The plant immune system. Nature, 444, 323-9.

Jones, J. D. G., Vance, R. E., and Dangl, J. L. (2016). Intracellular innate immune surveillance devices in plants and animals. Science. 354, pii: aaf6395

Juszczak, I., Cvetkovic, J., Zuther, E., Hincha, D. K., and Baier, M. (2016). Natural variation of cold deacclimation correlates with variation of cold-acclimation of the plastid antioxidant System in *Arabidopsis thaliana* Accessions. Front Plant Sci, 7, 305.

Kagale S., Robinson K.J., Nixon J., Xiao R., Huebert T., Condie J., Kessler D., Clarke W.E., Edger P.P., Links M.G., Sharpe A.G., and Parkin I. A.P. (2014). Polyploid Evolution of the Brassicaceae during the Cenozoic Era. Plant Cell, 26, 2777-2791.

Kalladan, R., Lasky, J. R., Chang, T. Z., Sharma, S., Juenger, T. E., Verslues, P. E., and Schroeder, J. I. (2017). Natural variation identifies genes affecting drought-induced abscisic acid accumulation in *Arabidopsis thaliana*, 114, 11536–11541.

Kasianov, A. S., Klepikova, A. V., Kulakovskiy, I. V., Gerasimov, E. S., Fedotova, A. V., Besedina, E. G., Penin, A. A. (2017). High-quality genome assembly of *Capsella bursa-pastoris* reveals asymmetry of regulatory elements at early stages of polyploid genome evolution. Plant J, 91, 278–291.

Kaul, S., Koo, H. L., Jenkins, J., Rizzo, M., Rooney, T., Tallon, L. J., Somerville, C. (2000). Analysis of the genome sequence of the flowering plant *Arabidopsis thaliana.* Nature, 408, 796–815.

Kerwin, R., Feusier, J., Corwin, J., Rubin, M., Lin, C., Muok, A., Kliebenstein, D. J. (2015). Natural genetic variation in *Arabidopsis thaliana* defense metabolism genes modulates field fitness. Elife, 13;4.

Kim, M. G., Geng, X., Lee, S. Y., and Mackey, D. (2009). The *Pseudomonas syringae* type III effector *AvrRpm1* induces significant defenses by activating the *Arabidopsis* nucleotide-binding leucine-rich repeat protein RPS2. Plant J, 57, 645–653.

Kim, S. H., Gao, F., Bhattacharjee, S., Adiasor,

J. A., Nam, J. C., and Gassmann, W. (2010). The *Arabidopsis* resistance-like gene SNC1 is activated by mutations in SRFR1 and contributes to resistance to the bacterial effector AvrRps4. PLoS Pathog, 6, e1001172.

Kinkema, M., Fan, W., and Dong, X. (2000). Nuclear Localization of NPR1 Is Required for Activation of PR Gene Expression. Plant Cell, 12, 2339.

Klauser, D., Flury, P., Boller, T., and Bartels, S. (2013). Several MAMPs, including chitin fragments, enhance AtPep-triggered oxidative burst independently of wounding. Plant Signal Behav, 8. pii: e25346.

Koch, E., and Slusarenko, A. (1990). *Arabidopsis* is susceptible to infection by a downy mildew fungus. Plant Cell, 2, 437–445.

Kong, Q., Qu, N., Gao, M., Zhang, Z., Ding, X., Yang, F., Zhang, Y. (2012). The MEKK1-MKK1/MKK2-MPK4 kinase cascade negatively regulates immunity mediated by a mitogen-activated protein kinase kinase kinase in *Arabidopsis.* Plant Cell, 24, 2225–2236.

Konieczny, A., and Ausubel, F. M. (1993). A procedure for mapping *Arabidopsis* mutations using co-dominant ecotype-specific PCR-based markers. Plant J, 4, 403–410.

Koornneef, M. (1990). Linkage map of *Arabidopsis thaliana* 2n=10. In genetic maps: Book 6; Plants, pp. 6–94.

Koornneef, Maarten, and Meinke, D. (2010). The development of *Arabidopsis* as a model plant. Plant J, 61, 909–921.

Korte, A., and Farlow, A. (2013a). The advantages and limitations of trait analysis with GWAS: a review. Plant Methods, 9, 29.

Krämer, U. (2015). Planting molecular functions in an ecological context with *Arabidopsis thaliana*. eLife. 2015, 4: e06100.

Kuai, X., MacLeod, B. J., and Després, C. (2015). Integrating data on the *Arabidopsis* NPR1/NPR3/NPR4 salicylic acid receptors; a differentiating argument. Front Plant Sci, 6, 235.

Laibach, F. (1943). *Arabidopsis thaliana* (L.) Heynh als objekt fur genetische und entwicklungsphysiologische Untersuchungenitle. Bot Archiv, 44, 439–455.

Laibach, F. (1951). Summer- and winter-annual races of *A. thaliana*. A contribution to the etiology of flower development. Beitr. Biol. Pflanzen, 28, 173–210.

Lawson, T. (2009). Guard cell photosynthesis and stomatal function. New Phytol, 181, 13-34.

Lebeis, S. L., Paredes, S. H., Lundberg, D. S., Breakfield, N., Gehring, J., McDonald, M., Dangl, J. L. (2015). Salicylic acid modulates colonization of the root microbiome by specific bacterial taxa. Science, 349, 860–864.

Lee, J., Garland, G. M., and Viscarra Rossel, R. A. (2018). Continental soil drivers of ammonium and nitrate in Australia. Soil, 4, 213–224.

Lenton, T. M., Dahl, T. W., Daines, S. J., Mills, B. J. W., Ozaki, K., Saltzman, M. R., and Porada, P. (2016). Earliest land plants created modern levels of atmospheric oxygen. Proc. Natl. Acad. Sci, 113, 9704–9709.

Leppyanen, I. V, Shakhnazarova, V. Y., Shtark, O. Y., Vishnevskaya, N. A., Tikhonovich, I. A., and Dolgikh, E. A. (2018). Receptor-like kinase *LYK9* in *Pisum sativum* L. Is the *CERK1-like* receptor that controls both plant immunity and AM symbiosis development. Int J Mol Sci, 19, e8.

Li, B., Li, G., Kronzucker, H. J., Baluška, F., and Shi, W. (2014). Ammonium stress in *Arabidopsis*: signaling, genetic loci, and physiological targets. Trends Plant Sci, 19, 107–114.

Li, Y., Li, S., Bi, D., Cheng, Y. T., Li, X., and Zhang, Y. (2010). SRFR1 negatively regulates plant NB-LRR resistance protein accumulation to prevent autoimmunity. PLoS Pathog, 6, e1001111.

Lindermayr, C., Sell, S., Müller, B., Leister, D., and Durner, J. (2010). Redox regulation of the *NPR1-TGA1* system of *Arabidopsis thaliana* by nitric oxide. Plant Cell, 22, 2894–2907.

Litrico, I., and Violle, C. (2015). Diversity in plant breeding: A new conceptual framework. Trends Plant Sci. 20, 604-613.

Liu, C., Atanasov, K. E., Tiburcio, AF., and Alcázar, R. (2019). The polyamine putrescine contributes to H2O2 and RbohD/F-dependent positive feedback loop of PAMP-triggered immunity in *Arabidopsis thaliana*. Submitted Front Plant Sci, (*submitted*).

Liu, J.-H., Wang, W., Wu, H., Gong, X., and Moriguchi, T. (2015). Polyamines function in stress tolerance: from synthesis to regulation. Front Plant Sci, 6, 827.

Lou, Y.-R., Bor, M., Yan, J., Preuss, A. S., and Jander, G. (2016). *Arabidopsis* NATA1 acetylates putrescine and decreases defense-related hydrogen peroxide accumulation. Plant Physiol, 171, 1443–1455.

Lu, H., Salimian, S., Gamelin, E., Wang, G., Fedorowski, J., Lacourse, W., and Greenberg, J. T. (2009). Genetic analysis of *acd6-1* reveals complex defense networks and leads to identification of novel defense genes in *Arabidopsis*. Plant Journal, 58, 401–412.

Lu, L., Shao, D., Qiu, X., Sun, L., Yan, W., Zhou, X., Xing, Y. (2013). Natural variation and artificial selection in four genes determine grain shape in rice. New Phytol, 200, 1269–1280.

Lysak, M. A., Koch, M. A., Pecinka, A., and Schubert, I. (2005). Chromosome triplication found across the tribe Brassiceae. Genome Res, 15, 516–525.

Macho, A. P., and Zipfel, C. (2014). Plant PRRs and the activation of innate immune signaling. Molecular Cell. 54, 263-272

Marina, M., Sirera, F. V., Rambla, J. L., Gonzalez, M. E., Blázquez, M. A., Carbonell, J., Ruiz, O. A. (2013). Thermospermine catabolism increases *Arabidopsis thaliana* resistance to *Pseudomonas viridiflava*. J Exp Bot, 64, 1393–1402.

Masclaux-Daubresse, C., Daniel-Vedele, F., Dechorgnat, J., Chardon, F., Gaufichon, L., and Suzuki, A. (2010). Nitrogen uptake, assimilation and remobilization in plants: challenges for sustainable and productive agriculture. Ann Bot, 105, 1141-57.

Mason, A., Takahira, J., Atri, C., Samans, B., Hayward, A., Cowling, W., Nelson, M. (2015). Microspore culture reveals complex meiotic behaviour in a trigenomic Brassica hybrid. BMC Plant Biol, 15, 173.

Matsuda, F., Nakabayashi, R., Yang, Z., Okazaki, Y., Yonemaru, J. I., Ebana, K., Saito, K. (2015). Metabolome-genome-wide association study dissects genetic architecture for generating natural variation in rice secondary metabolism. Plant J, 81, 13–23.

McHale, L., Tan, X., Koehl, P., and Michelmore, R. W. (2006). Plant NBS-LRR proteins: adaptable guards. Genome Biology. 7, 212

Meinke, D. W., Cherry, J. M., Dean, C., Rounsley, S. D., and Koornneef, M. (1998). *Arabidopsis thaliana*: a model plant for genome analysis. Science, 282, 662, 679–682.

Mélida, H., Sopeña-Torres, S., Bacete, L., Garrido-Arandia, M., Jordá, L., López, G., Molina, A. (2018). Non-branched β-1,3-glucan oligosaccharides trigger immune responses in *Arabidopsis*. Plant J, 93, 34–49.

Meyer, R. S., Choi, J. Y., Sanches, M., Plessis, A., Flowers, J. M., Amas, J., Purugganan, M. D. (2016). Domestication history and geographical adaptation inferred from a SNP map of African rice. Nature Genet, 48, 1083–1088.

Mitchell-Olds, T., and Schmitt, J. (2006). Genetic mechanisms and evolutionary significance of natural variation in *Arabidopsis*. Nature. Nature. 22; 441, 947-952.

Mitsuya, Y., Takahashi, Y., Berberich, T., Miyazaki, A., Matsumura, H., Takahashi, H., Kusano, T. (2009). Spermine signaling plays a significant role in the defense response of *Arabidopsis thaliana* to cucumber mosaic virus. Journal of Plant Physiol, 166, 626–643.

Mizuta, Y., Harushima, Y., and Kurata, N. (2010). Rice pollen hybrid incompatibility caused by reciprocal gene loss of duplicated genes. Proc Natl Acad Sci. 107, 20417–20422.

Moore, T. G. (2008). Global warming. The good, the bad, the ugly and the efficient. EMBO Rep, 9(Suppl 1), S41–S45.

Moorhead, G. B. G., Meek, S. E. M., Douglas, P.,

Bridges, D., Smith, C. S., Morrice, N., and MacKintosh, C. (2003). Purification of a plant nucleotide pyrophosphatase as a protein that interferes with nitrate reductase and glutamine synthetase assays. Eur J Biochem, 270, 1356–1362.

Mou, Z. (2017). Extracellular pyridine nucleotides as immune elicitors in *Arabidopsis*. Plant Signal Behav, 12, e1388977.

Mou, Z., Fan, W., and Dong, X. (2003). Inducer of plant systemic acquired resistance regulate NPR1 function through redox changes. Cell, 113, 815-816

Moyle, L. C., and Nakazato, T. (2008). Comparative genetics of hybrid incompatibility: Sterility in two solanum species crosses. Genetics, 179, 1437–1453.

Muller, H. (1942). Isolating mechanisms, evolution and temperature. In Biol. Symp. Vol. 6, pp. 71–125.

Mur, L. A. J., Simpson, C., Kumari, A., Gupta, A. K., and Gupta, K. J. (2017). Moving nitrogen to the centre of plant defence against pathogens. Ann Bot, 119, 703.

Nasrallah, M. E., Liu, P., Sherman-Broyles, S., Boggs, N. A., and Nasrallah, J. B. (2004). Natural variation in expression of self-incompatibility in *Arabidopsis thaliana*: Implications for the evolution of selfing. Proc Natl Acad Sci, 101, 16070-16074.

Neupane, S., Andersen, E. J., Neupane, A., and Nepal, M. P. (2018). Genome-wide identification of NBS-encoding resistance Genes in sunflower (*Helianthus annuus L.*). Genes, 9, 384.

Newman, T. E., Lee, J., Williams, S. J., Choi, S., Halane, M. K., Zhou, J., Sohn, K. H. (2019). Autoimmunity and effector recognition in *Arabidopsis thaliana* can be uncoupled by mutations in the RRS1-R immune receptor. New Phytol. 222, 954-965.

Niehl, A., Wyrsch, I., Boller, T., and Heinlein, M. (2016). Double-stranded RNAs induce a pattern-triggered immune signaling pathway in plants. New Phytol, 211, 1008–1019.

Nitta, Y., Ding, P., and Zhang, Y. (2014). Identification of additional MAP kinases activated upon PAMP treatment. Plant Signal Behav, 9, e976155.

Niu, Y., Chen, P., Zhang, Y., Wang, Z., Hu, S., Jin, G., Guo, L. (2018). Natural variation among *Arabidopsis thaliana* accessions in tolerance to high magnesium supply. Sci. Rep., 8, 13640.

Noguero, M., and Lacombe, B. (2016). Transporters involved in root nitrate uptake and sensing by *Arabidopsis*. Front Plant Sci, 7, 1391.

Nordborg, M., Borevitz, J. O., Bergelson, J., Berry, C. C., Chory, J., Hagenblad, J., Weigel, D. (2002). The extent of linkage disequilibrium in *Arabidopsis thaliana*. Nature Genet, 30, 190–193.

Noutoshi, Y., Ito, T., Seki, M., Nakashita, H., Yoshida, S., Marco, Y., Shinozaki, K. (2005). A single amino acid insertion in the *WRKY* domain of the *Arabidopsis TIR-NBS-LRR-WRKY*-type disease resistance protein SLH1 (*sensitive to low humidity 1*) causes activation of defense responses and hypersensitive cell death. Plant J, 43, 873–888.

Novikova, P. Y., Hohmann, N., Nizhynska, V., Tsuchimatsu, T., Ali, J., Muir, G., Nordborg, M. (2016). Sequencing of the genus *Arabidopsis* identifies a complex history of nonbifurcating speciation and abundant trans-specific polymorphism. Nature Genet, 48, 1077–1082.

Novikova, P. Y., Hohmann, N., and Van de Peer, Y. (2018). Polyploid *Arabidopsis* species originated around recent glaciation maxima. Curr Opin Plant Biol. 42, 8-15

Nunes-Nesi, A., Fernie, A. R., and Stitt, M. (2010). Metabolic and signaling aspects underpinning the regulation of plant carbon nitrogen interactions. Mol Plant. 3, 973-996

Okada, M., Yoshida, K., and Takumi, S. (2017). Hybrid incompatibilities in interspecific crosses between tetraploid wheat and its wild diploid relative *Aegilops umbellulata*. Plant Mol Biol, 95, 625–645.

Olukolu, B. A., Wang, G.-F., Vontimitta, V., Venkata, B. P., and Marla, S. (2014). A Genome-wide association study of the maize

hypersensitive defense response identifies genes that cluster in related pathways. PLoS Genet, 10, 1004562.

Orr, H. A. (2009). Fitness and its role in evolutionary genetics. Nat Rev Genet, 10, 531–539.

Østergaard, L., and King, G. J. (2008). Standardized gene nomenclature for the Brassica genus. Plant Methods, 4:10.

Park, B. S., Song, J. T., and Seo, H. S. (2011). *Arabidopsis* nitrate reductase activity is stimulated by the *E3 SUMO* ligase *AtSIZ1*. Nature Commu, 2, 400.

Pastor, V., Vicent, C., Cerezo, M., Mauch-Mani, B., Dean, J., and Flors, V. (2012). Detection, characterization and quantification of salicylic acid conjugates in plant extracts by ESI tandem mass spectrometric techniques. Plant Physiol Biochem, 53, 19–26.

Patel, D., Basu, M., Hayes, S., Majláth, I., Hetherington, F. M., Tschaplinski, T. J., and Franklin, K. A. (2013). Temperature-dependent shade avoidance involves the receptor-like kinase *ERECTA*. Plant J, 73, 980–992.

Petersen, M, Brodersen, P., Naested, H., Andreasson, E., Lindhart, U., Johansen, B., Mundy, J. (2000). *Arabidopsis* map kinase 4 negatively regulates systemic acquired resistance. Cell, 103, 1111–1120.

Petutschnig, E. K., Stolze, M., Lipka, U., Kopischke, M., Horlacher, J., Valerius, O., Lipka, V. (2014). A novel *Arabidopsis CHITIN ELICITOR RECEPTOR KINASE 1* (*CERK1*) mutant with enhanced pathogen-induced cell death and altered receptor processing. New Phytol, 204, 955–967.

Philippot, L., Raaijmakers, J. M., Lemanceau, P., and Van Der Putten, W. H. (2013). Going back to the roots: The microbial ecology of the rhizosphere. Nat Rev Microbiol, 11, 789-99.

Picó, F. X., Méndez-Vigo, B., Martínez-Zapater, J. M., and Alonso-Blanco, C. (2008). Natural genetic variation of *Arabidopsis thaliana* is geographically structured in the Iberian Peninsula. Genetics, 180, 1009–1021.

Pinheiro, F., Cafasso, D., Cozzolino, S., and Scopece, G. (2015). Transitions between self-compatibility and self-incompatibility and the evolution of reproductive isolation in the large and diverse tropical genus Dendrobium (Orchidaceae). Ann Bot, 116, 457–467.

Planas-Portell, J., Gallart, M., Tiburcio, A. F., and Altabella, T. (2013). Copper-containing amine oxidases contribute to terminal polyamine oxidation in peroxisomes and apoplast of *Arabidopsis thaliana*. BMC Plant Biol, 13, 109.

Platt, A., Vilhjálmsson, B. J., and Nordborg, M. (2010). Conditions under which genome-wide association studies will be positively misleading. Genetics, 186, 1045–1052.

Porra, R. J. (2002). The chequered history of the development and use of simultaneous equations for the accurate determination of chlorophylls a and b. Photosynth Res, 73, 149–156.

Posé, D., Verhage, L., Ott, F., Yant, L., Mathieu, J., Angenent, G. C., Schmid, M. (2013). Temperature-dependent regulation of flowering by antagonistic FLM variants. Nature, 503, 414–417.

Preiter, K., Brooks, D. M., Penaloza-Vazquez, A., Sreedharan, A., Bender, C. L., and Kunkel, B. N. (2005). Novel virulence gene of *Pseudomonas syringae pv. tomato* strain DC3000. J Bact, 187, 7805–7814.

Proell, M., Riedl, S. J., Fritz, J. H., Rojas, A. M., and Schwarzenbacher, R. (2008). The Nod-like receptor (NLR) family: A tale of similarities and differences. PLoS One, 3, e2119.

Provart, N. J., Alonso, J., Assmann, S. M., Bergmann, D., Brady, S. M., Brkljacic, J., McCourt, P. (2016). 50 years of *Arabidopsis* research: highlights and future directions. New Phytol, 209, 921–944.

Qi, J., Wang, J., Gong, Z., and Zhou, J.-M. (2017a). Apoplastic ROS signaling in plant immunity. Curr Opin Plant Biol, 38, 92–100.

Qi, J., Wang, J., Gong, Z., and Zhou, J. M. (2017). Apoplastic ROS signaling in plant immunity. Curr Opin Plant Biol. 38:92-100.

Qu, Z., Wang, J., Almøy, T., and Bakken, L. R.

(2014). Excessive use of nitrogen in Chinese agriculture results in high N(2) O/(N(2) O+N(2) product ratio of denitrification, primarily due to acidification of the soils. Global Change Biol, 20, 1685–1698.

Raiola, A., Errico, A., Petruk, G., Monti, D. M., Barone, A., and Rigano, M. M. (2018). Bioactive compounds in Brassicaceae vegetables with a role in the prevention of chronic diseases. Molecules, 23, pii: E15.

Rast, J. P., Smith, L. C., Loza-Coll, M., Hibino, T., and Litman, G. W. (2006). Genomic insights into the immune system of the sea urchin. Science. 314, 952-956.

Rathore, J. S., and Ghosh, C. (2018). Pathogen-associated molecular patterns and their perception in plants. In molecular aspects of plant-pathogen interaction. Singapore: Springer Singapore, pp. 79–113.

Rehmany, A. P. (2005). Differential recognition of highly divergent downy mildew avirulence Gene alleles by RPP1 resistance genes from two *Arabidopsis* Lines. Plant Cell, 17, 1839–1850.

Rico, A., and Preston, G. M. (2008). *Pseudomonas syringae* pv. tomato *DC3000* uses constitutive and apoplast-induced nutrient assimilation pathways to catabolize nutrients that are abundant in the tomato apoplast. Mol Plant Microbe Interact, 21, 269–282.

Rieseberg, L. H., and Willis, J. H. (2007). Plant speciation. Science. 317, 910-914.

Rodriguez, R. E., Debernardi, J. M., and Palatnik, J. F. (2014). Morphogenesis of simple leaves: Regulation of leaf size and shape. Wiley Interdisciplinary Reviews: Dev. Biol. 3, 41-57.

Rustagi, A., Singh, G., Agrawal, S., and Gupta, P. K. (2018). Proteomic studies revealing enigma of plant–pathogen interaction. In Molecular Aspects of Plant-Pathogen Interaction. Singapore: Springer Singapore, pp. 239–264.

Sadakierska-Chudy, A., and Filip, M. (2014). A comprehensive view of the epigenetic landscape. Part II: Histone post-translational modification, nucleosome level, and chromatin regulation by ncRNAs. Neurotox Res, 27, 172–197.

Sadhukhan, A., Kobayashi, Y., Nakano, Y., Iuchi, S., Kobayashi, M., Sahoo, L., and Koyama, H. (2017). Genome-wide association study reveals that the aquaporin *NIP1*;1 contributes to variation in hydrogen peroxide sensitivity in *Arabidopsis thaliana*. Mol Plant, 10, 1082–1094.

Sagor, G. H. M., Chawla, P., Kim, D. W., Berberich, T., Kojima, S., Niitsu, M., and Kusano, T. (2015). The polyamine spermine induces the unfolded protein response via the MAPK cascade in *Arabidopsis*. Front Plant Sci, 6, 687.

Sagor, G. H. M., Takahashi, H., Niitsu, M., Takahashi, Y., Berberich, T., and Kusano, T. (2012). Exogenous thermospermine has an activity to induce a subset of the defense genes and restrict cucumber mosaic virus multiplication in *Arabidopsis thaliana*. Plant Cell Rep, 31, 1227–1232.

Sánchez, M. I. G., McCullagh, J., Guy, R. H., and Compton, R. G. (2017). Reverse iontophoretic extraction of metabolites from living plants and their identification by ion-chromatography coupled to high resolution mass spectrometry. Phytochem Anal, 28, 195–201.

Sarasketa, A., Gonzalez-Moro, M. B., Gonzalez-Murua, C., and Marino, D. (2014). Exploring ammonium tolerance in a large panel of *Arabidopsis thaliana* natural accessions. J Exp Bot, 65, 6023–6033.

Saucet, S. B., Ma, Y., Sarris, P. F., Furzer, O. J., Sohn, K. H., and Jones, J. D. G. (2015). Two linked pairs of *Arabidopsis* TNL resistance genes independently confer recognition of bacterial effector *AvrRps4*. Nature Commun, 6, 6338.

Saur, I. M. L., Kadota, Y., Sklenar, J., Holton, N. J., Smakowska, E., Belkhadir, Y., Rathjen, J. P. (2016). NbCSPR underlies age-dependent immune responses to bacterial cold shock protein in *Nicotiana benthamiana*. Proc Natl Acad Sci, 113, 3389–3394.

Schmalenbach, I., Zhang, L., Ryngajllo, M., and Jiménez-Gómez, J. M. (2014). Functional analysis of the Landsberg erecta allele of FRIGIDA. BMC Plant Biol, 14, 218.

Schmickl, R., Paule, J., Klein, J., Marhold, K., and Koch, M. A. (2012). The evolutionary history of the *Arabidopsis arenosa* complex: Diverse tetraploids mask the Western Carpathian center of species and genetic diversity. PLoS One, 7, e42691.

Schumer, M., Cui, R., Rosenthal, G. G., and Andolfatto, P. (2015). Reproductive isolation of hybrid populations driven by genetic Incompatibilities. PLoS Genet, 11, e1005041.

Schwachtje, J., Fischer, A., Erban, A., and Kopka, J. (2018). Primed primary metabolism in systemic leaves: a functional systems analysis. Sci. Rep, 8, 216.

Shameer, K., Naika, M. B. N., Shafi, K. M., and Sowdhamini, R. (2018). Decoding systems biology of plant stress for sustainable agriculture development and optimized food production. Prog Biophys Mol Biol. pii: S0079-6107, 30089-30095.

Shammai, A., Petreikov, M., Yeselson, Y., Faigenboim, A., Moy-Komemi, M., Cohen, S., Schaffer, A. (2018). Natural genetic variation for expression of a SWEET transporter among wild species of *Solanum lycopersicum* (tomato) determines the hexose composition of ripening tomato fruit. Plant J, 96, 343–357.

Shan, L., He, P., Li, J., Heese, A., Peck, S. C., Nürnberger, T., Sheen, J. (2008). Bacterial effectors target the common signaling partner *BAK1* to disrupt multiple MAMP receptor-signaling complexes and impede plant immunity. Cell Host Microbe, 4, 17–27.

Sharma, A., Li, X., and Lim, Y. P. (2014). Comparative genomics of Brassicaceae crops. Breeding Science, 64, 3–13.

Sharma, B. B., Kalia, P., Singh, D., and Sharma, T. R. (2017). Introgression of black rot resistance from *Brassica carinata* to cauliflower (*Brassica oleracea* botrytis Group) through embryo rescue. Front Plant Sci, 8, 1255.

Shen, J., Chen, D., Bai, M., Sun, J., Coates, T., Lam, S. K., and Li, Y. (2016). Ammonia deposition in the neighbourhood of an intensive cattle feedlot in Victoria, Australia. Sci. Rep, 6, 32793.

Sicard, A., Kappel, C., Josephs, E. B., Lee, Y. W., Marona, C., Stinchcombe, J. R., Lenhard, M. (2015). Divergent sorting of a balanced ancestral polymorphism underlies the establishment of gene-flow barriers in *Capsella*. Nature Commun, 6, 7960.

Slatkin, M. (2008). Linkage disequilibrium - Understanding the evolutionary past and mapping the medical future. Nat Rev Genet, 9, 477-485

Slusarenko, A. J., and Schlaich, N. L. (2003). Downy mildew of *Arabidopsis thaliana* caused by *Hyaloperonospora parasitica* (formerly *Peronospora parasitica*). Mol Plant Pathol, 4, 159–170.

Smith, L. M., Bomblies, K., and Weigel, D. (2011). Complex evolutionary events at a tandem cluster of *Arabidopsis thaliana* genes resulting in a single-locus genetic incompatibility. PLoS Genet, 7, e1002164.

Solomon, P. S., Tan, K.-C., and Oliver, R. P. (2003). The nutrient supply of pathogenic fungi; a fertile field for study. Mol Plant Pathol, 4, 203–210.

Sonah, H., Deshmukh, R. K., Labbé, C., and Bélanger, R. R. (2017). Analysis of aquaporins in *Brassicaceae* species reveals high-level of conservation and dynamic role against biotic and abiotic stress in canola. Sci. Rep., 7, 2771.

Souza, C. de A., Li, S., Lin, A. Z., Boutrot, F., Grossmann, G., Zipfel, C., and Somerville, S. C. (2017). Cellulose-derived oligomers Act as damage-associated molecular patterns and trigger defense-like responses. Plant Physiol, 173, 2383–2398.

Stefanelli, C., Pignatti, C., Caldarera, C. M., Bonavita, F., Guarnieri, C., Flamigni, F., and Stanic', I. (2002). Spermine triggers the activation of caspase-3 in a cell-free model of apoptosis. FEBS Lett, 451, 95–98.

Stitt, M. (1999). Nitrate regulation. Curr Opin Plant Biol, 178–186.

Stringlis, I. A., Yu, K., Feussner, K., de Jonge, R., Van Bentum, S., Van Verk, M. C., Pieterse, C. M. J. (2018). MYB72-dependent coumarin exudation shapes root microbiome

assembly to promote plant health. Proc Natl Acad Sci, 115, E5213–E5222.

Stuttmann, J., Peine, N., Garcia, A. V., Wagner, C., Choudhury, S. R., Wang, Y., and Parker, J. E. (2016). *Arabidopsis thaliana* DM2h (R8) within the Landsberg *RPP1-like* resistance Locus underlies three different cases of EDS1-conditioned autoimmunity. PLoS Genet, 12, e1005990.

Sukno, S. A., Rivera, L. P., Rech, G. E., Vargas, W. A., Diaz-Minguez, J. M., Benito, E. P., Martin, J. M. S. (2012). Plant defense mechanisms are activated during biotrophic and necrotrophic development of *Colletotricum graminicola* in maize. Plant Physiol, 158, 1342–1358.

Sureshkumar, S., Todesco, M., Schneeberger, K., Harilal, R., Balasubramanian, S., and Weigel, D. (2009). A genetic defect caused by a triplet repeat expansion in *Arabidopsis thaliana*. Science, 323, 1060–1063.

Sweigart, A. L., and Willis, J. H. (2012). Molecular evolution and genetics of postzygotic reproductive isolation in plants. F1000 Biol Rep, 4, 23.

Świadek, M., Proost, S., Sieh, D., Yu, J., Todesco, M., Jorzig, C., Laitinen, R. A. E. (2017). Novel allelic variants in *ACD6* cause hybrid necrosis in local collection of *Arabidopsis thaliana*. New Phytol, 213, 900–915.

Tada, Y., Spoel, S. H., Pajerowska-Mukhtar, K., Mou, Z., Song, J., Wang, C., Dong, X. (2008). Plant immunity requires conformational changes of NPR1 via S-nitrosylation and thioredoxins. Science, 321, 952–956.

Takahashi, Y., Berberich, T., Miyazaki, A., Seo, S., Ohashi, Y., and Kusano, T. (2003). Spermine signalling in tobacco: Activation of mitogen-activated protein kinases by spermine is mediated through mitochondrial dysfunction. Plant J, 36, 820–829.

Takahashi, Y., Uehara, Y., Berberich, T., Ito, A., Saitoh, H., Miyazaki, A., Kusano, T. (2004). A subset of hypersensitive response marker genes, including HSR203J, is the downstream target of a spermine signal transduction pathway in tobacco. Plant J, 40, 586–595.

Tanaka, K., Choi, J., Cao, Y., and Stacey, G. (2014). Extracellular ATP acts as a damage-associated molecular pattern (DAMP) signal in plants. Front Plant Sci, 5, 446.

Tang, C., Toomajian, C., Sherman-Broyles, S., Plagnol, V., Guo, Y.-L., Hu, T. T., Nordborg, M. (2007). The evolution of selfing in *Arabidopsis thaliana*. Science, 317, 1070–1072.

Tavernier, V., Cadiou, S., Pageau, K., Laugé, R., Reisdorf-Cren, M., Langin, T., and Masclaux-Daubresse, C. (2007). The plant nitrogen mobilization promoted by *Colletotrichum lindemuthianum* in *Phaseolus* leaves depends on fungus pathogenicity. J Exp Bot, 58, 3351–3360.

Tavladoraki, P., Cona, A., and Angelini, R. (2016). Copper-Containing amine oxidases and FAD-dependent polyamine oxidases are key players in plant tissue differentiation and organ development. Front Plant Sci, 7, 824.

Teixeira, M. A., Wei, L., and Kaloshian, I. (2016). Root-knot nematodes induce pattern-triggered immunity in *Arabidopsis thaliana* roots. New Phytol, 211, 276–287.

Thalineau, E., Truong, H.-N., Berger, A., Fournier, C., Boscari, A., Wendehenne, D., and Jeandroz, S. (2016). Cross-regulation between N metabolism and nitric oxide (NO) Signaling during Plant Immunity. Front Plant Sci., 7, 472.

Thomma, B. P. H. J., Nürnberger, T., and Joosten, M. H. A. J. (2011). Of PAMPs and effectors: The blurred PTI-ETI dichotomy. The Plant Cell, 23, 4–15.

Tiburcio, A. F., Altabella, T., Bitrián, M., and Alcázar, R. (2014). The roles of polyamines during the lifespan of plants: from development to stress. Planta, 240, 1–18.

Tiku, A. R. (2018). Antimicrobial compounds and their role in plant defense. In Molecular Aspects of Plant-Pathogen Interaction (pp. 283–307). Singapore: Springer Singapore.

Tischner, R. (2000). Nitrate uptake and reduction in higher and lower plants. Plant Cell Environ, 23, 1005–1024.

Todesco, M., Kim, S.-T., Chae, E., Bomblies, K., Zaidem, M., Smith, L. M., and Laitinen, R. A. E. (2014). Activation of the *Arabidopsis thaliana* immune system by combinations of common *ACD6* Alleles. PLoS Genet, 10, e1004459.

Torres, M. A. (2010). ROS in biotic interactions. Physiol Plant, 138, 414-29.

Torres, M. A., Dangl, J. L. & Jones, J. D. G. (2002). *Arabidopsis* gp91phox homologues AtrbohD and AtrbohF are required for accumulation of reactive oxygen intermediates in the plant defense response. Proc. Natl. Acad. Sci. U. S. A. 99, 517–22

Torto, T. A., Li, S., Styer, A., Huitema, E., Testa, A., Gow, N. A. R., Kamoun, S. (2003). EST Mining and functional expression assays identify extracellular effector proteins from the plant pathogen *Phytophthora*. Genome Res, 13, 1675–1685.

Toruño, T. Y., Stergiopoulos, I., and Coaker, G. (2016). Plant-pathogen effectors: Cellular probes interfering with plant defenses in spatial and temporal manners. Annu Rev Phytopathol, 54, 419–441.

Town, C. D. (2006). Comparative genomics of *Brassica oleracea* and *Arabidopsis thaliana* reveal gene loss, fragmentation, and dispersal after polyploidy. Plant Cell, 18, 1348–1359.

Tran, D. T., Chung, E. H., Habring-Müller, A., Demar, M., Schwab, R., Dangl, J. L., Chae, E. (2017). Activation of a plant NLR complex through heteromeric association with an autoimmune risk variant of another NLR. Current Biology, 27, 1148–1160.

Trontin, C., bastien Tisné, S., Bach, L., and Loudet, O. (2011). What does *Arabidopsis* natural variation teach us (and does not teach us) about adaptation in plants? Curr Opin Plant Biol, 14, 225–231.

Tseng, P.-J., Wang, C.-Y., Huang, T.-Y., Chuang, Y.-Y., Fu, S.-F., and Lin, Y.-W. (2014). A facile colorimetric assay for determination of salicylic acid in tobacco leaves using titanium dioxide nanoparticles. Anal. Methods, 6, 1759–1765.

Turuspekov, Y., Ormanbekova, D., Rsaliev, A., and Abugalieva, S. (2016). Genome-wide association study on stem rust resistance in Kazakh spring barley lines. BMC Plant Biol, 16, 17–21.

Umezawa, Y., Hosono, T., Onodera, S. ichi, Siringan, F., Buapeng, S., Delinom, R., and Taniguchi, M. (2008). Sources of nitrate and ammonium contamination in groundwater under developing Asian megacities. Sci Total Environ, 404, 361–376.

Upadhyaya, P., Tyagi, K., Sarma, S., Tamboli, V., Sreelakshmi, Y., and Sharma, R. (2017). Natural variation in folate levels among tomato (*Solanum lycopersicum*) accessions. Food Chem, 217, 610–619.

Vaid, N., and Laitinen, R. A. E. (2019). Diverse paths to hybrid incompatibility in *Arabidopsis*. The Plant J, 97, 199–213.

Van Norman, J. M., and Benfey, P. N. (2009). *Arabidopsis thaliana* as a model organism in systems biology. Wiley Interdiscip Rev Syst Biol Med, 1, 372–379.

Van Wersch, R., Li, X., and Zhang, Y. (2016). Mighty Dwarfs: *Arabidopsis* autoimmune mutants and their usages in genetic dissection of plant immunity. Front Plant Sci, 7, 1717.

Velikova, V., Yordanov, I., and Edreva, A. (2000). Oxidative stress and some antioxidant systems in acid rain-treated bean plants protective role of exogenous polyamines. Plant Sci, 151, 59–66.

Vila-Aiub, M. M., Gundel, P. E., and Preston, C. (2015). Experimental methods for estimation of plant fitness costs associated with herbicide-resistance genes. Weed Sci, 63, 203–216.

Vilas, J. M., Romero, F. M., Rossi, F. R., Marina, M., Maiale, S. J., Calzadilla, P. I., Gárriz, A. (2018). Modulation of plant and bacterial polyamine metabolism during the compatible interaction between tomato and *Pseudomonas syringae*. Journal of Plant Physiol, 231, 281–290.

Vlot, A. C., Dempsey, D. A., and Klessig, D. F. (2009). Salicylic acid, a multifaceted hormone to combat disease. Annu Rev Phytopathol, 47, 177–206.

Wagner, M. R., Lundberg, D. S., del Rio, T. G., Tringe, S. G., Dangl, J. L., and Mitchell-Olds, T. (2016). Host genotype and age shape the leaf and root microbiomes of a wild perennial plant. Nature Commun, 7, 12151.

Wallington, E., Zipfel, C., Wang, H.-H., Schoonbeek, H., Ridout, C. J., Bowden, S., Stefanato, F. L. (2015). *Arabidopsis* EF-Tu receptor enhances bacterial disease resistance in transgenic wheat. New Phytol, 206, 606–613.

Wang, C., Zhou, M., Zhang, X., Yao, J., Zhang, Y., and Mou, Z. (2017). A lectin receptor kinase as a potential sensor for extracellular nicotinamide adenine dinucleotide in *Arabidopsis thaliana*. ELife, 6, e25474.

Wang, G. F., Ji, J., EI-Kasmi, F., Dangl, J. L., Johal, G., and Balint-Kurti, P. J. (2015). Molecular and functional analyses of a maize autoactive NB-LRR protein identify precise structural requirements for activity. PLoS Pathog, 11, e1004674.

Wang, H., Lu, Y., Liu, P., Wen, W., Zhang, J., Ge, X., and Xia, Y. (2013). The ammonium/nitrate ratio is an input signal in the temperature-modulated, *SNC1*-mediated and EDS1-dependent autoimmunity of nudt6-2 nudt7. The Plant J, 73, 262–275.

Wang, J., Tao, F., Marowsky, N. C., and Fan, C. (2016). Evolutionary fates and dynamic functionalization of young duplicate genes in *Arabidopsis* genomes. Plant Physiol. 172, 427-440.

Wang, Q., Xie, W., Xing, H., Yan, J., Meng, X., Li, X., Wang, G. (2015). Genetic architecture of natural variation in rice chlorophyll content revealed by a genome-wide association study. Mol Plant, 8, 946–957.

Wang, X., Zhang, C., Lin Lei, C., Chen, J., Li, X., Zhou, Z., Wu, J. (2016). Combined linkage and association mapping reveals QTL and candidate genes for plant and ear height in maize. Front. Plant Sci, 7, 833.

Wang, Y.-Y., Hsu, P.-K., and Tsay, Y.-F. (2012). Uptake, allocation and signaling of nitrate. Trends in Plant Sci, 17, 458–467.

Wang, Zheng, Meng, P., Zhang, X., Ren, D., and Yang, S. (2011). BON1 interacts with the protein kinases BIR1 and BAK1 in modulation of temperature-dependent plant growth and cell death in *Arabidopsis*. The Plant J, 67, 1081–1093.

Wang, Zhicai, Cui, D., Liu, J., Zhao, J., Liu, C., Xin, W., … Hu, Y. (2017). *Arabidopsis ZED1*-related kinases mediate the temperature-sensitive intersection of immune response and growth homeostasis. New Phytol, 215, 711–724.

Warwick, S. I., Francis, A., and Al-Shehbaz, I. A. (2006). Brassicaceae: Species checklist and database on CD-Rom. Plant Syst. Evol, 259, 249–258.

Warwick, S. I. (2010). Genetics and Genomics of the Brassicaceae. Genetics and Genomics of the Brassicaceae (Vol. 9). New York, NY: Springer New York.

Weigel, D., and Glazebrook, J. (2009). Dellaporta miniprep for plant DNA isolation. Cold Spring Harb Protoc, 2009, pdb.prot5178.

Westfall, P. H., Young, S. S., and Wright, S. P. (1993). On adjusting p-values for multiplicity. Biometrics, 49, 941.

Wiermer, M., Feys, B. J., and Parker, J. E. (2005). Plant immunity: The *EDS1* regulatory node. Curr Opin Plant Biol, 8, 383-389.

Wildermuth, M. C., Dewdney, J., Wu, G., and Ausubel, F. M. (2001). Isochorismate synthase is required to synthesize salicylic acid for plant defence. Nature, 414 562–565.

Wilkins, K. A., Bancroft, J., Bosch, M., Ings, J., Smirnoff, N., and Franklin-Tong, V. E. (2011). Reactive oxygen species and nitric oxide mediate actin reorganization and programmed cell death in the self-incompatibility response of Papaver. Plant Physiol, 156, 404–416.

Winck, F. V., Misra, B. B., Ferrante, A., Fernandez, E., Sanz-Luque, E., Chamizo-Ampudia, A., Galvan, A. (2015). Understanding nitrate assimilation and its regulation in microalgae. Front Plant Sci, 6, 899.

Withers, J., and Dong, X. (2017). Post-translational regulation of plant immunity. Curr Opin Plant Biol, 38, 124–132.

Wolf, D. E., Steets, J. A., Houliston, G. J., and Takebayashi, N. (2014). Genome size variation and evolution in allotetraploid *Arabidopsis kamchatica* and its parents, *Arabidopsis lyrata* and *Arabidopsis halleri*. AoB Plants.;6. pii: plu025

Wu, S., Lu, D., Kabbage, M., Wei, H.-L., Swingle, B., Records, A. R., Shan, L. (2011). Bacterial effector HopF2 suppresses *Arabidopsis* innate immunity at the plasma membrane. Mol Plant Microbe Interact, 24, 585–593.

Xin, X.-F., and He, S. Y. (2013). *Pseudomonas syringae* pv. tomato *DC3000*: A model pathogen for probing disease susceptibility and hormone signaling in plants. Annu Rev Phytopathol, 51, 473–498.

Xu, **G**., **Greene**, **G. H., Yoo**, **H**., **Liu**, **L**., **Marqués**, **J**., **Motley**, **J**., and **Dong**, **X**. (2017). Global translational reprogramming is a fundamental layer of immune regulation in plants. Nature, 545, 487–490.

Yamada, **K**., **Yamaguchi**, **K**., **Yoshimura**, **S**., **Terauchi**, **A**., and **Kawasaki**, **T**. (2017). Conservation of chitin-induced MAPK signaling pathways in rice and *Arabidopsis*. Plant Cell Physiol, 58, 993–1002.

Yamakawa, Kamada, Satoh, and Ohashi. (1998). Spermine is a salicylate-independent endogenous inducer for both tobacco acidic pathogenesis-related proteins and resistance against tobacco mosaic virus infection. Plant Physiol, 118, 1213–1222.

Yamamoto, E., Takashi, T., Morinaka, Y., Lin, S., Wu, J., Matsumoto, T., Ashikari, M. (2010). Gain of deleterious function causes an autoimmune response and Bateson–Dobzhansky–Muller incompatibility in rice. Mol Genet Genomics, 283, 305–315.

Yan, S., and Dong, X. (2014). Perception of the plant immune signal salicylic acid. Curr Opin Plant Bio; 20, 64-68.

Yang, H., Li, Y., and Hua, J. (2006). The C2 domain protein BAP1 negatively regulates defense responses in *Arabidopsis*. Plant J, 48, 238–248.

Yang, J., Liu, D., Wang, X., Ji, C., Cheng, F., Liu, B., Zhang, M. (2016). The genome sequence of allopolyploid *Brassica juncea* and analysis of differential homoeolog gene expression influencing selection. Nature Genet, 48, 1225–1232.

Yang, L., Li, B., Zheng, X., Li, J., Yang, M., Dong, X., Deng, X. W. (2015). Salicylic acid biosynthesis is enhanced and contributes to increased biotrophic pathogen resistance in *Arabidopsis* hybrids. Nature Commun., 6, 7309.

Yang, **S**., and **Hua**, **J**. (2004). A haplotype-specific resistance gene regulated by *BONZAI1* mediates temperature-dependent growth control in *Arabidopsis*. Plant Cell, 16, 1060–1071.

Yang, Shuhua, Yang, H., Grisafi, P., Sanchatjate, S., Fink, G. R., Sun, Q., and Hua, J. (2006). The *BON/CPN* gene family represses cell death and promotes cell growth in Arabidopsis. Plant J, 45, 166–179.

Yang, Sihai, Yuan, Y., Wang, L., Li, J., Wang, W., Liu, H., Tian, D. (2012). Great majority of recombination events in *Arabidopsis* are gene conversion events. Proc Natl Acad Sci, 109, 20992–20997.

Yang, Y., Gannon, P., Ding, P., Zhang, Y., Li, X., Zhang, Y., and Fang, B. (2010). *Arabidopsis snc2-1D* Activates receptor-like protein-mediated immunity transduced through *WRKY70*. The Plant Cell, 22, 3153–3163.

Yoda, H., Hiroi, Y., and Sano, H. (2006). Polyamine oxidase is one of the key elements for oxidative burst to induce programmed cell death in tobacco cultured cells. Plant Physiol, 142, 193–206.

Yoda, H., Yamaguchi, Y., and Sano, H. (2003). Induction of hypersensitive cell death by hydrogen peroxide produced through polyamine degradation in tobacco plants. Plant Physiol, 132, 1973–1981. Retrieved from

Yoshida, K. (2005). Evolutionary process of stress response systems controlled by abscisic acid in photosynthetic organisms. Yakugaku Zasshi, 125, 927-36.

Yoshioka, K., Kachroo, P., Tsui, F., Sharma, S. B., Shah, J., and Klessig, D. F. (2001). Environmentally sensitive, SA-dependent

defense responses in the cpr22 mutant of *Arabidopsis*. Plant J, 26, 447–459.

Yu, J., Pressoir, G., Briggs, W. H., Bi, I. V., Yamasaki, M., Doebley, J. F., Buckler, E. S. (2006). A unified mixed-model method for association mapping that accounts for multiple levels of relatedness. Nature Genet, 38, 203–208.

Yu, K. Q., Zhao, Y. R., Li, X. L., Shao, Y. N., Liu, F., and He, Y. (2014). Hyperspectral imaging for mapping of total nitrogen spatial distribution in pepper plant. PLoS One, 9, e116205.

Zamioudis, C., Korteland, J., Van Pelt, J. A., Van Hamersveld, M., Dombrowski, N., Bai, Y., Pieterse, C. M. J. (2015). Rhizobacterial volatiles and photosynthesis-related signals coordinate *MYB72* expression in *Arabidopsis* roots during onset of induced systemic resistance and iron-deficiency responses. Plant J, 84, 309–322.

Zandkamiri, H., Arceneaux, K., Harrison, S., Baisakh, N., and Pilcher, W. (2017). Genome-wide microarray analysis leads to identification of genes in response to herbicide, metribuzin in wheat leaves. PLOS One, 12, e0189639.

Zarza, X., Atanasov, K. E. K. E., Marco, F., Arbona, V., Carrasco, P., Kopka, J., Alcázar, R. (2016). Polyamine oxidase 5 loss-of-function mutations in *Arabidopsis thaliana* trigger metabolic and transcriptional reprogramming and promote salt stress tolerance. Plant Cell Environ, 40, 527-542

Zeng, W., Brutus, A., Kremer, J. M., Withers, J. C., Gao, X., Jones, A. D., and He, S. Y. (2011). A genetic screen reveals *Arabidopsis* stomatal and/or apoplastic defenses against *Pseudomonas syringae* pv. tomato *DC3000*. PLoS Pathog, 7, e1002291.

Zhang, H., Han, Z., Song, W., and Chai, J. (2016). Structural insight into recognition of plant peptide hormones by receptors. Mol Plant, 9, 1454-1463.

Zhang, Y., Cheng, Y. T., Qu, N., Zhao, Q., Bi, D., and Li, X. (2006). Negative regulation of defense responses in *Arabidopsis* by two *NPR1* paralogs. Plant J, 48, 647–656.

Zhang, Zhanying, Li, J., Pan, Y., Li, J., Zhou, L., Shi, H., Li, Z. (2017). Natural variation in CTB4a enhances rice adaptation to cold habitats. Nature Commun, 8, 14788.

Zhang, Zhiwu, Ersoz, E., Lai, C.-Q., Todhunter, R. J., Tiwari, H. K., Gore, M. A., Buckler, E. S. (2010). Mixed linear model approach adapted for genome-wide association studies. Nature Genet, 42, 355–360.

Zhou, B., Guo, Z., Xing, J., and Huang, B. (2005). Nitric oxide is involved in abscisic acid-induced antioxidant activities in *Stylosanthes guianensis*. J Exp Bot, 56, 3223–3228.

Zhou, J., Wu, S., Chen, X., Liu, C., Sheen, J., Shan, L., and He, P. (2014). The *Pseudomonas syringae* effector HopF2 suppresses *Arabidopsis* immunity by targeting BAK1. Plant J, 77, 235–245.

Zhu, W., Ausin, I., Seleznev, A., Méndez-Vigo, B., Picó, F. X., Sureshkumar, S., … Balasubramanian, S. (2015). Natural variation identifies *ICARUS1*, a universal gene required for cell proliferation and growth at high temperatures in *Arabidopsis thaliana*. PLoS Genet, 11, e1005085.

Zhu, W., Zaidem, M., Van de Weyer, A.-L., Gutaker, R. M., Chae, E., Kim, S.-T., Weigel, D. (2018). Modulation of ACD6 dependent hyperimmunity by natural alleles of an *Arabidopsis thaliana* NLR resistance gene. PLoS Genet, 14, e1007628.

Zipfel, C., and Felix, G. (2005). Plants and animals: A different taste for microbes? Curr Opin Plant Biol, 8, 353-360

Zipfel, C., and Robatzek, S. (2010). Pathogen-associated molecular pattern-triggered immunity: veni, vidi...? Plant Physiol, 154, 551–554.

Zottini, M., Costa, A., De Michele, R., Ruzzene, M., Carimi, F., and Schiavo, F. Lo. (2007). Salicylic acid activates nitric oxide synthesis in *Arabidopsis*. J Exp Bot, 58, 1397–1405.

ANNEX I

Supplemental material for Introduction

Supplemental Table ST 1: *Brassica* taxa members and their corresponding genomic charge and ploidy description.

Taxon	Family	Tribe	Genome size (Mbp)	Ploidy	Reference
Brassica rapa	Brassicaceae	Brassiceae	529	2n = 2x = 20	(Sharma *et al.*, 2014)
Brassica oleracea	Brassicaceae	Brassiceae	696	2n = 2x =18	(Yang *et al*., 2016)
Brassica nigra	Brassicaceae	Brassiceae	632	2n = 2x = 16	(Johnston *et al*., 2005a)
Brassic juncea	Brassicaceae	Brassiceae	534	2n = 4x = 36	(Mason *et al*., 2015)
Brassica napus	Brassicaceae	Brassiceae	566	2n = 4x = 38	(Cai *et al*., 2014)
Brassica carinata	Brassicaceae	Brassiceae	642	2n = 4x = 34	(Sharma *et al.*, 2017)

Supplemental Table ST 2: *Arabidopsis thaliana* taxa members and their corresponding genomic charge.

Taxon	Family	Tribe	Ploidy	References
Arabidopsis thaliana	Brassicaceae	Camelinae	2n = 2x = 10	(Koornneef, 1990)
Arabidopsis lyrata				
A. lyrata* spp. *lyrata	Brassicaceae	Camelinae	2n = 2x = 16	(Wolf *et al*., 2014)
A. arenicola	Brassicaceae	Camelinae	2n = 2x = 16	(Elven *et al.*, 2007)
A. lyrata* spp. *petrea	Brassicaceae	Camelinae	2n = 2x = 16	
A. lyrata* spp. *septentrionalis	Brassicaceae	Camelinae	2n = 2x= 16	
A. lyrata* spp. *umbrosa	Brassicaceae	Camelinae	2n =2x = 16	
Arabidopis halleri				
A. halleri* spp. *halleri	Brassicaceae	Camelinae	2n =2x = 16	(Briskine *et al*., 2017)
A. halleri* spp. *gemmifera	Brassicaceae	Camelinae	2n =2x = 16	(Wolf *et al*., 2014)
A. halleri* spp. *dacica	Brassicaceae	Camelinae	2n =2x = 16	(Novikova *et al*., 2016)
A. halleri* spp. *tatrica	Brassicaceae	Camelinae	2n =2x = 16	(Novikova *et al*., 2016)
A. halleri* spp. *ovirensis	Brassicaceae	Camelinae	2n =2x = 16	(Hohmann *et al*., 2014)
A. umezawana	Brassicaceae	Camelinae	2n =2x = 16	(Hohmann *et al*., 2014)
Arabidopsis arenosa				
A. arenosa* ssp. *arenosa	Brassicaceae	Camelinae	2n = 2x = 16	(Johnston *et al*., 2005b)
A. arenosa* ssp. *intermedia	Brassicaceae	Camelinae	2n = 4x = 32	(Schmickl *et al*., 2012)
A. arenosa* ssp. *borbasii	Brassicaceae	Camelinae	2n = 4x = 32	(Al-Shehbaz and O'Kane, 2002)

A. arenosa* ssp. *carpatica	Brassicaceae	Camelinae	2n = 2x = 16	(Schmickl *et al*., 2012)
A. neglecta* ssp. *neglzecta	Brassicaceae	Camelinae	2n = 2x = 16	(Al-Shehbaz and O'Kane, 2002)
A. neglecta* ssp. *robusta	Brassicaceae	Camelinae	2n = 4x = 32	(Novikova *et al*., 2016; Schmickl *et al*., 2012)
A. nitida	Brassicaceae	Camelinae	2n =2x = 16	
A. petrogena* ssp. *exoleta	Brassicaceae	Camelinae	2n = 4x = 32	(Schmickl *et al*., 2012)
A. petrogena* ssp. *petrogena	Brassicaceae	Camelinae	2n = 2x = 16	(Schmickl *et al*., 2012)
Arabidopsis cebennensis	Brassicaceae	Camelinae	2n =2x = 16	(Hohmann *et al*., 2014)
Arabidopsis pedemontana	Brassicaceae	Camelinae	2n = 2x = 16	(Al-Shehbaz and O'Kane, 2002)
Arabidopsis croatica	Brassicaceae	Camelinae	2n = 2x = 16	(Schmickl *et al*., 2012)
Allopolyploid taxa				
Arabidopsis suecica	Brassicaceae	Camelinae	2n = 4x = 26	(Johnston *et al*., 2005b)
Arabidopsis kamchatica* spp. *kamchatica	Brassicaceae	Camelinae	2n = 4x = 32	(Novikova *et al.*, 2018)
Arabidopsis kamchatica* ssp. *kawasakiana	Brassicaceae	Camelinae	2n = 4x = 32	(Wolf *et al*., 2014)
Other attractive allotetraploid taxa in plant research				
Capsella bursa-pastoris (L.) Medik.	Brassicaceae	Camelinae	2n = 4x =32	(Chen *et al.*, 2007)
Capsella grandiflora (Fauché & Chaub.) Boiss.	Brassicaceae	Camelinae	2n = 2x = 16	(Igic *et al*., 2009)
Capsella rubella Reut.	Brassicaceae	Camelinae	2n = 2x = 16	(Igic *et al*., 2009)

Supplemental Table ST 3: Genes and biological functions identified through natural variation studies in *A. thaliana* and other species.

Species	Gene name	Gene ID	Biologic process	Reference
A. thaliana	ICARUS1 (ICA1)	At2g31580	Growth	(Zhu *et al*., 2015)
A. thaliana	PHYB	AT2G18790	Red and white light sensing	(Filiault *et al*., 2008)
A. thaliana	ELF3	AT2G25930	Shade avoidance	(Coluccio *et al.*, 2011)
A. thaliana	Isopropyl malate isomerase large subunit 1(IIL1)	At4g13430	Growth	(Sureshkumar *et al*., 2009)
A. thaliana	Flowering locus M (FLM)	AT1G77080	Flowering	(Posé *et al*., 2013)
A. thaliana	Short vegetative phase (SVP)	AT2G22540	Flowering	
A. thaliana	FRIGIDA (FRI)	AT4G00650	Late-flowering	(Schmalenbach *et al*., 2014)
A. thaliana	ERECTA	AT2G26330	Shade avoidance	(Patel et al., 2013)
A. thaliana	Strubbelig-receptor family 3SRF3	AT4G03390	Immunity	(Alcázar *et al*., 2010)
A. thaliana	Heavy metal ATPase 3 (HMA3)	At4G30120	Cd^{2+} tolerance	(Fischer *et al.*, 2017)
A. thaliana	C-repeat binding factors (CBFs)	AT4G25470; AT4G25480; AT4G25490	Cold deacclimatation	(Juszczak *et al*., 2016)
O. sativa	cold tolerance at booting stage (CTB4a)	---	Cold adaptation	(Zhang *et al*., 2017)
O. sativa	Narrow leaf1 (NAL1)	---	Chlorophyll and chloroplast biosynthesis	(Wang *et al*., 2015)
Oryza sativa	Grain width and weight 2 (GW2); grain size 5 (GS5); seed width 5 (qSW5) and grain	---	Grain shape and size	(Lu *et al*., 2013)
S. lycopersicum	Several genes from the folate biosynthetic pathway	---	Folate biosynthesis and turnover	(Upadhyaya *et al*., 2017)
S. lycopersicum	SWEET transporter	---	Fruit ripening	(Shammai *et al*., 2018)
B. oleracea	Resistance genes analogs (RGA)	---	Immunity	(Bayer *et al*., 2018)

Supplemental Table ST 4: *Arabidopsis thaliana* NLR-based autoimmune hybrid incompatibilities and accessions involved.

Incompatible genes	Protein class	Accessions	Reference
RPP1-like; SRF3	TIR-NB-LRR; Leucine-rich repeat receptor kinase-like	Ler × Kas-2	(Alcázar *et al*., 2010, 2009, 2014; Atanasov *et al*., 2018)
RPP1 (DM2) / SSI4 (DM1)	TIR-NB-LRR	Uk-3 × Uk-1	(Bomblies *et al*., 2007b; Chae *et al*., 2014)
RPP1 (DM2); DM3	TIR-NB-LRR	Bla-1 × Hh-0	(Chae *et al*., 2014)
RPP1 (DM2); DM5	TIR-NB-LRR; unknown gene	Dog-4 × ICE163	(Chae *et al*., 2014)
intrinsic DM8 (RPP4/5)	TIR-NB-LRR	Ey1.5-2 × ICE228	(Chae *et al*., 2014)
RPP7 (DM6); RPW8 (DM7)	TIR-NB-LRR; RPW-NB-LRR	Fei-0 × Lerik1-3	(Bomblies *et al*., 2010; Chae *et al*., 2014)
RPP7 (DM6); RPW8 (DM7)	CC-NB-LRR; RPW-NB-LRR	KZ10 × Mrk-0	(Bomblies *et al*., 2010; Chae *et al*., 2014)
***RPP1 (*DM2); RPP8 (DM4)**	TIR-NB-LRR; CC-NB-LRR	TueWa1-2 × CE163	(Chae *et al*., 2014)
intrinsic ACD	Lipid transfer protein	Bla-1 × Hh-0	(Todesco *et al*., 2014a)
intrinsic ACD6	Lipid transfer protein	Mir-0 × Se-0	(Świadek *et al*., 2017; Todesco *et al*., 2014b)

ACD: accelerated cell death, RPP: recognition of *Peronospora parasitica* (*Hyaloperonospora arabidopsidis*), DM: dangerous mix, TIR-NB-LRR: Toll interleukin 1 nucleotide binding leucine rich repeats, CC-NB-LRR: Coiled-coil nucleotide-binding leucine rich repeats, RPW8-NB-LRR: resistance to powdery mildew 8

Supplemental Table ST5: Examples of PAMPs, DAMPs, NAMPs and effectors triggering defense responses.

Type	Organism	Molecule	Receptor	Immune response	Observed response	Reference
PAMP	Virus	dsRNA	Unknown, SERK1 dependent	PTI	MAPK, ROS, SA, gene expression	(Niehl *et al.*, 2016)
	Bacteria	csp22	LRR-RLP	PTI	ROS, Ca^{2+} influx, SA, MAPK, gene expression, cell wall reinforcement	(Saur *et al*., 2016)
	Bacteria	flg22	FLS2	PTI	Callose deposition, Ca^{2+} influx, ROS, SA, MAPK, gene expression, cell wall	(Teixeira *et al.*, 2016)
	Bacteria	elf18	EFR	PTI	Callose deposition, ROS, Ca^{2+} influx, SA, MAPK, gene expression, cell wall	(An *et al*., 2017; Wallington *et al*., 2015)
	Fungi	Chitin	CeBIP, CERK1,	PTI	MAPK, ROS, gene expression, SA, cell wall reinforcement	(Yamada *et al*., 2017)
	Fungi	β-Glucan	Beta glucan binding protein	PTI	ROS, MAPK, SA, gene expression, cell wall reinforcement	(Mélida *et al*., 2018)
	Bacteria	PGN	Lym1, Lym3	PTI	Gene expression, MAPK, ROS, cell wall reinforcement	(Gust, 2015)
DAMP	Plant	AtPeps	PEPR1, PEPR2	PTI/DTI	ROS production	(Bartels *et al*., 2013; Klauser *et al.*, 2013; Zhang *et al.*, 2016)
	Plant	Extracellular ATP (	DORN1	PTI/DTI	Ca^{2+} influx, ROS, SA	(Tanaka *et al.*, 2014)
	Plant	Extracellular NAD(P)	LecRK-I.8 (candidate receptor)	PTI/DTI	Ca^{2+} influx, ROS, SA	(Mou, 2017; Wang *et al*., 2017b)
	Plant	Ascarosides	Unknown	NTI/PTI	Callose deposition, gene expression, Ca^{2+} influx, suberin, lignin, cell wall	(Ali *et al*., 2018; Holbein *et al.*, 2016)

	Plant	Oligogalacturonides	WAK1	PTI/DTI	PR proteins, phytoalexins,	(Brutus *et al*., 2010)
	Plant	Xyloglucans	VvLYK1-1 and VvLYK1-2	PTI/DTI	ROS, MAPK, gene expression, ROS, callose deposition	(Claverie *et al*., 2018; Daire *et al*., 2018)
	Plant	Chitoligosaccharide	LysM-RLK	PTI/DTI	ROS, callose deposition, gene expression	(Leppyanen *et al*., 2018)
	Plant	PIPs	RLK7	PTI/DTI	Ca^{2+} influx, MAPK, callose deposition, cell wall reinforcement, gene	(Hou *et al*., 2014)
	Plant	Sucrose	Unknown	PTI/DTI	PR genes expression, SA, VOCs	(Chern *et al.*, 2008; Heil *et al*., 2012)
	Plant	Cellobiose	Pattern Recognition Receptor (PRR)	PTI/DTI	MAPK, Ca^{2+} influx, PR genes, suberin production	(Souza *et al*., 2017)
	Exogenous/Plant	Put	Unknown	DTI/PTI candidate	Callose deposition, gene expression, ROS, MAPK	(Liu *et al*., 2019)
	Exogenous/Plant	Spd	Unknown	DTI/PTI candidate	Gene expression, ROS, Ca^{2+}influx, MAPK, PCD	(Atanasov *et al*., 2019; Stefanelli *et al*., 2002; Yoda *et al.*, 2003)
	Exogenous/Plant	Cad	Unknown	DTI/PTI candidate	Gene expression, ROS, Ca^{2+}influx, MAPK	(Atanasov et al., 2019; Yoda et al., 2003)
	Exogenous/Plant	Spm	Unknown	DTI/PTI candidate	Gene expression, ROS, Ca^{2+}influx, MAPK	(Atanasov *et al*., 2019; Mitsuya *et al*., 2009; Sagor *et al*., 2015; Takahashi *et al*., 2003,
	Exogenous/Plant	t-Spm	Unknown	DTI/PTI candidate	Gene expression, ROS, Ca^{2+}influx, MAPK	(Atanasov *et al*., 2019; Marina *et al*., 2013; Sagor *et al*., 2012)
	Exogenous/Plant	HTD	Unknown	DTI/PTI candidate	Gene expression, ROS, Ca^{2+}influx, MAPK	(Atanasov *et al*., 2019)
Effector protein	Bacteria	AvrRps4	RRS1B/RPS4B	ETI/SAR	MAPK, hypersensitive response, oxidative stress, SA, gene expression	(Newman *et al*., 2019; Saucet *et al*., 2015)
	Bacteria	PopP2	RRS1-R/RPS4	ETI/SAR	MAPK, hypersensitive response, oxidative stress, SA, gene expression	(Newman *et al*., 2019)

	Bacteria	HopF2	Unknown, target BAK1	ETI/SAR	MAPK, hypersensitive response, oxidative stress, SA, gene expression	(Wu *et al*., 2011; Zhou *et al*., 2014)
	Bacteria	AvrPto and AvrPtoB	CERK1	ETI/SAR	MAPK, hypersensitive response, oxidative stress, SA, gene expression	(Gimenez-Ibanez *et al*., 2009; Shan *et al*., 2008)
	Oomycete	ATR1	RPP1	ETI/SAR	MAPK, hypersensitive response, oxidative stress, SA, gene expression	(Rehmany, 2005)
	Oomycete	ATR5	RPP5	ETI/SAR	MAPK, hypersensitive response, oxidative stress, SA, gene expression	(Bailey *et al*., 2011)
	Oomycete	ATR13	RPP13	ETI/SAR	MAPK, hypersensitive response, oxidative stress, SA, gene expression	(Grant *et al*., 1995)
	Oomycete	ATR39	RPP39	ETI/SAR	MAPK, hypersensitive response, oxidative stress, SA, gene expression	(Goritschnig *et al.*, 2012)
	Oomycete	HaRxL103	RPP4	ETI/SAR	MAPK, hypersensitive response, oxidative stress, SA, gene expression	(Asai *et al*., 2018)

PAMP: pathogen associated molecular patterns, DAMP: damage associated molecular patterns, NAMP: nematode associated molecular patterns, csp22: bacterial cold-shock proteins, flg22: flagellin 22, elf18: elongation factor Tu 18, PGN: peptidoglycan, AtPeps: *Arabidopsis thaliana* plant elicitor peptides, PIPs: PAMP-induced secreted peptides, Put; putrescine, Spd: spermidine, Spm: spermine, Cad: cadaverine, *t*-Spm: Thermo spermine, HTD: 1,7-diaminoheptane, PTI: pathogen triggered immunity, DTI: DAMP-triggered

ANNEX II

Supplemental material for Chapter 1

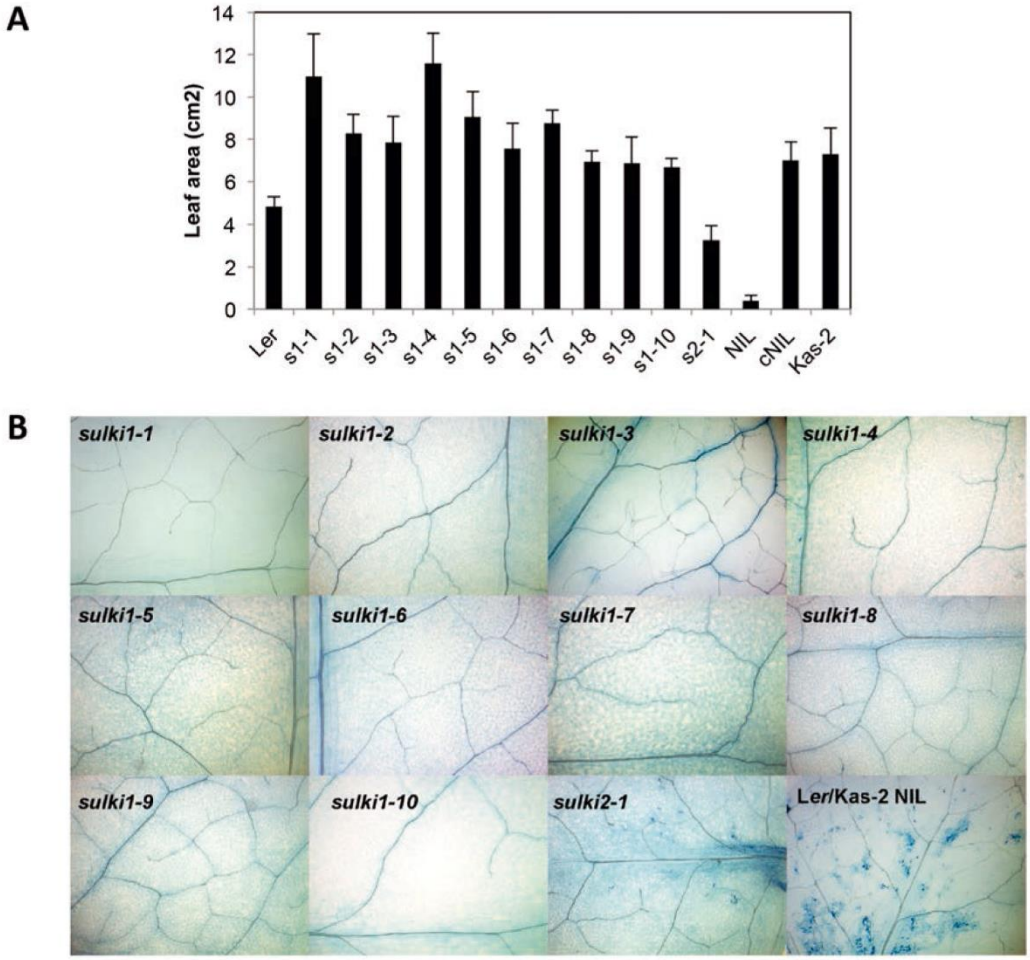

Supplemental Figure 1. Leaf area **(A)** and trypan blue staining **(B)** in 5-week-old *sulki1*, *sulki2*, L*er*/Kas-2 NIL, cNIL (Alcázar et al., 2010) and parental accessions grown at 14 - 16ºC. Error bars indicate standard deviation.

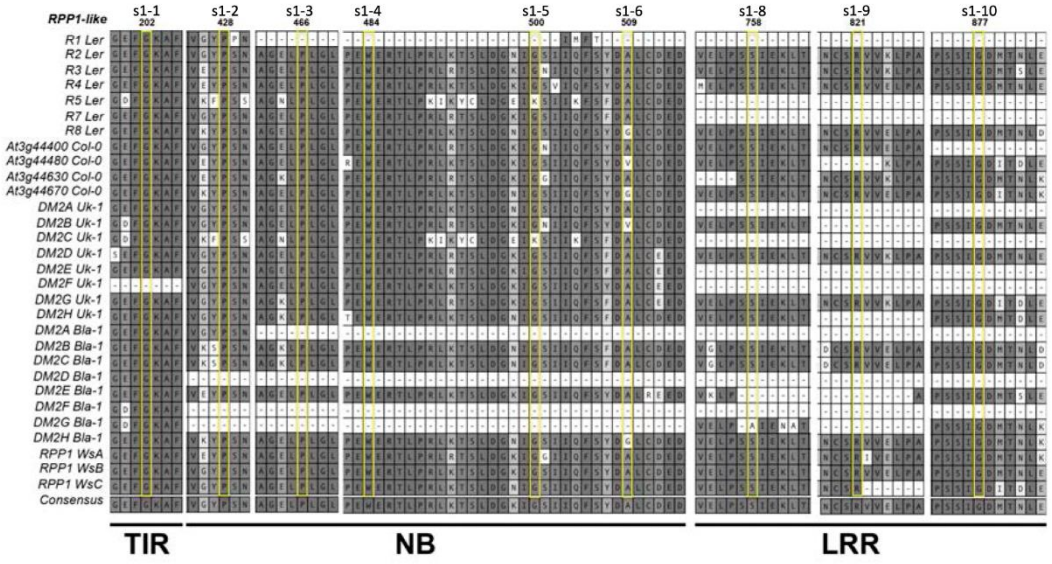

Supplemental Figure 2. Alignment of amino acid sequences for *RPP1-like* genes in L*er*, Col-0, Uk-1, Bla-1, and Ws. The position of amino acid variants in *sulki1* (*s1-1* to *s1-10*) mutants are shown on top and highlighted in yellow boxes within the aligned sequences.

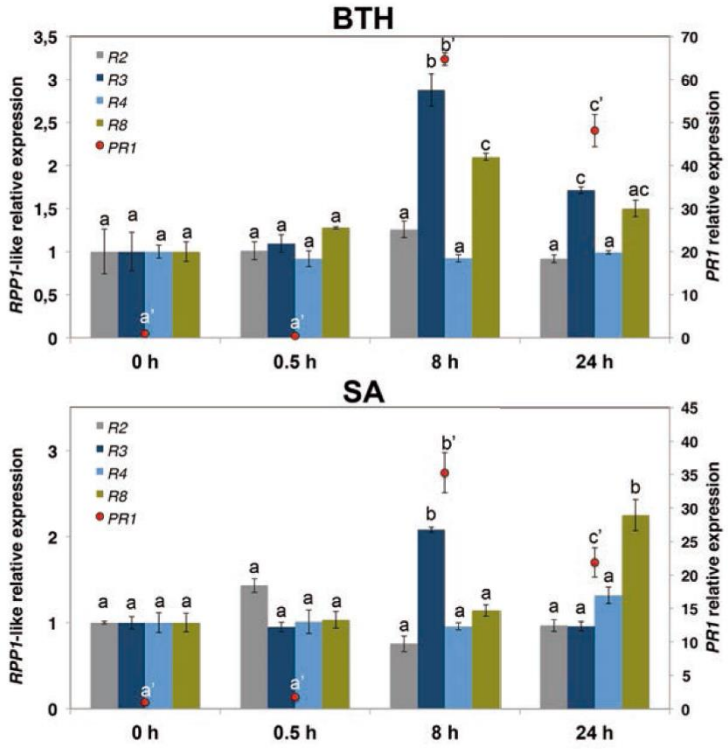

Supplemental Figure 3. RT-qPCR expression analyses of *PR1* (right axis), *RPP1-like* L*er R2*, *R3*, *R4*, and *R8* genes (left axis) in L*er* plants treated with 100 µM BTH or 100 µM SA. Samples were harvested at 0 h, 0.5 h, 8 h and 24 h after SA, BTH or mock treatment. Values are relative to mock-treated samples and are the mean ± SD of three biological replicates, each with three technical replicates. Letters indicate values that are significantly different according to Student–Newman–Keuls test at *P* value <0.05.

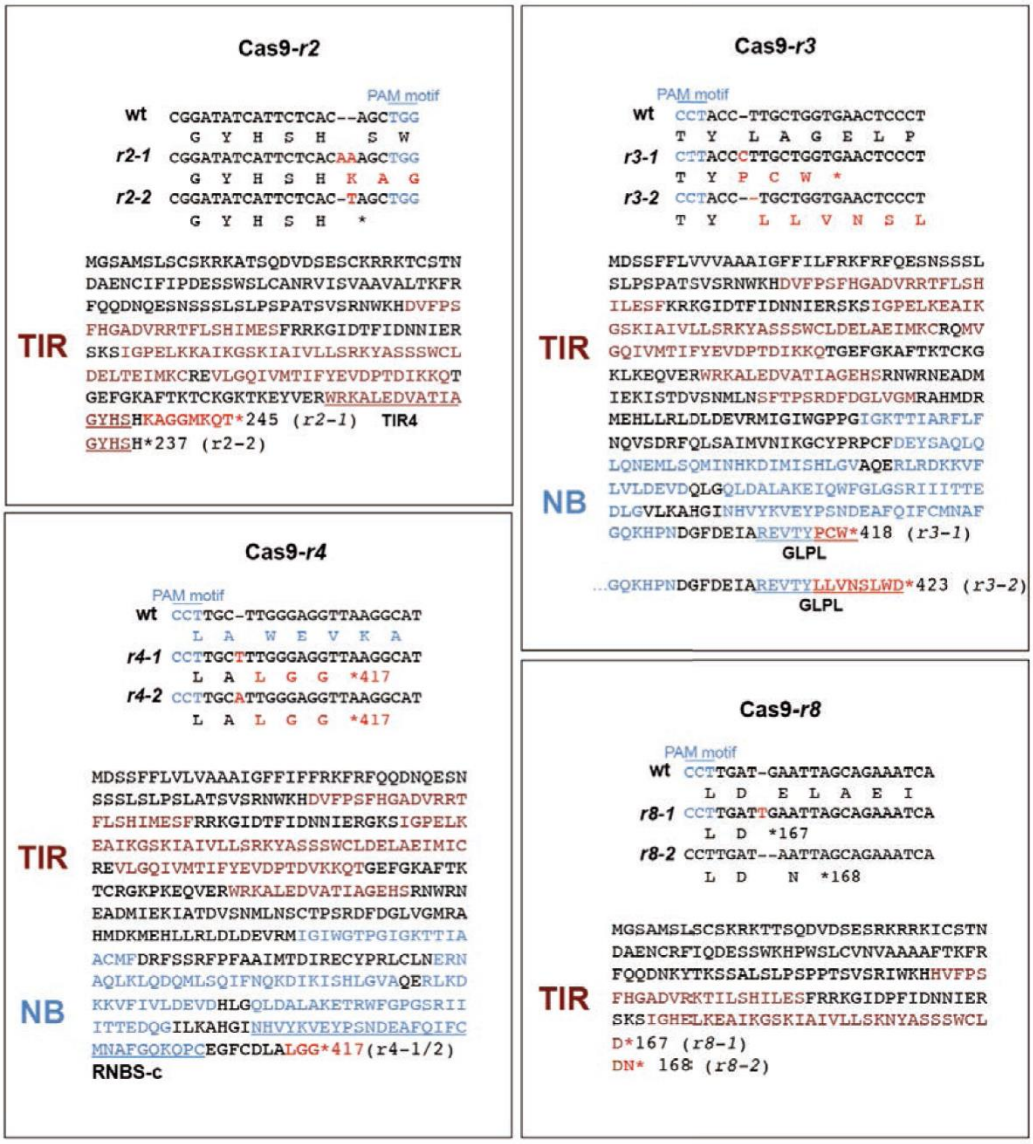

Supplemental Figure 4. CRISPR/Cas9-induced indel mutations in Cas9-*r2*, Cas9-*r3*, Cas9-*r4,* and Cas9-*r8* and their effects on protein translation. TNL domains and motifs are shown in different colors or underlined.

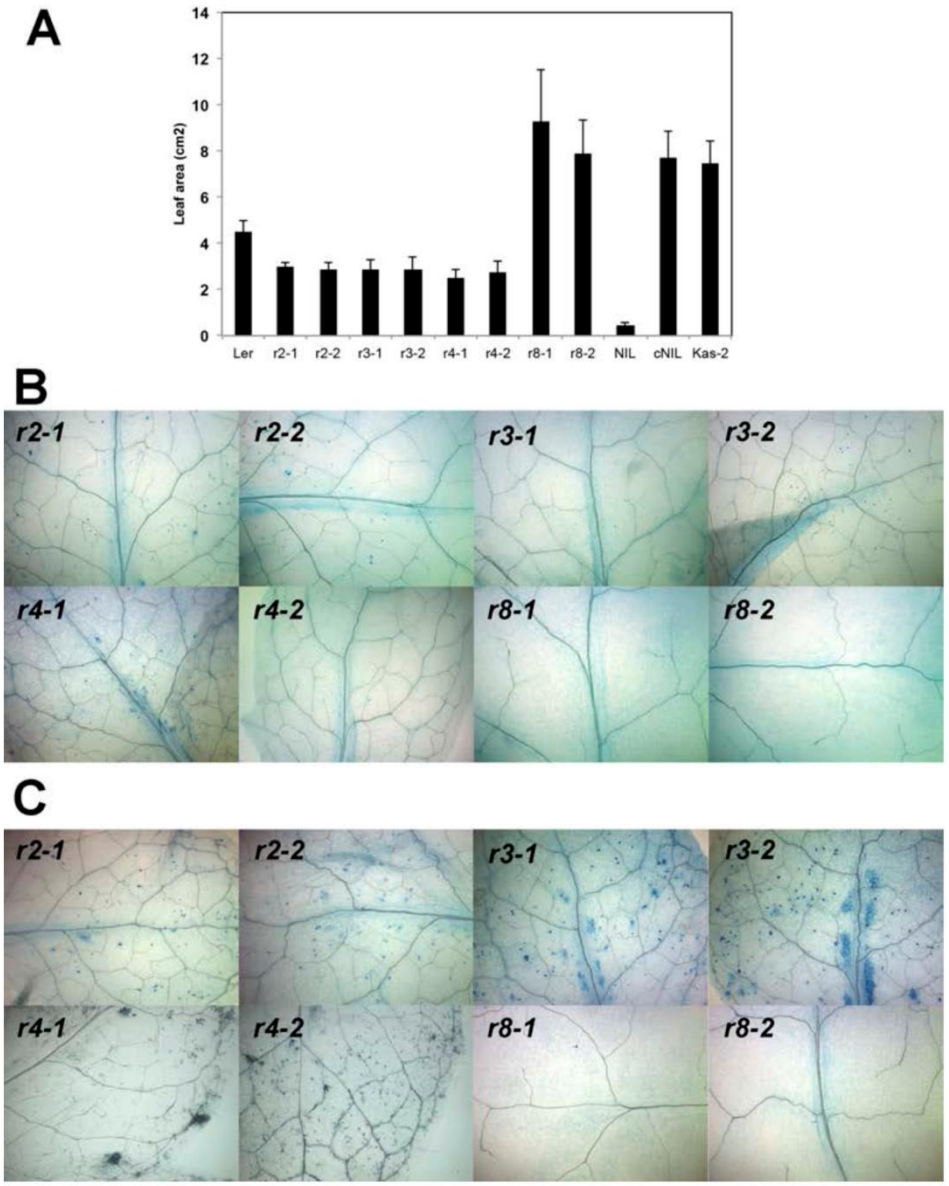

Supplemental Figure 5. Leaf area **(A)** and trypan blue staining **(B)** of 5-week-old CRISPR/Cas9 *RPP1-like* L*er* mutants grown at 14 - 16ºC. **(C)** Trypan blue staining in 7-week-old plants. Error bars indicate standard deviation.

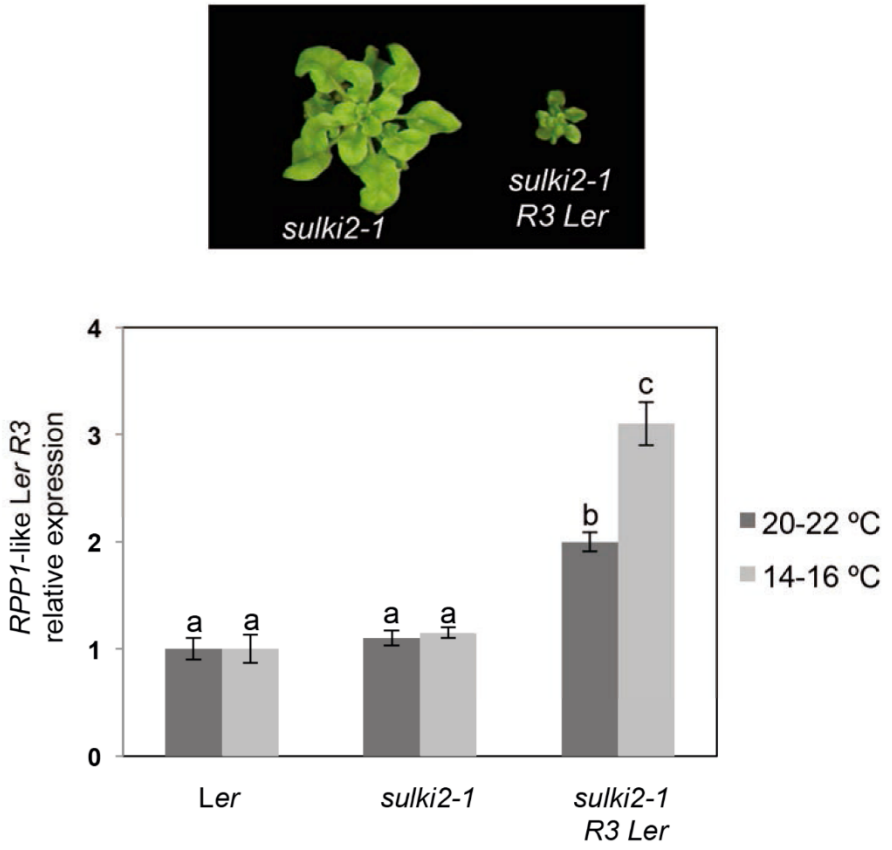

Supplemental Figure 6. Complementation of *sulki2-1* with *RPP1-like* L*er R3* gene reconstitutes L*er*/Kas-2 NIL phenotype. Pictures were taken 5 weeks after germination and growth at 14 - 16 ºC. Multiple independent *sulki2-1 RPP1-like* L*er R3* gene complemented lines (*sulki2-1 R3* L*er*) exhibited identical reconstitution of the phenotype. Quantitative expression analyses of *RPP1-like* L*er R3* in L*er*, *sulki2-1,* and one representative *sulki2-1 R3* L*er*. Letters indicate values that are significantly different according to Student–Newman–Keuls test at *P* value <0.05. Error bars indicate standard deviation.

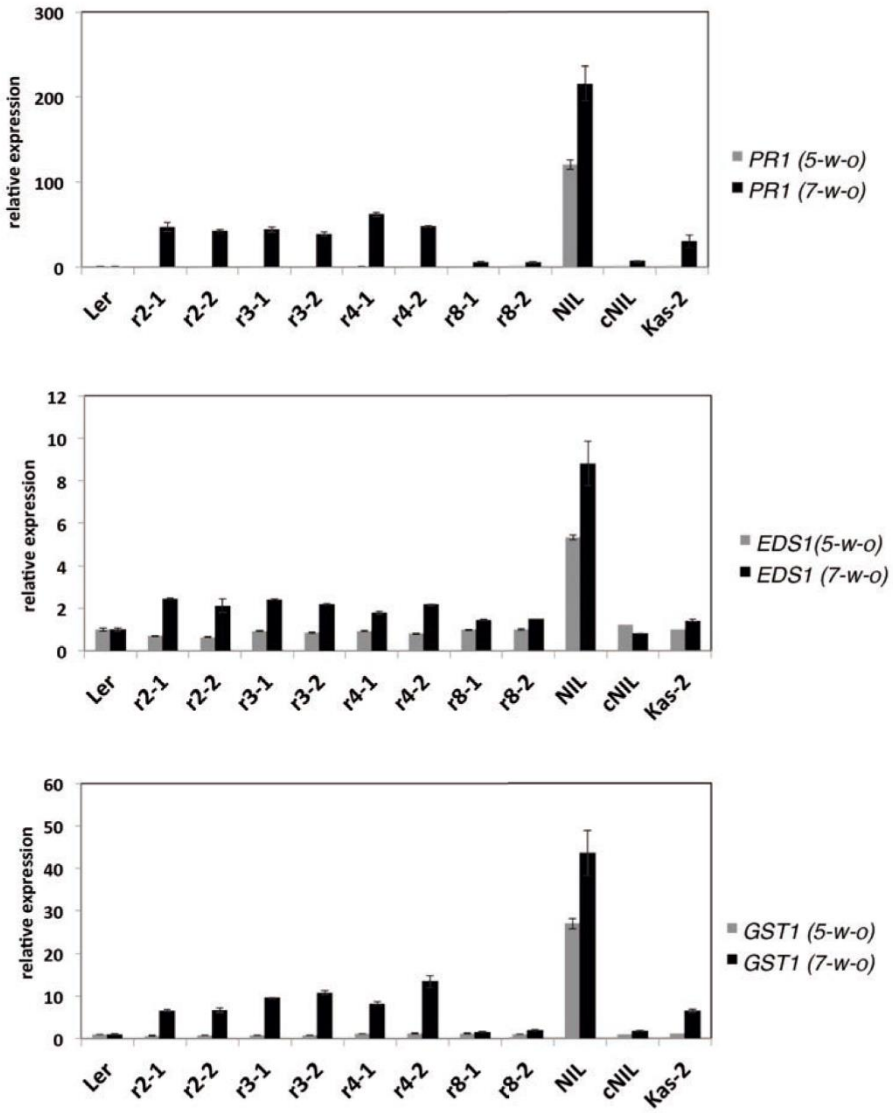

Supplemental Figure 7. *PR1*, *EDS1* and *GST1* expression analyses in 5- and 7-week-old (w-o) Cas9 *r2-1*, *r2-2*, *r3-1*, *r3-2*, *r4-1*, *r4-2*, *r8-1* and *r8-2*, L*er*, Kas-2, L*er*/Kas-2 NIL and cNIL plants grown at 14 - 16ºC. Error bars indicate standard deviation.

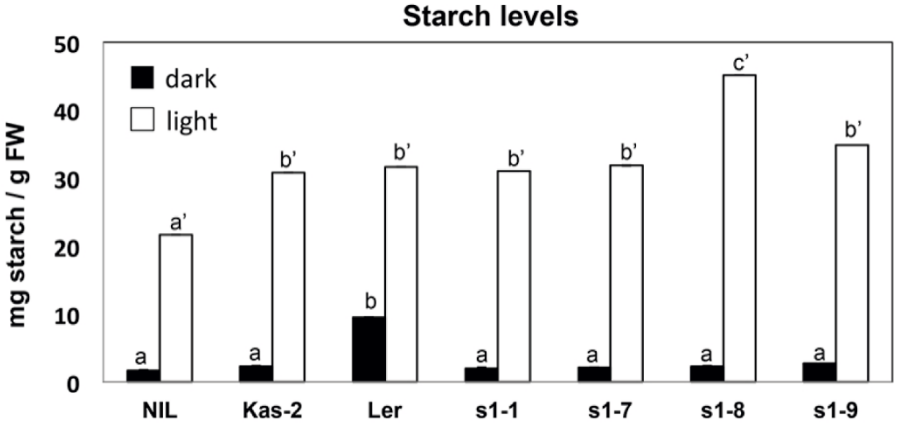

Supplemental Figure 8. Starch levels determined in leaves of 5-week old incompatible L*er*/Kas-2 NIL, Kas-2, L*er*, *sulki1-1*, *sulki1-7*, *sulki1-8* and *sulki1-9* grown at 14 - 16ºC. Letters indicate values that are significantly different according to Student–Newman–Keuls test at *P* value <0.05. FW, fresh weight. Error bars indicate standard deviation.

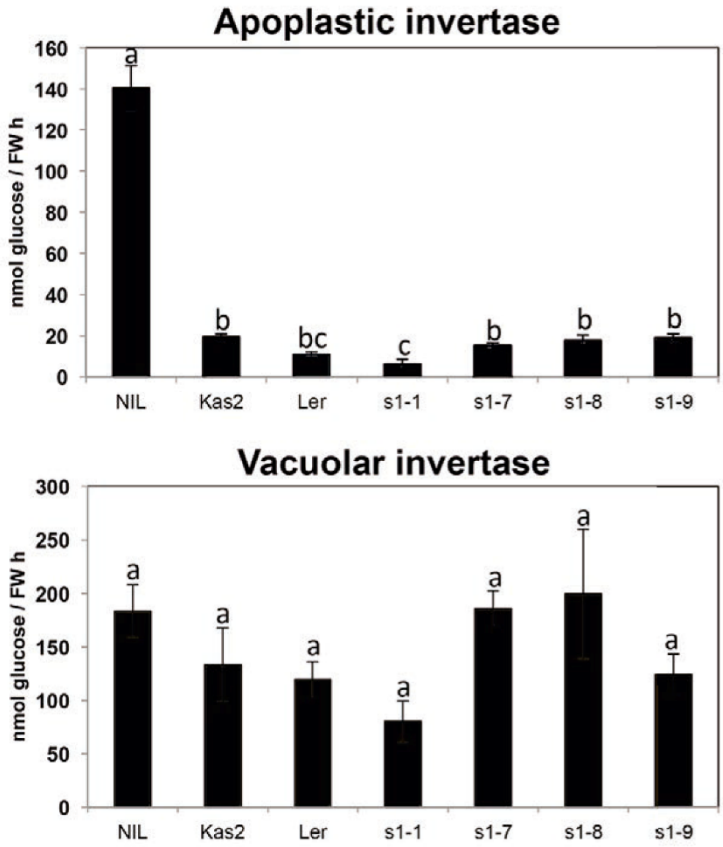

Supplemental Figure 9. Apoplastic and vacuolar invertase activities of 5-week-old incompatible L*er*/Kas-2 NIL, Kas-2, L*er*, *sulki1-1*, *sulki1-7*, *sulki1-8*, and *sulki1-9* grown at 14 - 16ºC. Letters indicate values that are significantly different according to Student–Newman–Keuls test at *P* value <0.05. FW, fresh weight. Error bars indicate standard deviation.

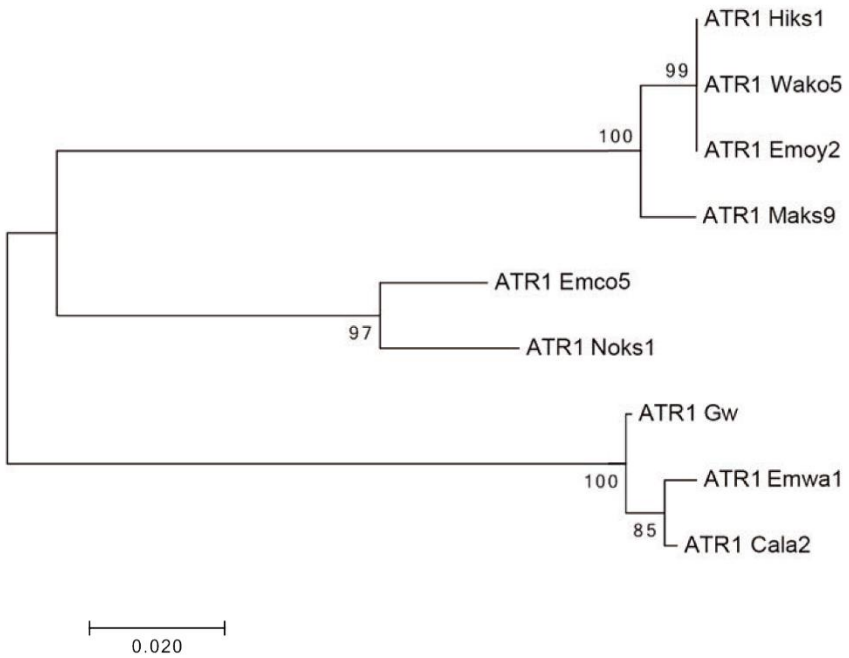

Supplemental Figure 10. Neighbor-joining phylogenetic analysis of ATR1 amino acid sequences from different *Hpa* isolates.

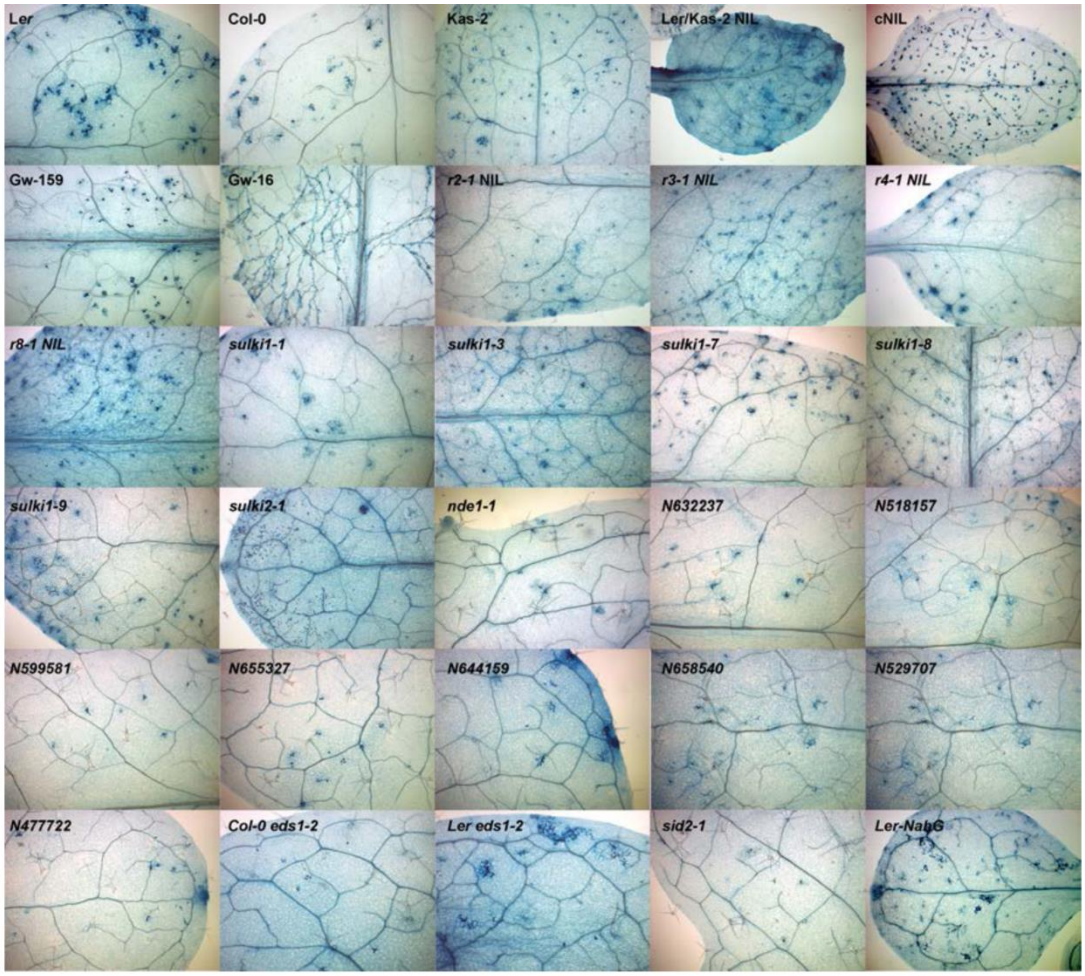

Supplemental Figure 11. Disease resistance phenotypes to *Hpa* Gw infection in different genotypes. L*er*, Col-0, Kas-2, L*er*/Kas-2 NIL, cNIL (Alcázar et al., 2010), Gw-159 (resistant genotype in the Gorzów population), Gw-16 (susceptible genotype in the Gorzów population), CRISPR/Cas9 NIL mutants, *eds1-2* (Feys et al. 2005), *nde1-1* (Stuttmann et al., 2016), L*er-NahG* (Bowling et al, 1997), *RPP1* and *RPP1-like* mutants in Col-0: *At3g44400* (N632237, N518154); *At3g44480* (N599581, N655327); *At3g44630* (N644159, N658450); *At3g44670* (N529707, N477722); *sid2-1* (Wildermuth et al., 2001).

- **Supplemental Tables can be found at:**

  http://www.plantphysiol.org/content/177/3/1152/tab-figures-data

ANNEX III

Supplemental material for Chapter 2

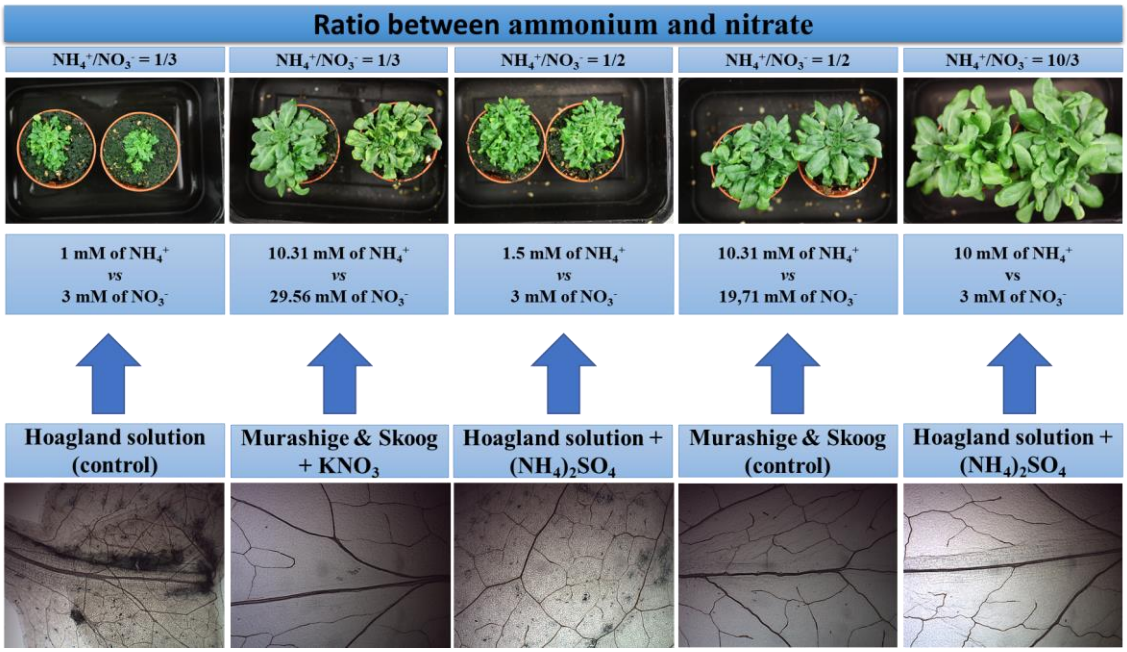

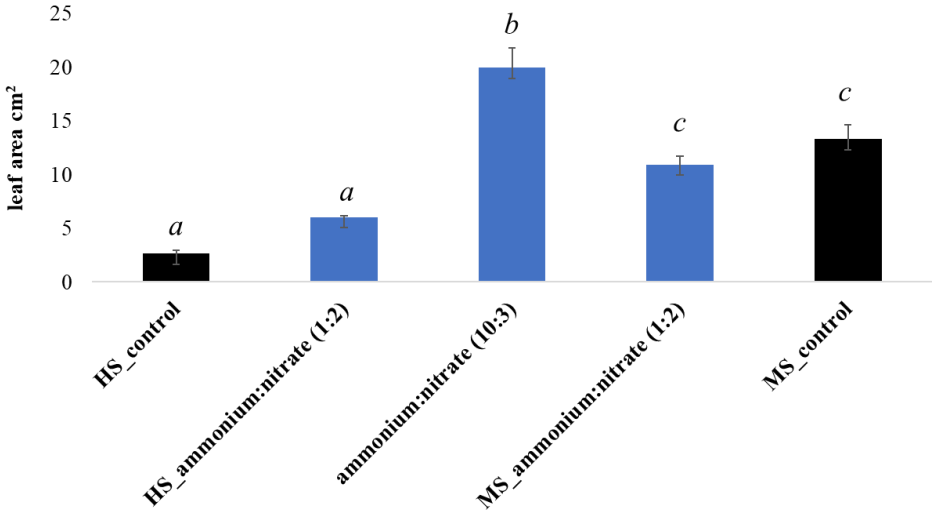

Supplemental Figure S1: Phenotype, trypan blue staining and leaf area measurements of eight-weeks old L*er*/Kas-2 NIL plants grown on soil at 14 ºC – 16 ºC. Plants were grown for four weeks under 0.5x HS irrigation media until different media treatments were initiated and maintained for four weeks. Significant differences are indicated by letters according to statistical analysis using the Student-Newman-Keuls test ($p<0.05$).

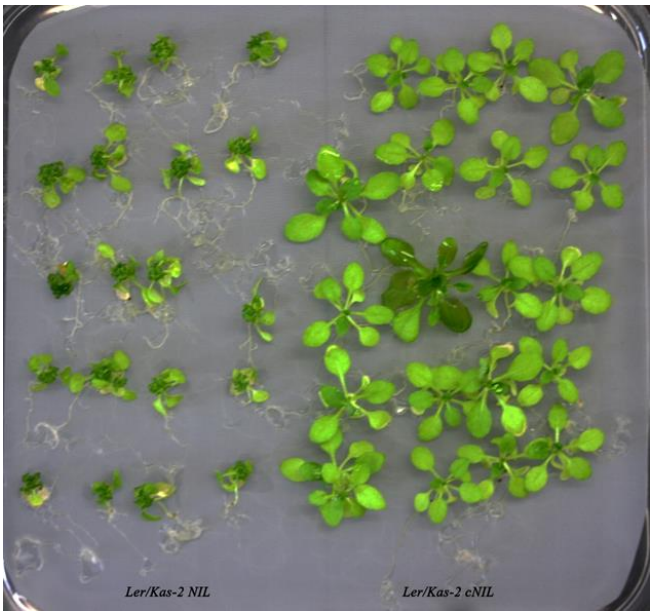

Supplemental Figure S2: Four-weeks old *A. thaliana* seedlings grown under in vitro (0.5x rMS-MES buffer pH=5.75, 1% of sucrose and 0.8% of Plant Agar) at natural temperature (14 ºC – 16 ºC). Image was acquired with Canon EOS 450D digital camera using a Macro Lens (EFS 60mm f/2.8 USM).

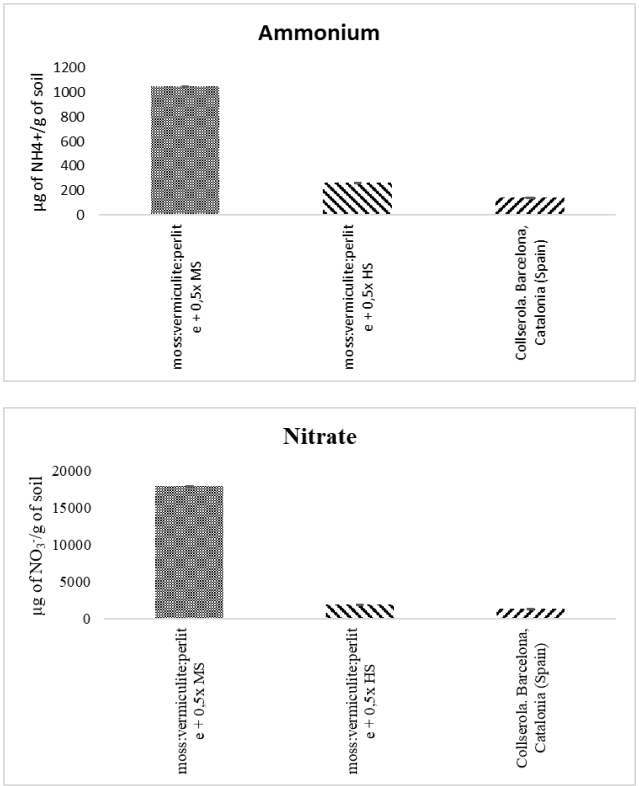

Supplemental Figure S3: Soil ammonium and nitrate quantification

Table 1: Composition of 0.5x Hoagland & Arnon nutrient solution (0.5x HS) and 0.5x Murashige & Skoog media (0.5x MS).

		0.5x HS	0.5x MS
Macronutrients	**NH_4NO_3**	1 mM	10.31 mM
	KNO_3	2 mM	9.40 mM
	$CaCl_2$	0 mM	1.50 mM
	KI	0 mM	2.5 µM
	$MgSO_4•7H_20$	500 µM	750 µM
	KH_2PO_4	1 mM	630 µM
	$Ca(NO_3)_2·2H_2O$	2 mM	0 mM
Micronutrients	**Fe- EDDHA**	19 µM	50 µM
	H_3BO_3	9 µM	50.14 µM
	$MnSO_4*H_2O$	15 µM	50 µM
	$ZnSO_4•7H_20$	5 µM	14.96 µM
	$CuSO_4$	5 µM	0.05 µM
	$CoCl_2$	0.3 µM	0.06 µM
	$Na_2MoO_3*2H_2O$	0.9 µM	0.52 µM
Vitamins	**Glycine**	0 µM	13.32 µM
	***myo*-Inositol**	0 µM	277.47 µM
	Nicotinic acid	0 µM	2.03 µM
	Pyridoxine-HCl	0 µM	1.22 µM
	Thiamine-HCl	0 µM	0.15 µM

Table 2.1: The reconstituted Murashige & Skoog media (0.5x rMS) consists of NH_4^+ concentration scaled down to HS.

		0.5x HS	0.5x MS	0.5x rMS
Macronutrients	**NH_4NO_3**	1 mM	10.31 mM	1 mM
	KNO_3	2 mM	9.40 mM	9.40 mM
	$CaCl_2$	0 mM	1.50 mM	1.50 mM
	KI	0 mM	2.5 µM	2.5 µM
	$MgSO_4•7H_20$	500 µM	750 µM	750 µM
	KH_2PO_4	1 mM	630 µM	630 µM
	$Ca(NO_3)_2·2H_2O$	2 mM	0 mM	0 mM
Micronutrients	**Fe- EDDHA**	19 µM	50 µM	50 µM
	H_3BO_3	9 µM	50.14 µM	50.14 µM
	$MnSO_4*H_2O$	15 µM	50 µM	50 µM
	$ZnSO_4•7H_20$	5 µM	14.96 µM	14.96 µM
	$CuSO_4$	5 µM	0.05 µM	0.05 µM
	$CoCl_2$	0.3 µM	0.06 µM	0.06 µM
	$Na_2MoO_3*2H_2O$	0.9 µM	0.52 µM	0.52 µM

Table 2.2: Supplementation of the 0.5x HS and 0.5x MS media to reach NH_4^+/NO_3^- ratio of 1:2 in 0.5x HS, 10:3 in 0.5x HS, and 1:3 in the 0.5x MS. References ration for the conventional 0.5x HS and 0.5x MS are 1/3 and 1/2, respectively.

Nutrient	1:2 in 0.5x HS	10:3 in 0.5x HS	1:3 in the 0.5x MS
$(NH_4)SO_4$	0.5 mM	9	-
KNO_3	-	-	9.85

Table 3: NH_4^+ and NO_3^- quantification from different soils used in this work.

	NH4+		**NO3-**	
	µg/ g of soil	**SE**	**µg/ g of soil**	**SE**
Moss: vermiculite: perlite + 0,5x MS (40:50:10)	1047,5	0,18	17976,9	3,59
Moss: vermiculite: perlite + 0,5x HS (40:50:10)	264,1	1,02	1929,7	0,17
Soil from wild population in Collserola, Barcelona	142,7	0,47	1363,6	1,78

Table 4: List of qRT-PCR oligonucleotides used in this work**.**

Gene	**Name**	**Sequence**
At3g18780	*ACTIN2*_Fwd	GATTCAGATGCCCAGAAGTCTTGT
	*ACTIN2*_Rev	TGGATTCCAGCAGCTTCCAT
At3g48090	*EDS1*_Fwd	GGAGAATGGATCACAGACGGG
	*EDS1*_Rev	CGTAATCCACCACTTTCTAAACGTT
At1g02930	*GST1*_Fwd	CTTCTCTCAACTGGCAAGGACA
	*GST1*_Rev	TGAACCAACTGGGTCAAACTC
At2g14610	*PR1*_Fwd	CTTTGTAGCTCTTGTAGGTGCTCTT
	*PR1*_Rev	TGGTTGTGAACCCTTAGATAATCTT

Table 5: *Pseudomonas spp*. media preparation.

NAME	Recipe	Annotation
NYGA	5g of Bacto Peptone.	If solid media is required, add 10 g of Bacto Agar.
	3g of Yeast Extract.	
	20 ml of Glycerol.	
	Adjust pH to 7.0 with NaOH.	
	Bring up to 1L with distill water.	
Rifa50	Scale 50mg and add 50 ml of DMSO	*Pst DC3000* and *Pst DC3000 hrcC*

Table 6: Recipes used in the modified Dellaporta protocol.

NAME	Stock Solution	Working Solution
Extraction Buffer 1 (EB1)	0.5 M EDTA pH=8.0	50 mM EDTA pH=8.0
	1 M Tris pH=8.0	100 mM Tris pH=8.0
	4 M NaCl	500 mM NaCl
		0.07% (v/v) of 2-Mercaptoethanol
Extraction Buffer 2 (EB2)	0.5 M EDTA pH=8.0	10 mM EDTA pH=8.0
	1 M Tris pH=8.0	50 mM Tris pH=8.0
20% Sodium dodecyl sulphate (SDS) in water	20 g of SDS in 100 ml	
5 M Potassium acetate (KAc) in water	49.1 g in 100 ml	
3 M Sodium acetate (NaAc) in water	24.6 g in 100 ml	
Isopropanol (IPA)	100% of IPA	
Ethanol (EtOH)	70% EtOH	

Table 7: Sequences, PCR program, enzymes and amplicon sizes of makers used for mapping.

Name and sequence	Annotations	
F9K21_Fwd: TTCGTTGCAATGTACAGATC F9K21_Rev: CTATGGAGGGAATGTACTTAA	NmucI (Tsp45I). Incubate at 37ºC o/n. Enzyme cuts in Kas-2.	95ºC for 5 min. **95ºC for 15 sec.** **50ºC for 45 sec.** **72ºC for 2 min.** **x32 cycles** 72ºC for 10 min. 20ºC forever
F4C21.22_Fwd: AAGACCCAACATTTCCTCTCAACCAA F4C21.22_Rev: AGCTCCGTGGAATCCATTTGTTTTAATA	ApoI. Incubate at 50ºC o/n. Enzyme cuts in *Ler*.	
MVA3_Fwd: ATACCAACAAGAATATGAAATCTGTC MVA3_Rev: CATTGTTAGTTCGGTGATTAGG	AccI. Incubate at 37ºC o/n. Enzyme cuts in Kas-2.	
F11P17-4615_Fwd: CGCAATCGATTTTATTTAAATCC F11P17-4615_Rev: TTTCAGTTTGATGATTTATTCGC	Position 22.60 Mb. Amplicon of 209 bp in Col-0 and 190 bp in Kas-2.	
F5I14_Fwd: CTGCCTGAAATTGTCGAAAC F5I14_Rev: GGCATCACAGTTCTGATTCC	Position 24.37 Mb. Amplicon of 196 bp in Col-0 and 295 bp in Kas-2.	

Table 8: Sequences used for *NPR1* gene amplification and SANGER sequencing.

Name and sequence	**PCR program**
*NPR1*_Fwd_v2: CGCTACCGATAACACCGACT *NPR1*_Rev_v2: TCGTTTCTCAGCAGTGTCGT	95ºC for 5 min. **95ºC for 15 sec.** **55ºC for 45 sec.** **72ºC for 2 min.** **x32 cycles** 72ºC for 10 min. 20ºC forever Amplicon size: 1852 bp

ANNEX IV

Supplemental material for Chapter 3

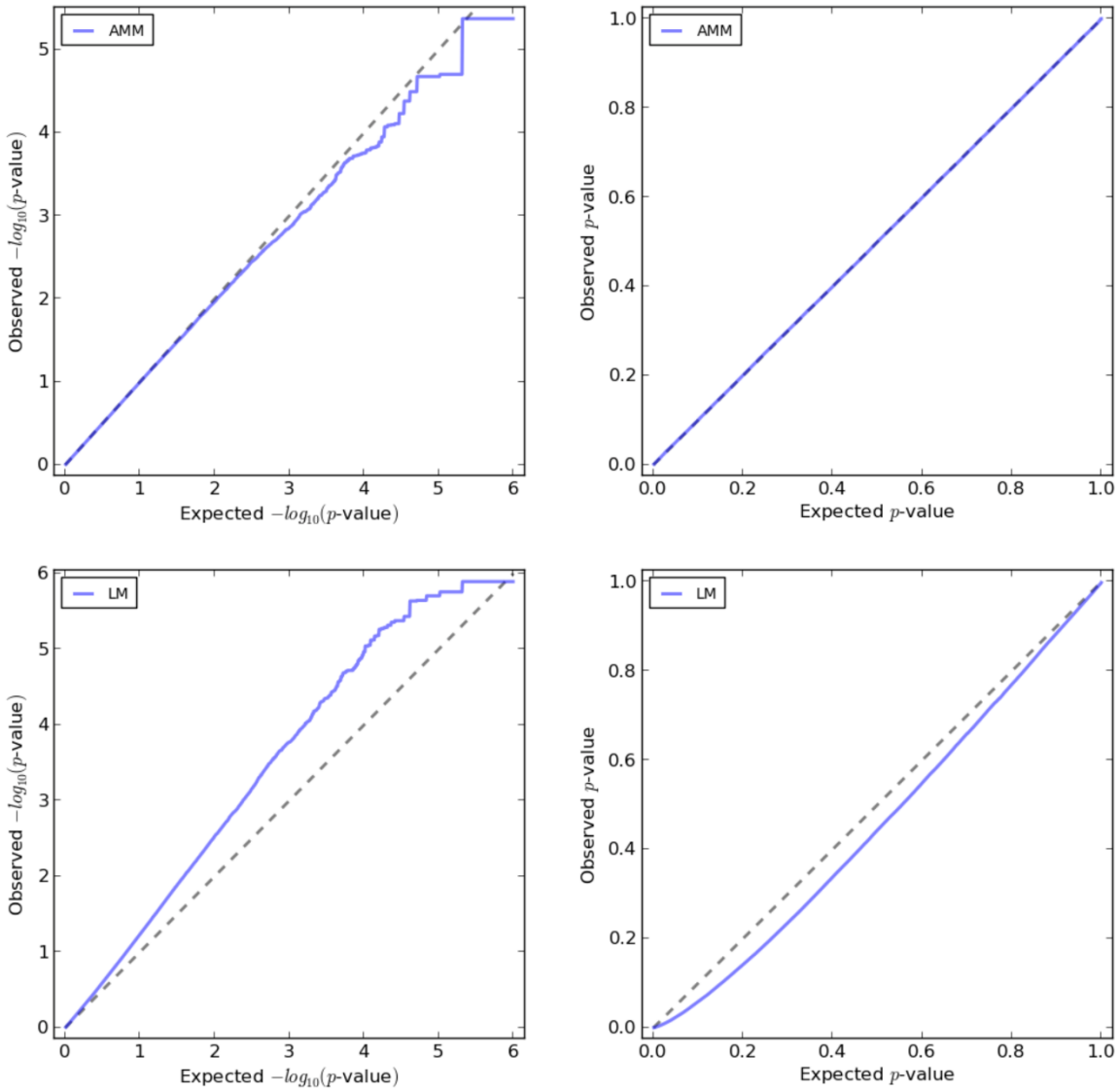

Supplemental Figure S1: Quantile-Quantile (Q–Q) plots for GWAS analysis of chlorophyll levels in response to guazatine using AMM and LM methods.

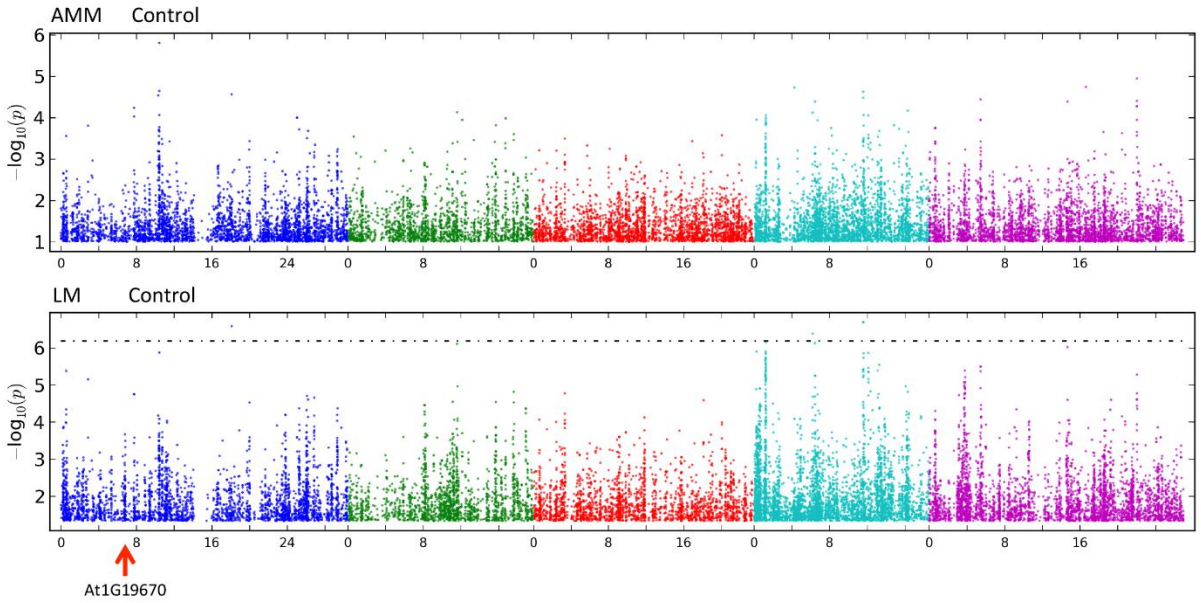

Supplemental Figure S2: Genome wide association mapping profile for chlorophyll levels under control conditions (0 μM guazatine) in 107 Arabidopsis accessions analyzed with the AMM and LM methods

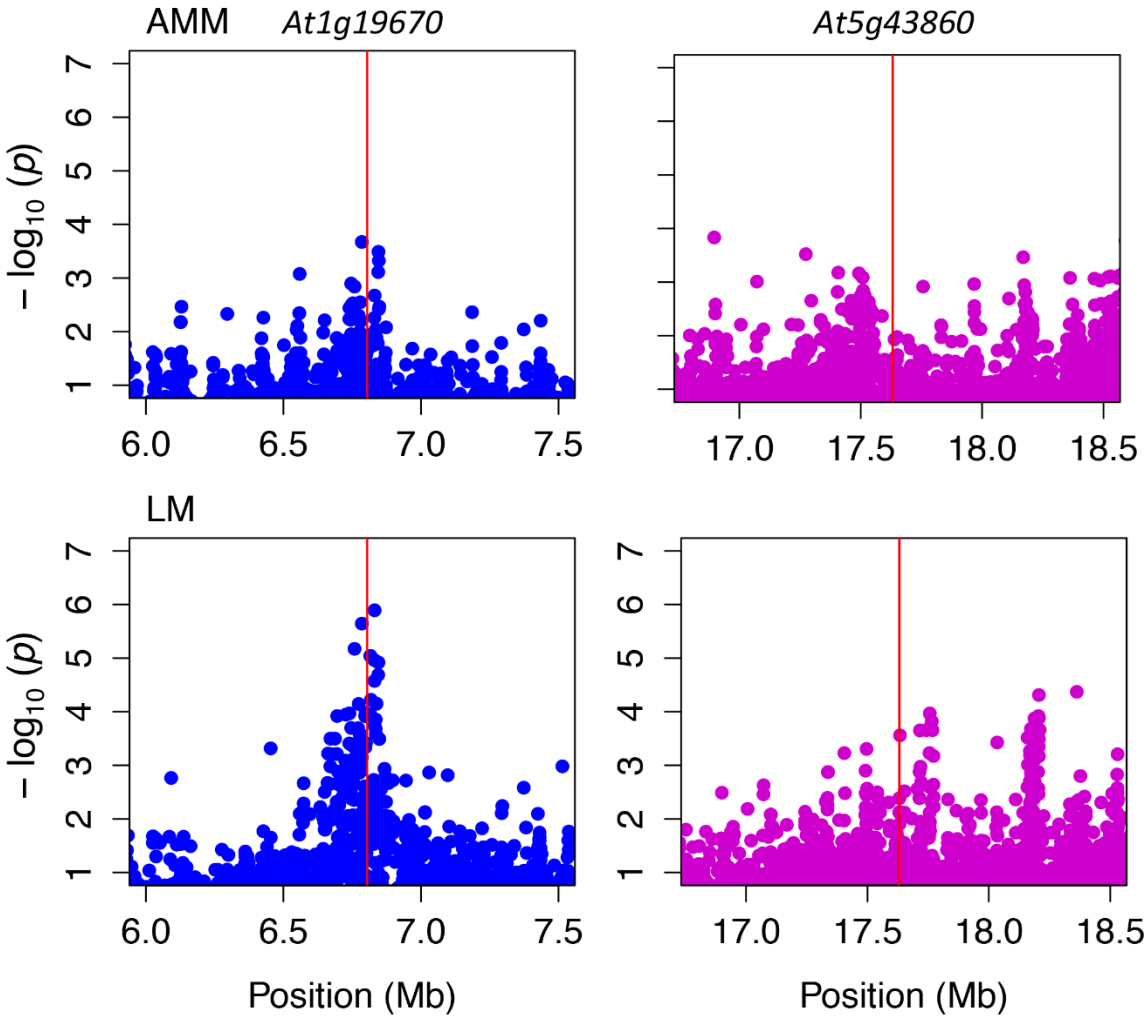

Supplemental Figure S3: Detailed view of the genome wide association mapping profile for guazatine tolerance in 107 Arabidopsis accessions analyzed with the AMM and LM methods in the *CLH1* (At1g19670) and *CLH2* (At5g43860) loci.

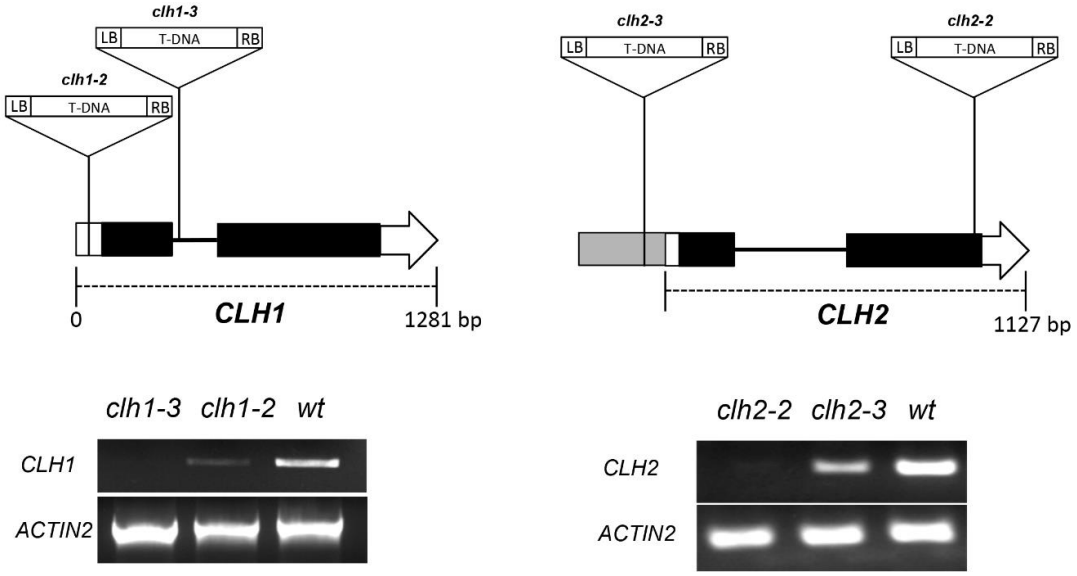

Supplemental Figure S4: Schematic representation of 5′ and3′ UTRs (white), exons (black), introns (lines), and promoter region (gray) in *CLH1* (At1g19670) and *CLH2* (At5g43860) genes. The position of T-DNA insertion in *clh1-2*, *clh1-3*, *clh2-2*, and *clh2-3* is indicated. The expression of *CLH1* and *CLH2* in7-days-old *clh1* and *clh2* seedlings, respectively, was determined by RT-PCR using gene-specific primers and ACTIN2 as housekeeping control.

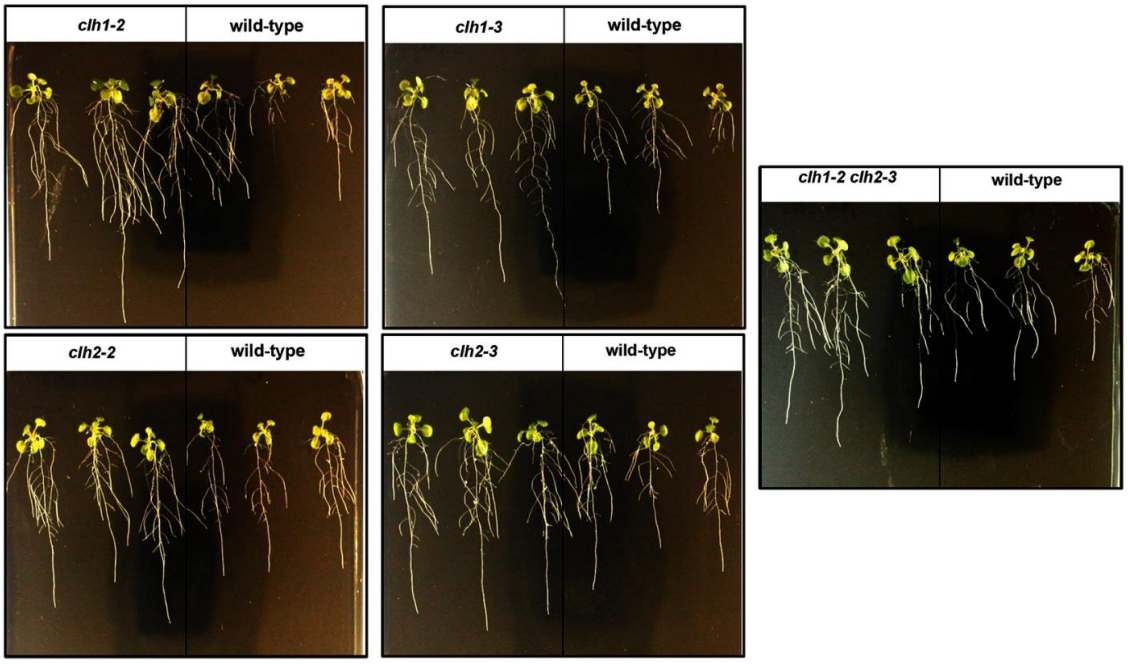

Supplemental Figure S5: Root phenotype of *clh1-2*, *clh1-3*, *clh2-2*, *clh2-3* and double *clh1-2/clh2-3* 16-days-oldseedlings. Seedlings were germinated and grown in the absence of guazatine during 4 days, and then transferred to vertical plates containing1.5 µM guazatine. Pictures were taken 12days after treatment.

Supplemental Table T1: List of *Arabidopsis thaliana* accessions used in this work.

ABRC Stock number	Accession name	Latitude	Longitude	Country
CS76100	Bor-4	49.4013	16.2326	Czech Rep.
CS28344	Hey-1	51.25	5.9	Netherlands
CS28847	Zu-1	47.3667	8.55	Switzerland
CS28814	Wc-2	52.6	10.0667	Germany
CS28492	Mh-0	50.95	7.5	Poland
CS28420	Kro-0	50.0742	8.96617	Germany
CS28373	Jm-1	49	15	Czech Rep.
CS28128	Ca-0	50.2981	8.26607	Germany
CS28280	Gie-0	50.584	8.67825	Germany
CS28350	Hn-0	51.3472	8.28844	Germany
CS76105	Bur-0	54.1	-6.2	Ireland
CS28135	Chat-1	48.0717	1.33867	France
CS76152	Kelsterbach-4	50.0667	8.5333	Germany
CS76136	Got-7	51.5338	9.9355	Germany
CS76143	Hovdala-2	NA	NA	Central Asia
CS76106	C24	41.25	-8.45	Portugal
CS28812	WAR	41.7302	-71.2825	USA
CS76088	Alc-0	40.31	-3.22	Spain
CS76150	Kas-1	35	77	India
CS76124	Duk	49.1	16.2	Czech Rep.
CS28369	Jl-3	49.2	16.6166	Czech Rep.
CS76140	Hi-0	52	5	Netherlands
CS28633	PHW-33	52.25	4.5667	Netherlands
CS28013	Alst-1	54.8	-2.4333	UK
CS28017	An-2	51.2167	4.4	Belgium
CS28018	Ang-0	50.3	5.3	Belgium
CS28049	Ann-1	45.9	6.13028	France
CS28091	Boot-1	54.4	-3.2667	UK
CS76101	Br-0	49.2	16.6166	Czech Rep.
CS76114	Ct-1	37.3	15	Italy
CS76129	Fei-0	40.5	-8.32	Portugal
CS76135	Ge-0	46.5	6.08	Switzerland
CS76139	Gy-0	49	2	France
CS76145	Hs-0	52.24	9.44	Germany
CS76153	Kin-0	44.46	-85.37	USA
CS76168	Lip-0	50	19.3	Poland
CS76173	Lm-2	48	0.5	France
CS76137	Gr-1	47	15.5	Austria
CS28394	Kl-5	50.95	6.9666	Germany
CS28495	Mnz-0	50.001	8.26664	Germany
CS28210	Do-0	50.7224	8.2372	Germany
CS76103	Bu-0	50.5	9.5	Germany
CS76127	Est-1	58.3	25.3	RUS
CS28326	Gr-5	47	15.5	Austria
CS28336	Ha-0	52.3721	9.73569	Germany
CS28729	Sei-0	46.5438	11.5614	Italy
CS28650	Pog-0	49.2655	-123.206	Canada
CS28201	Da(1)-12	NA	NA	Czech Rep.

ABRC Stock number	Accession name	Latitude	Longitude	Country
CS76133	Ga-0	50.3	8	Germany
CS76174	Lom1-1	56.09	13.9	Sweden
CS28732	Sg-1	47.6667	9.5	Germany
CS76176	Lp2-2	49.38	16.81	Czech Rep.
CS76148	JEA	43.6833	7.33333	France
CS76166	Liarum	55.95	13.85	Sweden
CS76084	11PNA4.101	42.0945	-86.3253	USA
CS76085	328PNA054	42.0945	-86.3253	USA
CS28053	Ba-1	56.5459	-4.79821	UK
CS76107	CAM-16	48.2667	-4.58333	France
CS76108	CAM-61	48.2667	-4.58333	France
CS76111	CIBC-17	51.4083	-0.6383	UK
CS28163	Co-2	40.12	-8.25	Portugal
CS28165	Co-4	40.12	-8.25	Portugal
CS76113	Col-0	38.3	-92.3	USA
CS28193	Com-1	49.416	2.823	France
CS28181	CSHL-5	40.8585	-73.4675	USA
CS28200	Da-0	49.8724	8.65081	Germany
CS28208	Di-1	47	5	France
CS76119	DraIV 1-14	49.4112	16.2815	Czech Rep.
CS76120	DraIV 1-5	49.4112	16.2815	Czech Rep.
CS76122	DraIV 6-16	49.4112	16.2815	Czech Rep.
CS76123	DraIV 6-35	49.4112	16.2815	Czech Rep.
CS28236	Ep-0	50.1721	8.38912	Germany
CS28252	Fi-1	50.5	8.0167	Germany
CS28268	Fr-4	50.1102	8.6822	Germany
CS28274	Ga-2	50.3	8	Germany
CS76134	Gd-1	53.5	10.5	Germany
CS28277	Ge-1	46.5	6.08	Switzerland
CS28282	Go-0	51.5338	9.9355	Germany
CS28332	Gu-1	50.3	8	Germany
CS76144	HR-5	51.4083	-0.6383	UK
CS76146	HSm	49.33	15.76	Czech Rep.
CS76149	Ka-0	47	14	Austria
CS76154	Kno-18	41.2816	-86.621	USA
CS28419	Kr-0	51.3317	6.55934	Germany
CS28423	Krot-2	49.631	11.5722	Germany
CS76158	LAC-5	47.7	6.81667	France
CS76160	LDV-14	48.5167	-4.06667	France
CS76162	LDV-34	48.5167	-4.06667	France
CS76163	LDV-58	48.5167	-4.06667	France
CS28457	Li-5:2	50.3833	8.0666	Germany
CS28459	Li-6	50.3833	8.0666	Germany
CS28461	Li-7	50.3833	8.0666	Germany
CS76165	LI-OF-095	40.7777	-72.9069	USA
CS76169	Lis-1	56	14.7	Sweden
CS76172	LL-0	41.59	2.49	Spain
CS76179	Lz-0	46	3.3	France
CS76181	MIB-15	47.3833	5.31667	France
CS28527	Nc-1	48.6167	6.25	France
CS28550	NFC-20	51.4083	-0.6383	UK

ABRC Stock number	Accession name	Latitude	Longitude	Country
CS28575	Nw-2	50.5	8.5	Germany
CS22689	RRS-10	41.5609	-86.4251	USA
CS28713	RRS-7	41.5609	-86.4251	USA
CS28720	S96	NA	NA	UNK
CS28725	Sav-0	49.1833	15.8833	Czech Rep.
CS28734	Sh-0	51.6832	10.2144	Germany
CS28800	Ven-1	52.0333	5.55	Netherlands
CS28833	Wt-3	52.3	9.3	Germany

En memòria de la meva mare

…

Anka K. Trayanova

…

Мила ми е мойта майка,

макар стара била,

макар да е сиромашка,

тя ме е родила.

И да бъде ощ по-бедна,

долня - прост бял камък,

аз когато я погледна

тя е безцен камък.

И да беше тя прост възел

в дрипа еднокрайка,

тя за мен е все пак тази

сладка, мила майка.

Мила си ми, майко моя,

за теб ще милея,

ще те мисля, ще те помня,

чак доде живея.

Petko R. Slaveykov